Determining the *in vitro* anti-cancer effects of various novel indoles and an anti-microbial peptide towards a potential treatment of glioma.

by

Saurabh Prabhu

A thesis submitted in partial fulfilment for the requirements for the degree of PhD at the University of Central Lancashire.

October 2014.

Abstract

Substituted indoles (2-arylindoles) and related structures are known to exhibit potent anti-cancer activity against human breast cancer cell lines, and a range of other therapeutic targets. This activity, and other factors such as their biological activity, the fact that they are privileged structures, and the presence of the indole nucleus in various commercial anti-cancer drugs led to the choosing of indoles for the current study as a starting point for the development of new treatments against glioma. Investigation began on determining the anti-cancer activity of a variety of indoles against glioma cell lines (1321N1 and U87MG) using a number of different cell-based assays and also to compare them with conventional anti-cancer drugs. The aim was to find potent anti-cancer compound(s), amongst the compounds tested, and by studying its preliminary structure-activity-relationships (SAR), try to determine how the active compound(s) may be exerting their effects.

The SAR screening was divided into two main groups: indoles without a 2-aryl group and indoles with a 2-aryl group. The most potent compound identified, and its analogues, were further tested on the non-cancerous SVGp12 cell line to check for specificity of these indoles towards cancer cells, wherein it was found that these compounds were not specific to any particular cell type. Furthermore, activity was also observed for the best lead compound in the glioblastoma short-term culture, IN859, in which it gave a relatively low micromolar IC_{50} value (400 μM).

The results indicated that the anti-cancer activity of these compounds started within 2 h and therefore it was speculated that the mechanism of action of these compounds might work through the generation of reactive oxygen species (ROS). A ROS-detection kit was used to demonstrate this hypothesis, a result which was later corroborated using flow cytometry, and also provided quantitative analysis of the amount of ROS generated. It was further hypothesised that in the cells studied, autophagy was mediated due to excessive ROS generation. This was also confirmed over a similar time course by quantifying the amount of fluorescence generated in the 1321N1 and U87MG cell lines when labelled with acridine orange (a dye used to detect the formation of autophagosomes during autophagy)

using flow cytometry. Moreover, the use of an autophagy inhibitor, 3-methyladenine, was shown to inhibit autophagy in these cell lines, again validating this hypothesis.

In conclusion, it has been demonstrated that the ability of certain substituted privileged indoles possessing a 2-aryl group and having an attached –OH group to it may have a rapid, deleterious effect on the viability of a primary short term culture (IN859) and glioma cell lines (1321N1 and U87MG). The mechanism of action of these indoles to cause cell death may be via the generation of ROS, leading to cell death initiated by autophagy.

Another short separate study was also performed in order to investigate the anti-cancer activity of an anionic host defence peptide, *Cn*-AMP2, on the above mentioned cell lines. This peptide was found to exhibit a modest cytostatic effect on both the cell lines but at higher concentrations (> 1 mM) and only when the serum concentrations were weaned down from 10 % to 2.5 %.

List of Figures

Figure 1: Coloured computed tomography (CT) brain scan showing a large intracranial tumour, the large round mass (green) seen at centre. Within the tumour, spots indicate fluid-filled cysts (Image available at https://sciencephoto.com/media/254804/view)..... 2

Figure 2: Data provided in the graph are for adults aged 15-99 diagnosed in England and Wales which predicts the survival estimates. Brain tumour shows insignificant increase in the median survival rate over three decades (Rachet *et al.*, 2009)..... 5

Figure 3: Different representations of the chemical structure of indole. 15

Figure 4: Baeyer's original structure for indole (Baeyer and Emmerling, 1869)..... 16

Figure 5: Formation of indole-3-carbinol. (Available at http://lpi.oregonstate.edu/infocenter/phytochemicals/i3c/fig1.html)..... 19

Figure 6: The structure of DIM..... 20

Figure 7: Structure of sunitinib with the 2- indolinone (indole-like) core highlighted..... 21

Figure 8: Structure of enzastaurin with the two indoles highlighted. 22

Figure 9: Structure of cediranib with the indole core highlighted. 23

Figure 10: Structure of vinblastine with the two indoles highlighted..... 24

Figure 11: Structure of vincristine with the two indoles highlighted. 25

Figure 12: Structure of 1-benzyl-indole-3-carbinol with the indole core highlighted..... 26

Figure 13: Structure of SR13668 with the two indoles highlighted. 27

Figure 14: Structure of INF55 and bazedoxifene..... 29

Figure 15: Diagram showing the important steps during autophagy..... 34

Figure 16: Diagrammatic representation of a haemocytometer..... 43

Figure 17: Diagrammatic representation of the MTS assay (Image available at http://spotlite.nih.gov/assay/images/2/26/Terry_Riss_aDream_Slides.pdf). 47

Figure 18: Structures of MTS tetrazolium [3-(4,5-dimethylthiazol-2-yl)-5-(3-carboxymethoxyphenyl)-2-(4-sulfophenyl)-2H-tetrazolium] and its formazan product (Adapted from Promega)..... 48

Figure 19: Diagrammatic representation of the ATP assay (assay (Image available at http://spotlite.nih.gov/assay/images/2/26/Terry_Riss_aDream_Slides.pdf). 49

Figure 20: Mono-oxygenation of luciferin is catalysed by luciferase in the presence of $Mg2^{+}$, ATP and molecular oxygen (Adapted from Promega). 50

Figure 21: Compounds used in the present study. 53

Figure 22: Selected ^{1}H NMRs of compounds 209 and 223a showing their level of purity. 54

Figure 23: Detection of ROS generation by Image-iT™ LIVE Green Reactive Oxygen Species Detection Kit. 58

Figure 24: Growth analysis of the non-cancerous foetal glial cell line, SVGp12, and the human glioma cell lines 1321N1 and U87MG by Neubauer's Haemocytometer method. . 68

Figure 25: Growth analysis of glioma cell lines 1321N1 and U87MG using the ATP assay where the R^2 value is the correlation coefficient. 69

Figure 26: Dose response curves of cisplatin, carmustine, etoposide, gemcitabine and temozolomide on the 1321N1 cell line after treatment for 48 h. The data points are means of 4 repeats and the error bars represent ±SD. 72

Figure 27: Dose response curves of cisplatin, carmustine, etoposide, gemcitabine and temozolomide on the U87MG cell line after treatment for 48 h. The data points are means of 4 repeats and the error bars represent ±SD. 73

Figure 28: Various novel compounds tested in comparison with cisplatin and resveratrol for 48 h on the 1321N1 cell line. The data points are means of 4 repeats and the error bars represent ±SD. 77

Figure 29: Various novel compounds tested in comparison with cisplatin and resveratrol for 48 h on the U87MG cell line. The data points are means of 4 repeats and the error bars represent ±SD. 78

Figure 30: Diagram showing the structures of the tested indoles and the structural similarity between resveratrol and compound 193 (box). 81

Figure 31: Various indoles tested in comparison with cisplatin and resveratrol on the 1321N1 cell line after treatment for 48 h. The data points are means of 4 repeats and the error bars represent ±SD. 82

Figure 32: Various indoles tested in comparison with cisplatin and resveratrol on the U87MG cell line after treatment for 48 h. The data points are means of 4 repeats and the error bars represent ±SD. 83

Figure 33: Chemical structures of indole-3-carbinol (147 (I3C), a 2-arylindole (compound 193) and their proposed structural hybrids (compound 223a and 209). 85

Figure 34: Indoles tested on the 1321N1 cell line for 48 h. The data points are means of 4 repeats and the error bars represent ±SD. 87

Figure 35: Indoles tested on the U87MG cell line for 48 h. The data points are means of 4 repeats and the error bars represent ±SD. 88

Figure 36: Diagram depicting the acid instability of compound 147 (I3C) and the analogous structure for the presumably more stable acid-degradation product from compound 223a. 90

Figure 37: Diagram showing the structure of a generic 2-arylindole (left) and the potent compound (209, right). 91

Figure 38: Diagram representing the analogues of compound 209 without the aryl–OH group, but with the 2-aryl ring. 93

Figure 39: 1321N1 cell line treated with compound 209 at two different concentrations... 99

Figure 40: 1321N1 cell line treated with resveratrol at two different concentrations. 100

Figure 41: U87MG cell line treated with compound 209 at two different concentrations. 102

Figure 42: Images of human glioma cells 1321N1 showing membrane lysis (as indicated by trypan blue staining) after treatment with compound 209 (1000 µM) at different time points at 20X magnification. 104

Figure 43: Images of human glioma cells U87MG showing membrane lysis (as indicated by trypan blue staining) after treatment with compound 209 (1000 µM) at different time points at 20X magnification. 104

Figure 44: Indoles tested on the 1321N1 cell line for 2 h using the MTS assay. The data points are means of 4 repeats and the error bars represent ±SD. 108

Figure 45: Indoles tested on the U87MG cell line for 2 h using the MTS assay. The data points are means of 4 repeats and the error bars represent ±SD. 109

Figure 46: Indoles tested on the SVGp12 cell line for 2 h using the MTS assay. The data points are means of 4 repeats and the error bars represent ±SD. 110

Figure 47: Confocal acquisitions of human glioma cell line 1321N1 at 40X magnification after 1 h of incubation with Image-iT ™ LIVE Green Reactive Oxygen Species Detection Kit and compound 209. 116

Figure 48: 1321N1 cells were treated with compound 209 and analogues for 1 h. 119

Figure 49: U87MG cells were treated with compound 209 and analogues for 1 h. 120

Figure 50: Dot plot with a gate encompassing the A) 1321N1 and B) U87MG cell populations by scatter. 121

Figure 51: The vicious cycle of ROS stress in cancer (Trachootham *et al.*, 2009). 126

Figure 52: 1321N1 (A) and U87MG (B) cells co-treated with compound 209 (500 µM) and ascorbic acid (500 µM) for 1 h. Ascorbic acid was used as a scavenger for hydroxyl reactive oxygen species and the MTS assay was used to measure the cell viability. The data points are means of 4 repeats and the error bars represent ±SD. 130

Figure 53: Acidic vesicular organelle (AVO) formation in 1321N1 cells. 136

Figure 54: Acidic vesicular organelle (AVO) formation in U87MG cells. 137

Figure 55: Compound 209 tested on the IN859 primary cell line for 2 h. The data points are means of 4 repeats. 143

Figure 56: Flowchart model depicting ROS mediated cell death mechanism. 145

Figure 57: The morphology of 1321N1 cell line after incubation with *Cn*-AMP2. 148

Figure 58: Peptides represented as two-dimensional axial projections. 150

Figure 59: Dose response curves using the MTS assay for the action of *Cn*-AMP2 against the 1321N1 and U87MG glioma cell lines when cultured in DMEM with an FBS concentration of 2.5 % (v/v). The data points are means of 4 repeats and the error bars represent ±SD. 152

List of Tables

Table 1: WHO classification of glioma (Louis *et al.*, 2007)..... 8

Table 2: Media, reagents, supplements and storage conditions. 40

Table 3: Log P values (calculated using ChemBioDraw Ultra 11.0) of some of the indoles tested. 56

Table 4: Drug/compound preparation: Stock solutions were made prior to use..... 57

Table 5: Showing the IC_{50} values of cisplatin, and the indoles against the two different cell lines after being exposed for 48 h using the MTS assay. The values shown are the standard deviations of four repeats. 89

Table 6: Showing the IC_{50} values of indoles against the two different cell lines after being exposed for 2 h using the MTS assay. The values shown are the standard deviations of four repeats. 107

Table 7: Showing the IC_{50} values of the indoles tested against the two different cell lines after being exposed for 2 h using the ATP assay. The values shown are the standard deviations of four repeats. 111

Table 8: The percentage of ROS positive cells when treated with compounds 209, 193, 223 and TBHP for 1 h. Carboxy-H_2DCFDA staining intensity was quantified by flow cytometry and the following values are the means of 3 repeats. (t-test, $P < 0.05$ for compound 209, SD = Standard deviation). 118

Table 9: The percentage of ROS positive cells when treated with compound 209 at various concentrations for 1 h. Carboxy-H_2DCFDA staining intensity was quantified by flow cytometry and the following values are the means of 3 repeats. 123

Table 10: The percentage of ROS positive cells when treated with compound 209 at various concentrations for 48 h. Carboxy-H_2DCFDA staining intensity was quantified by flow cytometry and the following values are the means of 3 repeats. 124

Table 11: The percentage of ROS positive cells when treated with compound 209 and compound 209 + ascorbic acid for 1 h. Carboxy-H_2DCFDA staining intensity was quantified by flow cytometry and the following values are the means of 3 repeats. (t-test, $P < 0.05$ for compound 209, SD = Standard deviation). 131

Table 12: The percentage of acridine orange positive cells when treated with compound 209 and 3- methyladenine for 1 h. Acridine orange staining intensity was quantified by flow cytometry and the following values are the means of 3 repeats. (t-test, $P < 0.05$ for compound 209, SD = Standard deviation). 135

Acknowledgements

I would like to take this opportunity to express my extreme gratefulness and appreciation to all those people without whom, it wouldn't have been possible for me to complete my doctoral research. I would like to dedicate this thesis to my grandmother, parents and my sisters, Apurva and Swati, without whom it would have been impossible for me to complete my research. They all have been a constant source of motivation, encouragement and inspiration. I am deeply grateful to my parents for their unconditional love, support and providing the finances for me to study away from home and believing in me that I could get through this.

I am extremely grateful to my Director of Studies, Dr Timothy Snape for his extensive knowledge and rational way of thinking, which has been of great importance to me. His understanding, patience and personal guidance provided a good foundation for this thesis. I want to sincerely thank my second supervisors, Professor Robert Lea and Dr Fredrick Harris for their detailed and constructive comments throughout this work. Hours of discussions with Fred have proved to be a very good confidence booster. I would also like to thank my Research Degree Tutor, Professor Jaipaul Singh for his unparalleled support in completing all the legal documentation required during these three years. I owe my most sincere gratefulness to Dr Julie Shorrocks for introducing me to cell culture and providing patient and persistent help in my laboratory work throughout these four years of research. I would also like to thank Dr Sarah Rachel Dennison for her guidance in various areas of my research and Clare Altham for helping me with all the paperwork requirements throughout these years.

Last but not the least, I would like to specially acknowledge and extend my heartfelt thankfulness to my friends Varun, Abhijit and Chaitanya for keeping me cheerful always.

List of Abbreviations

µM	micro-molar
µl	micro-litre
2-ME	2-methoxyestradiol
3-MA	3-methyladenine
AA	anaplastic astrocytoma
ADME	absorption, distribution, metabolism, and excretion
AG	angiocentric glioma
AKT	protein Kinase B
AO	acridine orange
AP-1	activator protein 1
ASK1	apoptosis signal-regulated kinase 1
ATCC	American Type Culture Collection
ATG	autophagy related genes
ATM	ataxia telangiectasia mutated
ATP	adenosine triphosphate
AVO	acidic vesicular organelles
BBB	blood-brain barrier
BCNU	carmustine
BNIP3	BCL2/adenovirus E1B 19 kDa protein-interacting protein 3
BRU	Biomedical research unit
CCNU	lomustine
Cdk	cyclin-dependent kinase
CMA	chaperone-mediated autophagy
CNS	central nervous system
CT	computed Tomography
CYP	cytochrome P450
DIM	3,3'-diindolylmethane

DMEM	Dulbeccos's modified eagle's medium
DMSO	dimethyl Sulfoxide
DNA	deoxyribonucleic acid
ECACC	European Collection of Cell Cultures
EGFR	epidermal growth factor receptor
EMEM	Essential minimum eagle medium
EMT	epithelial-to-mesenchymal transition
EPR	electron paramagnetic resonance
ERK	extracellular signal-regulated kinases
FBS	foetal bovine serum
FITC	fluorescein isothiocyanate
FSC	forward scatter
GBM	glioblastoma multiforme
Gy	Gray (unit)
H	hours
HBSS	Hanks' balanced salt solution
H_2O_2	hydrogen peroxide
HDPs	host defence peptides
HO·	hydroxyl radical
HPLC	high-performance liquid chromatography
IC_{50}	inhibition concentration causing 50% cell death
JNK	c-Jun N-terminal kinase
KDa	dalton
MALDI	matrix-assisted laser desorption/ionization
MAPK	mitogen-activated protein kinase
min	minutes
ml	milli-litre
mM	milli-molar

MRI	magnetic resonance imaging
MRS	magnetic resonance spectroscopy
mTOR	mammalian target of rapamycin
MTS	4,5-dimethylthiazol-2-yl)-5-(3-carboxymethoxyphenyl)-2-(4-sulfophenyl)-2H-tetrazolium
NADP	nicotinamide adenine dinucleotide phosphate
NEAA	non-essential amino acids
NF-κB	nuclear factor kappa-light-chain-enhancer of activated B cells
NMR	nuclear magnetic resonance
NQO	NAD(P)H:quinone acceptor oxidoreductase
NQ1Q	NAD(P)H:quinone oxidoreductase
$O_2^{\cdot -}$	superoxide radical
PBS	phosphate buffered saline
PCD	programmed cell death
PDGFR	platelet-derived growth factor receptor
PKC	protein kinase C
PEITC	phenylethyl isothiocyanate
PI	propidium iodide
PMA	pilomyxoid astrocytoma
ROS	reactive oxygen species
SD	standard deviation
SERM	selective oestrogen receptor modulators
SSC	side scatter
TBHP	*tert*-butyl hydroperoxide
TMZ	temozolomide
USFDA	U S Food and Drug Administration
v/v	volume by volume
VEGF	vascular endothelial growth factor
WHO	World Health Organisation

The only source of knowledge is experience.

-Albert Einstein.

Table of Contents

1. INTRODUCTION 2
1.1 Brain tumours 2
1.1.1 Glioma 3
1.1.1.1 Epidemiology of glioma 4
1.1.1.2 Classification 6
1.1.1.3 Diagnosis of glioma 8
1.1.1.4 Treatments for glioma 9
1.1.1.4.1 Surgery 10
1.1.1.4.2 Radiation 11
1.1.1.4.3 Chemotherapy 11
1.2 Small molecules 13
1.2.1 Indoles 14
1.2.1.1 History 15
1.2.1.2 Synthesis 16
1.2.2 The importance of the indole motif in drug design 16
1.2.2.1 Biological activity 17
1.2.2.2 Indoles in cancer 18
1.2.2.2.1 Indole-3-carbinol 19
1.2.2.2.2 Sunitinib 21
1.2.2.2.3 Enzastaurin 22
1.2.2.2.4 Cediranib 23
1.2.2.2.5 Vinblastine 24
1.2.2.2.6 Vincristine 25
1.2.2.2.7 1-Benzyl-indole-3-carbinol 26
1.2.2.2.8 SR13668 27
1.2.2.3 Indoles as privileged structures 28
1.3 *Cn*-AMP2; a host defence peptide 30
1.4 Mechanisms involved in cell death 31
1.4.1 Apoptosis 32
1.4.2 Autophagy 33

1.4.3 Necrosis 35
1.5 Hypothesis and aims of the research 35
2. MATERIALS AND METHODS 38
2.1 Cell culture 38
2.1.1 Thawing cryopreserved cells 41
2.1.2 Subculture 41
2.1.3 Cell Counting 42
2.1.4 Cell freezing 43
2.2 Growth curves 44
2.3 Cell proliferation assays 45
2.3.1 MTS assay 46
2.3.2 ATP assay 49
2.3.3 Trypan blue dye exclusion test 51
2.4 Preparation of stock solutions of commercial anti-cancer agents and novel compounds 52
2.4.1 Physiochemical properties of novel indoles 55
2.5 Image-iT™ LIVE Green Reactive Oxygen Species Detection Kit 58
2.5.1 Confocal microscopy 59
2.5.2 Flow cytometry analysis 60
2.5.3 Acridine orange staining 60
2.6 Graphical analysis and stock solution preparation of the host defence peptide (HDP), *Cn*-AMP2 62
2.7 Statistical and Data analyses 64
3. RESULTS AND DISCUSSION 66
3.1 Establishing the growth curves for the glioma cell lines 66
3.2 Cell proliferation and viability measurements of glioma cell lines in the presence of the test compounds. 70
3.2.1 Determining the best commercial compound to be used as a positive control *in vitro* 70
3.2.1.1 Cisplatin as a positive control 74
3.2.2 Preliminary test compounds in comparison with cisplatin and resveratrol 75
3.2.3 Privileged indoles in comparison with cisplatin and resveratrol 80
3.2.4 Testing the hybrid compounds and their analogues on glioma cell lines 86
3.2.5 The instability of compound 223a in acidic media 89

3.3 Structure-activity-relationship of compound 209 with its analogues 90
3.3.1 Indoles without the 2-aryl group 91
3.3.2 Indoles with the 2-aryl group 92
3.4 The importance of phenols and phenolic fragments 96
3.5 Time course studies of compound 209. 98
3.5.1 Time course study using the MTS assay 98
3.5.2 Time course study using the trypan blue exclusion test 103
3.6 The activity of various indoles on the 1321N1, U87MG and SVGp12 cell lines (2 h) 105
3.6.1 Corroborative study of compound 209 using the ATP assay. 111
3.7 Detection of Reactive Oxygen Species (ROS). 113
3.7.1 Possible cellular mechanism of action of compound 209 113
3.7.2 Confocal microscopy using an "Image-iT LIVE Green Reactive Oxygen Species Detection Kit". 114
3.7.3 Flow cytometry analysis using Image-iT LIVE Green Reactive Oxygen Species Detection Kit. 117
3.7.3.1 Treatment with the test compounds for 1 h 117
3.7.3.2 Dot plots for the selection of cells used in Figure 48 and Figure 49 121
3.7.3.3 Treatment with compound 209 at various concentrations 122
3.7.3.4 Treatment with compound 209 for 48 h 123
3.7.4 Reactive oxygen species (ROS) 125
3.7.5 Co-treatment of the cells with compound 209 and a ROS scavenger (ascorbic acid) 129
3.8 Detection of Autophagy 132
3.9 Effects of compound 209 on a primary cell culture 142
3.10 Summary of the proposed ROS-induced mechanisms of cell death 144
3.11 *Cn*-AMP2, a host defence peptide (HDP) against the glioma cell lines, 1321N1 and U87MG. 146
4. Conclusion and future work 156
4.1 General conclusions 156
4.2 Scope for future studies 157
5. Appendices 200
5.1 Appendix I 200
5.2 Appendix II 203

5.3 Appendix III 204
5.3.1 List of research outcomes 204
5.3.2 List of conferences attended 205

Chapter I

1.INTRODUCTION

1.1 Brain tumours

Brain tumours are masses or growths of abnormal cells in the brain and are typically categorised as either primary or secondary. Those which originate in the brain are called primary tumours while secondary tumours are formed when cancer cells from body parts such as lung or breast, spread to the brain (Aminoff, 2011).

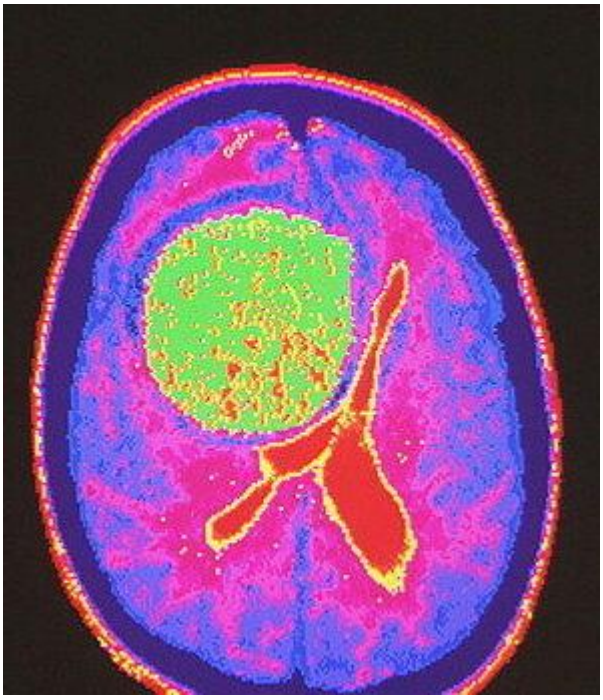

Figure 1: Coloured computed tomography (CT) brain scan showing a large intracranial tumour, the large round mass (green) seen at centre. Within the tumour, spots indicate fluid-filled cysts (Image available at https://sciencephoto.com/media/254804/view).

Primary brain tumours can be non-cancerous (benign) or cancerous (malignant) and are less common compared to secondary brain tumours. However, unlike cancers elsewhere in the body, primary malignant brain tumours rarely spread from the brain. Primary

tumours are mostly benign which means that they remain located in the area where they originated and do not spread to the other parts of the body. Benign tumours can be operated upon and taken out completely and if successful they do not cause any further problems. Successful removal of a benign tumour also depends upon the location of the tumour. Sometimes it is difficult to remove benign tumours as doing so might damage the surrounding sensitive brain cells (Aminoff, 2011).

Malignant brain tumours grow more rapidly than benign tumours and destroy surrounding brain cells. A brain tumour, primary or secondary, can cause a variety of signs and symptoms because it can directly press on or invade brain tissue (Figure 1). The signs and symptoms include severe headaches, difficulties with balancing, personality or behavioural changes, hearing problems, vision problems including blurred vision, double or loss of peripheral vision (Aminoff, 2011).

1.1.1 Glioma

Brain tumours arising from the glial cells in the brain are known as gliomas. Gliomas are a heterogeneous group of neoplasms and comprise the majority of tumours which originate in the central nervous system (CNS) (Burton and Prados, 2000). Glial cells are the most common cells in the brain and their important functions include supporting and protecting the nerve cells, supplying energy and nutrients and maintaining the blood- brain barrier (BBB). Each type of glial cell has its own independent function, for example, astrocytes help in the transportation of nutrients and help in supporting neurons in place, oligodendrocytes provide insulation to the neurons, microglia digest dead neurons and pathogens and ependymal cells line the ventricles and also secrete cerebrospinal fluid (Louis *et al.*, 2001).

Gliomas are comprised of a mix of neoplastic and non-neoplastic cells, which include native and recruited cells and there is a vast diversity among the tumour cells with respect to *in vitro* growth, a key property for cell differentiation. Tumourigenic cells, which are undifferentiated and have the capacity for developing into tumours, are termed stem cells (Park and Rich, 2009). Gliomas vary in their aggressiveness, or malignancy and as such, there is a gradation of gliomas, which is based on how normal or abnormal the tumour cells appear when examined under a microscope. Glioma cases are mostly observed in industrial and developed countries and among them, glioblastoma is the most frequent and malignant histological type (Fisher *et al.*, 2007). It is very important to study the genomic conditions along with the continued evaluation of environmental and development factors for gliomas. To achieve this goal, large sample sizes and multidisciplinary teams with expertise in neuropathology, genetics, epidemiology, functional genomics, bioinformatics, biostatistics, immunology and neuro-oncology are required, all of which can help to explore relevant pathways and the modifying effects of other genes, to avoid false positive findings (Fisher *et al.*, 2007).

1.1.1.1 Epidemiology of glioma

Brain tumours are one of the most devastating forms of cancer and are the second leading cause of death in men and children and the fifth leading cause of death in women (Jemal *et al.*, 2010). The worldwide annual incidence rate of primary malignant brain tumours ranges from 5.8 per 100,000 for males and 4.1 per 100,000 for females in developed countries (Jain *et al.*, 2008; Schwartzbaum *et al.*, 2006). In 2008, 4,785 people in Europe were diagnosed with malignant brain tumours with 4,552 people being diagnosed with other non-invasive types of brain tumour (Crocetti *et al.*, 2012). The rate of incidence

of primary brain tumour in the US increases steadily with increase in age, which peaks at 65.5/100,000 person years (ABTA, 2010). Gliomas account for 86 % of primary tumours and strongly influence the statistical data for primary tumours in the UK (McKinney, 2004). The incidence of primary tumours also shows a variation with sex, race, age and geography (Moore and Kim, 2010), and approximately 13,000 deaths and 18,000 new cases of primary malignant brain and CNS tumours occur annually in the US (Schwartzbaum *et al.*, 2006). About 4,500 new cases of glioma occur every year in the UK, of which 20 % are low grade gliomas and the remaining 80 % are high grade gliomas (Efird, 2011). In Europe, cases of primary brain tumour comprising of high grade glioma and brain metastasis observed range from 4.5 to 11.2 cases per 100,000 in men and from 1.6 to 8.5 per 100,000 in women (Crocetti *et al.*, 2012).

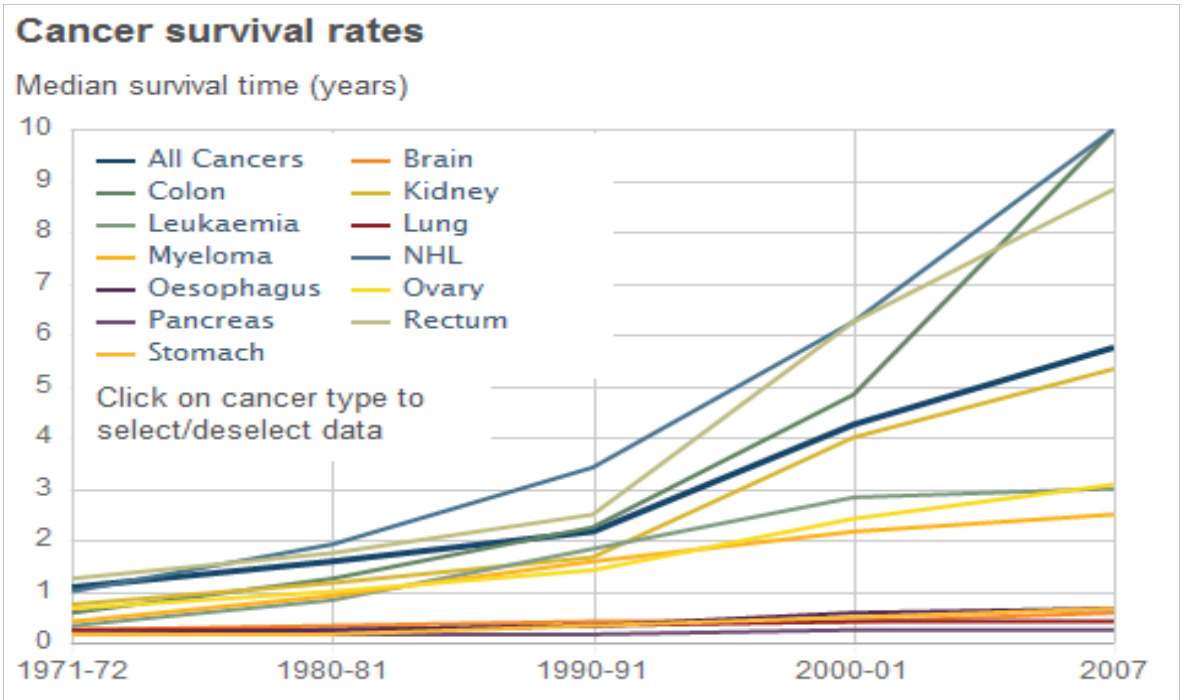

Figure 2: Data provided in the graph are for adults aged 15-99 diagnosed in England and Wales which predicts the survival estimates. Brain tumour shows insignificant increase in the median survival rate over three decades (Rachet *et al.*, 2009).

A report by Macmillan Cancer Support stated that over the past three decades, brain tumour treatment has not led to an increase in the survival period of brain tumour patients (Figure 2) (Rachet *et al.*, 2009). The survival of glioma patients is still poor, with pilocytic astrocytoma being an exception. The 5-year survival rate of glioblastoma patients is less than 3 % (Burkhard *et al.*, 2003), and a number of epidemiological studies have revealed that certain occupations have an increased brain tumour risk. However, no epidemiological analyses have led to identification of an environmental carcinogen that could be unequivocally linked to brain tumour development (Ohgaki and Kleihues, 2005).

1.1.1.2 Classification

Based on presumed cell origin, gliomas are classified as astrocytic, oligodendrocytic and mixed gliomas (Louis *et al.*, 2001). The following criteria are used for grading: increase in cellular density, nuclear atypias, mitosis, vascular proliferation and necrosis. Pilocytic astrocytomas are benign and are classified as grade I gliomas. Low-grade (II) or high-grade tumours (III and IV) are diffuse astrocytomas, oligodendrogliomas and oligoastrocytomas, while glioblastomas are grade IV astrocytomas (Louis *et al.*, 2007). Several molecular genetic alterations have been characterised in gliomas in the past years. Molecular profiles have been associated with specific histological and prognostic tumour subgroups, contributing to improve the classification of gliomas. At least two alternative molecular pathways have been suggested in the astrocytoma progression involving TP53 inactivation (secondary glioblastomas) and EGFR amplification (*de novo* glioblastomas) (Frankel *et al.*, 1992; Biernat *et al.*, 1995). Oligodendroglial tumours have demonstrated recurrent combined loss of chromosome 1p/19q, which represent a favourable prognosis

marker and probably a predictor of a good chemosensitivity of the tumour (Hoang-Xuan *et al.*, 2005).

In adults, the most frequently encountered tumours are high-grade or malignant neoplasms of astrocytic and oligodendrocytic lineage (Burton and Prados, 2000). Malignant gliomas are the most common primary CNS tumours (Zhu *et al.*, 2005) and in spite of intensive clinical investigation and many therapeutic approaches, the treatment for primary brain tumours remains inadequate (Kim and Glantz, 2006). The WHO system further grades these on the basis of histological degrees of malignancy with grade I being the least malignant to grade IV being the most malignant (Louis *et al.*, 2001). Low-grade tumours (grade I and II) are usually circumscribed and grow slowly over a period of time while high-grade tumours (grade III and IV) are comparatively aggressive having poor prognosis. Some of the low-grade gliomas undergo malignant transformation to high-grade neoplasms with age, lifestyle and time. Glioblastoma multiforme (GBM) and anaplastic astrocytoma (AA) are the most malignant and aggressive high-grade gliomas (WHO grade IV and III respectively), having a combined incidence of 5-8/100,000 population (Koukourakis *et al.*, 2009). WHO revised the classification and added three new tumours in 2007: angiocentric glioma (AG), pilomyxoid astrocytoma (PMA) and pituicytoma (table 1) (Louis *et al.*, 2007; Brat *et al.*, 2007).

Table 1: WHO classification of glioma (Louis *et al.*, 2007).

WHO Grade / Tumour type	Grade I	Grade II	Grade III	Grade IV
Astrocytic Tumours	Pilocytic astrocytoma	Pilomyxoid astrocytoma, Diffuse astrocytoma	Anaplastic astrocytoma	Glioblastoma Multiforme
Oligodendroglial Tumours		Oligodendroglioma	Anaplastic oligodendroglioma	
Ependymal tumours	Subependymoma	Ependymoma	Anaplastic ependymoma	
Mixed and other common types of glioma	Angiocentric glioma, pituicytoma	Oligoastrocytoma	Anaplastic oligoastrocytoma	

1.1.1.3 Diagnosis of glioma

Patients with malignant gliomas have to undergo tissue diagnosis to undertake further clinical management. The tumours are visualised by Magnetic Resonance Imaging (MRI) scanning using an intravenous contrast dye while the grade and type of tumour can be identified using magnetic resonance spectroscopy (MRS) (Shah *et al.*, 2006). Optical methods like confocal imaging, multi-photon imaging and microscopic imaging are also being used in current cancer research. These imaging techniques usually do not validate the diagnosis with certainty, and therefore the gold standard for diagnosis is a brain biopsy. The microscopic appearance of biopsied tissue, with the help of special tissue stains, usually yields a definitive diagnosis (Nikiforova and Hamilton, 2011). Diagnosis of high-grade glioma is usually made through a Computed Tomography (CT) scan or MRI. With the help of a CT and MRI scan, the tumour can be detected as well obtaining information on size, location, morphology and spread of the tumour. The diagnosis is then established and the

tumour is classified histologically, either at the time of surgical resection or by a single-event biopsy if surgery is not possible. There is a growing understanding of the molecular genetics of gliomas, which allows a more accurate classification of glioma to take place and may give an indication of prognosis and likely response to treatment.

Glioblastoma multiforme is diagnosed by a fine needle aspiration biopsy (Schultz *et al.*, 2005), whilst histological diagnosis of gliosarcoma is confirmed on the presence of tissue with gliomatous or mesenchymal differentiation as well as reticulin formation (Hoang-Xuan *et al.*, 2005; Boerman *et al.*, 1996; Reis *et al.*, 2000). Oligodendroglioma is diagnosed histologically on the presence of mild to moderate glial neoplasms with no or low mitotic activity (Kleihues and Cavenee, 2000). Also, further research on the diagnosis of gliomas is being done by designing immunotherapeutic strategies based on pharmacogenomic findings (Yamanaka and Itoh, 2007).

1.1.1.4 Treatments for glioma

Gliomas are among the most common brain tumours leading to mortality, since they are difficult to treat. On diagnosis of glioma, the standard form of treatment consists of maximal surgical resection of the tumour, radiotherapy and concomitant and adjuvant chemotherapy. This treatment is standard because of major challenges like tumour heterogeneity, location of the tumour (as it can be beyond the reach of surgical intervention) and rapid, aggressive tumour relapse, therefore success of therapy depends on the grade of the tumour, extent of surgical tumour removal, location and age. Recurrent gliomas can be treated by surgery in appropriate patients, since low grade tumours are less likely to resurface, while older patients are treated with less aggressive therapy like radiation etc. Surgery cannot be used to treat glioma developed in the brain stem since it is

too delicate to be operated on (Barnet, 2007). High grade tumours are treated with surgery followed by radiotherapy as this treatment pattern helps to control the growth, spread and symptoms of the tumour. Long courses of radiotherapy are not suitable for patients who are not fit or do not take enough self-care, and these patients may be offered a short course of palliative radiotherapy or conformal radiotherapy in which the radiation beam is shaped to fit the tumour (Chang *et al.*, 2005).

Surgery and radiation continue to be the prime modalities of therapy for malignant brain tumours. However, chemotherapy is another option for the treatment of glioma, but the role of such a therapy in malignant gliomas has been inconclusive (Kim and Glantz, 2006). Nevertheless, a phase II study of bevacizumab plus temozolomide (TMZ), during and after radiation therapy for patients with newly diagnosed glioblastoma multiforme, showed a significant survival benefit over radiation therapy alone (Lai *et al.*, 2011).

1.1.1.4.1 Surgery

The role of surgery in the treatment of malignant gliomas includes establishing a pathological diagnosis, relief of mass effect, and cytoreduction (Laws *et al.*, 2003; Rampling *et al.*, 2004). The indications for surgical intervention can be divided into practical and theoretical considerations. The practical indications are: to obtain a histological diagnosis, given the lack of absolute specificity of modern radiographic imaging; to improve neurologic symptoms and/or signs in patients for whom the mass effect of their tumour, and its surrounding oedema, is a direct cause of disability; to delay the onset of new symptoms; and to improve survival by removing immediately life-threatening lesions. Theoretical indications for surgical intervention are controversial but are generally thought to improve the patient's response to adjunctive or combination

chemotherapy and include removal of poorly oxygenated and radiation-resistant tumour cells, the removal of poorly vascularised regions of the tumour that are sequestered from systemic chemotherapy on the basis of marginal blood supply, and the overall reduction of tumour cells that have the potential to proliferate (DeAngelis *et al.*, 2002).

1.1.1.4.2 Radiation

The most important achievement of radiation therapy is to specifically kill tumour cells in order to leave normal brain tissues unharmed (Shaw *et al.*, 2006). Multiple treatments of standard-dose "fractions" of radiation are applied to the brain in a standard external beam radiation therapy. Unfortunately, each treatment leads to the destruction of the healthy as well as normal tissue. Until the next treatment, most of the normal cells have managed to repair any damage caused, while the tumour tissue is unable to repair the damage as quickly as the normal tissue. This particular procedure is repeated at least 10 to 30 times depending on the type of tumour and such extra treatment gives some patients improved results and longer survival rates (Fisher *et al.*, 1998). Even though survival in patients with malignant gliomas remains restricted, there is optimism with the emergence of such treatment strategies (Avgeropoulos and Batchelor, 1999).

1.1.1.4.3 Chemotherapy

Chemotherapy refers to drugs used for cancer treatment. Irrespective of treatment with surgery and radiotherapy, their unavoidable recurrence makes high-grade gliomas the most devastating neoplasms leading to death. Since the late 1970s, various randomised clinical trials have also tried to evaluate the role of adjuvant chemotherapy in the improvement of survival for glioma patients, but such studies still remain inconclusive (Lonardi *et al.*, 2005).

Chemotherapy is a form of systemic treatment in which the drugs travel through the body to reach the cancer cells. There are numerous drugs which are used as chemotherapeutic agents to treat the many cancers which exist, and these drugs can be used alone or can be coupled and used in combination with other drugs or even other treatments (Sersa *et al.*, 2008).

Chemotherapy is a systemic treatment, unlike radiation and surgery which target the tumour directly, and hence these are termed local treatments. They act in one specific area like the breast, lung or prostate. Research on this subject is growing rapidly and more and more drugs are becoming available. For an anti-cancer drug to be effective, it must satisfy numerous features, such as: the drug must reach the cancer cells; sufficiently toxic amounts of drug (or its active metabolite) must enter the cells and remain there for a long enough period of time; the cancer cells must be sensitive to the effects of the drug, and all this must occur before resistance emerges (Galanis and Buckner, 2000). In addition the patient must be able to withstand the adverse effects of treatment.

One of the first promising compounds identified as useful anti-cancer chemotherapeutic agents were the alkylating agents with their distinctive property of adding alkyl groups to the DNA in tumour cells, thus forming a variety of interstrand cross-links (Espinosa *et al.*, 2003). These adducts cause alterations in the DNA's structure and interfere with DNA transcription and replication thus leading to growth inhibition of tumour cells (Schilsky, 1996). These drugs are most effective on rapidly proliferating cells and are independent of the mitotic rate of the tumour (Newton, 2006). Temozolomide, nitrosourea compounds, such as ACNU (nimustine), BCNU (carmustine), and CCNU (lomustine), have been successfully used as single agents as well as in various

combinations in the salvage treatment of gliomas as they are highly lipid soluble and readily cross the BBB. Conversely, cisplatin and carboplatin are platinum based drugs which are water-soluble alkylating (methylating) agents and are given via intra-arterial or intravenous routes (Bernstein and Berger, 2008). They cause DNA damage via intrastrand crosslink formation and chelation. Their penetration through the BBB is restricted due to their water soluble nature; cisplatin is almost never used on its own and is mostly given in combination with other drugs because of its toxic nature, which may result in renal failure, peripheral neuropathy and hearing loss (Brown, 2004).

In the current study, privileged indoles were tested on various glioma cell lines. These indoles were tested in comparison with commercially used drugs so that the dosage and the minimum/maximum time for treatment could be estimated and compared. For that reason, various commercially available drugs such as cisplatin, temozolomide, gemcitabine, carmustine and etoposide were tested and compared on both the 1321N1 and U87MG glioma cell lines.

1.2 Small molecules

All the indoles screened in the current study have molecular weights lower than 351 g/mol and therefore come under the category of small molecules according to the upper molecular weight limit (800 g/mol) for a compound to be termed a small molecule (Surhone *et al.*, 2010). All the compounds tested in this study, excluding the antimicrobial peptide, follow one of the most important rules in drug development; Lipinski's “Rule of Five”. It is a well-established rule of thumb used to determine if a chemical compound with specific biological or pharmacological activity has certain properties that would make it an

orally active drug. This rule was formulated by Christopher A. Lipinski in 1997, based on the observation that most medicines are relatively small and lipophilic molecules (Lipinski *et al.*, 2001). This rule describes the molecular properties which are important for a drug to possess suitable pharmacokinetics in the human body, including their absorption, distribution, metabolism, and excretion (ADME) (Lipinski *et al.*, 2001). However, the rule does not predict if a compound is pharmacologically active. Lipinski's rule states that, in general, an orally active drug has no more than one violation of the following criteria:

- Not more than 5 hydrogen bond donors (nitrogen or oxygen atoms with one or more hydrogen atoms attached)
- Not more than 10 hydrogen bond acceptors (nitrogen or oxygen atoms)
- A molecular mass less than 500 g/mol
- An octanol-water partition coefficient, log P, not greater than 5

The origin of the term “Rule of Five” is that all the numbers above are multiples of five. The rule is important for drug development where a pharmacologically active lead structure is optimised gradually for amplified activity and specificity, as well as drug-like properties such as lipophilicity, solubility, permeability, chemical and metabolic stability (Oprea *et al.*, 2001).

1.2.1 Indoles

Indoles are natural compounds that are found in many plants, but particularly those associated with cruciferous vegetables such as broccoli, cauliflower, cabbage and Brussels sprouts. Indoles are of great interest to the pharmaceutical industry, and at the present time several thousand specific derivatives are reported annually. Chemically, indoles (Figure 3)

are aromatic heterocyclic organic compounds which contain an indole ring; a bicyclic structure, involving a six-membered benzene ring fused to a five-membered nitrogen-containing pyrrole ring (Sundberg, 1996).

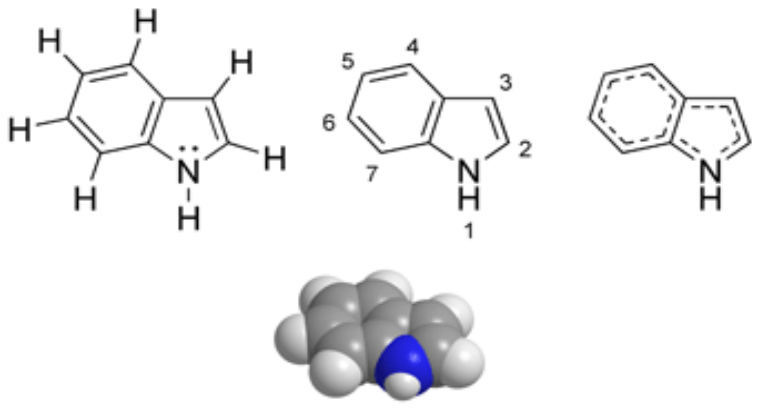

Figure 3: Different representations of the chemical structure of indole.

1.2.1.1 History

The first preparation of indole dates from 1866 and certain indole derivatives were vital dyestuffs until the end of the 19th century. Indole chemistry started developing with the study of the dye indigo, and in 1866, Adolf von Baeyer reduced oxindole to indole using zinc dust and proposed a formula for the product (Figure 4) (Baeyer and Emmerling, 1869). In the 1930s, interest in indole strengthened when it was identified that the indole nucleus is present in numerous alkaloids, tryptophan and auxins (VanOrder and Lindwall, 1942).

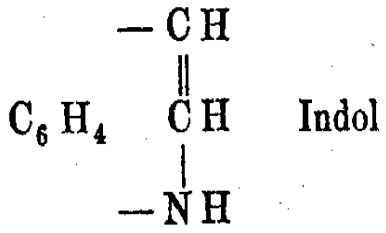

Figure 4: Baeyer's original structure for indole (Baeyer and Emmerling, 1869).

1.2.1.2 Synthesis

Fischer's indole synthesis remains the most versatile method for preparing indoles and was first reported in 1883 (Sumpter and Miller, 1954). The principal commercial source of indole is extraction from coal tar, even though the feasibility of industrial synthesis from starting materials such as aniline and ethylene glycol, N-ethylaniline or 2-ethylaniline has been demonstrated (Sundberg, 1996).

1.2.2 The importance of the indole motif in drug design

Substituted indoles and related structures are known to exhibit potent anti-cancer activity against human breast cancer cell lines (Wang *et al.*, 2006; Brew *et al.*, 2009) and it has also been observed that indoles possess a wide range of biological activity in different therapeutic areas (Joshi and Chand, 1982). Moreover, various commercially available anti-cancer drugs such as indole-3-carbinol (I3C), vinblastine, vincristine and sunitinib contain an indole ring, indicating that the indole nucleus may be one of the important subunits for the above mentioned compounds' anti-tumour activities to exist. As a result, a considerable amount of research is currently taking place on numerous indole derivatives and their potential anti-cancer activities are being evaluated (Chao *et al.*, 2007; Aronchik *et al.*, 2012; Nguyen *et al.*, 2010). Having such precedent, in the current study it was decided to investigate the effects of structurally similar substituted indoles on human glioma cell lines

1321N1 and U87MG which act as models for glioma and which, to date, have not been extensively studied to ascertain their effects with indoles. Below are the key aspects which were considered when selecting indole derivatives as novel compounds to be used in this study.

1.2.2.1 Biological activity

The synthesis and reactivity of indole derivatives has been a topic of research importance for more than a century. The primary reason for this continued interest is the wide range of biological activity found among indoles (Joshi and Chand, 1982). For example, the indole ring appears in the amino acid tryptophan, and metabolites of tryptophan are vital in the biological chemistry of both animals and plants. 3-(2-Aminoethyl)-5-hydroxyindole (serotonin) is the key neurotransmitter in animals (Osborne *et al.*, 1982), while indole-3-acetic acid is the most abundant and basic auxin natively occurring and functioning in plants, generating the majority of auxin effects in intact plants (Sundberg, 1996). The indole nucleus is also found in several natural products such as the catharanthus alkaloids, which are well-established mitotic inhibitors (Brancale and Silvestri, 2007; De Martino *et al.*, 2006; Jordan and Wilson, 2004), and the marine alkaloid eudistomin K, which has been shown to have an *in vitro* IC_{50} = 0.01 g/mL against the tumour P-388 mouse leukaemia cell line (Gul and Hamann, 2005; Lake *et al.*, 1989).

The search for specific agonists and antagonists of the receptors for these and other indole metabolites has been an active pursuit of pharmaceutical chemistry for nearly half a century, and not surprisingly, since the indole ring also appears in several natural products such as indole alkaloids (Southon and Buckingham, 1989), fungal metabolites (Horakova and Betina, 1977) and marine natural products which have potent biological activities

(Christophersen, 1983). The dimeric indole vinca alkaloid, vincristine, and closely related compounds, were among the first of the anti-mitotic class of chemotherapeutic agents for cancer (Brossi, 1992), and likewise, the anti-tumour antibiotic mitomycin C, which after bio-reductive activation, forms inter- and intra-strand cross-links with DNA, contains an oxidised indole nucleus (Tomasz, 1995).

1.2.2.2 Indoles in cancer

Privileged structures represent various classes of different molecules which are known to bind to multiple receptors with high affinity. As such, the study of these molecules in drug discovery is rapidly emerging in medicinal chemistry, especially since it is considered that such privileged structures could allow medicinal chemists to discover biologically active compounds, across a broad range of therapeutic areas, in a reasonable time scale (Horton *et al.*, 2003). As alluded to above, one such class of privileged structures is the indole class, and because of its presence in a broad range of pharmacologically active molecules, it has been proposed that indoles possibly represent the most important of all structural classes in drug discovery (Horton *et al.*, 2003; Joshi and Chand, 1982). As a result, it is predictable that the indole motif will have made its way into clinically useful drugs, and discussed below are the various commercially available drugs and indole derivatives currently being used/developed for the treatment of cancer.

1.2.2.2.1 Indole-3-carbinol

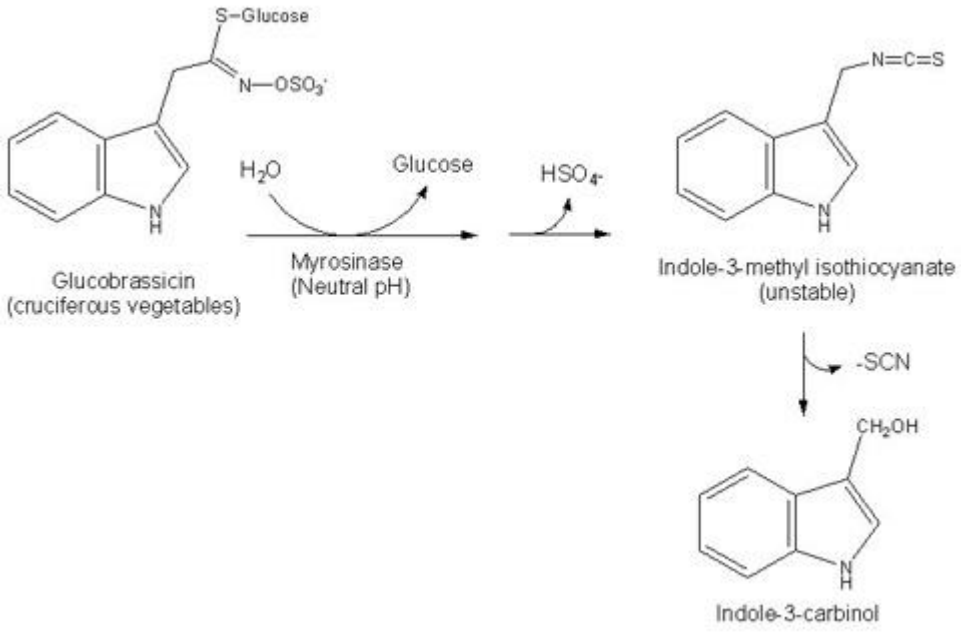

Figure 5: Formation of indole-3-carbinol. (Available at http://lpi.oregonstate.edu/infocenter/phytochemicals/i3c/fig1.html).

Indole-3-carbinol (I3C) is an alkaloid with an indole core, and it is found in some fruits and vegetables, including members of the cruciferous family and, in particular, members of the genus *Brassica* (Higdon *et al.*, 2007). It is derived from the hydrolysis of glucobrassicin, a glucosinolate, which is predominant in brassica vegetables, it is synthesized from indole-3-glucosinolate by the action of the enzyme myrosinase (Verhoeven *et al.*, 1997) (Figure 5). The stability of glucosinolates is heavily influenced by external factors and therefore the amount of I3C formed from glucobrassicin in foods is variable and relies on the processing and preparation of those foods. Its anti-tumour effects in experimental animals (Oganesian *et al.*, 1997; Jin *et al.*, 1999; Kojima *et al.*, 1994) and humans (Wong *et al.*, 1997; Yuan *et al.*, 1999) are well documented, and previous studies have shown that I3C activates specific transcriptional factors, signal transduction, and metabolic cascades that lead to cell cycle arrest, apoptosis, down-regulation of cancer cell

migration, and modulation of hormone receptor signaling (Aggarwal and Ichikawa, 2005; Safe *et al.*, 2008; Kim and Milner, 2005; Firestone and Bjeldanes, 2003; Sundar *et al.*, 2006). Indole-3-carbinol, in the acidic environment of the stomach, dimerizes to form a complex mixture of biologically active compounds, identified collectively as acid condensation products (Shertzer and Senft, 2000). The most important one is the dimer, 3,3'-diindolylmethane (DIM), which is readily detectable in the liver and feces of rodents that are fed I3C (Grose and Bjeldanes, 1992) (Figure 6).

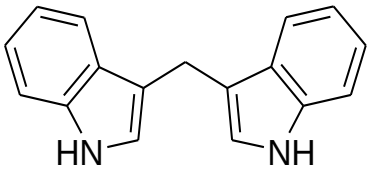

3,3'-Diindolylmethane (DIM)

Figure 6: The structure of DIM.

Previous studies on I3C and its dimeric product, DIM, suggest that these compounds exhibit the ability to regulate multiple cellular signaling pathways, including the PI3K/Akt/mTOR signaling pathway (Rahman and Sarkar, 2005; Wang *et al.*, 2008) which is responsible for regulating apoptosis, and therefore may be important in controlling cancer. These natural compounds are also active modulators of downstream transcription factor nuclear factor kappa-light-chain-enhancer of activated B cells (NF-κB) signaling which might help explain their ability to inhibit angiogenesis and reverse the epithelial-to-mesenchymal transition (EMT) phenotype (Ahmad *et al.*, 2013). Since the structure of I3C is almost exclusively indole itself, with only the pendant methane chain extra, its biological activity is almost certainly related to this important privileged motif.

1.2.2.2.2 Sunitinib

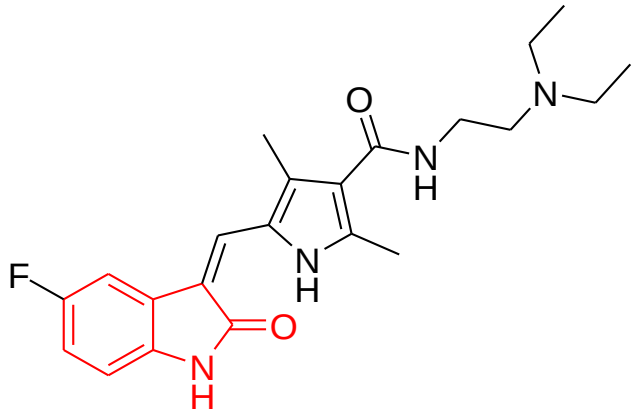

Figure 7: Structure of sunitinib with the 2- indolinone (indole-like) core highlighted.

Sunitinib (Sutent™, Pfizer) (Figure 7), previously known as SU11248, is an orally available, small-molecule, which targets multiple tyrosine kinases and was approved by the United States Food and Drug Administration (USFDA) for the treatment of renal cell carcinoma and imatinib-resistant gastrointestinal stromal tumour in 2006 (FDA, 2006). It was the first cancer drug simultaneously approved for two different cancers i.e., renal cell carcinoma and imatinib-resistant gastrointestinal stromal tumour. The simultaneous inhibition of its target kinases leads to decreased tumour vascularisation and cancer cell death. A recent study showed that sunitinib could induce apoptosis in glioblastoma multiforme (GBM) cells (Joshi *et al.*, 2012), and accordingly it has been studied in more than 435 clinical trials for various cancers and its phase II trials for recurrent anaplastic astrocytoma and GBM has just been completed (Clinicaltrials.gov, 2013). However, importantly, its improved biological activity over the related compound, imatinib, can be associated with this indole like structural motif, since such a core is not present in imatinib.

1.2.2.2.3 Enzastaurin

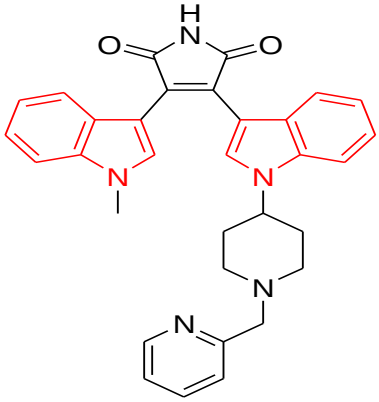

Figure 8: Structure of enzastaurin with the two indoles highlighted.

Enzastaurin (LY317615.HCl) (Eli Lilly), (Figure 8) is a novel, synthetic, acyclic *bis*indolylmaleimide anti-angiogenic and anti-neoplastic agent which acts by inhibiting protein kinase C (PKC) (Chen and LaCasce, 2008), and a notable feature of its structure is that it contains two indoles in its core. Enzymes of the PKC family regulate various cellular functions such as cell growth, tumour cell proliferation and apoptosis (Parker, 1999) and it has been suggested that PKC-β is the major mediator of vascular endothelial growth factor (VEGF)-induced cell proliferation (Takahashi *et al.*, 1999). Moreover, enzastaurin acts as a selective inhibitor of PKC-β resulting in the blockade of the VEGF pathway and the intracellular Akt signalling (Graff *et al.*, 2005); it has direct anti-cancer activity either alone or in combination with other anti-neoplastic agents (Dreicer *et al.*, 2013).

1.2.2.2.4 Cediranib

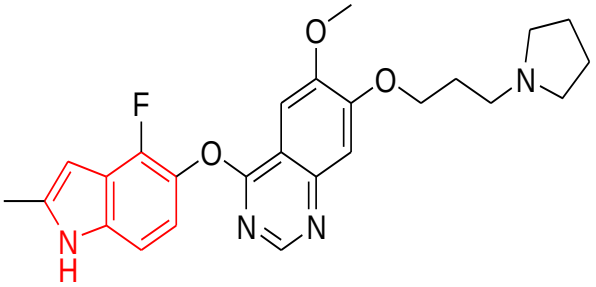

Figure 9: Structure of cediranib with the indole core highlighted.

Cediranib (AZD2171) (Recentin^{TM}, AstraZeneca) (Figure 9) is a potent small molecule TKI of VEGFRs, which also targets c-KIT (stem-cell factor) and platelet derived growth factor receptor-α (PDGFR-α) (Wedge *et al.*, 2005; Brave *et al.*, 2011) and it is an indole-ether quinazoline derivative with potent anti-cancer activities. Research has shown promising results in glioma treatments, leading to a 6-month progression-free survival in phase II clinical trials (Batchelor *et al.*, 2010). The effectiveness of cediranib has been associated with its anti-angiogenic properties and the ability to normalise tumour vasculature and alleviate oedema in glioma patients (Kamoun *et al.*, 2009). Regardless of the potential this agent holds for the treatment of glioma, the identification of biomarkers for response prediction to its therapy is still a major issue that needs to be addressed (Martinho *et al.*, 2013), a limitation that could be solved by developing new compounds for the treatment of this disease.

1.2.2.2.5 Vinblastine

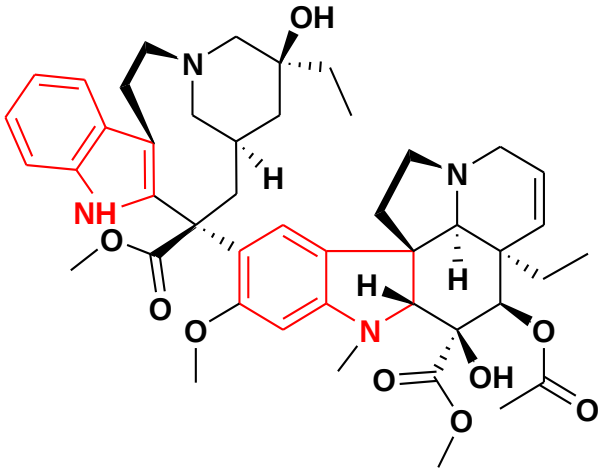

Figure 10: Structure of vinblastine with the two indoles highlighted.

Vinblastine (Velbe®, Genus Pharmaceuticals) (Figure 10), is a microtubule inhibitor of the vinca alkaloid class and is used to treat various kinds of cancers, such as non-small cell lung cancer, head and neck cancer, testicular cancer, breast cancer and Hodgkin's lymphoma (Evans, 2009). The vinca alkaloids are just some of the *bis*-indole alkaloids which are known to possess anti-cancer activity by inhibiting mitosis and microtubule formation (Evans, 2009). Research has shown that treatment of cells with vinblastine causes M-phase specific cell cycle arrest by disrupting microtubule assembly, improper formation of the mitotic spindle and the kinetochore (Jordan *et al.*, 1992). Both of these factors are essential for the separation of chromosomes during anaphase of mitosis. While many microtubule-targeting agents can either inhibit or promote microtubule polymerization, vinblastine can accomplish both of these functions. For example, at low concentrations (<100 nM), vinblastine inhibits the exchange of tubulin subunits at the plus ends of microtubules, effectively stabilizing its dynamics. At medium concentrations (100 nM – 1 μM), vinblastine promotes depolymerisation of microtubules, while at higher concentrations (>1 μM), it causes the formation of tubulin paracrystals (Jordan *et al.*,

1992); the result of disrupting the microtubule dynamics is usually apoptosis and cell death, therefore such compounds are currently of high interest in the development of new cancer treatments.

1.2.2.2.6 Vincristine

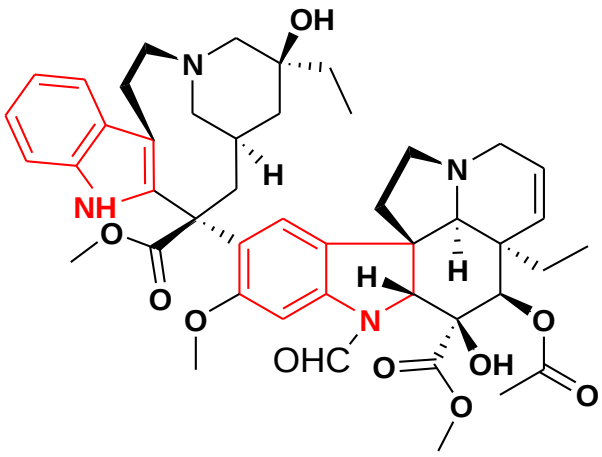

Figure 11: Structure of vincristine with the two indoles highlighted.

Vincristine (Oncovin ®, Genus Pharmaceuticals) (Figure 11), is also a vinca alkaloid and is therefore structurally similar to vinblastine. It is formed by the coupling of the indole alkaloids vindoline and catharanthine in the vinca plant, and it too causes mitotic inhibition which is beneficial for cancer chemotherapy (Evans, 2009). Vincristine binds to tubulin dimers, inhibiting the assembly of microtubule structures and arresting mitosis in metaphase (Owellen *et al.*, 1972).

1.2.2.2.7 1-Benzyl-indole-3-carbinol

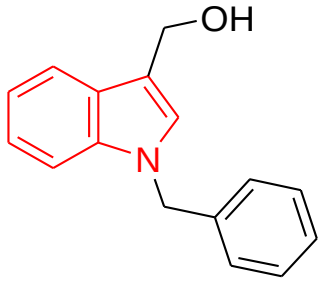

Figure 12: Structure of 1-benzyl-indole-3-carbinol with the indole core highlighted.

1-Benzyl-indole3-carbinol (Figure 12) is a new and significantly more potent I3C analogue. A recent study reported that 1-benzyl-I3C is the most effective synthetic derivative of I3C to date (Aronchik *et al.*, 2012; Nguyen *et al.*, 2010), and in comparison to I3C, this novel derivative exhibited *circa* 1000-fold enhanced potency in suppressing the growth of both oestrogen independent (MDA-MB-231) and oestrogen responsive (MCF-7) human breast cancer cells (Nguyen *et al.*, 2010).

1-Benzyl-I3C induces G1 cell cycle arrest at very low concentrations (IC_{50} of 0.05 μM) and causes the key I3C-specific effects on the expression and activity of G1 acting cell cycle genes, including the disruption of endogenous interactions of the Sp1 transcription factor with the CDK6 promoter. It also inhibits the *in vivo* growth of human breast cancer cell-derived tumour xenografts in athymic mice (Nguyen *et al.*, 2010). Since the only treatment options currently available for breast cancer are chemotherapy, radiation therapy, hormone therapy, immune therapy and/or the surgical removal of the breast, the *in vivo* and cellular anti-proliferative properties of 1-benzyl-I3C and the low effective dose makes this novel I3C-derivative a promising drug candidate for its future development as a therapeutic agent for human reproductive cancers, and an attractive lead compound for the treatment of other cancers too.

1.2.2.2.8 SR13668

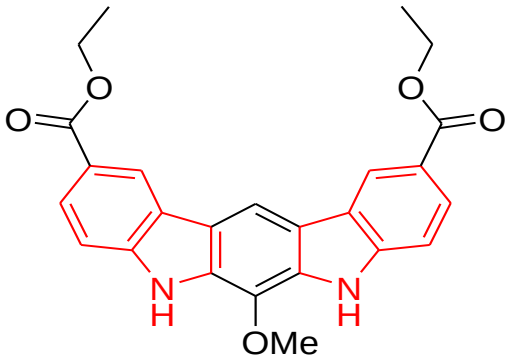

Figure 13: Structure of SR13668 with the two indoles highlighted.

Indole-3-carbinol, is extremely unstable under physiological conditions and upon degradation produces four condensation products, all of which possess anti-cancer activity (Rahman and Sarkar, 2005). Based on this, these four products were used as the starting point to design a novel class of indole analogue in order to find the most potent protein kinase B inhibitor (Akt). SR13668 (Figure 13), the most promising analogue discovered (Chao *et al.*, 2007), is a *bis*-indole with potent *in vitro* and *in vivo* activity against various cancers and promises to be a cancer chemopreventive agent too (Green *et al.*, 2011). It is a serine/threonine Akt inhibitor with potential anti-neoplastic and anti-angiogenic activities and it inhibits the activity of Akt, which may result in the inhibition of the PI3K/Akt signalling pathway and tumour cell proliferation, leading to cellular apoptosis. It has improved *in vitro* and *in vivo* stability and activity in comparison to I3C (Chao *et al.*, 2007) and is not mutagenic (Doppalapudi *et al.*, 2007).

Many more indole containing compounds or indole derivatives are being researched and tested worldwide for various different types of cancer, and if pursued appropriately, this class of compound might open a much needed new avenue for the treatment of glioma.

Having such precedent in support of this current study prompted the testing of indoles for the treatment of glioma, and if successful, to determine their mechanism of action too.

1.2.2.3 Indoles as privileged structures

Privileged structures promise to be an effective approach towards the discovery and optimization of novel compounds. Over the past 20 years the privileged structure concept has arisen as a productive approach towards the discovery of novel biologically active molecules and compounds (DeSimone *et al.*, 2004; Horton *et al.*, 2003). Privileged structures are molecular scaffolds with versatile binding properties, such that a single scaffold is able to provide potent and selective ligands for numerous biological targets through modification i.e. the addition or removal of functional groups. Moreover, privileged structures typically show promising drug-like properties such as greater absorption, distribution, metabolism, and permeability, which in turn lead to more drug-like compound libraries and leads (Horton *et al.*, 2003). The ultimate result is the creation of high quality leads that provide a solid base for further development. The crux of the identification of 'privileged' structures is on highlighting the significance of the structure-target relationships that confer 'privileged' status. This understanding allows 'privileged' structure based libraries to be targeted at distinct target families (e.g. ROS, autophagy, enzymes/kinases).

The 'privileged' nature of the indole-class of compounds suggests that changing the substituents at various positions around the indole nucleus will generate new compounds with diverse biological activities. In this regard, the 2-arylindole class appears to be one of the most promising sub-structures of the indole family which should be researched in more depth for their anti-cancer potential. The 2-arylindole sub-structure has shown tremendous

biological activity across various biological targets and is present in various anti-tumour agents, selective oestrogen receptor modulators (SERM), efflux pump inhibitors and COX-2 inhibitors (Lal and Snape, 2012). For example, 2-aryl-indolyl maleimides have shown potent anti-cancer activity in various *in vivo* and *in vitro* models as protein kinase inhibitors (Hendricks *et al.*, 1995) whilst the 2-arylindole analogue, 4-(3-phenyl-1H-indol-2-yl)benzene sulphonamide, is a potent and selective COX-2 inhibitor (Hu *et al.*, 2003). INF55 (Figure 14), a substituted 2-arylindole, is a known NorA efflux pump inhibitor in *S. aureus* (Samosorn *et al.*, 2006) whilst, bazedoxifene (Figure 14), a SERM, is one of the earliest known examples which shows good receptor binding affinity and mammary tumour inhibition in rats (von Angerer *et al.*, 1984). A previous study also showed that 2-aryl-3-substituted indole derivatives inhibit tubulin polymerisation by binding selectively at the colchicine binding site of tubulin and thus inhibiting the cell cycle at the G2/M phase and inducing apoptosis (Kaufmann *et al.*, 2007). Moreover, in an *in vitro* assay against breast cancer cell lines, these indole derivatives exhibited comparable potency to combretastatin A-4 and vincristine (Kaufmann *et al.*, 2007).

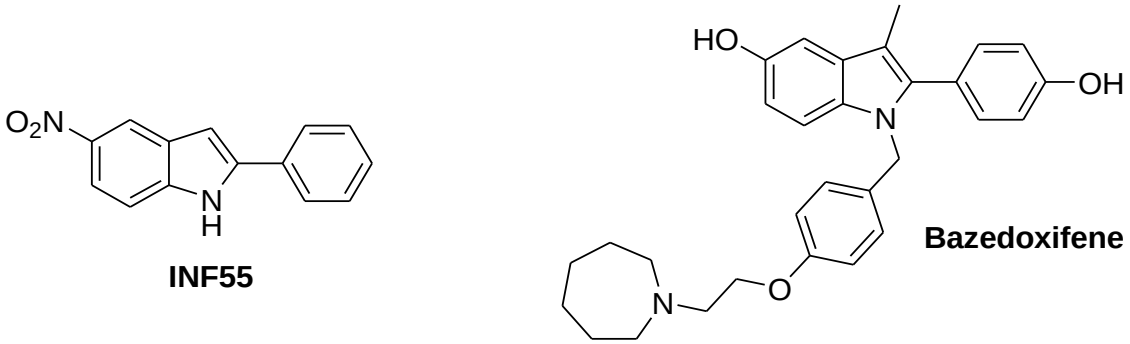

Figure 14: Structure of INF55 and bazedoxifene.

Based on this plethora of indole-based research the indole class of molecules are imaginably the most important class of privileged motif in biology. Even within the

privileged structural class of the indoles, the 2-arylindoles, just a subset, still demonstrate wide-ranging and potent activities. Whether this activity is due to the indole as a whole or due to the aromatic moiety at the 2-position, or a combination of the two, remains to be seen. Having such a precedent generated strong interest in testing 2-arylindoles as a treatment for glioma in this study.

1.3 *Cn*-AMP2; a host defence peptide

In addition to conventional approaches for the development of anti-cancer compounds (i.e. small molecules obeying Lipinski's rules), a number of innovative research initiatives have recently been taken to try and identify alternative natural therapies (Harris *et al.*, 2013b). One such initiative has involved research on host defence peptides (HDPs), which primarily function as innate immune antibiotics but have also been shown to kill cancer cells (Hoskin and Ramamoorthy, 2008; Dennison *et al.*, 2006b; Dennison *et al.*, 2005; Prabhu *et al.*, 2013b). Their anti-cancer activity is facilitated by the fact that, in a similar fashion to microbial cells, cancer cells carry an overall negative charge on their outer surface, thus allowing their targeting by HDPs, which are generally cationic (Harris *et al.*, 2013b; Dennison *et al.*, 2006b). In contrast, around 100 anionic HDPs are known and despite their same charge as the cell membrane, it has recently been proposed that, due to a unique feature of their cell-death mechanism, these peptides could be investigated for their anti-cancer potential (Harris *et al.*, 2013b). In response, the present study has investigated the ability of the HDP, *Cn*-AMP2, from *C. nucifera* (coconuts), to kill cancer cells (Harris *et al.*, 2009b). This peptide was originally isolated from green coconut water, which is the clear liquid inside young coconuts and is a popular drink in the tropics, especially in Tropical Asia and Latin America. Characterisation of *Cn*-AMP2 showed that it has a net

charge of -1, a molecular weight of 1265 g/mol and that it exhibits broad-spectrum anti-microbial activity, which was predicted to involve the adoption of α-helical secondary structure (Pelegrini *et al.*, 2011; Mandal *et al.*, 2009). As such, it was studied here in order to ascertain if it also possesses anti-cancer activity, not least because the molecular weight of this peptide fits nicely between small molecules (molecular weight <800 g/mol – see section 1.2) and mAbs (molecular weight ~150 kDa, of which bevacizumab belongs and is approved for the treatment of various cancers), and thus its study may provide access to further lead compounds with which to develop into useful therapies for glioma.

1.4 Mechanisms involved in cell death

Having outlined the types of compounds of interest to us, it is important to be able to determine the type of cell death occurring and the mechanism of action taking place with any active compounds developed. Knowing such information should therefore aid in the future development of the compounds identified.

Cell death can be classified according to its morphological appearance (which may be apoptotic, necrotic, autophagic or associated with mitosis), enzymological (with and without the involvement of nucleases or of distinct classes of proteases, such as caspases, calpains, cathepsins and transglutaminases) and functional aspects (programmed or accidental, physiological or pathological) (Melino, 2001). A cell should be considered dead when any one of the following molecular or morphological criteria is met: (i) the cell has lost the integrity of its plasma membrane, as defined by the incorporation of vital dyes (e.g., PI and trypan blue) *in vitro*; (ii) the cell, including its nucleus, has undergone complete fragmentation into discrete bodies (which are frequently referred to as ‘apoptotic bodies’);

and/or (iii) its corpse (or its fragments) has been engulfed by an adjacent cell *in vivo* (Kroemer *et al.*, 2009).

Programmed cell-death (PCD) is the death of a cell in any form mediated by an intracellular programme (Engelberg-Kulka *et al.*, 2006), as opposed to necrosis, which is a form of traumatic cell-death that results from acute tissue injury and aggravates an inflammatory response. Type I and Type II PCD are regularly carried out in a regulated process which usually results in an advantage developing during an organism's life cycle. There are three main types of programmed cell death known:

- Apoptosis or Type I programmed cell-death
- Autophagic or Type II programmed cell-death
- Necrosis or Type III programmed cell-death

1.4.1 Apoptosis

The expression ‘apoptosis’ was coined by Kerr *et al.* in 1972, and it is one of the main types of PCD and comprises a series of biochemical events leading to a characteristic cell morphology and death. More precisely, a series of biochemical events that lead to various morphological changes, including changes to the cell membrane, such as loss of membrane integrity and attachment, cell shrinkage, blebbing, nuclear fragmentation, chromosomal DNA fragmentation and chromatin condensation (Keith, 2008). One of the main differences in apoptosis and necrosis is the process of cellular debris disposal whose result does not cause any harm to the organism. Apoptosis, in general, results in advantages during an organism's life cycle as opposed to necrosis which is a form of traumatic cell death resulting from acute cellular injury. For example, the fingers and toes in a developing

human embryo are differentiated because the cells between the fingers apoptose, resulting in separate digits. For an average child between the ages of 8 and 14, approximately 20 to 30 billion cells die per day while 50 to 70 billion cells die per day due to apoptosis in the average human adult. In a year, this accounts for the subsequent destruction and proliferation of a mass of cells equal to an individual's body weight (Mukherjee, 2008).

1.4.2 Autophagy

Autophagy is a highly conserved process of cellular degradation in eukaryotes by which damaged cytoplasmic proteins and organelles are delivered to the lysosome for degradation (Klionsky, 2007). It was originally named as a process of protein recycling and is termed as Type II PCD. The process is characterised by sequestration of bulk cytoplasmic proteins and organelles in autophagic vesicles, and subsequent delivery, to and degradation by, the lysosomal system. The process of autophagy is, in-part, characterised by the formation of acidic vesicular organelles (AVOs) which can be detected and measured by staining with acridine orange (Prabhu *et al.*, 2013a). During autophagy, parts of the cytoplasm or organelles are sequestered into double-membrane structures termed autophagosomes or autophagic vacuoles (Figure 15) (Klionsky, 2007). Two important functions have been suggested for this process. Firstly, autophagy is a short-term stress response to a nutrient starved condition or during amino-acid insufficiency; by degrading the cell's own cytoplasmic components into lysosomes, cells get substrates for both vital protein synthesis and energy metabolism (Meijer and Codogno, 2004). Secondly, autophagy has been proposed to play a role in Type II cell death (Gozuacik and Kimchi, 2004). Cells treated with chemical agents such as arsenic trioxide (Kanzawa *et al.*, 2003; Kanzawa *et al.*, 2005) or cells which overexpress tumour suppressor proteins, such as the

short mitochondrial form of p19^{ARF}, induce an autophagic response that causes cell death (Reef *et al.*, 2006).

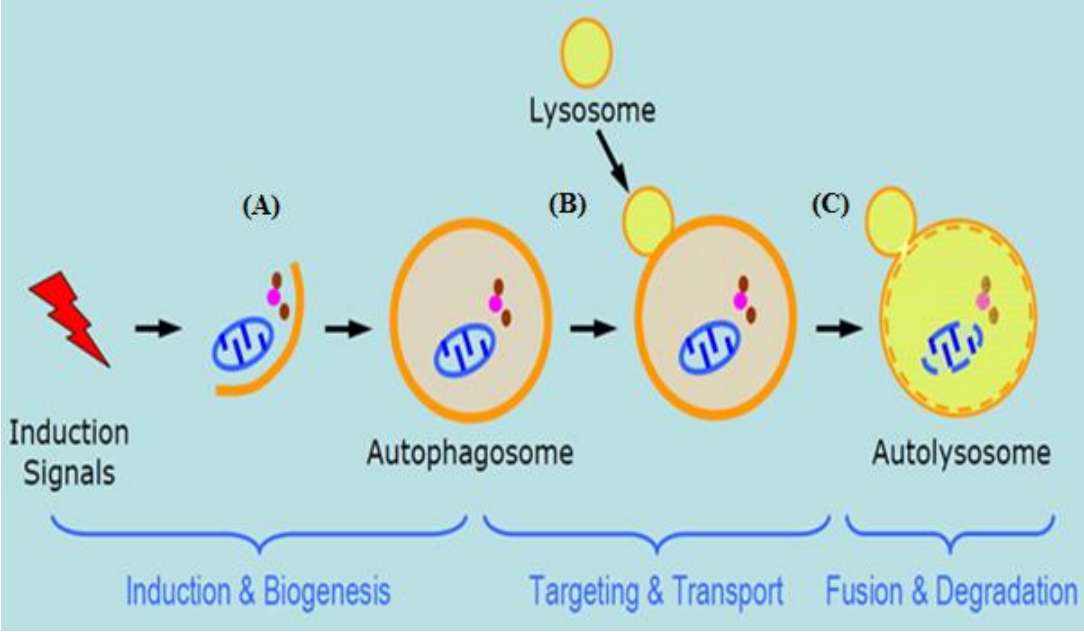

Figure 15: Diagram showing the important steps during autophagy.

(Available at http://www.mc.uky.edu/biochemistry/labs/wang/interests1.htm) (A) Induction of autophagy leads to cytoplasm sequestering into double-membrane structures called autophagosomes, (B) autophagosome fuses in the cytoplasm with a lysosome, and (C) lysosome is converted into an autolysosome where the contents are degraded.

Autophagy has been a topic of great interest for scientists for over 50 years, but has been limited due to the lack of knowledge about the molecular machinery behind this process (Reggiori and Klionsky, 2002), however, extensive research and genetic screens in yeast (*S. cerevisiae*) have led to the identification of over 30 autophagy-related genes (ATG) (Klionsky *et al.*, 2003). Autophagy can be separated into three types viz: macro-autophagy, micro-autophagy and chaperone-mediated autophagy (CMA), these three types vary in their physiological functions and modes of degradation but all have in common the degradation of intracellular components via the lysosome (Maria Cuervo, 2004).

1.4.3 Necrosis

Necrosis, in contrast to apoptosis, which is a naturally occurring cause of cellular death, has been observed to be a form of accidental cell death brought about by injury to the cell by pathogens or toxins (Kroemer *et al.*, 2009). It is caused by factors external to the cell or tissue, such as infection or trauma and is a Type III PCD. Necrosis is almost always unfavourable and can be fatal, in contrast to apoptosis, which often provides beneficial effects to the organism. It is often necessary to remove necrotic tissue surgically by a process known as debridement, because cells undergoing necrotic cell death do not usually send the same chemical signals to the immune system as cell undergoing apoptosis. This prevents nearby phagocytes from finding and engulfing the dead cells, which leads to the deposition of cell debris at or near the site of cell death (Kroemer *et al.*, 2009).

1.5 Hypothesis and aims of the research

Substituted indoles and related structures are known to exhibit potent anti-cancer activity against human breast cancer cell lines (Wang *et al.*, 2006), and various other factors, such as their biological activity, the fact that they are privileged structures, and the presence of the indole nucleus in various commercial anti-cancer drugs, therefore led to the choosing of indoles for the current study. As such, it was decided to investigate if there was any anti-cancer activity with indoles against glioma cell lines (1321N1 and U87MG) using a number of different cell-based assays and also comparing them with conventional anti-cancer drugs *in vitro*.

Once lead compounds were identified, the aim would be to optimise their structures and try to determine preliminary structure-activity-relationships and try to find out how

they may be exerting any observed effects. Therefore, various analogues, structurally similar to the potent compounds, would be purchased, or prepared, in an attempt to see if activity could be affected in any way through structural manipulations.

Research has shown that, in general, 2-arylindoles are known to be active in a wide range of therapeutic areas (Horton *et al.*, 2003; Lal and Snape, 2012) and therefore, the structure-activity-relationship screening would be divided into two main categories: indoles without the 2-aryl group and indoles with the 2-aryl group. For clarification, aryl refers to any functional group or substituent derived from a simple aromatic ring, be it phenyl, thienyl, indolyl, etc. The most promising compounds would also be tested on the non-cancerous SVGp12 cell line to check for compound specificity towards cancer cells.

In addition, a separate short study was conducted in response to recent studies at UCLan (Harris *et al.*, 2013b; Harris *et al.*, 2009b) which suggest that anionic host defence peptides (HDPs) may possess anti-cancer potential, and therefore using the assays and expertise developed during the work with indoles, the ability of the plant HDP, *Cn*-AMP2, to kill cancer cells, was investigated on glioma cells lines *in vitro* as well.

Chapter II

2. MATERIALS AND METHODS

2.1 Cell culture

Commercially available glioma cell lines 1321N1 (astrocytoma grade II) and U87MG (astrocytoma grade IV/glioblastoma) were obtained from the European Collection of Cell Cultures (ECACC) while SVGp12, a non-cancerous foetal glial cell line was obtained from the American type culture collection (ATCC). As this project was focussed on finding novel compounds for glioma treatment, the novel compounds used in this study were tested on the 1321N1 and U87MG cell lines since both cell lines were derived from malignant gliomas. SVGp12 being a non-cancerous cell line was used in certain experiments only, to determine the specificity of the compounds towards cancerous cells.

1321N1 is a human astrocytoma cell line isolated in 1972 as a sub clone of the cell line 1181N1 which in turn was isolated from the parent line U-118 MG [one of a number of cell lines derived from malignant gliomas by J. Ponten (Ponten and Macintyre, 1968)]. U87MG was derived from a malignant glioma from a female patient by explant culture. Explant culture is a technique used for the isolation of cells from a piece or pieces of tissue. This is also one of a number of cell lines derived from malignant gliomas by J. Ponten and associates from 1966 to 1969 (Ponten and Macintyre, 1968). The SVGp12 cell line was established by transfecting cultured human foetal glial cells from brain material dissected from 8 to 12 week old embryos with DNA from a Simian vacuolating virus 40 (SV40) and is a non-cancerous cell line. Both 1321N1 and U87MG cell lines exhibit an epithelial morphology (ECACC, UK) while the non-cancerous SVGp12 cell line shows fibroblastic

morphology (ATCC, UK). All the above cell lines used in this study were characterised within the biomedical research unit (BRU) at UCLan and indicated that the above mentioned cell lines were glial and of human origin.

The 1321NI cell line was maintained in Dulbeccos's Modified Eagle's Medium (DMEM) supplemented with 10 % (v/v) FBS and 2 mM L-glutamine, while the U87MG and SVGp12 cell lines were maintained in Essential Minimum Eagle Medium (EMEM) supplemented with 10 % (v/v) FBS, 2 mM L-glutamine, 1 mM sodium pyruvate and 1% (v/v) non-essential amino acids (NEAA) (Lonza, UK). Short-term glioma cell cultures derived from surgical biopsies from patients with WHO grade IV astrocytoma designated as IN859 was generously given by Professor Tim Dawson from the Royal Preston Hospital. The primary cell line was maintained in Ham's F-10 medium supplemented with 10% (v/v) FBS. All the cell lines were cultured in 75 cm^2 tissue culture treated flasks (Thermo Scientific Nunc, UK) and maintained in a 37°C humidified incubator supplied with 5% CO_2. For all the experiments, each of the glioma cell lines were used between passages 2-20 while the primary cell line was used between passages 3-7.

Table 2: Media, reagents, supplements and storage conditions.

Reagents	Abbreviations and storage temperature	Formulations	Suppliers
Dulbecco's modified eagle's medium	DMEM, 2-8 °C	25 mM HEPES, 1.0 g/l glucose, 1.0 mM sodium bicarbonate, 0.011g/l phenol red.	Lonza, UK
Eagle's minimum essential medium	EMEM, 2-8 °C	10 mM HEPES, 4.5 g/l glucose, 2.0 g/l sodium bicarbonate, 1.0mM sodium pyruvate, 0.0053 g/l phenol red.	Lonza, UK
Foetal bovine serum, Australian origin foetal bovine serum (for primary cells)	FBS, -20 °C	Heat inactivated FBS.	GIBCO, UK
L-glutamine	-20 °C	200 mM L- glutamine.	Lonza, UK
0.5% Trypsin-EDTA (10x)	-20 °C	0.21 mM trypsin, 146 mM sodium chloride, 4.8 mM EDTA	Gibco, UK
Non essential amino acid	2-8 °C	100 X non-essential amino acid.	Lonza, UK
Phosphate buffer saline (PBS, 1x)	2-8 °C	8 g/l NaCl, 0.2 g/l KCl, 1.44 g/l Na_2HPO_4 0.24 g/l KH_2PO_4.	Fisher, UK
Trypan blue (0.4 %)	Room temperature	0.81 % sodium chloride, 0.06 % potassium phosphate, dibasic	Sigma, UK
Dimethyl sulfoxide	DMSO, Room temperature	99.5 % dimethyl sulfoxide, 0.81 % sodium chloride	Sigma, UK
Ham's F-10 medium	2-8 °C	20 mM HEPES, 1.2 g/l sodium bicarbonate	Sigma, UK
Hank's balanced salt solution	HBSS, 2-8 °C	1 mM calcium chloride, 0.49 mM magnesium chloride, 0.40 mM magnesium sulfate, 5.3 mM potassium chloride, 0.44 mM potassium phosphate monobasic, 4.1 mM sodium bicarbonate, 138 mM sodium chloride, 0.34 mM sodium phosphate dibasic, 5.5 mM D-glucose	Gibco, UK

2.1.1 Thawing cryopreserved cells

The cryopreserved cells were fragile and required careful handling. These cells were thawed as quickly as possible and plated into the fresh growth medium. However, if the cells were sensitive to the cryopreservative like DMSO, they were centrifuged before plating so as to remove the cryopreservative. In this study, the culture medium was pre-warmed to 37°C and 10 ml of it was pipetted into the 75 cm^2 culture flasks per 1 ml of frozen cells. Cryovials were removed from liquid nitrogen and quickly defrosted in a 37°C water bath. Once thawed, the vials were sprayed with 70 % ethanol and the contents of the vial directly transferred into fresh media contained in a culture flask, in the laminar flow hood. After 12-24 h of incubation the medium was replaced with fresh growth medium to remove the cryopreservative.

2.1.2 Subculture

Once the cells achieved 70-80% monolayer confluency they were sub cultured/passaged in a laminar flow hood to maintain sterile conditions and to avoid contamination. The respective culture medium for the cell line to be passaged, phosphate buffered saline (PBS), and trypsin (all sterile) were all pre-warmed in the 37°C water bath for about 30 min to equilibrate the temperature. The medium from the flask to be passaged was aspirated and the flask was washed with PBS (5 ml for 75 cm^2 and 2 ml for 25 cm^2 flasks) to remove any trace of serum from the cells. The PBS was then removed and 1X trypsin was added to the flask (2 ml for 75 $cm^2$and 1ml for 25 cm^2 flasks) and incubated at 37°C for 2-5 min to detach the adherent cells. After 5 min the flask was viewed under the inverted light microscope to check for the detachment of cells and was tapped gently to aid removal. To this trypsinised flask, 2 ml of the respective culture medium was then added to

neutralize the trypsin reaction and prevent any damage to the cell membranes. The medium was pipette mixed to break down any large cell clumps and the cell suspension was transferred to a 15 ml centrifuge tube (Fisher Scientific, UK). The cell suspension was centrifuged at 1000 rpm for 5 min and the supernatant was then carefully aspirated, leaving a small amount of medium above the pellet. The pellet was then flicked, resuspended in the appropriate volume of respective medium and mixed well to obtain a homogenous and evenly distributed cell suspension. Cell viability was determined by staining cells with trypan blue (Sigma-Aldrich, UK) and the cell count monitored using a Neubauer Haemocytometer. The cells were then re-cultured at a cell density of $5x10^5$ cells/ml in a 75 cm^2 flask containing 10 ml of fresh medium to maintain a working stock.

2.1.3 Cell Counting

Once the cells were trypsinised, a volume of 50 µl of cell suspension was pipetted into a sterile eppendorf. To this suspension another 50 µl of trypan blue (Sigma Aldrich, UK) was added. Trypan blue staining helps in counting the number of dead cells. The live cells do not take up the stain while the dead cells are stained blue in colour and this can also be used as an assay (section 2.3.3) to detect the anti-cancer activity of potential compounds. On the Neubauer Haemocytometer (Figure 16A), a cover slip was attached onto the slide over the chambers of the haemocytometer using a small amount of moisture, such as an exhaled breath.

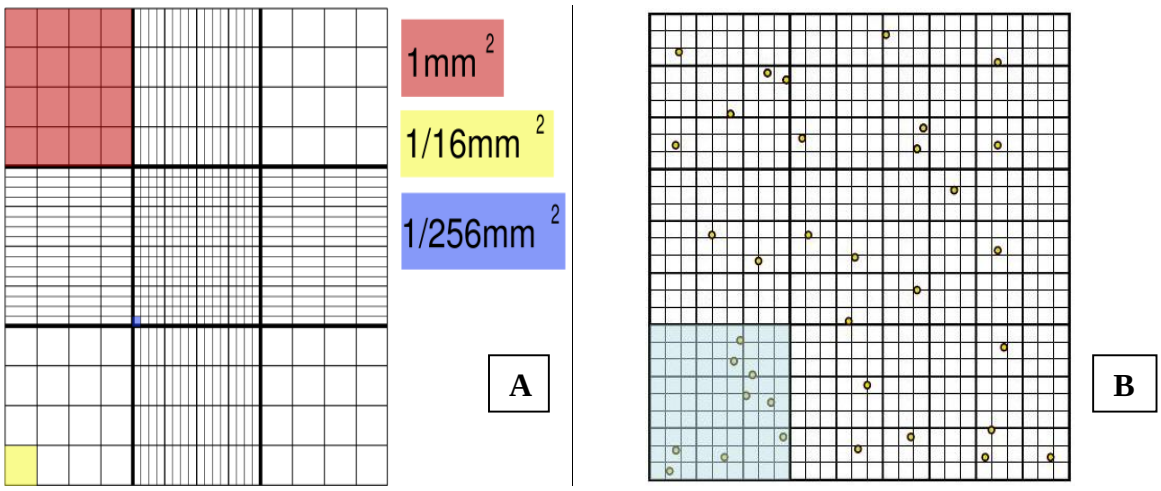

Figure 16: Diagrammatic representation of a haemocytometer.

(A) A haemocytometer with its dimensions. (B) A haemocytometer loaded with cell suspension (Images taken from http://en.wikipedia.org/wiki/File:Haemocytometer_grid.svg and http://www.gene-delivery.ox.ac.uk/Protocols/Tissue%20Culture%20Protocols/Counting%20Cells/counting_cells.htm).

The cell suspension (20 µl) containing 10 µl trypan blue was pipetted out on to the haemocytometer and was viewed under an inverted light microscope. The microscope was focused on 25 squares of one chamber and the number of cells in these squares were counted, this step was then repeated for the other chambers as well (Figure 16B). The average number of cells in the centre grid ($1mm^2$) of each chamber was counted and this number was multiplied by $2x10^4$ to obtain the number of cells per 1 ml of suspension. This number would be then used either for seeding the cells in 96 microtiter well plates, tissue culture flasks or for cryopreservation.

2.1.4 Cell freezing

The cells were passaged and counted as described earlier. The cell pellet was resuspended in 1 ml of cell freezing medium consisting of complete growth medium and 10 % dimethyl sulfoxide (DMSO) for glioma cell lines (1321N1 and U87MG). The cryovial containing this cell suspension was placed in 'Mr. Frosty' (Nalgene, UK) freezer

container filled with isopropanol and stored overnight at -80°C. The following day the cryovials were transferred into liquid nitrogen.

2.2 Growth curves

The generation of a growth curve aided the evaluation of the growth characteristics of the cells and ensured suitable tissue culture technique was being developed. This study was performed to analyse the growth characteristics of the non-cancerous foetal glial cell line SVGp12 and human glioma cell lines 1321N1 and U87MG so that the population doubling time, exponential phase and lag phase could be determined. The time at which the compounds/drugs should be administered on these cell lines would be determined by the data obtained from growth curves.

To generate the growth curves of the cell lines 1321N1, U87MG and SVGp12 each cell line was grown in thirty 25 cm^2 flasks at a cell density of 10,000 cells/flask with a total volume of 5 ml/flask. The day the cells were seeded was considered as day zero. Every day three of these flasks (n=3) were trypsinised and the cell count was determined as described earlier until the cells reached 100 % confluency.

Growth curves of cancer cell lines (1321N1 and U87MG) were also generated using a CellTiter-Glo® Luminescent Cell Viability Assay (commonly known as the ATP assay, Promega UK Ltd) (section 2.3.2). On day zero, 1000 cells/100 µl were seeded in 10 of the opaque white 96-well plates. On day one, one of the 96-well plates was equilibrated for 30 min at room temperature followed by addition of 100 µl of the CellTiter Glo® Reagent in the dark. The contents in the wells were mixed for 2 min in the plate reader to induce cell lysis and the plate was then incubated at room temperature for 10 min to stabilise the

luminescent signal. The luminescence was then recorded using the Tecan GENios Pro® microplate reader. This was repeated every day until day 10 and on each occasion cells from two separate wells were counted (n=2). A standard ATP curve was determined by seeding a known number of cells (1000, 2000, 4000, 8000, 16000) in the 96 well plates and recording their corresponding luminescence on the consecutive day. This standard curve was used to determine the number of cells corresponding to a particular luminescence.

2.3 Cell proliferation assays

The cell proliferation assays were used for carrying out the *in vitro* cytotoxicity tests to determine the most potent compounds against the glioma cell lines. Commercial drugs cisplatin, temozolomide, carmustine, etoposide and gemcitabine were tested on the 1321N1 and U87MG glioma cell lines to compare and find the most potent drug which can be further used as a positive control in the testing of the novel compounds.

The cells were prepared for this assay by trypsinising the cells out from the T75 flasks and then counting them using the techniques described in section 2.1.3 Once the cells were counted, approximately 4000 cells/200µl were seeded in 96-well plates (appendix 2) (Sarstedt, Leicester, UK). The cells were allowed to attach overnight, fresh drug was added the following day and the well plates were incubated according to suitable time points and cell viability was measured using two different cytotoxicity assays. The sensitivity of the above mentioned glioma cell lines to various anti-cancer drugs and novel compounds were tested using a CellTiter 96® AQueous One Solution Cell Proliferation Assay (commonly known as the MTS assay, Promega, UK) and a CellTiter-Glo® Luminescent Cell Viability Assay (commonly as known as the ATP assay, Promega, UK). Each concentration of the

drugs was added into four separate wells (n=4) and each experiment was repeated at least three times.

The next part of this study was to analyse the cytotoxicity of the novel compounds and compare their activity with cisplatin and resveratrol on the above mentioned glioma cell lines. For these studies, the glioma cell lines were treated with the commercial drugs and resveratrol for 48 h and each concentration of the drug was added into four separate wells (n=4) and each experiment was repeated at least three times. Moreover, the non-cancerous, SVGp12 cell line was also and only used to determine whether the potent compounds found in this study were specific to cancer cells.

A primary short-term culture, IN859 was also used at the end of the study to support the results obtained using established continuous cell lines because it resembles more similarity towards *in vivo* testing in comparison to established cell lines, as these cell lines may mutate over time.

2.3.1 MTS assay

The MTS assay (Figure 17) was used in this study because it gives a quantitative result, as opposed to the trypan blue or propidium iodide (PI) assays which only offer a qualitative result. This assay was the primary assay used for performing all cell viability studies because it is cheaper and less time consuming than the ATP assay. Nevertheless, the ATP assay was used on occasion to validate the MTS assay results. Research laboratories extensively use such assays across the world to detect cytotoxicity in various compounds, and medical agents and evaluating cell membrane integrity is one of the most common ways to measure cell viability and cytotoxic effects. Compounds that have cytotoxic effects

often cause cell membrane lysis. Vital dyes, such as trypan blue or PI normally cannot enter healthy cells; however, if the cell membrane has been compromised, they freely cross the membrane and stain intracellular components (Riss and Moravec, 2004). On the other hand, some compounds or medical agents can prove toxic without damaging the cell membrane i.e. without causing cell lysis and such cytotoxicity cannot be measured using trypan blue or PI. In such cases the MTS or similar assays have to be used. The MTS assay measures cell viability using a colorimetric reaction in lieu of membrane lysis. It measures the dehydrogenase enzyme activity found in the mitochondria of metabolically active cells (McGowan *et al.*, 2011).

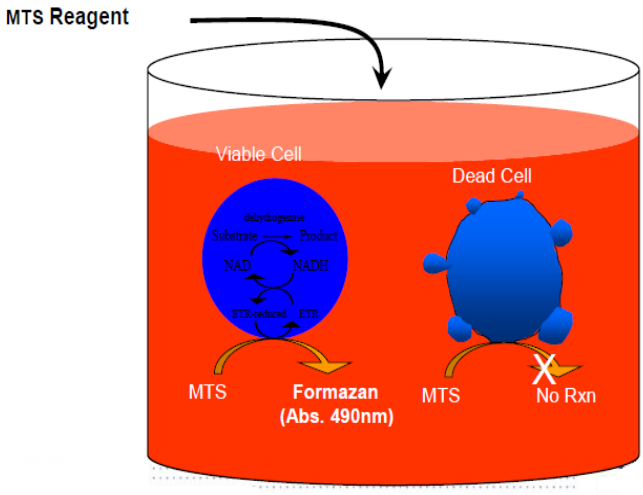

Figure 17: Diagrammatic representation of the MTS assay (Image available at http://spotlite.nih.gov/assay/images/2/26/Terry_Riss_aDream_Slides.pdf).

Viable cells will reduce the MTS reagent to a coloured formazan product which has an absorbance maximum at 490-500 nm in phosphate-buffered saline (Mosmann, 1983). The main application of this kit allows an assessment of the viability and proliferation of cells in cell culture based assays (Petty *et al.*, 1995). The assay can also be used to determine the potential cytotoxicity of novel compounds and toxic materials since those agents would inhibit or stimulate cell viability and proliferation. The MTS tetrazolium

compound (Owen's reagent) is bio-reduced by cells into a coloured formazan product that is soluble in the tissue culture media (Figure 18). This conversion is thought to be accomplished by NADPH or NADH produced by dehydrogenase enzymes in metabolically active cells. When the amount of purple formazan generated by cells treated with an agent is compared with the quantity of formazan produced by untreated vehicle control cells, the efficiency of the test agent in causing death, or changing the metabolism of cells, can be deduced through the production of a dose-response curve (Wilson, 2000).

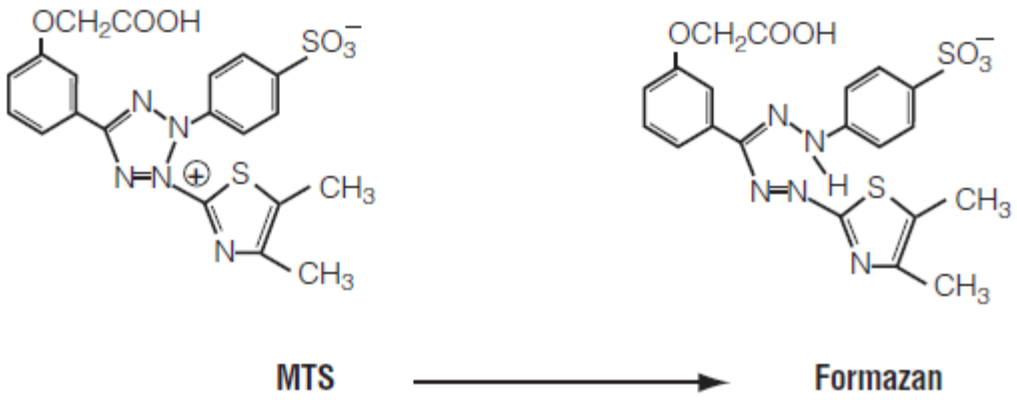

Figure 18: Structures of MTS tetrazolium [3-(4,5-dimethylthiazol-2-yl)-5-(3-carboxymethoxyphenyl)-2-(4-sulfophenyl)-2H-tetrazolium] and its formazan product (Adapted from Promega).

Assay protocol:

The 1321N1, U87MG and SVGp12 cell lines were trypsinised and cultured overnight at a cell density of 3500 cells/200 µl/well, 4000 cells/200 µl/well and 5000 cells/200 µl/well respectively in 96-well microtitre plates (appendix 2) (Sarstedt, UK). The following day when the cells appeared 50-60 % confluent, each concentration of the commercial drugs and novel compounds to be studied were added in quadruplicates and left for incubation for 48 h. After 48 h, 20 µl of the pre-warmed MTS reagent (Promega, UK) was added to each of the wells and the 96-well plates were incubated at 37°C for 60 min. At the end of the 60 min period, the absorbance was recorded at 490 nm using the Tecan

GENios Pro® microplate reader. The absorbance is directly proportional to the number of live cells. Thus, the percentage of cell survival can then be determined using the following equation:

$$\text{Cell survival (\%)} = \frac{\text{Absorbance of treated cells} \times 100}{\text{Absorbance of vehicle control group (untreated cells + solvent)}}$$

2.3.2 ATP assay

The ATP assay was only used in this study to further validate the results generated by the MTS assay. Unlike the MTS assay, the ATP assay can measure cells as low as 4 cells per well, in contrast to the MTS assay which can only detect samples containing more than 1000 cells per wells, as such this makes the ATP assay highly sensitive (Petty *et al.*, 1995), and thus a good assay for the corroboration of the MTS assay results, thus proving any activity seen is real and repeatable.

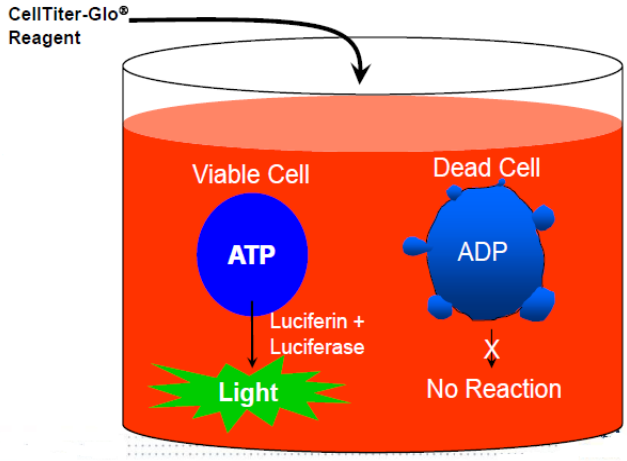

Figure 19: Diagrammatic representation of the ATP assay (assay (Image available at http://spotlite.nih.gov/assay/images/2/26/Terry_Riss_aDream_Slides.pdf).

The ATP assay is a homogeneous method for determining the number of viable cells in culture based on the quantitation of the ATP present, a process which signals the presence of metabolically active cells (Kangas *et al.*, 1984). The homogeneous "add-mix-

measure" format results in cell lysis and generation of a luminescent signal proportional to the amount of ATP present (Figure 19). The amount of ATP present is directly proportional to the number of live cells present in the culture. The ATP assay relies on the properties of a proprietary thermostable luciferase (Ultra-Glo™ Recombinant Luciferase), which generates a stable long lived glow-type luminescent signal with a half-life of more than five hours. Using firefly (*P. pyralis*) luciferase this luminescence assay is an alternative to colorimetric, fluorometric and radio-isotopic assays for the quantitative assessment of cytotoxicity and proliferation of cultured mammalian cells (Crouch *et al.*, 1993).

ATP monitoring can be used to measure the cytocidal, cytostatic and proliferative effects of various biological response modifiers, drugs and biological compounds. ATP is an indicator for cell viability because it exists in all metabolically active cells and the concentration declines significantly when the cells undergo apoptosis or necrosis (Cree and Andreotti, 1997). The assay is based on the production of light caused by the reaction of ATP with added luciferase and D-luciferin (Figure 20).

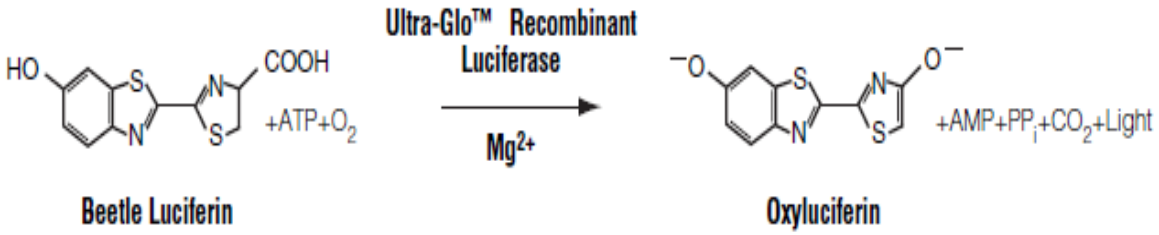

Figure 20: Mono-oxygenation of luciferin is catalysed by luciferase in the presence of $Mg2^{+}$, ATP and molecular oxygen (Adapted from Promega).

Assay protocol:

The 1321N1 and the U87MG cells were trypsinised and cultured overnight at a cell density of 3500 cells/200 µl/well and 4000 cells/200 µl/well respectively in 96-well

microtitre plates (appendix 2) (Sarstedt, UK). The following day when the cells appeared 50-60 % confluent each concentration of the novel compounds mentioned above were added in quadruplicates and left to incubate for 48 h. After 48 h, the media was removed and replaced with warm PBS and the 96-well plates were equilibrated for 30 min at room temperature followed by the addition of 100 µl of ATP Reagent in the dark. The contents in the wells were mixed for 2 min using the Tecan GENios Pro® microplate reader to induce cell lysis and the plates were then incubated at room temperature for 10 min to stabilise the luminescent signal. The luminescence was then recorded using the Tecan GENios Pro® microplate reader. The luminescence obtained is directly proportional to the number of live cells. Thus, the percentage of cell survival was then determined using the following equation:

$$\text{Cell survival (\%)} = \frac{\text{Luminescence of treated cells x 100}}{\text{Luminescence of vehicle control group (untreated cells + solvent)}}$$

2.3.3 Trypan blue dye exclusion test

The trypan blue dye exclusion test was used in this study to check the time required for membrane lysis (cell death) to occur after treatment with certain compounds as this cannot be detected by the MTS or the ATP assay. The trypan blue dye exclusion test is used for determining the amount of living cells present in a cell suspension and is based on the principle that live cells possess intact cell membranes that exclude certain dyes such as trypan blue, PI or eosin, whereas dead cells become stained. In this test, the cell suspension is mixed with the trypan blue dye in a 1:1 ratio and then visually observed under the microscope to determine whether cells take up or exclude the dye. A viable cell will have a clear cytoplasm whereas a dead cell will have a blue stained cytoplasm.

Assay protocol:

Cells were trypsinised and 4000 cells/200 µl/well were seeded in 96 well plates (appendix 2) (BD Biosciences, UK) and were allowed to attach overnight. Cells were treated with 1000 µM and 750 µM of the test compound for various time points (15 min, 45 min, 75 min, 90 min, 120 min). After the desired treatment time, a volume of around 10 µl of trypan blue dye (Sigma Aldrich, UK) was added into the well plate and the cells were observed under the microscope for potential trypan blue staining.

2.4 Preparation of stock solutions of commercial anti-cancer agents and novel compounds

The anti-cancer commercial drugs used in this study were cisplatin, carmustine, temozolomide, etoposide and gemcitabine. Stock solutions of each drug were prepared as mentioned in table 3 and were stored in the freezer at -20°C until required. Either ethanol or dimethyl sulfoxide (DMSO) was used to dissolve the various commercial drugs and novel compounds. The drugs and compounds were then subsequently dissolved in the culture medium of the respective cell line; the final concentration of ethanol or DMSO used was no more than 0.5 %. The untreated vehicle controls also contained 0.5 % absolute ethanol or DMSO. These concentrations of ethanol and DMSO have no toxic effects on the cell lines (Kiyozuka *et al*., 2001).

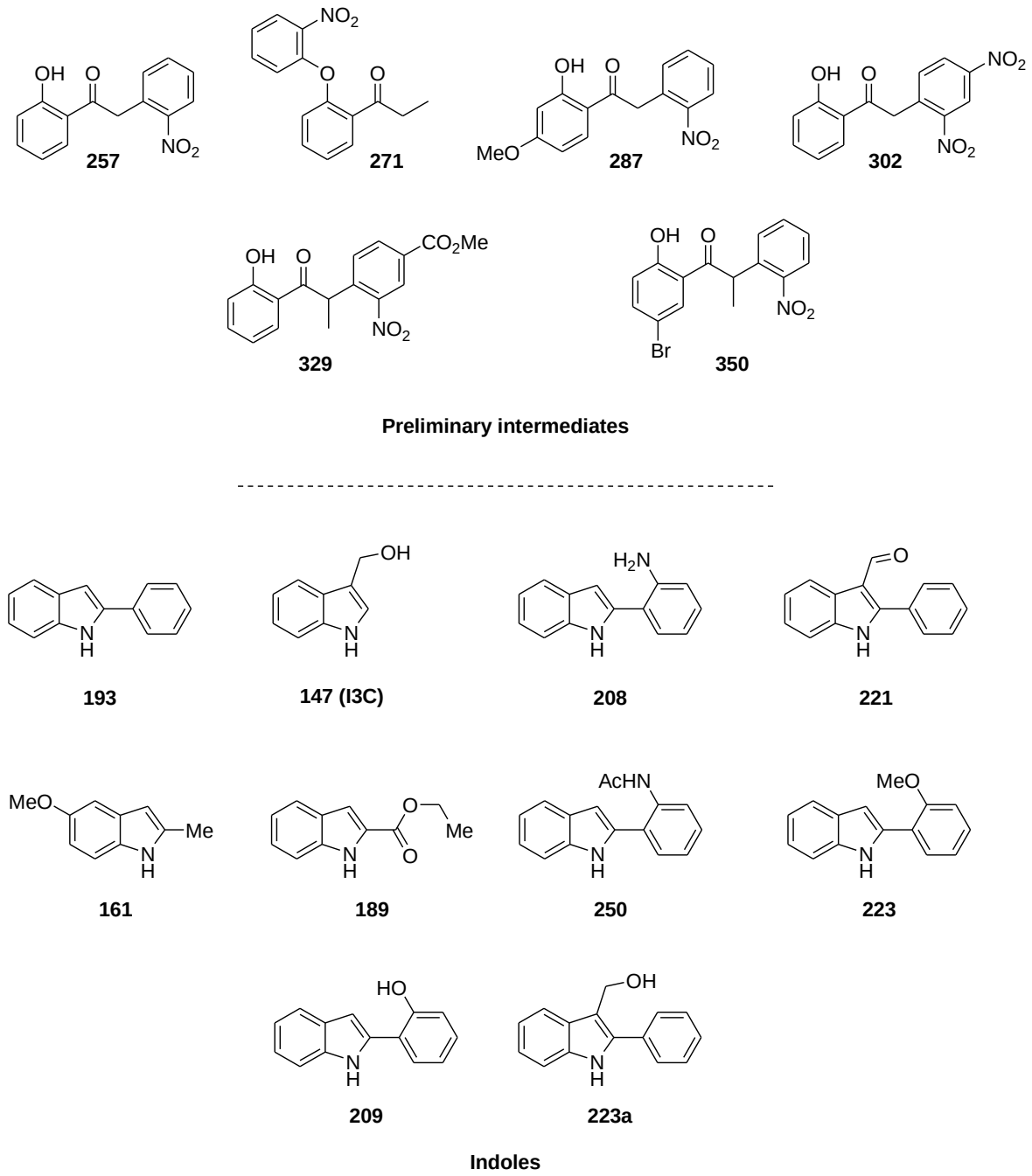

Figure 21: Compounds used in the present study.

All the compounds in Figure 21 were either synthesised or purchased and were labelled according to their molecular weights for simplicity and all of these compounds were at least 95 % pure, as determined by ^{1}H and ^{13}C NMR, and HPLC; as an example of the purity of the prepared test compounds, the ^{1}H NMRs for 209 and 223a (Figure 22) are shown below,

whilst those compounds that were commercially available (Sigma-Aldrich, UK) were used as purchased. For example, indole-3-carbinol (147) and the negative control, 2-phenylindole (193), were both at least 95 % pure, whilst all other commercially available test compounds were also at least 95 % pure, as determined by gas chromatography.

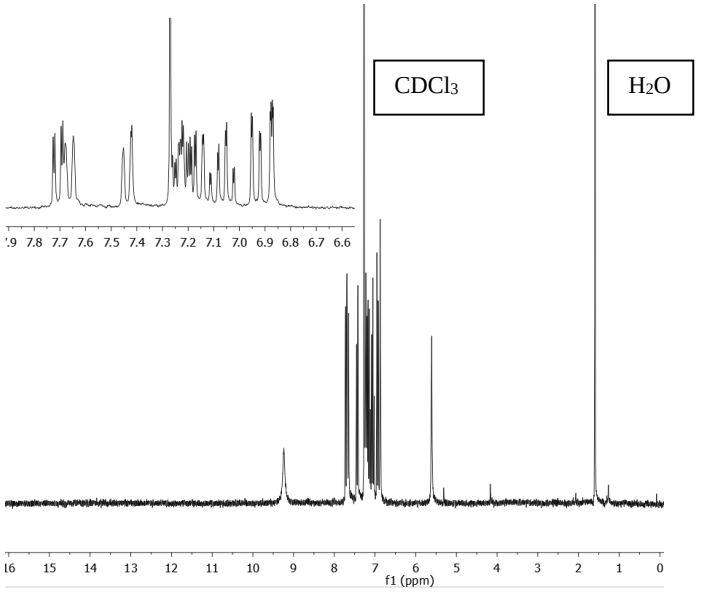

Compound 209

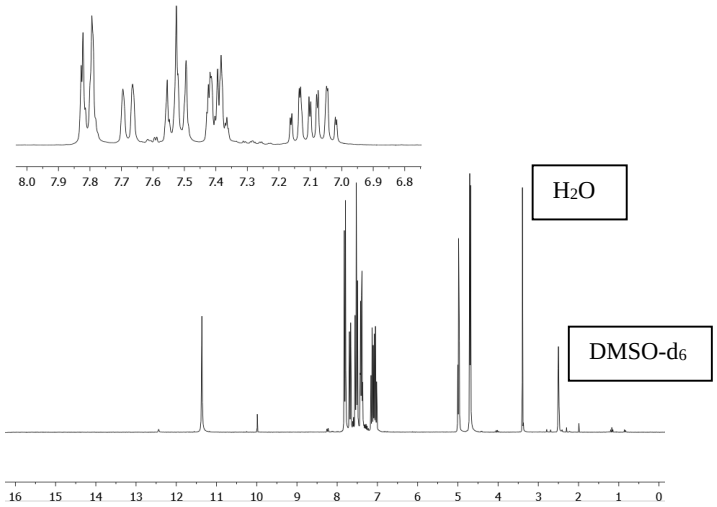

Compound 223a

Figure 22: Selected ^{1}H NMRs of compounds 209 and 223a showing their level of purity.

For the synthetic protocols and characterisation of the indoles prepared by the Snape group and tested herein, see Appendix I.

2.4.1 Physiochemical properties of novel indoles

An octanol-water partition coefficient (Log P) is the ratio of the concentrations of a compound in two phases of a mixture of two immiscible liquids at equilibrium (Leo *et al.*, 1971). Generally, one of the solvents chosen is water, whereas the second is hydrophobic such as octanol (Sangster, 1997). Therefore, the partition coefficient is a measure of how hydrophilic or hydrophobic a compound is. One rule of Lipinski's "Rule of Five" (section 1.2) states that, an orally active drug's Log P should not be greater than five if the compound is to freely distribute around the body and traverse cell membranes; with that in mind, table 3 shows the Log P values for the indoles used herein, where it can be seen that all values are < 5, as required.

The indoles used in the current study were found to be lipophilic (table 3) and therefore were only soluble in the cell culture media with the concomitant use of an organic solvent [ethanol or DMSO]. Whilst this lipophilicity may be problematic for the determination of biological activity, it may be beneficial for *in vivo* activity, since the compounds are more likely to be able cross cell membranes and act upon their intracellular target(s).

Table 3: Log P values (calculated using ChemBioDraw Ultra 11.0) of some of the indoles tested.

Entry	Compounds	Log P
1	**209**	2.92
2	**223a**	2.73
3	**223**	3.18
4	**193**	3.31

Table 4: Drug/compound preparation: Stock solutions were made prior to use.

Drugs/compounds (Supplier)	**Solvent used**	**Stock concentration (mM)**	**Final concentrations used (µM)**
Cisplatin (Sigma-Aldrich,UK)	Culture media	1	10, 20, 50, 100, 300, 500
Carmustine (Sigma-Aldrich,UK)	Dissolved in ethanol, subsequently in culture media	1	50, 100, 300, 500
Temozolomide (Sigma-Aldrich,UK)	Culture media	1	50, 100, 300, 500
Etoposide (Sigma-Aldrich,UK)	Dissolved in ethanol, subsequently in culture media	1	50, 100, 300, 500
Gemcitabine (Sigma-Aldrich,UK)	Dissolved in ethanol, subsequently in culture media	1	50, 100, 300, 500
Novel compounds: 209, 287, 221, 223, 223a, 250, 147 (I3C) (Sigma-Aldrich,UK)	Dissolved in ethanol, subsequently in culture media	2	1000, 750, 400, 200, 100
Novel compounds: 302, 350, 271, 329, 257, 208, 189, 161, 193, Resveratrol	Dissolved in DMSO, subsequently in culture media	2	1000, 750, 400, 200, 100
Ascorbic acid (Sigma-Aldrich,UK)	Culture media	1	500
3-Methyladenine (Sigma-Aldrich,UK)	Culture media	5	5000
Acridine orange (Sigma-Aldrich,UK)	Ethanol	0.1	3
Carboxy-H_2DCFDA (Invitrogen LTD, UK)	DMSO	10	25
TBHP (Invitrogen LTD, UK)	HBSS	100	100
Cn-AMP2 (Pepsyn, UK)	DMSO	4	2000, 1000, 500

2.5 Image-iT™ LIVE Green Reactive Oxygen Species Detection Kit

The Image-iT™ LIVE Green Reactive Oxygen Species (ROS) Detection Kit (Invitrogen Ltd, UK) was used in this study to validate the hypothesis that certain compounds may cause ROS production in the cells leading to oxidative stress. This kit provides the key reagents necessary for the detection of ROS in live cells. In addition to carboxy-H_2DCFDA, the kit provides the common inducer of ROS production, *tert*-butyl hydroperoxide (TBHP), as a positive control. Using this ROS detection kit, oxidatively stressed and nonstressed cells are reliably distinguished by fluorescence microscopy. The generation of ROS is inevitable for aerobic organisms, and, in healthy cells, occurs at a controlled rate. Under conditions of oxidative stress, ROS production is dramatically increased, resulting in subsequent alteration of membrane lipids, proteins, and nucleic acids.

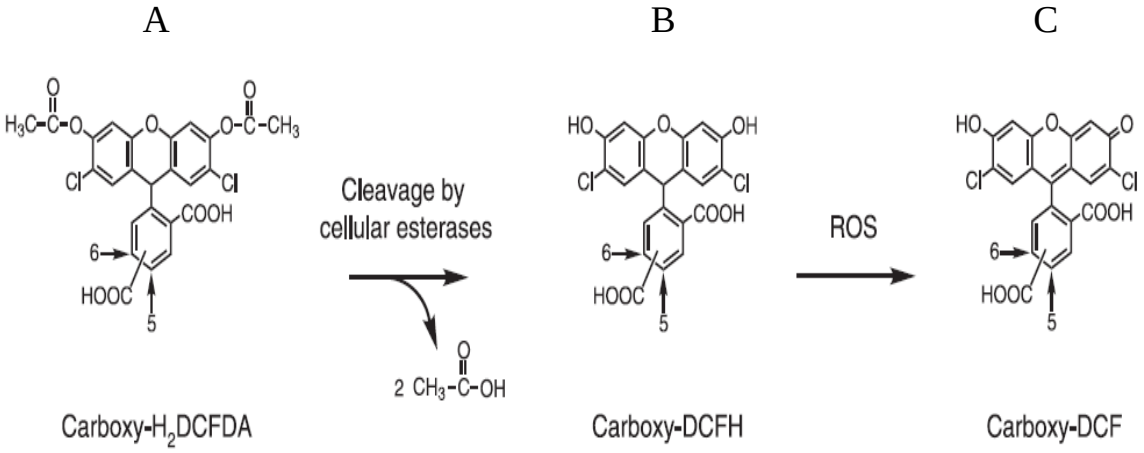

Figure 23: Detection of ROS generation by Image-iT™ LIVE Green Reactive Oxygen Species Detection Kit.

The carboxy-H_2DCFDA permeates live cells (Figure 23A). It is deacetylated in the live cell by nonspecific intracellular esterases and is converted to carboxy-DCFH (Figure 23 B). In the presence of nonspecific ROS (produced throughout the cell, particularly

during oxidative stress) the reduced fluorescein compound, carboxy-DCF (Figure 23C) is oxidised and emits bright green fluorescence which can be detected using a confocal microscope or a flow cytometer.

2.5.1 Confocal microscopy

The above mentioned Image-iT ™ LIVE Green ROS Detection Kit was used to detect the reactive oxygen species in the glioma cell lines. The assay was based on carboxy-H_2DCFDA, a reliable fluorogenic marker for ROS in live cells which would fluoresce green on the detection of ROS in live cells (Figure 23). A confocal microscope was used to visualise the amount of fluorescence produced. As a test run, to make sure that the assay worked, it was initially performed using a confocal microscope. Once confirmed it was working as expected, all future experiments were performed on a flow cytometer so that the amount of fluorescence produced could be quantified.

Assay protocol:

Glioma cell lines were trypsinised and 2 x 10^4 cells of each cell line were seeded in 6-well plate/ml/well (appendix 2) (BD Biosciences, UK) and the cells were allowed to attach overnight. On the day of experiment, cells were treated with 500 µM of the test compound and the positive control [*tert*-butyl hydroperoxide (TBHP) (100 µM)] for 1 h followed by labelling with a sufficient amount of 25 µM carboxy-H_2DCFDA dye and incubated for 30 min at 37°C, protected from light. Cells were gently washed with Hank's balanced salt solution (HBSS) warm buffer three times and were imaged immediately on the Zeiss LSM510 laser confocal microscope at an excitation/emission of 495/529 nm.

2.5.2 Flow cytometry analysis

Flow cytometry is a powerful technology for the simultaneous measurement and analysis of multiple parameters of individual cells within heterogeneous populations. It has an array of applications ranging from subset identification of heterogeneous cell populations, fluorescence-activated cell sorting (FACS) to rare-event detection in stem cell analysis. In order to quantify the amount of ROS produced in the glioma cell lines, Image-iT ™ LIVE Green ROS Detection Kit was again used.

Assay protocol:

Glioma cell lines were trypsinised and 2 x 10^4 cells/ml/well of each cell line were seeded in 6-well plates (appendix 2) (BD Biosciences, UK) and were allowed to attach overnight. On the day of the experiment, cells were treated with 500 µM of the test compound and the positive control [*tert*-butyl hydroperoxide (TBHP) (100 µM)] for 1 h followed by labelling with sufficient amount of 25 µM carboxy-H_2DCFDA dye and incubation for 30 min at 37°C, protected from light. The ascorbic acid study followed the same protocol with the exception being that cells were co-treated with the test compound (500 µM) and ascorbic acid (500 µM) for 1 h. Cells were gently washed with HBSS warm buffer three times and then trypsinised, centrifuged and resuspended in 300 µl PBS. Cells were filtered through cell strainer caps (35µm mesh) (BD Biosciences) to obtain a single cell suspension and analysed using a FACSAria flow cytometer using FITC fluorochrome at an excitation/emission of 488/519 nm (BD Biosciences).

2.5.3 Acridine orange staining

Acridine orange staining was used in this study to validate the hypothesis that the quick cell death caused by one of the test compounds may be due to autophagy, mediated

by ROS (oxidative stress). Acridine orange (AO) is a nucleic-acid selective fluorescent cationic dye useful for cell cycle determination (Darzynkiewicz, 1990), and it is commonly used to study autophagy since it accumulates in acidic organelles in a pH-dependent manner (Han and Burgess, 2010). Acridine orange, due to its metachromatic properties, is widely used in fluorescence microscopy and flow cytometry analysis (Darzynkiewicz, 1991). At neutral pH, AO is a hydrophobic green fluorescent molecule but during autophagy, AO becomes protonated and trapped within the acidic vesicles of the organelle and emits orange light. It is cell-permeable, and interacts with DNA and RNA by intercalation or electrostatic attractions respectively. When bound to DNA, it has an excitation maximum at 502 nm and an emission maximum at 525 nm (green). On binding with RNA, the excitation maximum shifts to 460 nm (blue) and the emission maximum shifts to 650 nm (red) (Darzynkiewicz and Juan, 1997). Acridine orange enters acidic compartments such as lysosomes and gets protonated and sequestered. Cells illuminated with blue (488 nm) excitation light were measured with flow cytometry. In these low pH conditions (during AVO formation), the dye will emit orange light when excited by blue light. Thus, AO can be used to isolate engulfed cells, because it will fluoresce upon engulfment (Darzynkiewicz and Juan, 1997).

Assay protocol:

Glioma cell lines were trypsinised and 2 x 10^4 cells/ml/well were seeded in 6-well plates (appendix 2) (BD Biosciences, UK) and were allowed to attach overnight. After 24 h of incubation, the cells were treated with 500 µM of the test compound or the test compound (500 µM) + 3-methyladenine (5 mM) for 1 h. After 1 h incubation with the compound the cells were stained with 3 µM acridine orange (Sigma, UK) and incubated for 15 min at 37°C, protected from light. Cells were gently washed with PBS, trypsinised,

centrifuged and were re-suspended in 300 µl PBS. Cells were filtered through cell strainer caps (35 µm mesh) to obtain a single cell suspension and analysed using a FACSAria flow cytometer using a PE-Texas Red fluorochrome at an excitation/emission of 488/615 nm (BD Biosciences).

2.6 Graphical analysis and stock solution preparation of the host defence peptide (HDP), *Cn*-AMP2

The sequence of the HDP, *Cn*-AMP2 [TESYFVFSVGM, Thr-Glu-Ser-Tyr-Phe-Val-Phe-Ser-Val-Gly-Met (where, Thr- threonine, Glu- glutamic acid, Ser- serine, Tyr- tyrosine, Phe- phenylalanine, Val- valine, Gly- glycine, Met- methionine)], was obtained from Mandal *et al*, (2009) and that of temporin 1-Ja (ILPLVGNLLNDLL), an amphibian host defence peptide, was obtained from Isaacson *et al*. (2002). The latter peptide was chosen as a reference HDP based on its structural similarities to *Cn*-AMP2, namely, its similarity in length and net charge, and its ability to form a well-defined α-helix. The sequence of each of these peptides was then represented as an α-helical wheel, which is a two-dimensional axial projection assuming an angular periodicity of 100° (Schiffer and Edmundson, 1967), using the software, AntheProt v 5.0 (VanOrder and Lindwall, 1942; Deleage *et al.*, 2001). *Cn*-AMP2 was supplied by Pepsyn (Liverpool, UK), produced by solid phase synthesis and purified by HPLC to greater than 95 %, which was confirmed by Pepsyn, UK. The peptide was stored as a stock solution of 4 mM in DMSO at -20 °C. The peptide was tested for anti-cancer activity on the 1321N1 and U87MG glioma cell lines in 96-well plates (Sarstedt, Leicester, UK) using the technique described in section 2.3.1 *Cn*-AMP2 (final concentrations of 2 mM and 1 mM) was incubated with the 1321N1 and U87MG cell lines, which had been cultured in Dulbeccos's Modified Eagle's Medium

(DMEM), prepared as described in section 2.1, except that the FBS concentration of the medium was varied [10 % and 2.5 % (v/v)]. The percent viability of the cells was then determined according to the MTS cell viability assay, as described in section 2.3.1, except that an incubation period of 72 h was employed. The effect of *Cn*-AMP2 on the morphology of these cells was examined by recording images using an inverted microscope. The ability of *Cn*-AMP2 to lyse membranes of the 1321N1 and U87MG cell lines was assayed as described in section 2.3.3 except that: cells were grown in DMEM containing 2.5 % (v/v) FBS, and incubated with the peptide at levels of 1 mM and 2 mM for 72 h. As controls, these experiments were repeated in the absence of the peptide and, in all cases, experiments were performed in quadruplicate. The untreated vehicle controls contained 0.5 % DMSO.

2.7 Statistical and Data analyses

Data obtained from these experiments were subjected to statistical analyses using GraphPad Prism software (version 6.0, USA) to analyse and compare the control and test values. The flow cytometry results were analysed on the BDS FACS DIVA software. All data are expressed as mean ±standard deviation (SD). The Log P value of the novel compounds was calculated using ChemBioDraw Ultra (version 11.0, PerkinElmer Informatics). The data was considered as significant when $p < 0.05$.

Chapter III

3.RESULTS AND DISCUSSION

Section A: Determination of anti-cancer activity using cell viability assays

3.1 Establishing the growth curves for the glioma cell lines.

To analyse the growth characteristics of the human glioma cell lines 1321N1, U87MG and the non-cancerous foetal glial cell line, SVGp12, their growth curves were established. This study was performed to determine the population doubling time, exponential and lag phases and also to verify and compare the growth patterns obtained from the literature to ensure suitable tissue culture technique was being developed. Growth curves were plotted using two methods; the flask method and the plate method. In the flask method, the cell count was acquired using Neubauer's Haemocytometer method (Strober, 2001) and it was observed that the rate of proliferation for the 1321N1 cells was faster than the U87MG cell line and both of the cancer cell lines were faster than the non-cancerous SVGp12 cell line (Figure 24). The population doubling time for 1321N1, U87MG and SVGp12 cell lines was 22 ±2 h, 25 ±3 h and 30 ±2 h respectively. Values which are consistent with both the cell types and other studies (Kim *et al.*, 2012; Ke *et al.*, 2000). In the plate method (figures 25C and 25D), only the growth curves of the cancerous cell lines (1321N1 and U87MG) were determined, and this was performed using the CellTiter-Glo® Luminescent Cell Viability Assay. The cell count was acquired by plotting a standard curve of cell count against luminescence and comparing the absorbance value obtained with the

value obtained in the standard curve. The cell count was acquired using the equation of the straight line since the growth is linear ($R^2 \sim 1$), as demonstrated on the standard curve (figures 25A and 25B). Similar to the flask method, it was observed that the 1321N1 cells proliferate at a faster rate than U87MG. The exponential phase observed by the flask method for the 1321N1 cell line was from the 3rd to 6th day while for the U87MG was from the 4th to 9th day. The exponential phase observed by the flask method for the non-cancerous foetal glial cell line, SVGp12 cell line was from the 5th to 8th day. The exponential phase observed by the plate method for the 1321N1 cell line was from 4th to 6th day while for the U87MG was from the 4th to 7th day. Previous studies have shown that the doubling time for the 1321N1 cell line to be 22 h (Kim *et al.*, 2012) while that of the U87MG cell line to be 29 h (Ke *et al.*, 2000), results which were similar to the those obtained from the current study and thus confirmed that the results were consistent with the growth patterns shown in the literature for the above mentioned glioma cell lines.

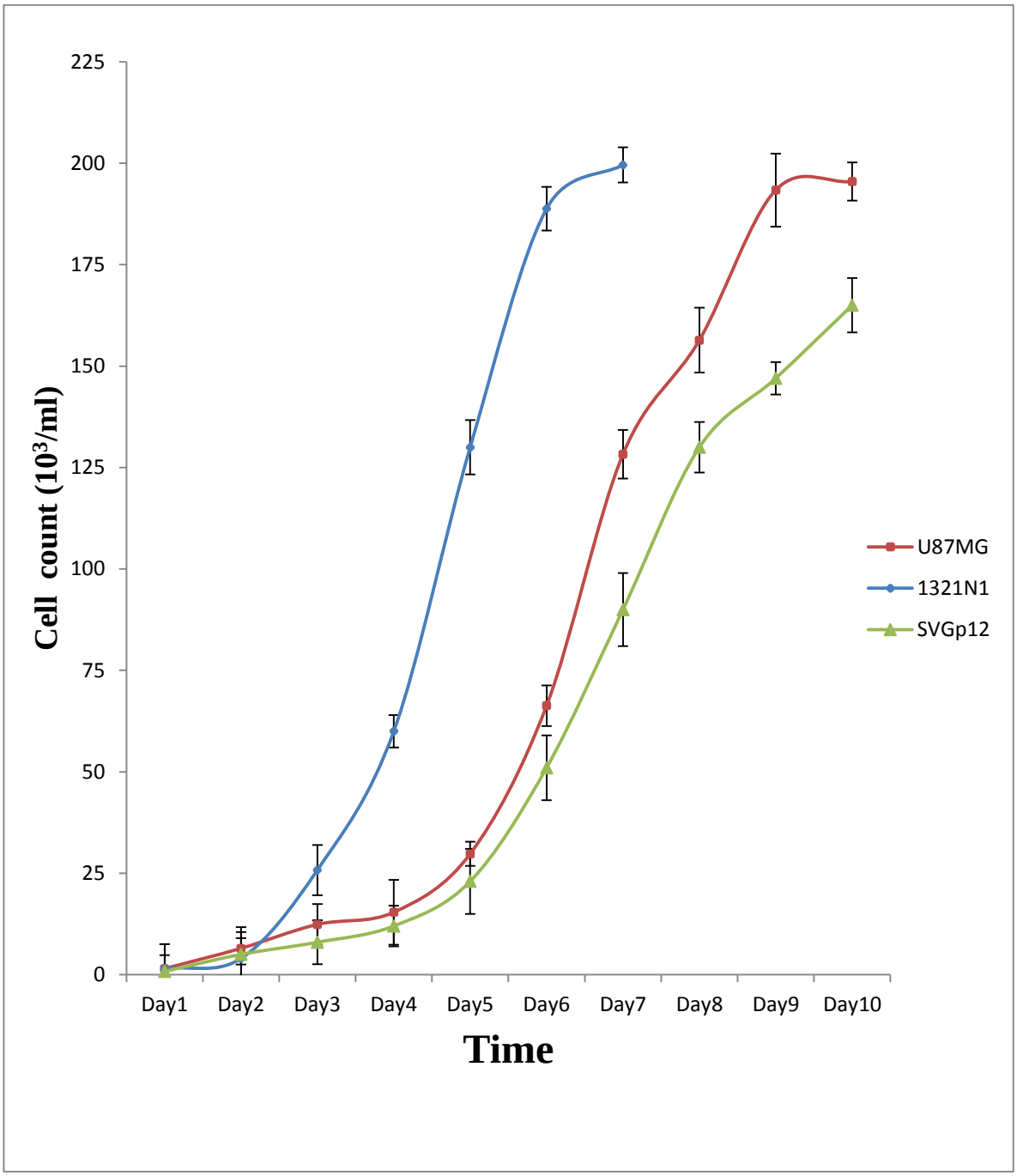

Figure 24: Growth analysis of the non-cancerous foetal glial cell line, SVGp12, and the human glioma cell lines 1321N1 and U87MG by Neubauer's Haemocytometer method.

Note that the exponential phase is reached on the 3rd day for the 1321N1, 4th day for the U87MG and on the 5th day for the SVGp12 cell lines while the plateau phase is reached from the 6th day for the 1321N1 cell line and 9th day for the U87MG cell line. The data points are means of three repeats and the error bars represent ± standard deviation (±SD).

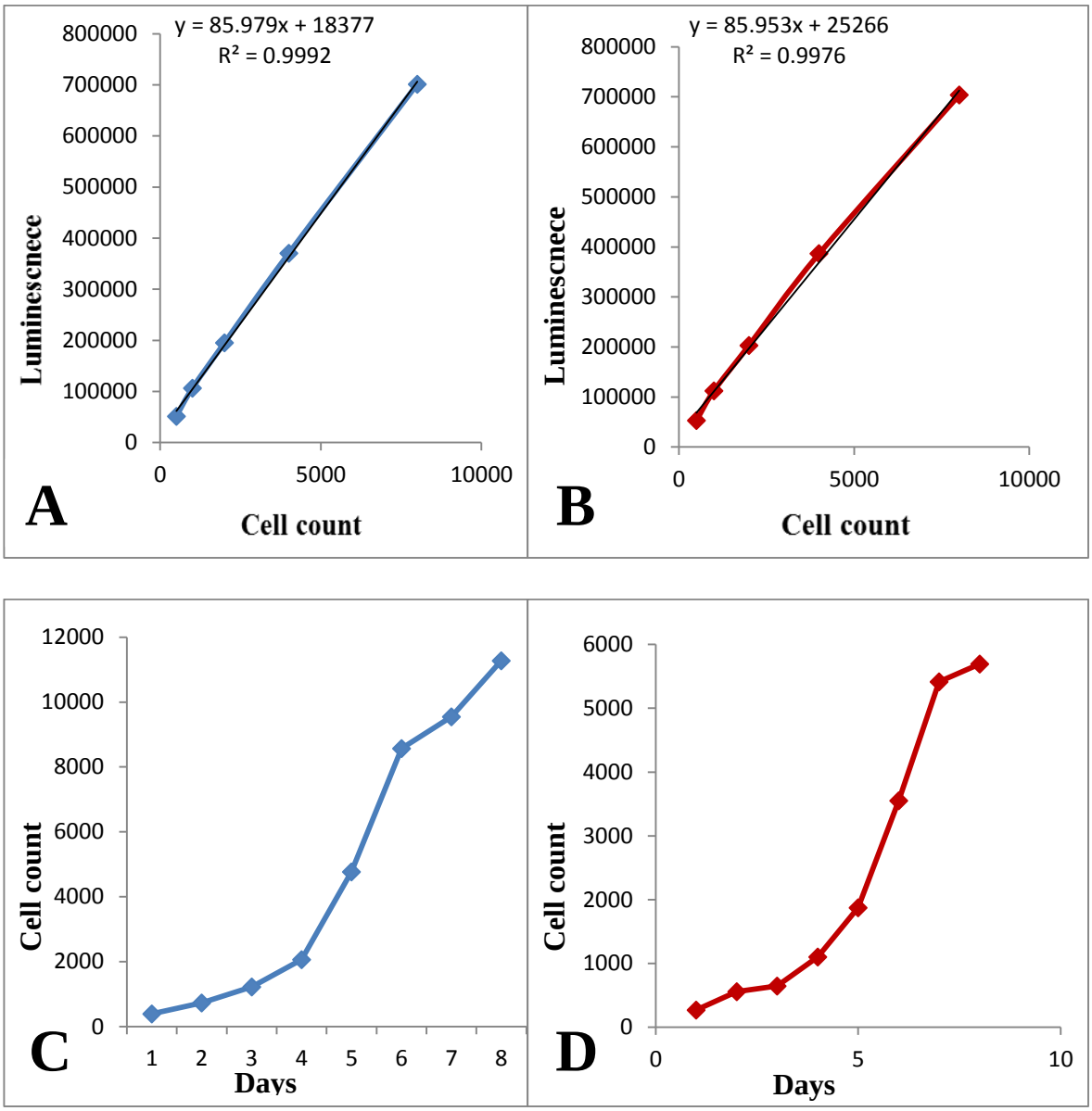

Figure 25: Growth analysis of glioma cell lines 1321N1 and U87MG using the ATP assay where the R^2 value is the correlation coefficient.

A) Standard curve for the 1321N1 cell line. **B)** Standard curve for the U87MG cell line. **C)** Growth curve for the 1321N1 cell line where the exponential phase is from the 4th-6th day. **D)** Growth curve for the U87MG cell line where the exponential phase is from the 4th-7th day. The data points are means of 2 repeats.

Typical cell growth shows three phases, viz; a lag phase, which denotes the time taken by the cells to recover from subculture, attach to the surface of the flask or well and spread; the log phase which represents the phase in which the cell numbers begin to proliferate exponentially, and a second lag phase in which the cell culture becomes confluent and the growth rate slows down or stops and the curve looks like a plateau when plotted on a graph. It was observed by both the methods used, that the rate of proliferation in the exponential phase for the 1321N1 cell line was faster than the U87MG (section 3.1). The doubling time of the SVGp12 cell line was the slowest throughout, making it the most slow growing cell line compared to the two cancerous cell lines tested; it is clear therefore that cancer cells multiply faster than the non-cancerous ones, as expected and shown in the literature (Cooper, 2000).

3.2 Cell proliferation and viability measurements of glioma cell lines in the presence of the test compounds.

3.2.1 Determining the best commercial compound to be used as a positive control *in vitro*

The commercial drugs cisplatin, carmustine, etoposide, gemcitabine and temozolomide were used in this study and tested on both the 1321N1 (Figure 26) and U87MG (Figure 27) cell lines in order to find the most potent drug which can be further used as a positive control in the testing of these compounds. This would also enable to allow a comparison to be made between these established anti-cancer drugs and the compounds tested later. The concentrations used were 10 µM, 20 µM, 50 µM, 100 µM, 300

µM and 500 µM. The IC_{50} value was reached at a concentration of 11 ±2 µM after treating with cisplatin and 50 ±2 µM for gemcitabine after 48 h on the 1321N1 cell line. However, the more malignant U87MG cell line was resistant to all the above commercial drugs, except for cisplatin, where the IC_{50} value was reached at a concentration of 310 ±4 µM after treatment for 48 h. The following dose response curves were plotted using the MTS cell proliferation assay.

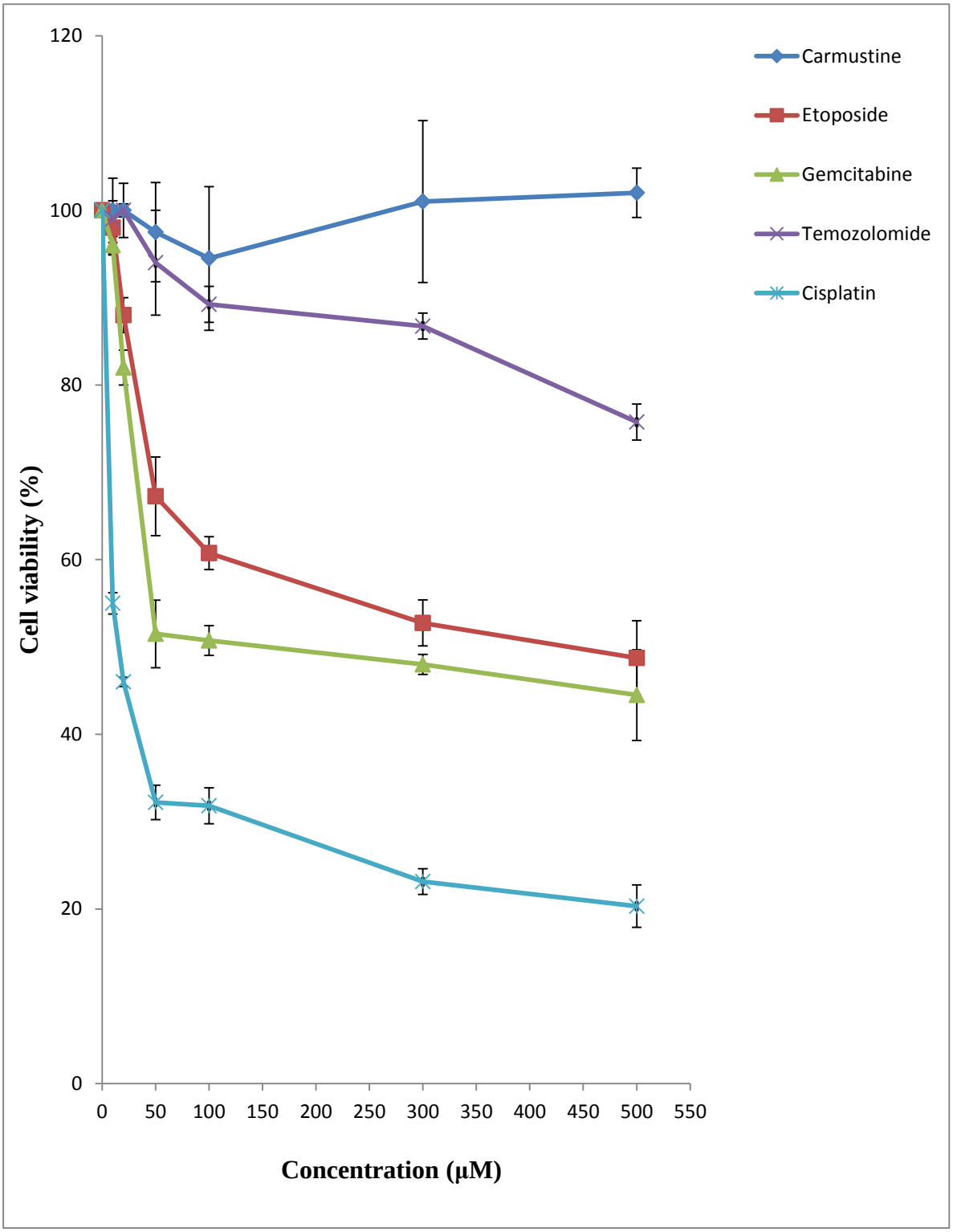

Figure 26: Dose response curves of cisplatin, carmustine, etoposide, gemcitabine and temozolomide on the 1321N1 cell line after treatment for 48 h. The data points are means of 4 repeats and the error bars represent ±SD.

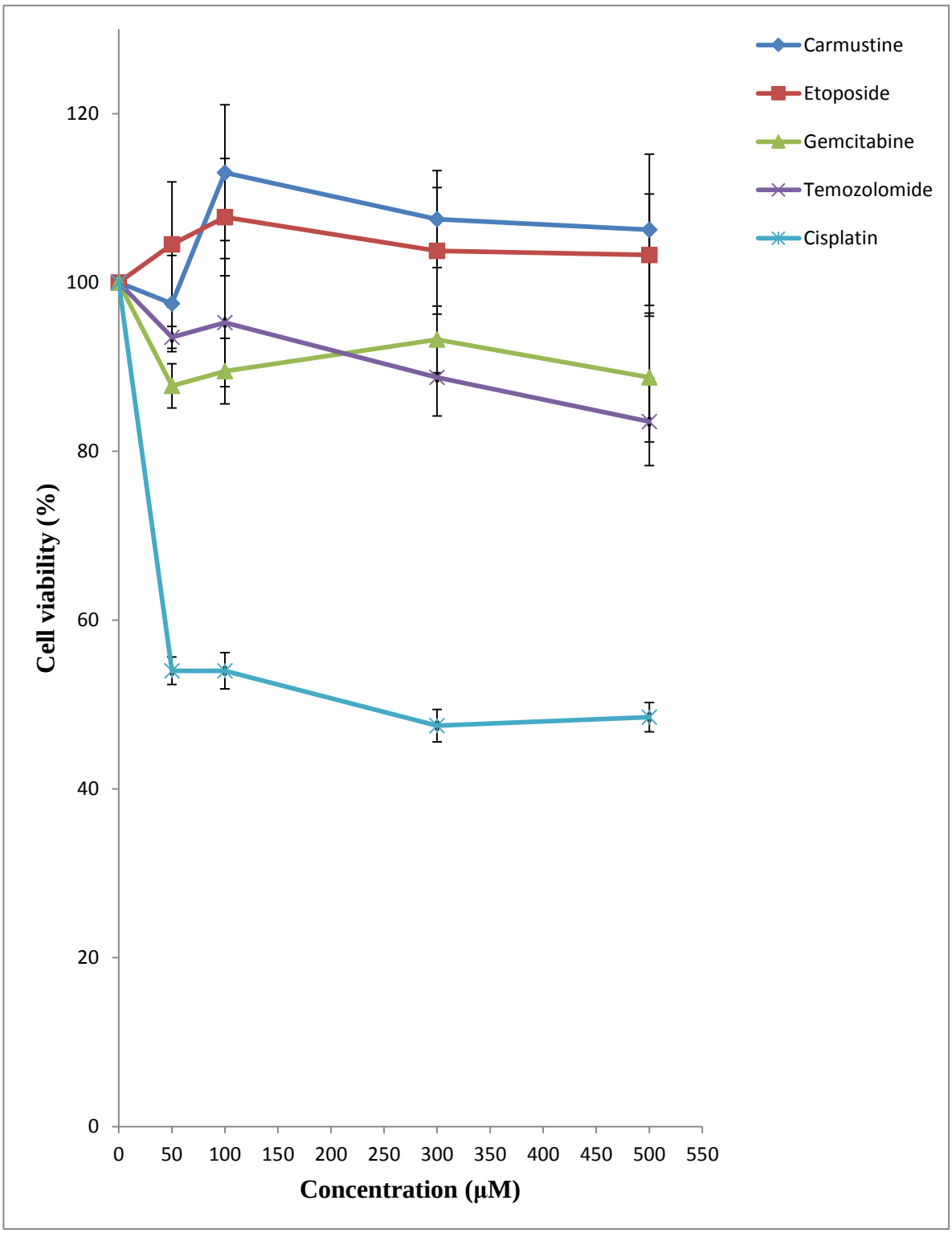

Figure 27: Dose response curves of cisplatin, carmustine, etoposide, gemcitabine and temozolomide on the U87MG cell line after treatment for 48 h. The data points are means of 4 repeats and the error bars represent ±SD.

3.2.1.1 Cisplatin as a positive control

The results of the cytotoxic analysis showed that cisplatin was the most potent of all commercial drugs (etoposide, carmustine, temozolomide and gemcitabine) tested (Figure 26 and Figure 27) and therefore it was used from here on as a standard comparison against all other test compounds. These cytotoxicity results showed that the IC_{50} values were reached on both of the glioma cell lines (1321N1 and U87MG) within 48 h of treatment with cisplatin. These results are consistent with previous studies which have shown that both these glioma cell lines are sensitive to cisplatin and cell death is induced through apoptosis (Raaphorst *et al.*, 1998; Shervington *et al.*, 2009).

Cisplatin possesses its anti-cancer activity because of its interaction with chromosomal DNA after it enters into the cell via either active or passive diffusion (Kazanietz, 2010). Over the years cisplatin has shown significant impact on the treatment of multiple neoplasms and was also one of the key reasons behind selecting this drug herein as a comparison against the test compounds on the glioma cell lines (Helm and States, 2009; Matsuzaki *et al.*, 2000). For example, research has shown that cisplatin is also a Fas inducer which makes oesophageal tumours susceptible to the Fas antigen, a feature which results in apoptosis (Matsuzaki *et al.*, 2000); the Fas receptor is a death receptor on the surface of cells that leads to apoptosis, and these studies have shown that the anti-cancer effect of an anti-Fas antibody on the oesophageal cancer cell line was enhanced by pre-treatment with cisplatin. DNA fragmentation was observed in a cell line that was treated with both cisplatin and this anti-Fas antibody and it ultimately led to cell apoptosis, whilst an anti-Fas neutralising antibody inhibited this cytotoxicity (Matsuzaki *et al.*, 2000). Therefore, comparing the results of the test compounds developed herein with cisplatin,

using the same cell lines, will enable the potential of the compounds, as leads, to be determined.

3.2.2 Preliminary test compounds in comparison with cisplatin and resveratrol

The interest in indoles, and in particular 2-arylindoles, by the Snape research group (Snape, 2008; Lal and Snape, 2012) has resulted in a number of pure synthetic intermediates being available which share structural similarities to the 2-arylindoles for which they are precursors, as such, the initial study began by testing a few of these intermediates (Snape, 2008) in the hope of a) discovering novel anti-cancer activity and b) providing basal activity which could potentially be improved upon if the compounds were converted to their indole counterparts. Moreover, in support of this study, these intermediates share structural similarities with resveratrol, a known anti-cancer agent which has been the subject of a vast amount of research over the past 15 years (Jo Atten *et al.*, 1998; Jiang *et al.*, 2005; Li *et al.*, 2009; Gagliano *et al.*, 2010; Wcislo, 2014; Liu *et al.*, 2014).

Dose response curves of cisplatin, resveratrol and the various novel intermediates (Figure 28 and Figure 29) on the 1321N1 and U87MG cell lines were plotted using the MTS cell proliferation assay, wherein both these cell lines were exposed to different concentrations of the compounds for 48 h, in order to assess this cytotoxicity; cisplatin and resveratrol were used as positive controls. As mentioned above, these intermediates were compared to cisplatin, since it was found to be the most potent compound on both the glioma cell lines of interest (section 3.2.1), amongst all other commercial drugs tested, and also with resveratrol, because the test compounds share structural similarities with

resveratrol, a known anti-cancer agent (Gagliano *et al.*, 2010). As shown in Figure 28 and Figure 29, the IC_{50} value of cisplatin was 11 ±2 µM on the 1321N1 cell line and 310 ±4 µM on the U87MG cell line, whilst, resveratrol showed moderate activity on the 1321N1 cell line but proved inactive on the U87MG cell line. For the structures of the intermediates tested, see Figure 21, section 2.4.

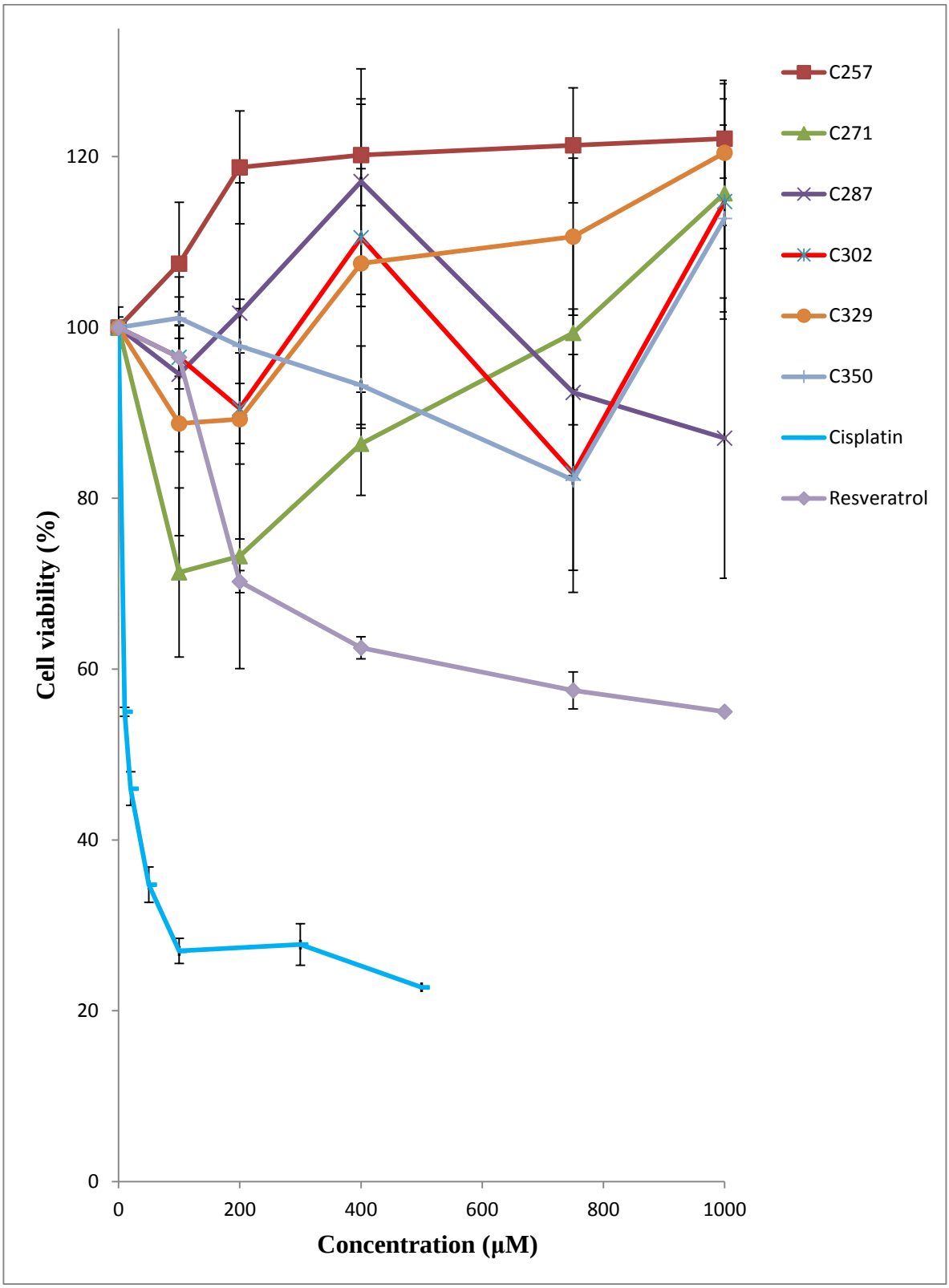

Figure 28: Various novel compounds tested in comparison with cisplatin and resveratrol for 48 h on the 1321N1 cell line. The data points are means of 4 repeats and the error bars represent ±SD.

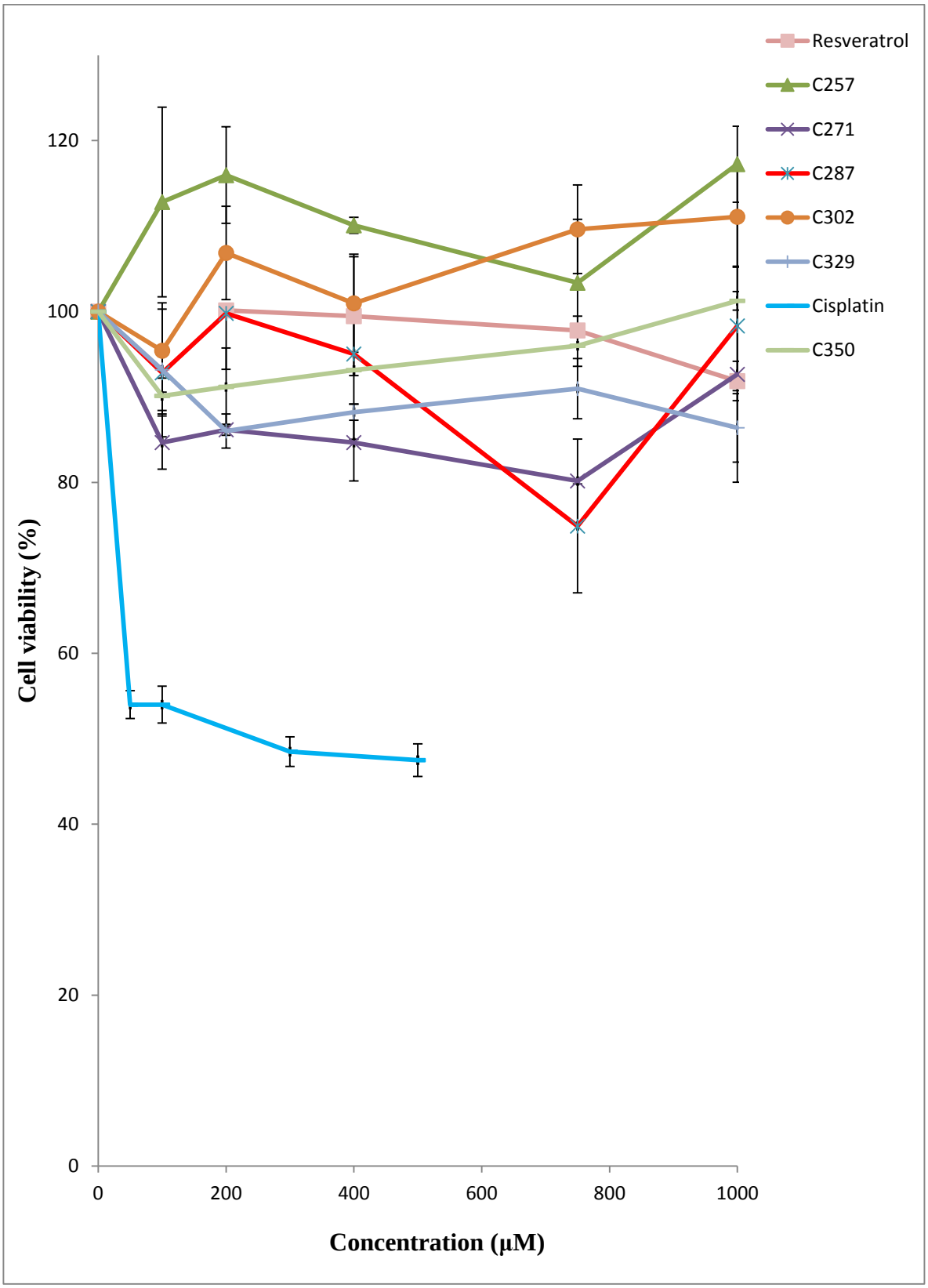

Figure 29: Various novel compounds tested in comparison with cisplatin and resveratrol for 48 h on the U87MG cell line. The data points are means of 4 repeats and the error bars represent ±SD.

Without exception, all of the above test compounds failed to show any significant activity compared to either cisplatin or resveratrol, on both the glioma cell lines studied. Within the experimental variation obtained by the error bars, none of the compounds, against either cell line, managed to reduce the cell viability below 80 %. Unlike cisplatin, which saw a rapid fall to approximately 30 % and 50 % cell viability, in 1321N1 and U87MG respectively, at relatively low concentrations.

Despite this, a previous study in A549 lung cancer cells showed that resveratrol acts by up-regulating p53 and p21 proteins and induces apoptosis by the activation of caspases by disrupting the mitochondrial membrane complex after exposing the cells for 48 h with resveratrol (Whyte *et al.*, 2007). Thus, the results from the current study in accordance with the above mentioned literature indicate that resveratrol behaves differently with different cell types even when the exposure time is kept constant, as evidenced by the activity of resveratrol observed on the 1321N1 and A549 cell lines but none on the U87MG cell line.

These results suggest that although the test compounds are phenolic and structurally similar to the known anti-cancer agent resveratrol, there must be some other particular structural feature of resveratrol which is responsible for its activity against the 1321N1 cancer cell line, a feature which is not present in the above tested intermediates.

3.2.3 Privileged indoles in comparison with cisplatin and resveratrol

Since the test compounds in Figure 28 and Figure 29 did not show any significant activity, six indoles were purchased including compounds 193 and 147 (I3C). Compounds 147 (I3C) and 193 were chosen since it has been shown that both have established activity against cancer cells (Lal and Snape, 2012), moreover, compound 193 is also a 2-arylindole, compounds which are known to be biologically potent (section 1.2.2.3). Compounds 208 and 221 are also readily available 2-arylindoles with further structural modifications which may be useful for producing structure-activity-relationships, whilst compounds 161 and 189 are indoles which lack the 2-aryl group for comparison (Figure 30). As discussed previously, resveratrol (a naturally occurring phytoalexin that is present in grapes, red wine, berries and peanuts and has been studied extensively for its anti-cancer properties (Gagliano *et al.*, 2010; Li *et al.*, 2009; Jiang *et al.*, 2005)) was also used here as a comparison since it is structurally similar to the 2-arylindoles and is also a known natural anti-cancer agent (Gagliano *et al.*, 2010). As Figure 30 (box) shows the aromatic rings and linking carbons of compound 193 and resveratrol overlap well, although the hydroxyl groups of resveratrol are superfluous. Nevertheless, the importance of these hydroxyl groups' presence, and their positions will become clear when these structurally related compounds are tested.

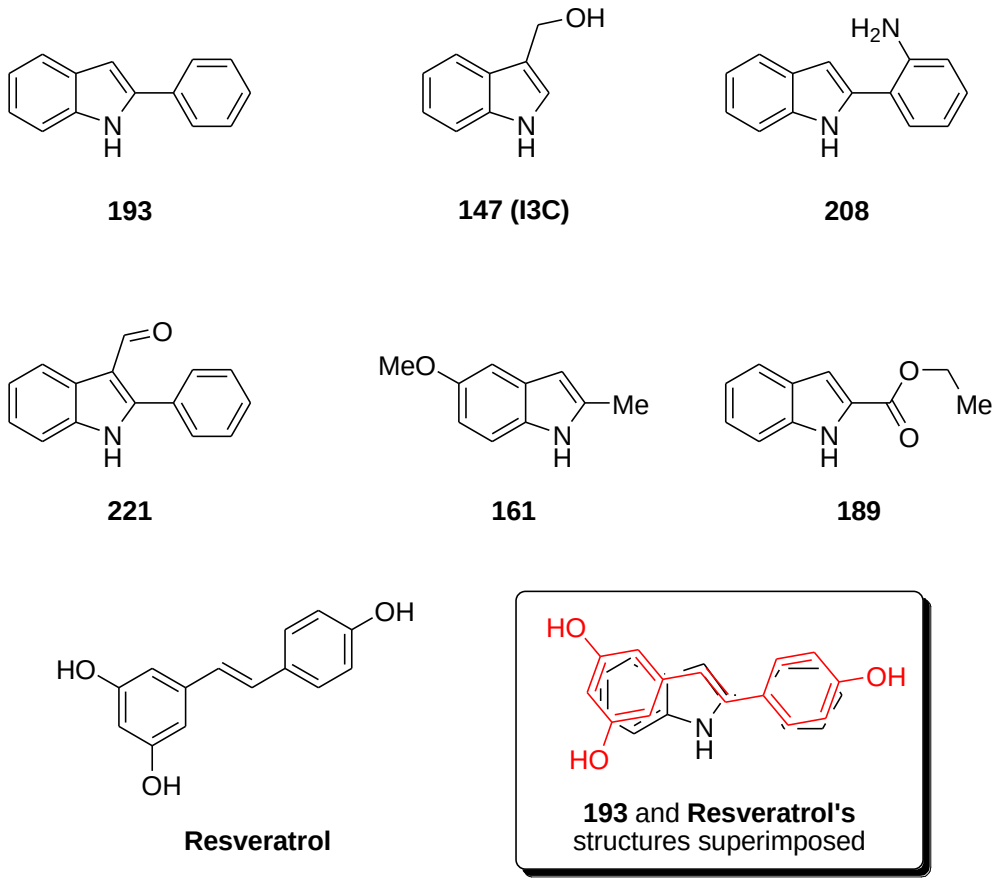

Figure 30: Diagram showing the structures of the tested indoles and the structural similarity between resveratrol and compound 193 (box).

In this regard, the dose response curves of cisplatin, resveratrol, and the various indoles mentioned above were plotted against the 1321N1 and U87MG cell lines using the MTS cell proliferation assay, wherein both these cell lines were exposed to different concentrations of the compounds for 48 h.

As shown in Figure 31 and Figure 32, the IC_{50} value of cisplatin was 11 ±2 µM on the 1321N1 cell line and 310 ±4 µM on the U87MG cell line. The results also showed that whilst compound 147 (I3C) had modest activity [IC_{50} = 309 ± 2 µM (1321N1) and 670 ± 2 µM (U87MG)], compound 193 did not reach its IC_{50} over the same time frame (48 h) but

only reached a maximum growth inhibition of 7 % (U87MG) at 400 µM, however, compound 193 was not able to inhibit the growth of the 1321N1 cell line at all.

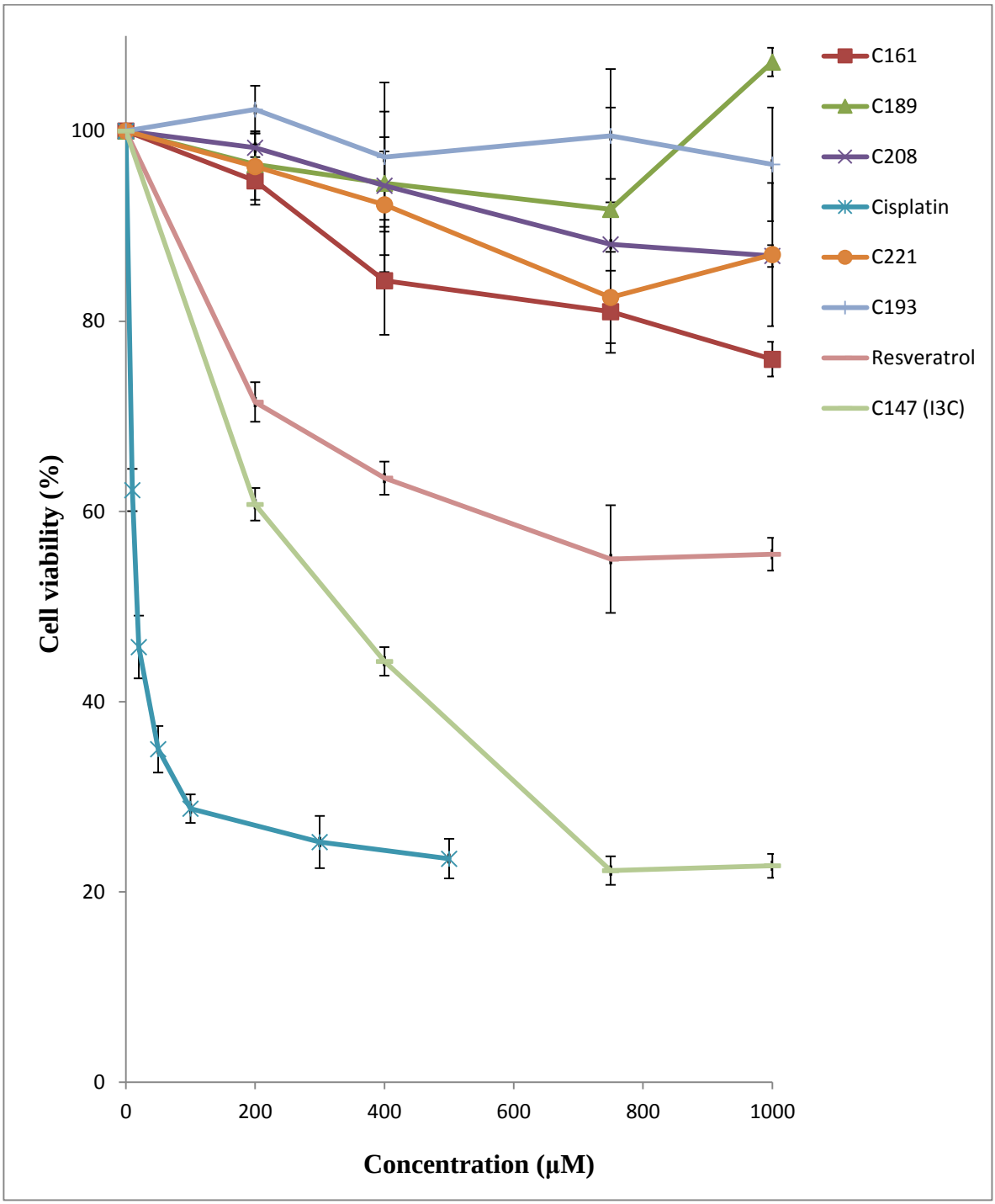

Figure 31: Various indoles tested in comparison with cisplatin and resveratrol on the 1321N1 cell line after treatment for 48 h. The data points are means of 4 repeats and the error bars represent ±SD.

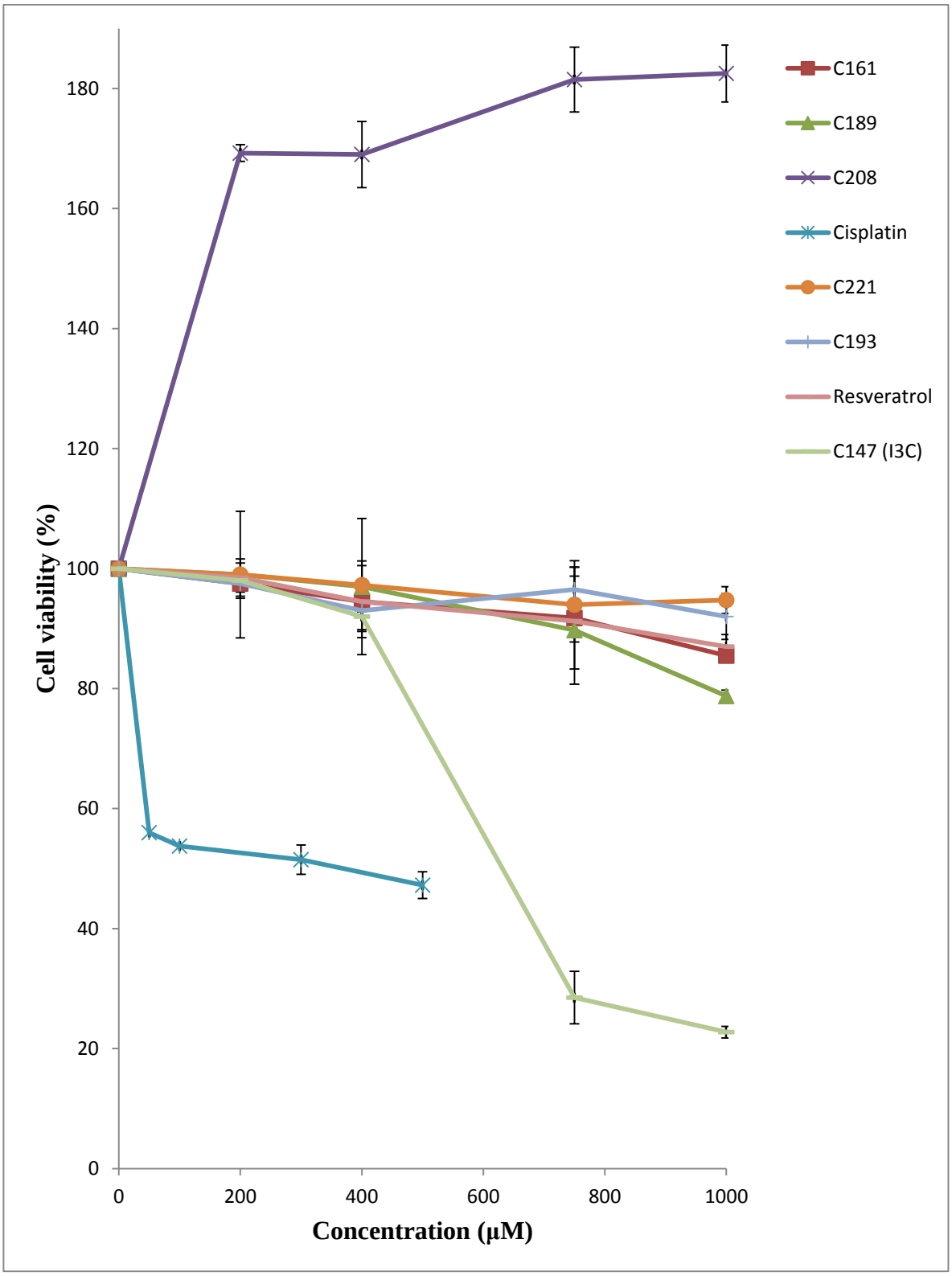

Figure 32: Various indoles tested in comparison with cisplatin and resveratrol on the U87MG cell line after treatment for 48 h. The data points are means of 4 repeats and the error bars represent ±SD.

In support of these results, studies increasingly indicate that dietary I3C prevents the development of oestrogen-enhanced cancers including breast, endometrial and cervical cancers (Brew *et al.*, 2009; Auborn *et al.*, 2003; Mori *et al.*, 2001). For example, the cell division cycle 25A (Cdc25A) phosphatase is overexpressed in a variety of human cancers and I3C induces degradation of Cdc25A, and arrest of the G1 cell cycle, which inhibits the growth of breast cancer cells (Wu *et al.*, 2010). Recent studies showed that the serine124 site of Cdc25A, which is related to cyclin-dependent kinase 2 (Cdk2), is required for I3C-induced degradation of Cdc25A in breast cancer cells, and that interruption of the ATM-Chk2 pathway suppressed I3C-induced destruction of Cdc25A. CHK2 is a protein kinase that is activated in response to DNA damage via the ATM-Chk2 pathway and is involved in cell cycle arrest (Matsuoka *et al.*, 1998) while Cdk2 is directly involved in cell cycle regulation (Morgan, 2007). Another recent study on MDA-MB-231 breast cancer cells showed that I3C induced stress fibres and peripheral focal adhesions in a Rho kinase-dependent manner that led to an inhibition of motility in human breast cancer cells. I3C significantly decreased the *in vitro* migration of these cells and therefore it may be a useful agent in reducing the metastatic spread of tumours (Brew *et al.*, 2009).

An unexpected, yet reproducible and statistically significant result also evident from these results (Figure 32) is that compound 208 appears to *induce* cell proliferation on the U87MG glioma cell line (compared to control cells), but is inactive on the 1321N1 cell line, an intriguing feature which was not pursued here, but may be worth following up in the future. Compounds 189, 161 and 221 were found to be inactive against both cell lines.

Based on the results in Figure 31 and Figure 32, whilst bearing in mind the observed importance of both compound 147 (I3C) and the 2-phenyl group in indoles (Gastpar *et al.*, 1998), it was of interest to know whether or not the preparation of hybrid

structures of compounds 147 (I3C) and 193, thus generating 223a and 209 (Figure 33), would result in improved activity against these cell lines in comparison with the activities of indoles 147 (I3C) and 193 themselves. In the event, indoles 223a (Leete, 1959) and 209 (Snape, 2008) were prepared as previously reported, and both were subjected to the same assay as indoles 147 (I3C) and 193 above. Such compounds would introduce hydroxyl groups into these molecules, a structural feature which appears to be important in the activity of resveratrol (when compared to compound 193) and 147 (I3C) itself (Figure 30).

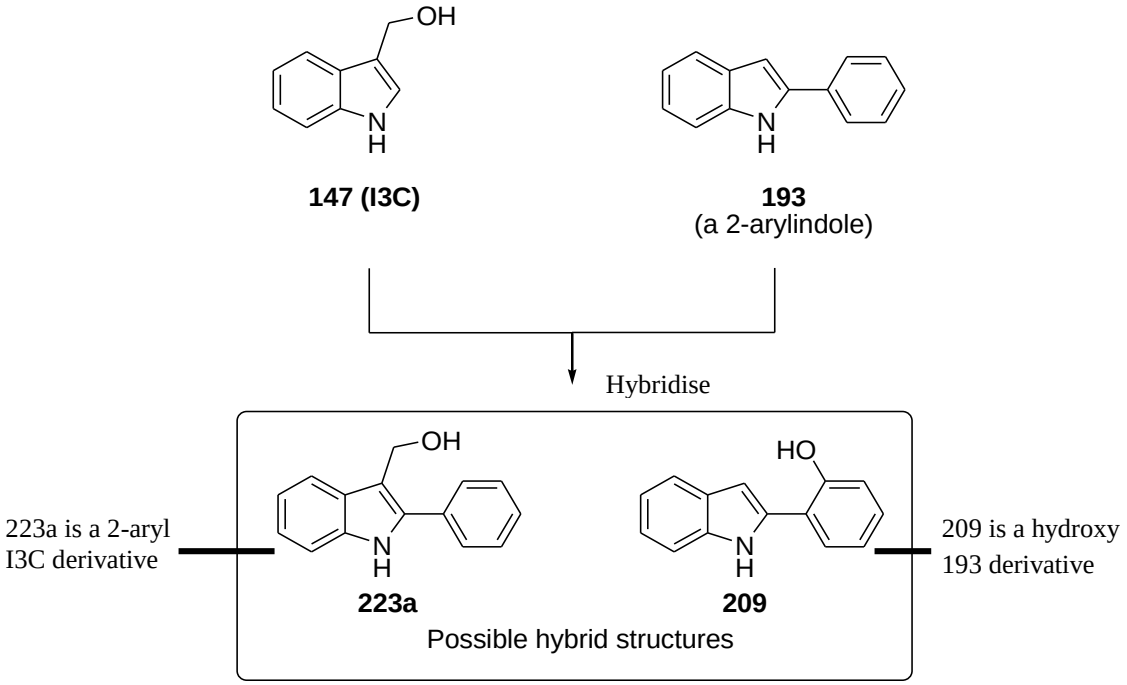

Figure 33: Chemical structures of indole-3-carbinol (147 (I3C), a 2-arylindole (compound 193) and their proposed structural hybrids (compound 223a and 209).

In addition, two further analogues, compounds 223 (So *et al.*, 2007) and 250 were prepared by synthetic chemists in the Snape research group (Prabhu *et al.*, 2013a) and also included as test compounds to determine if there was any influence induced by the hydroxyl group on activity.

For example, a direct comparison between compounds 223a and 147 (I3C) or 193, and between 209 with 193 would allow the importance of the inclusion of the hydroxyl group to be made. Moreover, a direct comparison between compounds 223a and 209 will enable the importance of the position of the hydroxyl group to be made. Furthermore, the readily prepared compound 223 will allow a comparison to be made between the hydroxyl group (in compound 209) and the methoxy group (in compound 223), i.e. is the –OH important for hydrogen bonding donation or will oxygen alone suffice? Similarly, comparison between compounds 208 and 250 will enable the importance of $–NH_2$ vs.–NHAc to be made. All the above-mentioned novel compounds were tested in comparison with cisplatin as the positive control (section 3.2.1.1).

3.2.4 Testing the hybrid compounds and their analogues on glioma cell lines

The newly synthesised hybrid compounds and their analogues (section 3.2.3 above) were tested on the 1321N1 and U87MG glioma cell lines. As before, dose response curves on these cell lines using compounds 209, 223a, 223, 250 and 193 were plotted using the MTS cell proliferation assay, wherein the cell lines were exposed to different concentrations (200 µM, 400 µM, 750 µM and 1000 µM) of these compounds for 48 h.

As shown in Figure 34 and Figure 35, both the hybrid compounds (209 and 223a) were more active than compounds 147 and 193, in both cell lines. Compounds 193 and 223 were found to be inactive, whilst the IC_{50} values were reached at concentrations of 586 ±4 µM and 396 ±4 µM (compound 209) and 111 ±1 µM and 176 ±1 µM (compound 223a) over 48 h on the 1321N1 and U87MG cell lines respectively. Compound 250 reached its

IC_{50} value at concentrations of 695 ±4 µM and 600 ±2 µM on the 1321N1 and U87MG cell lines respectively, table 5 summarises these results.

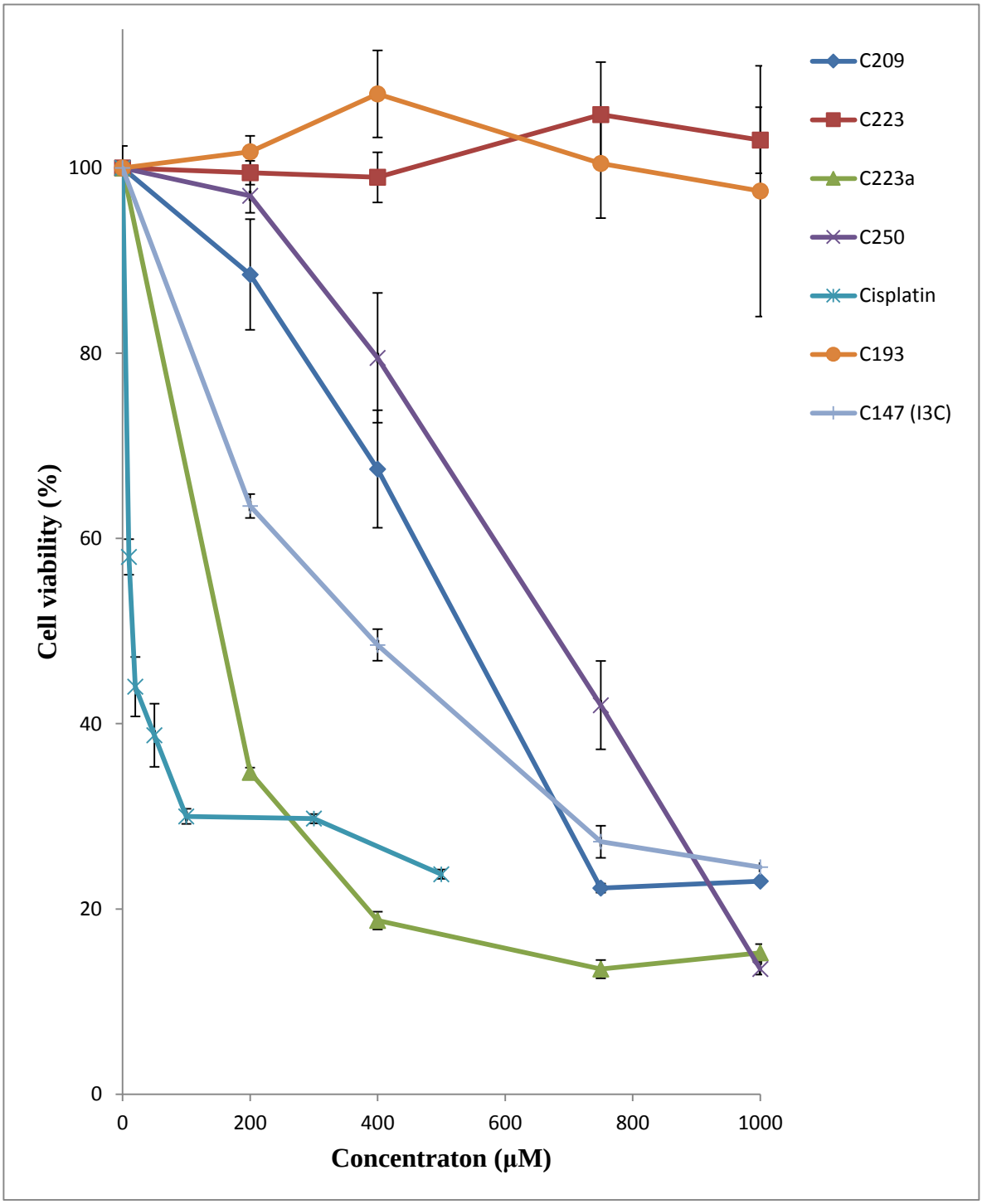

Figure 34: Indoles tested on the 1321N1 cell line for 48 h. The data points are means of 4 repeats and the error bars represent ±SD.

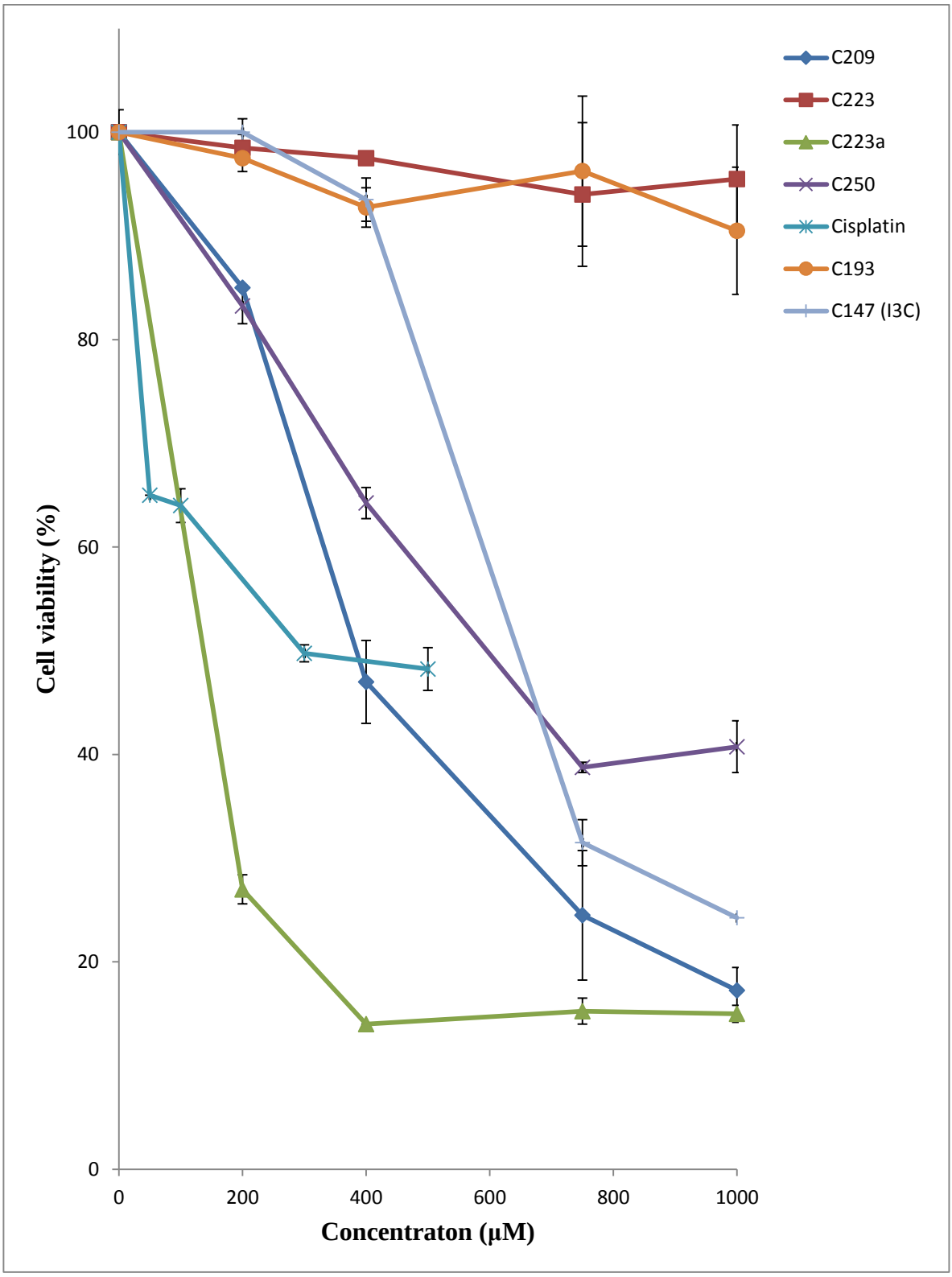

Figure 35: Indoles tested on the U87MG cell line for 48 h. The data points are means of 4 repeats and the error bars represent ±SD.

Table 5: Showing the IC_{50} values of cisplatin, and the indoles against the two different cell lines after being exposed for 48 h using the MTS assay. The values shown are the standard deviations of four repeats.

		MTS assay IC_{50} values	
Entry	Compounds	1321N1 (µM)	U87MG (µM)
1	**147**(I3C)	309±2	670±2
2	**223**	>1000	>1000
3	**223a**	111±1	176±1
4	**209**	586±4	396±4
5	**193**	>1000	>1000
6	**250**	695±4	600±2
7	**221**	>1000	>1000
8	**Cisplatin**	11±2	310±4

The compounds with IC_{50} values > 1000 µM were considered to be inactive in these assays.

3.2.5 The instability of compound 223a in acidic media

As shown in section 3.2.4 (Figure 34 and Figure 35), compound 223a is one of the most potent indoles tested against these cell lines. Unfortunately, it proved to be unstable under acidic conditions, and such behaviour is well documented for similar structures (Bradlow, 2008; Rogan, 2006; Weng *et al.*, 2008), as such, this inherent instability did not justify further investigation here and therefore it was not used in future experiments. As Figure 36 shows, upon exposure to acid, it is known that compound 147 (I3C) loses a molecule of water to give the positively charged species shown. Thus, in the same vein, a similar chain of events is likely to occur in compound 223a, however, in this case, the

addition of the 2-aryl ring in compound 223a may cause further instability by increasing the conjugation of the vinylogous hemiaminal of compound 147 (I3C), and thus increasing the stability of the acid degradation products and rendering the compound more acid sensitive.

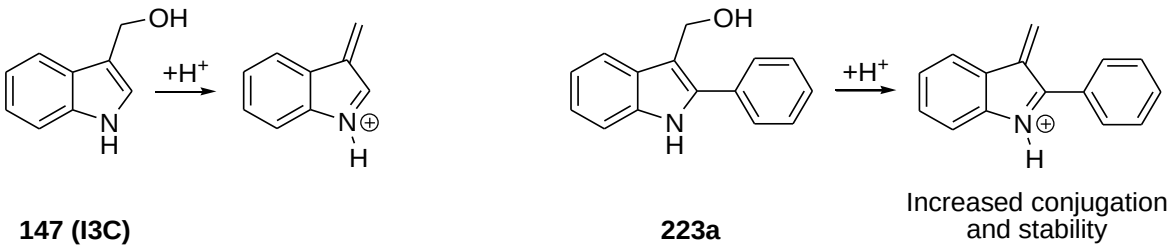

Figure 36: Diagram depicting the acid instability of compound 147 (I3C) and the analogous structure for the presumably more stable acid-degradation product from compound 223a.

An interesting feature of the acid instability of compound 147 (I3C) is that the resulting positively charged species can dimerize to form a compound known as 3,3'-diindolylmethane (DIM), the compound which appears to be the biologically active species of I3C. However, it is unlikely that such dimerization can occur with compound 223a due to the bulky phenyl ring in the 2-position preventing two molecules joining together.

3.3 Structure-activity-relationship of compound 209 with its analogues

As shown above (section 3.2.4), compound 209 was found to be the most active, stable indole tested, and in the event of having to halt the further evaluation of compound 223a due to its instability issues, the aim now was to determine preliminary structure-activity-relationships of compound 209 and try to determine how it may be exerting its effect. Research has shown that in general, 2-arylindoles (Figure 37) are known to be active in a wide range of therapeutic areas (Lal and Snape, 2012), therefore, the structure-activity-

relationship screening was categorised into two main groups: indoles without the 2-aryl group and indoles with the 2-aryl group.

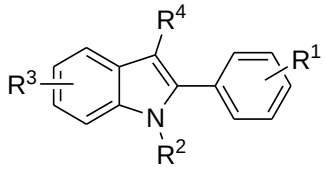

Generic structure of a 2-arylindole

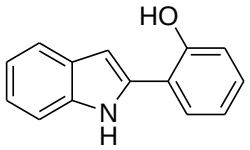

209

Figure 37: Diagram showing the structure of a generic 2-arylindole (left) and the potent compound (209, right).

3.3.1 Indoles without the 2-aryl group

As shown above in Figure 31 and Figure 32, compounds 161 and 189, which lack a 2-aryl group, are completely inactive. The exception being compound 147 (I3C), which is known to possess anti-cancer activity (Safe *et al.*, 2008; Bradlow, 2008; Firestone and Bjeldanes, 2003). That said, of the three compounds which lack a 2-aryl group, compound 147 (I3C) uniquely possesses a hydroxyl group, a functional group which appears to be important when the activities of resveratrol and compounds 209 and 223a are considered, all of which contain at least one hydroxyl group. Based on this, it was hoped that it would be possible to ascertain how important the –OH group was to the activity seen here. A recent study on melanoma cells showed that doxycycline, a member of the tetracycline antibiotics group induced intra-cellular ROS generation and led to c-Jun N-terminal kinase (JNK) activation and cellular apoptosis (Shieh *et al.*, 2010). Observations regarding its structure indicated that doxycycline has multiple –OH groups and that such groups may be playing an important part in inducing cell death. Previous studies have also shown that various naturally occurring dietary compounds like capsaicin, gingerol, 6-paradol and 6-

dihydrocapsaicin protect against experimentally-induced mutagenesis and tumourigenesis (Surh, 1999), and that the anti-cancer effects of these compounds is thought to be due to the common factor that all of them possess –OH groups, and thus this feature may be one of the reasons for their shared anti-cancer activity.

3.3.2 Indoles with the 2-aryl group

In order to test this hypothesis, analogues of compound 209 were purchased or prepared which possessed the 2-aryl group, but lacked the –OH group, in order for them to be screened in the MTS assay so as to determine if this group was important for anti-cancer activity (Figure 38). Compound 193 lacks any substituent on the 2-aryl group and was found to be inactive, as already shown, suggesting that in this case, the –OH may be important for activity. Similarly, to further test its importance, analogues 223 and 221, which also both lack the –OH group, were prepared (223) by the members of the Snape research group or bought (221), and tested. In the case of compound 223, oxygen was present on the 2-aryl group, but not as an –OH group, but rather as an –OMe group. In contrast, compound 221 possesses an aldehyde on the indole ring but no substituents on the 2-aryl group. Upon testing, both of these compounds were found to be inactive, again suggesting that the –OH group may be essential for activity to exit, either on the ring (as with 209 compared to 193) or on the indole ring (as with I3C compared with 221).

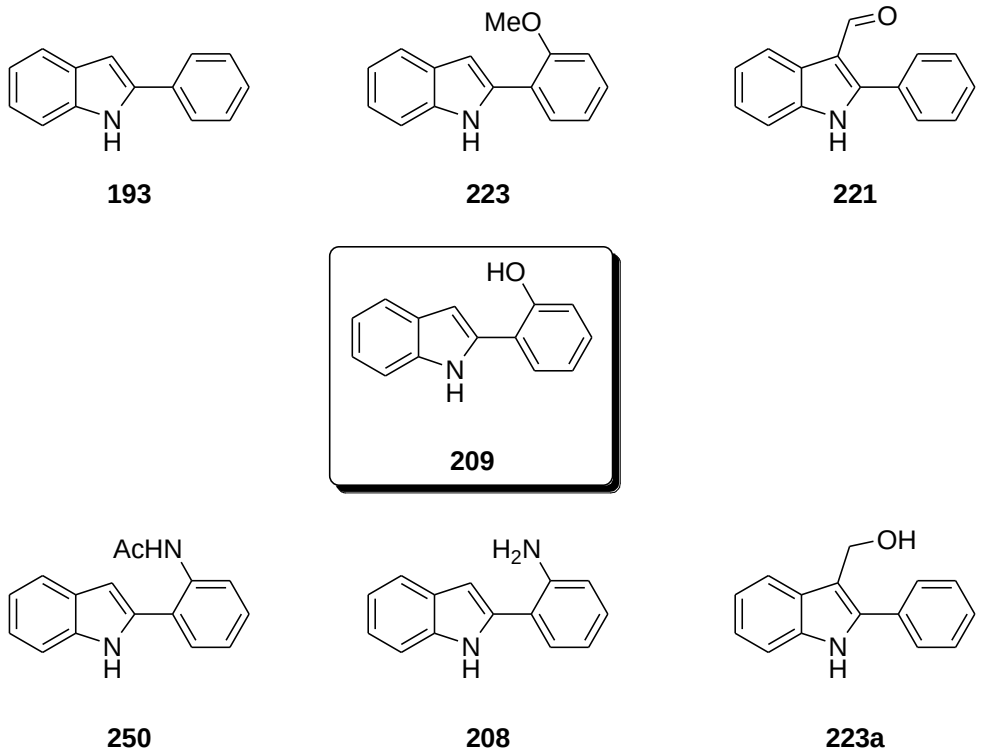

Figure 38: Diagram representing the analogues of compound 209 without the aryl–OH group, but with the 2-aryl ring.

Further analogues of 209 were obtained to ascertain whether an $–NH_2$ group (an amine) on the benzene ring was as active as the –OH group of compound 209. These analogues (208 and 250) were also found to be inactive, or only active at a very high concentration (IC_{50} value of compound 250 is > 600 µM) indicating, once again, that the –OH group seems to be important for their anti-cancer activity in some way.

As alluded to earlier, compound 208 appeared to induce cell growth on the U87MG cell line, however, upon its derivatization to form an acetamide group (-NHAc, compound 250), the compound no longer induced cell growth, but was active at rendering the cells non-viable at very high concentrations.

In Figure 31 and Figure 32, compound 221 was shown to be inactive, therefore it was decided to reduce its aldehyde to the primary alcohol, thus generating the hybrid

compound 223a (Figure 33). The rationale for this decision was that unlike 221 and 193 which had no –OH group on the benzene ring (and were therefore shown to be inactive), 223a had an –OH group that was not on the benzene ring, but was in fact in a similar position to that of indole-3-carbinol's –OH, group and that compound was found to be active (IC_{50} value of indole-3-carbinol on the 1321N1 cell line = 309 µM and U87MG = 670 µM). Clearly, the –OH group was having a large influence on the activity of these indoles.

The results of compound 223a, as determined by the MTS assay, show that it is active on both the 1321N1 and U87MG cell lines suggesting, once again, that the –OH group was very important, but that it does not necessarily need to be attached directly to the benzene ring as in compound 209 (IC_{50} value of compound 223a on the 1321N1 cell line = 111 µM and U87MG = 176 µM). However, it is important to note that whilst all of the initial intermediates tested contain an aromatic –OH group, they were all inactive (section 3.2.2) further corroborating that the indole nucleus, as a whole, appears to be important. This suggestion is supported by the fact that indoles appear to be privileged in their ability to possess activity in a number of therapeutic areas (Horton *et al.*, 2003; Lal and Snape, 2012). Further structure-activity-relationship studies would be the subject of future work on this project to attempt to optimise activity further still.

Having discovered potentially new lead cytotoxic indoles against the glioma cell lines (1321N1 and U87MG), it was essential to determine the mechanism of action of the more active (and stable) indole (compound 209) in the hope that the biological target(s) identified could be used to help with future rounds of lead development by incorporating *in silico* modeling. Preliminary insights into their mechanism of action were gleaned from the

structure of the active compounds, since it was insightful that compounds 147, 209 and 223a were active, yet analogues such as 193, 223 and 221 were not; the hydroxyl group was evidently having an effect. Furthermore, a previous study showed that the phenol group of a related indole was reported as having a large influence on the activity of similar compounds against breast cancer cell lines MDA-MB 231 and MCF-7 (Gastpar *et al.*, 1998), further indicating that the –OH group may be important. Additionally, a recent study has shown that 2-(2,4-dihydroxyphenyl)-8-hydroxy-1,4-naphthoquinone, a derivative of an aromatic compound, juglone, which possesses hydroxyl groups, showed significant anti-cancer activity by inducing apoptosis on immortalised human glioma cell line GLI36 and in a primary human glioblastoma cell culture (Zagotto *et al.*, 2011).

In the compounds studied herein, it was assumed that such a difference in activity between the compounds possessing a hydroxyl group and those that did not, could not be due to differences in hydrogen-bonding, and therefore the hydroxy or phenoxy groups in these compounds may be responsible for the observed cell death in another way.

Recent and previous studies have shown that hydroxy and phenoxy containing compounds may act as anti-oxidants as well as pro-oxidants under certain conditions (Fujisawa *et al.*, 2005; Iwasaki *et al.*, 2011). For example, it is known that certain phenoxy compounds act as anti-oxidants at low concentrations, whereby they are used to scavenge free radicals in the cell, yet they are able to cause cell death at high concentrations, due to themselves forming cell-damaging free radicals. In addition, such a switch can also occur in the presence of Cu^{2+} whereby the chelated compounds are able to induce ROS production and subsequently cause DNA damage (Iwasaki *et al.*, 2011). Factors which may need to be taken into account when the mechanism of action of compound 209 is being considered.

It has been proposed that ortho-dihydroxy groups that can chelate Cu^{2+} induce the greatest pro-oxidant activity (Brown and Kelly, 2007), and a recent study showed that compounds such as ferulic acid, quinic acid and resveratrol did not induce ROS by Cu^{2+}, because they have no ortho-dihydroxy groups (Iwasaki *et al.*, 2011). A result which also agrees with the data of this current study (section 3.5.1), in which resveratrol took more than 24 h to cause cells to become non-viable, possibly suggesting that this compound was acting via a different mechanism other than simply generating ROS at the concentrations used.

3.4 The importance of phenols and phenolic fragments

As shown throughout this thesis so far, it is known that certain indoles possess potent anti-cancer activity which is of great interest to the pharmaceutical industry, and numerous specific derivatives are reported annually (Shankar and Srivastava, 2012). The synthesis and reactivity of these indole derivatives has been a topic of research importance for more than a century, and the primary reason for this continued interest is the wide range of biological activity found among indoles (Sharma *et al.*, 2010; Lal and Snape, 2012). Research has also shown that sterically hindered phenolic motifs in indoles could give rise to added anti-oxidant properties, and such sterically hindered phenols also constitute structural fragments of a number of non-indole drugs too (Nugumanova *et al.*, 2007). Therefore, compounds derived from both indoles and sterically hindered phenols may have promising biological activity, as has been shown here.

Research by others has also shown that phenols may directly contribute to high anti-proliferative and pro-apoptotic activity (Marian *et al.*, 2004; Zagotto *et al.*, 2011). For

example, carnosic acid, a rosemary phenolic compound, has been shown to display anti-cancer activity and induce ROS mediated apoptosis in human neuroblastoma IMR-32 cells (Tsai *et al.*, 2011). Their results also suggested that down-regulation of the anti-apoptotic Bcl-2 protein occurred in cells treated with carnosic acid. This effect was accompanied by increased activation of p38 and by decreased activation of extracellular signal-regulated kinase (ERK) as well as activation of JNK (Tsai *et al.*, 2011).

Furthermore, curcumin, the principal curcuminoid of the popular Indian spice turmeric, is known to show high anti-tumour activity on malignant cells (Tuttle *et al.*, 2011; Youssef and El-Sherbeny, 2005). The role of curcumin in inhibiting malignancy can also be due to its anti-oxidant activity (Nagabhushan M and SV, 1987), and Sreejayan and Rao have reported that the phenolic hydroxyl and methoxy groups on the phenyl ring, and the 1,3-diketone system are the two most important structural features that contribute to its anti-oxidant properties (Sreejayan and Rao, 1996; Sreejayan and Rao, 1997; Jovanovic *et al.*, 2001; Sun *et al.*, 2002; Anto *et al.*, 2002). Taken together, the importance of the indole nucleus and phenolic compounds suggests that the potent compound 209 used in this study (Figure 33), which possesses a phenolic group attached to indole, may be partly responsible for its activity.

3.5 Time course studies of compound 209.

3.5.1 Time course study using the MTS assay

During the MTS cell viability assay, at relatively high concentrations, visual morphological changes were observed to take place on the cells treated with compound 209, an effect which was detected within the first hour of treatment. Based on this rapid result, a time course study was performed to determine the minimum time necessary for compound 209 to cause the cells to become non-viable (as determined by the MTS assay). In the event, as shown in Figure 39 and Figure 40, the cytotoxic effect of compound 209 (750 µM and 1000 µM) starts 1.5 h after the treatment on the 1321N1 and U87MG cell lines.

As highlighted in Figure 30 (box), the structural similarity between resveratrol and compound 193 is high. Based on this structural overlay, compound 209 has even greater similarity to resveratrol than compound 193 due to the presence of the hydroxyl group on the aryl ring in compound 209, therefore resveratrol was also used in this time course study, however, resveratrol was only used on the 1321N1 cell line since U87MG was found to be resistant to resveratrol (Figure 41).

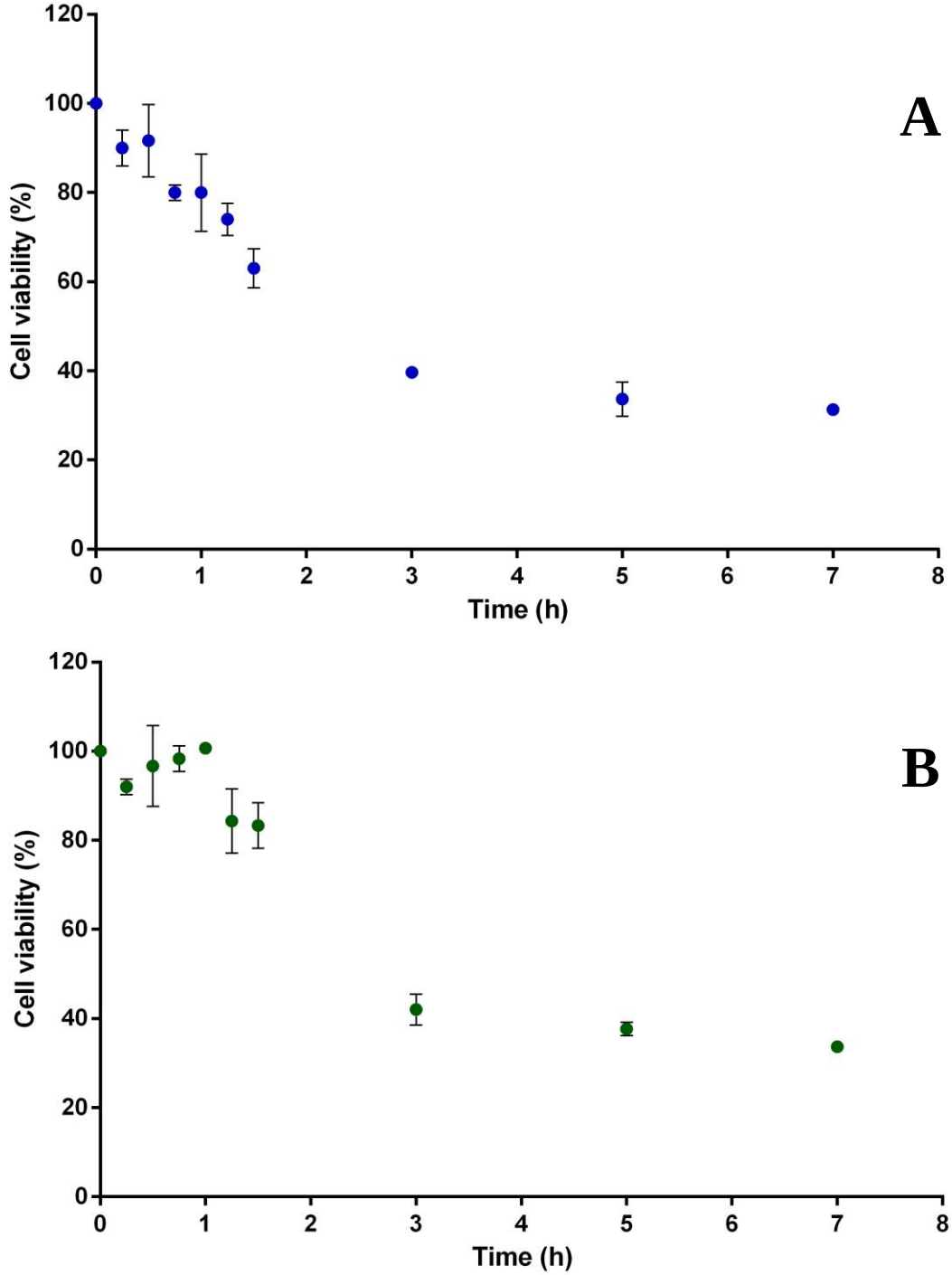

Figure 39: 1321N1 cell line treated with compound 209 at two different concentrations.

(A) 1000 µM and (B) 750 µM at various time points where it can be seen that the cytotoxic effect starts after 1.5 h after treatment. The data points are means of 4 repeats and the error bars represent ±SD.

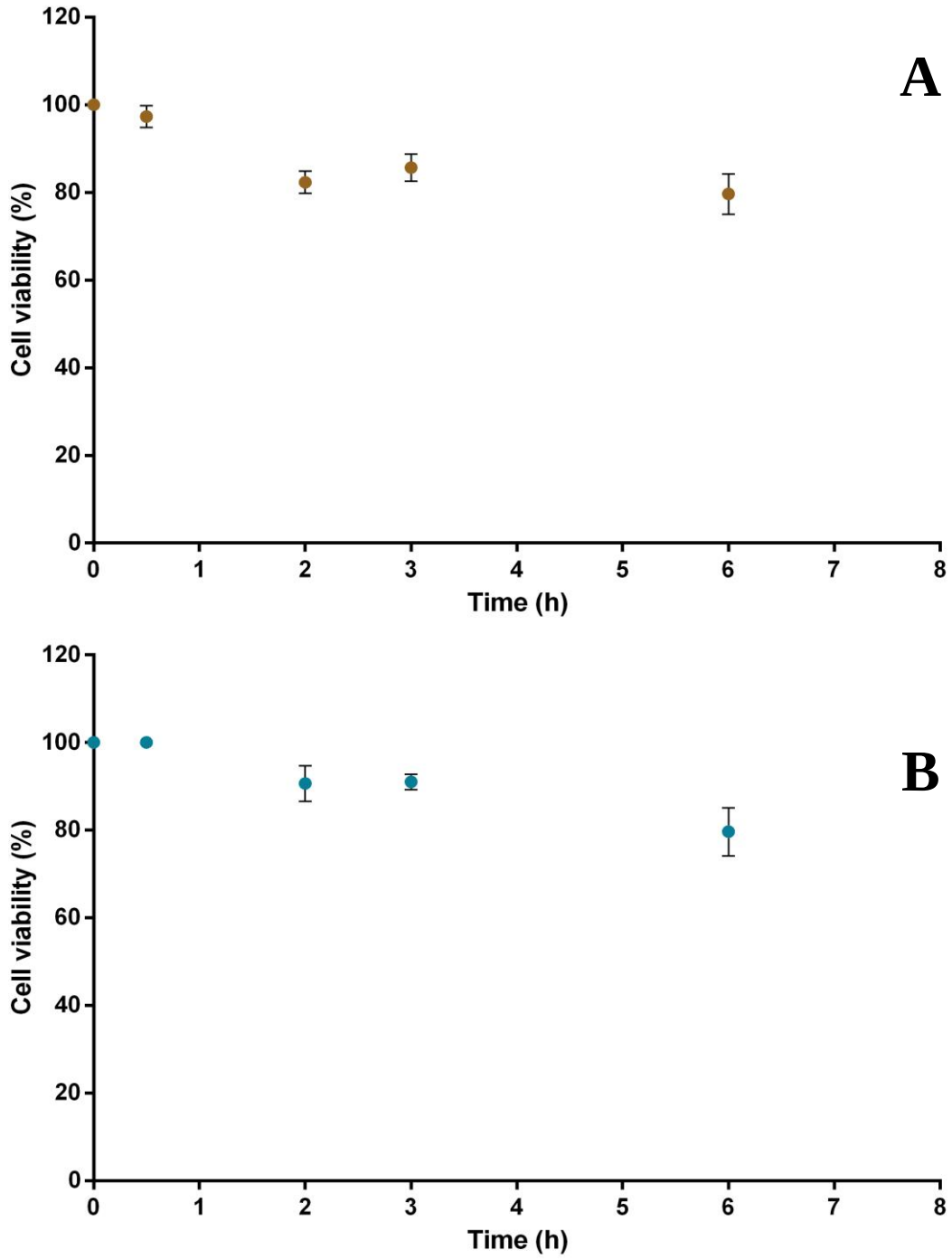

Figure 40: 1321N1 cell line treated with resveratrol at two different concentrations.

(A) 1000 µM and (B) 750 µM at various time points. It can be clearly seen that there is no immediate cytotoxic effect like that observed with compound 209. The data points are means of 4 repeats and the error bars represent ±SD.

The time course study for resveratrol (Figure 40) suggested that it required more than 24 h to display its effects, a result which is in contrast to compound 209 which exhibited up to 40 % cell death within 2 h on both cell lines (Figure 39 and Figure 41). This suggests that the mechanism of action of compound 209 is different to that of resveratrol, despite being structurally comparable and both possessing phenolic group(s), results which may indicate that the entire structure (and possibly the indole nucleus itself), as a whole, may be required for quick cell death to occur. Despite their structural similarities, the differing time taken for resveratrol and compound 209 to exert their anti-cancer effects, suggests that their mechanisms of action must be different.

As seen here in glioma cells, previous research has showed that resveratrol induces cell death within 24 h in ovarian cancer cells, and that the mitochondrial release of cytochrome c, formation of the apoptosome complex, and caspase activation was observed after treatment with resveratrol (Opipari *et al.*, 2004). Remarkably, even with such molecular features of apoptosis, analysis of resveratrol-treated cells by light and electron microscopy revealed morphological and structural changes indicating autophagy, rather than apoptosis in these ovarian cancer cells (Opipari *et al.*, 2004). This may indicate that resveratrol can induce cell death through two distinct pathways, but that both of these pathways are not able to induce the quick cell death seen by treatment with compound 209 on the glioma cells.

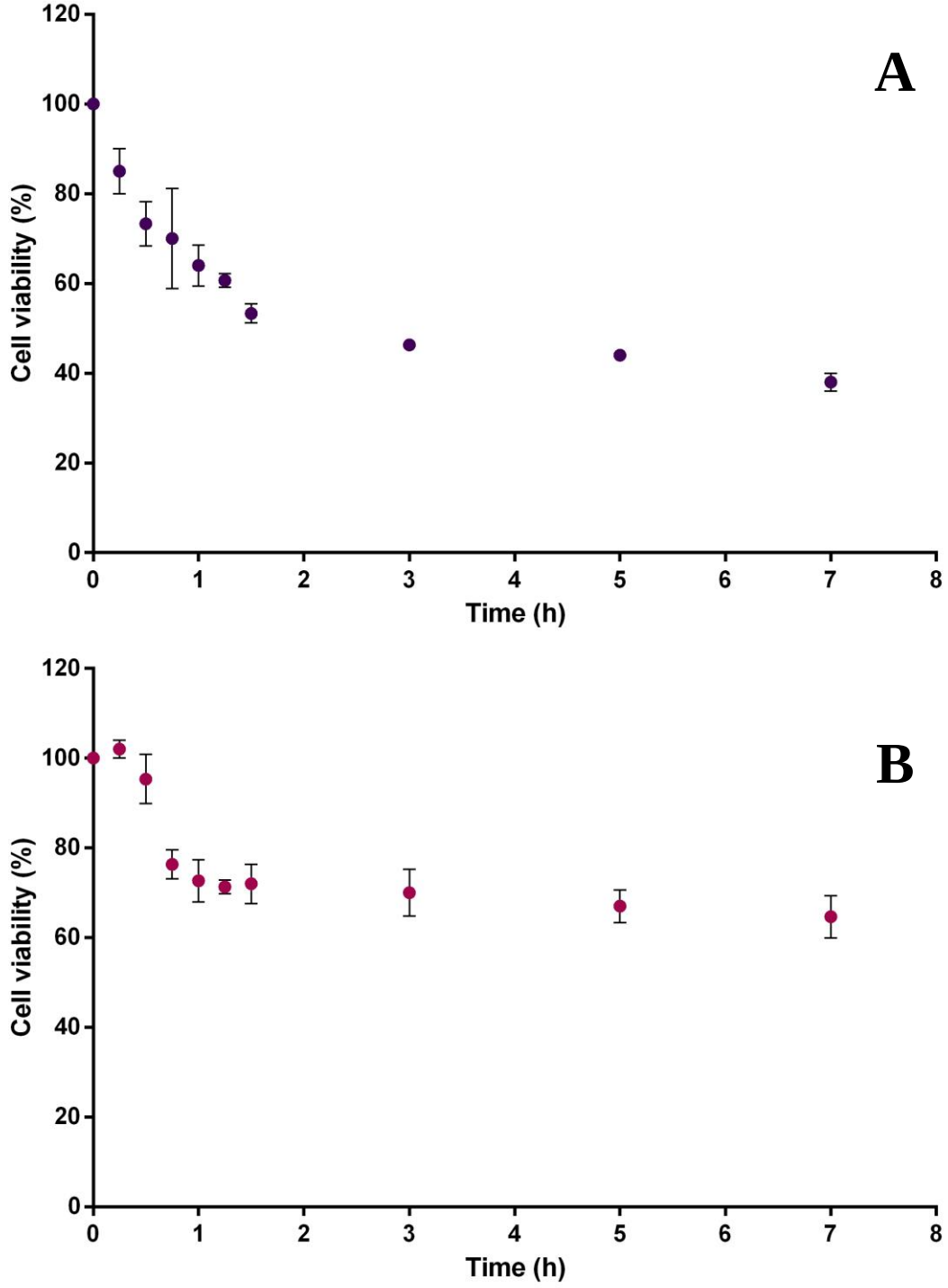

Figure 41: U87MG cell line treated with compound 209 at two different concentrations.

(A) 1000 µM and (B) 750 µM at various time points where it can be seen that the cytotoxic effect starts after 1.5 h after treatment. The data points are means of 4 repeats and the error bars represent ±SD.

3.5.2 Time course study using the trypan blue exclusion test

In addition to the onset of cell death occurring after 1.5 h on both cell lines, as indicated with the MTS assay (section 3.5.1), a time course study using trypan blue was also performed to find out the time required by compound 209 to cause membrane lysis, a feature indicated by the cell being stained blue, signifying cell death has occurred (section 2.3.3).

In the event, membrane lysis (as indicated by trypan blue staining) was observed on both 1321N1 [Figure 42 D] and U87MG [Figure 43 D] cell lines after 1.5 h of treatment with compound 209. Representative images from one of three experiments yielding similar results are shown.

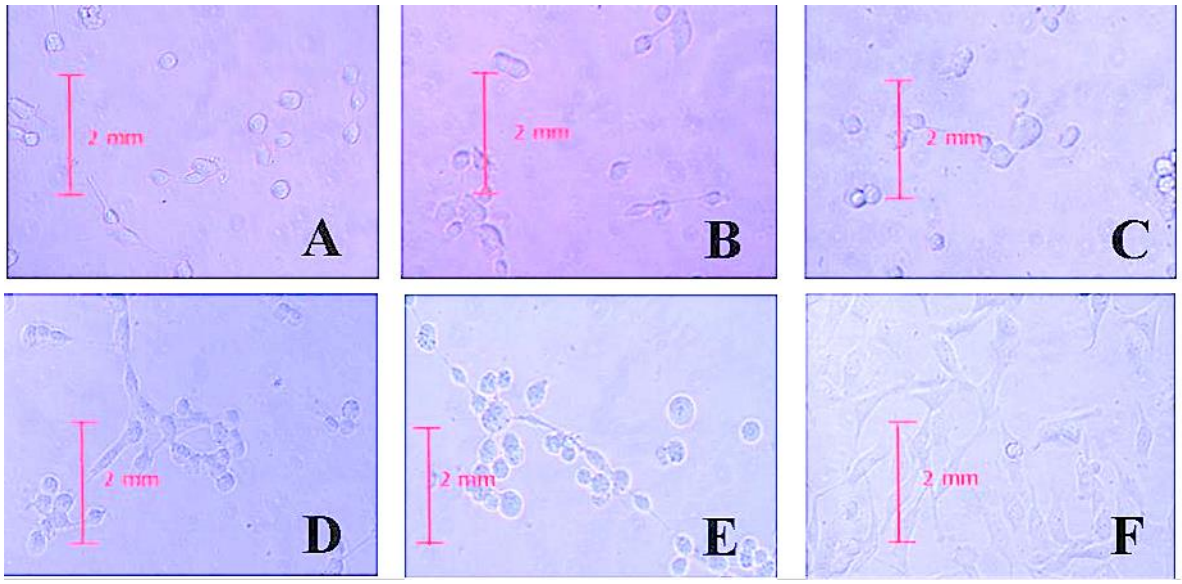

Figure 42: Images of human glioma cells 1321N1 showing membrane lysis (as indicated by trypan blue staining) after treatment with compound 209 (1000 µM) at different time points at 20X magnification.

A) 15 min (0.25 h) B) 45 min (0.75 h) C) 75 min (1.25 h) D) 90 min (1.5 h) E) 120 min (2 h) F) control untreated cells.

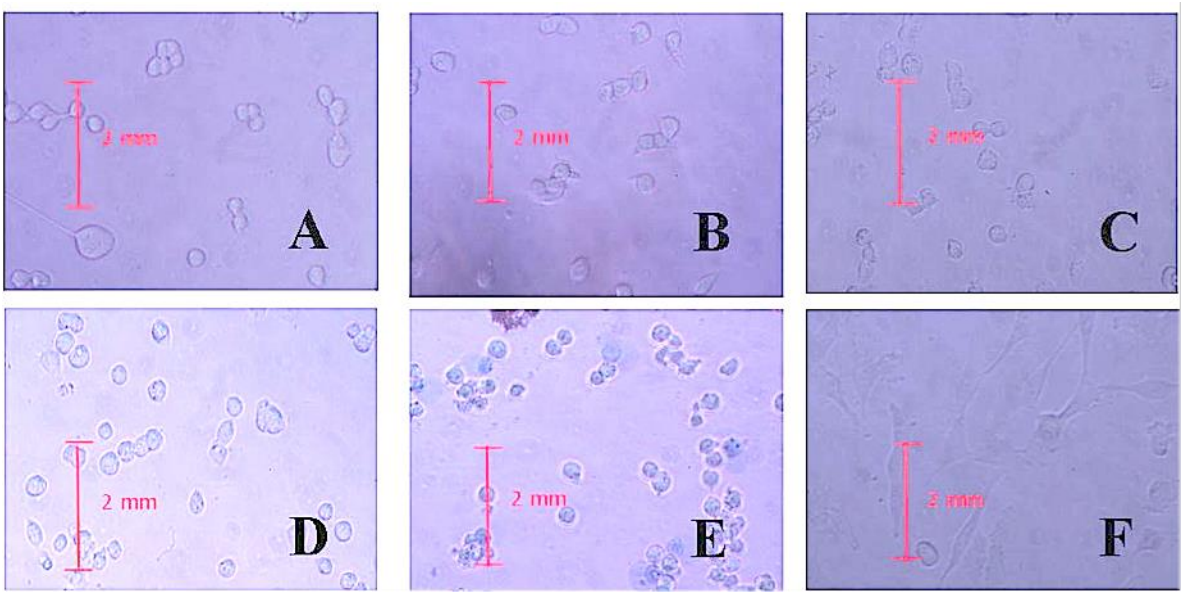

Figure 43: Images of human glioma cells U87MG showing membrane lysis (as indicated by trypan blue staining) after treatment with compound 209 (1000 µM) at different time points at 20X magnification.

A) 15 min (0.25 h) B) 45 min (0.75 h) C) 75 min (1.25 h) D) 90 min (1.5 h) E) 120 min (2 h) F) control untreated cells.

As can be seen from Figure 42 and Figure 43, cell death (i.e. cells are stained blue) was observed with 1000 μM of compound 209, between 90-120 min (D and E in Figure 42 and Figure 43), data which supports the results observed with the MTS assay (section 3.5.1). Together, these time course studies suggest that at high concentrations, compound 209 has a rapid effect on cell viability which may be an indication of necrosis. This suggests that the concentrations of compound 209 may play an important role in deciding the type of cell death pathway to be followed, as has been observed for other phenolic compounds which are either anti-oxidant (at low concentrations) or pro-oxidants (at high concentrations) (Iwasaki *et al.*, 2011; Fujisawa *et al.*, 2005).

3.6 The activity of various indoles on the 1321N1, U87MG and SVGp12 cell lines (2 h)

Up until this point the best compounds discovered were indoles 209 and 223a, a feature which was temporarily put down due to the presence of the hydroxyl group in these structures, a feature which they share with the active compound 147 (I3C). Contrastingly, it was possible to use indoles 193 and 223 as negative controls, since both had the hydroxyl group either missing or masked, and are consequently inactive, a feature which suggests that the hydroxyl group is important. Having established an apparent rapid mechanism of action for indole 209 (section 3.5), compounds 209, 193 and 223 were further tested on the 1321N1, U87MG and SVGp12 cell lines for 2 h. The previous time course study using compound 209 on the glioma cell lines (section 3.5) showed that this indole exhibited its anti-cancer activity within 2 h. The following study was therefore performed to determine their IC_{50} values at the 2 h time point, and to see whether they all act and exhibit an effect, in a similar way as seen at the 48 h time point (Figure 34 and Figure 35). As seen

previously in Figure 31 and Figure 32, cisplatin was used as a positive control, whereas, in this 2 h study cisplatin was not used because it needs at least 48-72 h to exert its cytotoxic effect (Shervington *et al.*, 2009; Pisanu *et al.*, 2014). The SVGp12 cell line (non-cancerous) was also introduced in this study to determine whether compound 209 was specific to cancer cells or whether it exhibits cytotoxicity on all cell types, including non-cancerous ones.

Dose response curves of compounds 209, 193 and 223 on 1321N1, U87MG and SVGp12 cell lines were plotted using the MTS cell proliferation assay, wherein the cell line was exposed to different concentrations of these compounds for 2 h. The active compound 209 and two inactive compounds (223 and 193) were chosen to be tested on the above cell lines according to the results obtained in section 3.2.4. Compound 193, being completely inactive on the 1321N1 and U87MG cells lines, was used as a negative control, whereas compound 223, which was only weakly active and therefore did not reach the IC_{50} value, was also included. Compound 250 was not used in this study as its IC_{50} value (> 600 µM on both the cell lines) was considered too high compared to compound 209.

In the 2 h time course experiments (Figure 44 and Figure 45), IC_{50} values of 996 ±5 µM and 700 ±3 µM were obtained for compound 209 on the 1321N1 and U87MG cell lines respectively (table 6). In addition, as shown in Figure 46, the IC_{50} value of compound 209 was 750 ±2 µM on the SVGp12 cell line. As expected, compound 223 was only weakly active and did not reach the IC_{50} value, whereas compound 193 was completely inactive (table 6).

Table 6: Showing the IC_{50} values of indoles against the two different cell lines after being exposed for 2 h using the MTS assay. The values shown are the standard deviations of four repeats.

		MTS assay IC_{50} values		
Entry	Compounds	1321N1 (µM)	U87MG (µM)	SVGp12 (µM)
1	**209**	996 ±5	700 ±3	750 ±2
2	**223**	>1000	>1000	>1000
3	**193**	>1000	>1000	>1000

Those compounds with low activity (i.e. less than 10 % cell death) at a concentration of 1000 µM were considered to be inactive in these assays.

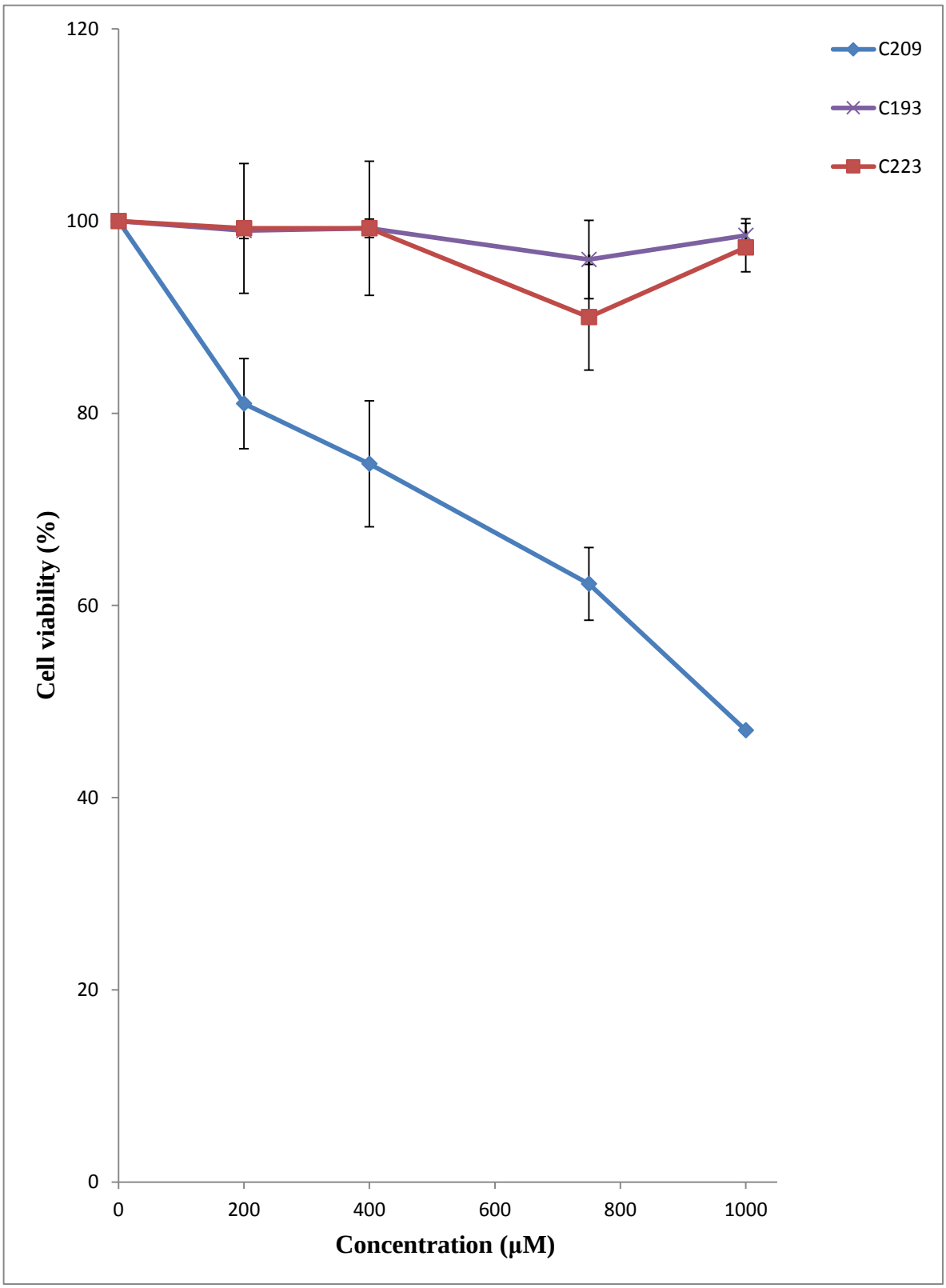

Figure 44: Indoles tested on the 1321N1 cell line for 2 h using the MTS assay. The data points are means of 4 repeats and the error bars represent ±SD.

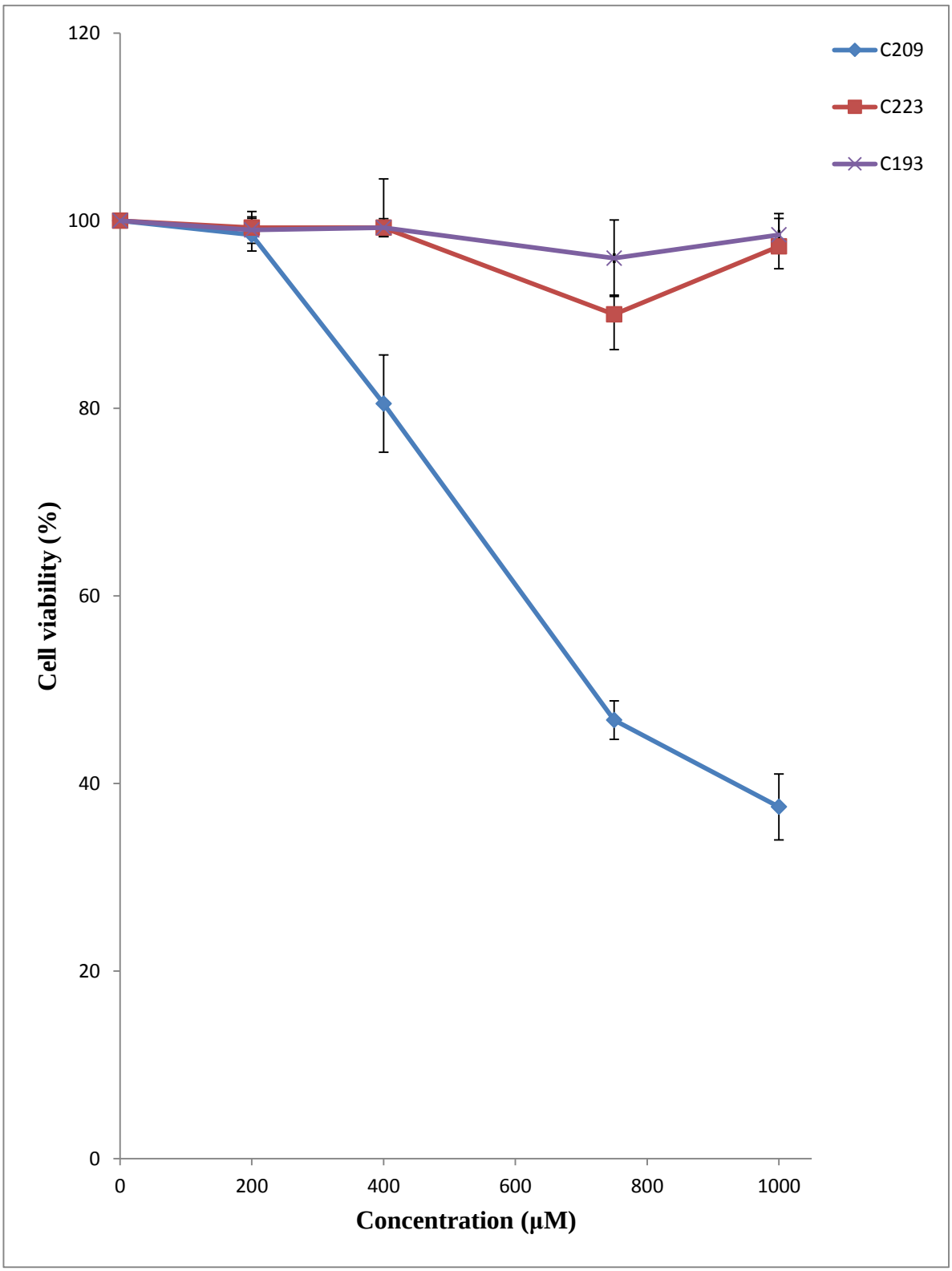

Figure 45: Indoles tested on the U87MG cell line for 2 h using the MTS assay. The data points are means of 4 repeats and the error bars represent ±SD.

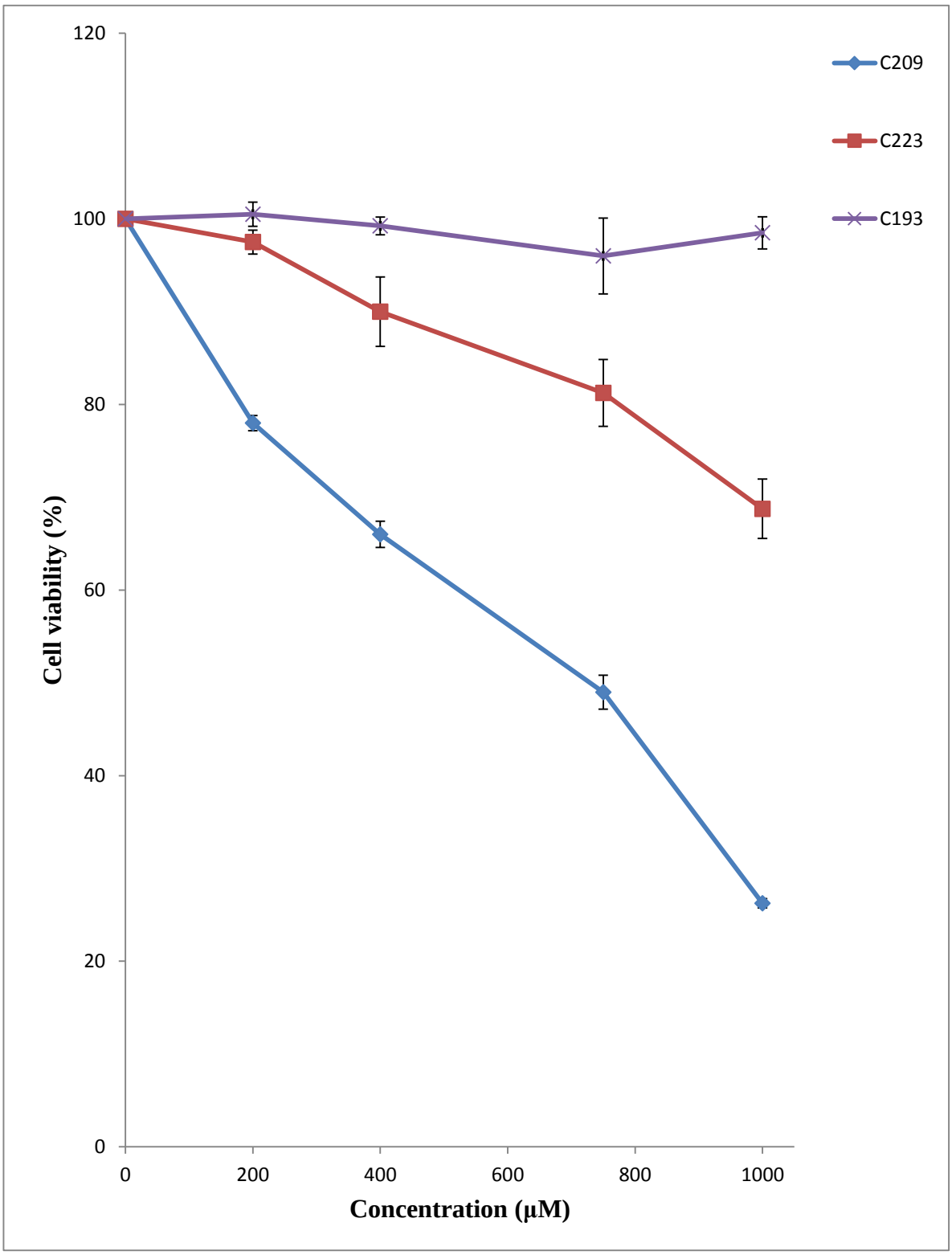

Figure 46: Indoles tested on the SVGp12 cell line for 2 h using the MTS assay. The data points are means of 4 repeats and the error bars represent ±SD.

3.6.1 Corroborative study of compound 209 using the ATP assay.

Up to this point the cytotoxicity of the test compounds had only been examined using the MTS assay, however, before further mechanistic studies were carried out, it was felt prudent to corroborate these results using a second cell viability assay.

During these experiments, dose response curves of compounds 209, 193 and 223 were obtained, on both the 1321N1 and U87MG cell lines, using an ATP cell viability assay (section 2.3.2). The cell lines were exposed to different concentrations of these compounds for 2 h, wherein compounds 193 and 223 were included as negative controls, as per the results obtained from the MTS assay (section 3.2.4).

Table 7 outlines the IC_{50} results of the ATP assay on both the cell lines vs. the test compounds.

Table 7: Showing the IC_{50} values of the indoles tested against the two different cell lines after being exposed for 2 h using the ATP assay. The values shown are the standard deviations of four repeats.

		ATP assay IC_{50} values	
Entry	Compounds	1321N1 (µM)	U87MG (µM)
1	**209**	1000 ±4	878 ±3
2	**223**	>1000	>1000
3	**193**	>1000	>1000

Those compounds with low activity (i.e. less than 10 % cell death) at a concentration of 1000 µM were considered to be inactive in these assays. Unlike the MTS assay, the ATP assay can measure cells as low as 4 cells per sample, in contrast to MTS assay which can only detect samples containing more than 1000 cells, as such, the ATP assay is highly

sensitive (Petty *et al.*, 1995) and thus is considered a more accurate assay and thus can be used for corroborating the results obtained using the MTS assay. Despite this increased accuracy, the ATP assay was not used throughout the whole of my PhD project because, not only is it a more expensive protocol, it is also more time consuming compared to the MTS assay. As such, the use of the MTS assay allowed quick and inexpensive data to be obtained, thus enabling structure-activity data to be more easily achieved.

The data obtained from the ATP assay (table 7) gave a similar pattern of activity for both the cell lines to that of the MTS assay, thus enabling me to confidently trust the results obtained throughout by the MTS assay. Although the activity obtained with the ATP assay is only modest, the values in table 7 are IC_{50}s, showing that 50 % cell death had occurred at the concentration quoted in the table.

Section B: Preliminary investigation into the mechanism of action of the most potent indole

3.7 Detection of Reactive Oxygen Species (ROS).

3.7.1 Possible cellular mechanism of action of compound 209

It was important to determine the cellular mechanism(s) via which the most potent compound could induce cell death as this would help in narrowing down the cellular processes which is active indole may be targeting. The effects of compound 209 were rapid (2 h) as opposed to other conventional drugs which require at least 48 h of treatment to induce cell death.

Different classes of anti-cancer drugs act via differing mechanisms to induce cell death; these include: apoptosis, derangement in calcium homeostasis, cell cycle arrest and alteration in gene expressions (Pratheeshkumar *et al.*, 2012). The challenge here was to find a cell death mechanism which was as quick as that observed (i.e. within 2 h). Since the above mentioned cell death mechanisms cannot complete their cycle in such a short time span of 2 h, it was hypothesised that such quick cell death might be mediated by oxidative stress [generation of excessive reactive oxygen species (ROS)]. For example, in a recent study on the U87MG cell line, it has been observed that basal ROS levels can increase to toxic levels within 30 min following treatment with β-lapachone, a natural naphthoquinone compound (Park *et al.*, 2011).

Moreover, another separate study showed that oncogenic transformation of ovarian epithelial cells with a human plasmid [H-Ras^{V12}] caused elevated ROS levels within 5 h and rendered the malignant cells highly sensitive to beta-phenylethyl isothiocyanate

(PEITC, a chemopreventive agent found in abundance in watercress), a process which effectively disabled the glutathione anti-oxidant system and caused severe ROS accumulation preferentially in the transformed cells due to their active ROS output. This excessive ROS production caused oxidative mitochondrial damage and inactivation of redox-sensitive molecules (Trachootham *et al.*, 2006). Such precedent prompted a new study in this project directed at identifying if any ROS mediated cell death was occurring in the glioma cell lines by the most suitable compound identified by the MTS assay (section 3.2.4). Therefore, in this regard, both the glioma cell lines (1321N1 and U87MG) were studied for ROS generation post-treatment with the most potent novel (and stable) indole, compound 209.

3.7.2 Confocal microscopy using an "Image-iT LIVE Green Reactive Oxygen Species Detection Kit".

This study was performed to help understand the possible mechanism behind the apparent quick cell death caused by compound 209 on the 1321N1 glioma cell lines. An Image-iT™ LIVE Green Reactive Oxygen Species Detection Kit was used to detect the reactive oxygen species in the 1321N1 and the glioma cell lines. The assay is based on the compound, carboxy-H_2DCFDA, a reliable fluorogenic marker for ROS in live cells, whereby oxidatively stressed cells fluoresce when labelled with the carboxy-H_2DCFDA dye provided in the kit. The results can then be observed by either confocal microscopy (qualitative only) or by flow cytometry (quantitative).

Initial qualitative data was obtained using confocal microscopy which was used to visualise any fluorescence produced, before moving on to use flow cytometry to quantify the amount of fluorescence produced. This additional observational step was required

because a previous kit ordered for detecting ROS, for some unknown reason, did not work. Therefore, in all future experiments with this kit, to ensure that the assay was working properly, it was performed using a confocal microscope as well using the positive control, *tert*-butyl hydroperoxide (TBHP), supplied by the assay manufacturing company. For conformation of the assay working properly, the 1321N1 cell line was used (Figure 47). Once it was confirmed that the assay was working, all future experiments were then performed on a flow cytometer so that the amount of fluorescence produced could be quantified.

During the experiment, cells were thoroughly washed at each step to prevent background staining and were imaged immediately and fluorescence was observed. The results with compound 209 (500 µM), for 1 h, suggested that the cells were under oxidative stress during this time, as indicated by the increased levels of fluorescence visualised as compared to the control cells (Figure 47). The positive control used in this experiment was *tert*-butyl hydroperoxide (TBHP) (100 µM) which is a common inducer of ROS (Bhattacharya *et al.*, 2011) and was suggested and provided by Invitrogen Ltd.

It is known that ROS generation is instantaneous and at optimum levels within 2 h, but then reduces considerably after 24 h, as has been shown before by (Rogalska *et al.*, 2011), and thus the conditions used here were focussed on a 1 h timeframe.

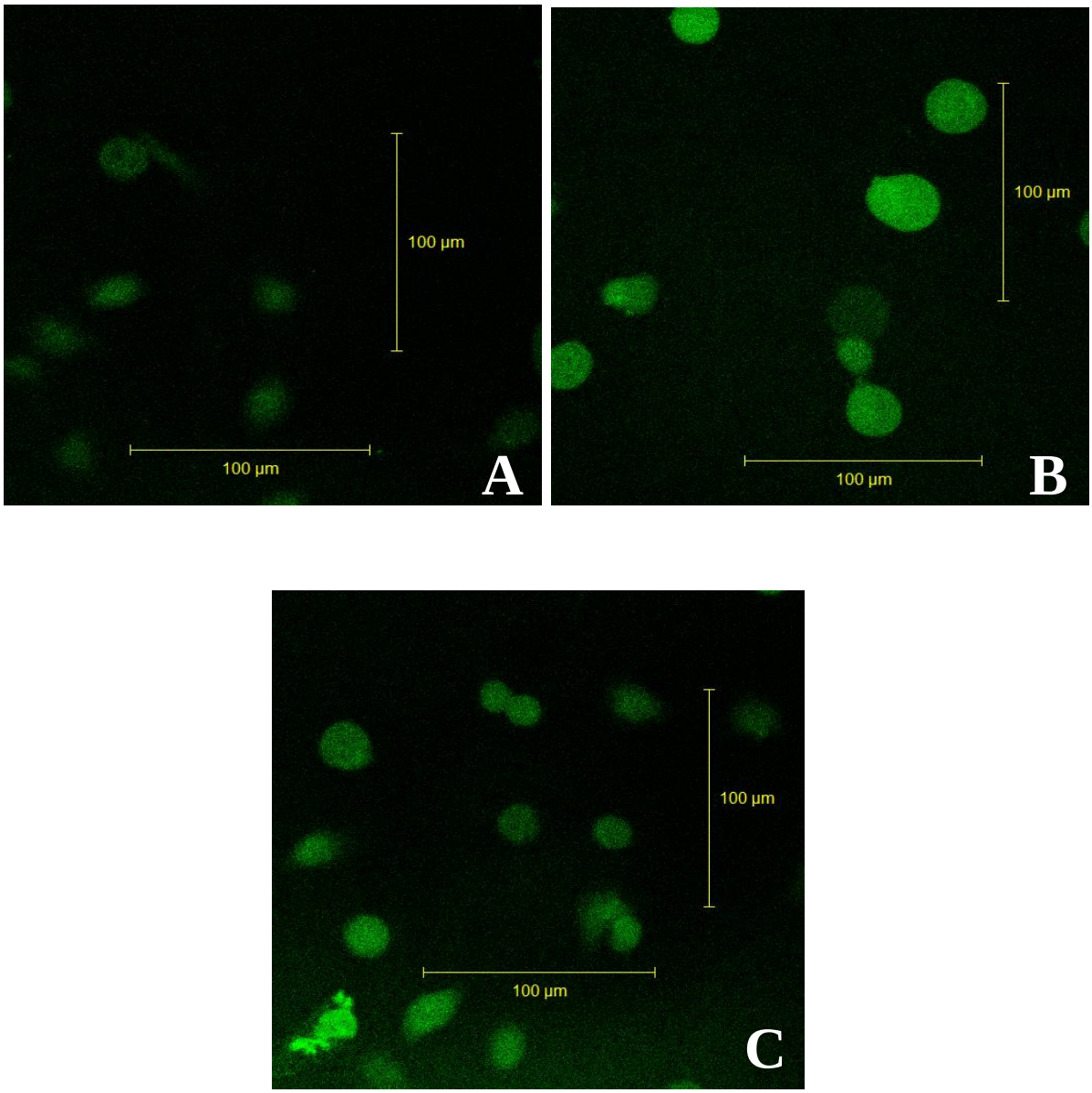

Figure 47: Confocal acquisitions of human glioma cell line 1321N1 at 40X magnification after 1 h of incubation with Image-iT ™ LIVE Green Reactive Oxygen Species Detection Kit and compound 209.

(A) 1321N1 control untreated cells. (B) 1321N1 cells treated with positive control [(*tert*-butyl hydroperoxide (TBHP) (100 µM)]. (C) 1321N1 cells treated with compound 209 (500 µM). Representative data from one of three experiments yielding similar results are shown.

The concentration used in this study was not greater than 500 µM because anything greater than that caused the cells to detach making it difficult for confocal imaging to take place. One possible reason the cell detachment caused may have been due to cells being in

a necrotic stage (as witnessed by membrane lysis, section 3.1.2) since the trypan blue exclusion test indicated membrane lysis occurs within 1.5 h of treatment with compound 209 at high concentrations.

3.7.3 Flow cytometry analysis using Image-iT LIVE Green Reactive Oxygen Species Detection Kit.

3.7.3.1 Treatment with the test compounds for 1 h

The ROS data accrued to this point was merely qualitative, however, in order to quantify the fluorescence produced in the cells, both the 1321N1 and U87MG cell lines were analysed using flow cytometry. The cells were treated with compound 209, compounds 193 and 223 (used as negative controls, according to the results in section 3.2.4) and a positive control [*tert*-butyl hydroperoxide (TBHP)] for 1 h followed by incubation with the dye as per the provided protocol (section 2.5.2). On analysing the results (FACSAria machine, BD Biosciences), a significant shift in the peak, which indicates an increase in the amount of fluorescence in the cells treated with compound 209, was observed when compared to the control cells; such results indicate that excessive generation of ROS is taking place, i.e. the cells are under oxidative stress (Figure 48D and Figure 49D).

The cell lines 1321N1 and U87MG showed 94 % and 79 % ROS positive cells respectively, when treated with compound 209 for 1 h suggesting that this indole generates substantial amounts of ROS. The percentage of ROS positive cells was calculated by comparison to the control cells, thus eliminating the basal levels of ROS which are present in each of the cells (table 8).

Table 8: The percentage of ROS positive cells when treated with compounds 209, 193, 223 and TBHP for 1 h. Carboxy-H_2DCFDA staining intensity was quantified by flow cytometry and the following values are the means of 3 repeats. (t-test, $P < 0.05$ for compound 209, SD = Standard deviation).

Cell lines / Compounds	1321N1 (%)	U87MG (%)
TBHP (positive ctrl)	11 ± 2.95 SD	11 ± 0.5 SD
193 (negative ctrl)	3 ± 0.25 SD	1 ± 0.1 SD
223 (negative ctrl)	9 ± 4.78 SD	3.5 ± 0.25 SD
209 (test compound)	94 ± 2.08 SD	79 ± 6.5 SD

Previous and recent studies have shown similar results where ROS-mediated cell death occurred (Zhang *et al.*, 2014; Zhu *et al.*, 2014; Park *et al.*, 2011). For example, a recent study showed that sodium arsenite induced ROS-dependent autophagic cell death in pancreatic β-cells (Zhu *et al.*, 2014). Another separate study also showed that gambogic acid, the main active component of gamboge resin, induced ROS-mediated autophagy in colorectal cancer cells (Zhang *et al.*, 2014). Such literature supports the results obtained in the current study whereby the cell death which has been observed was mediated by ROS.

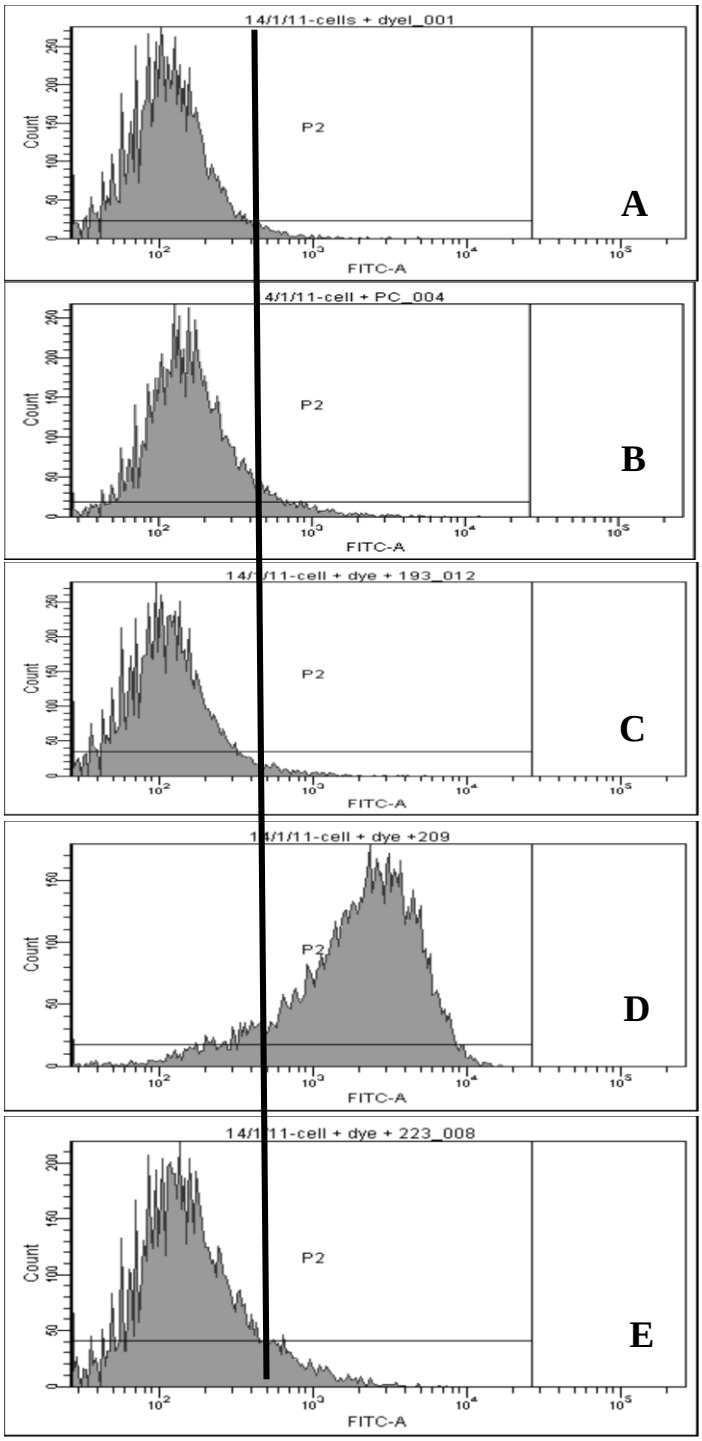

Figure 48: 1321N1 cells were treated with compound 209 and analogues for 1 h.

(A) Cells + Dye (Control cells) (B) Cells treated with positive control [100 µM *tert*-butyl hydroperoxide (TBHP)] (C) Cells treated with compound 193 (500 µM) (D) Cells treated with compound 209 (500 µM) (E) Cells treated with compound 223 (500 µM). Carboxy-H_2DCFDA staining intensity was quantified by flow cytometry. Representative data from one of three experiments yielding similar results are shown.

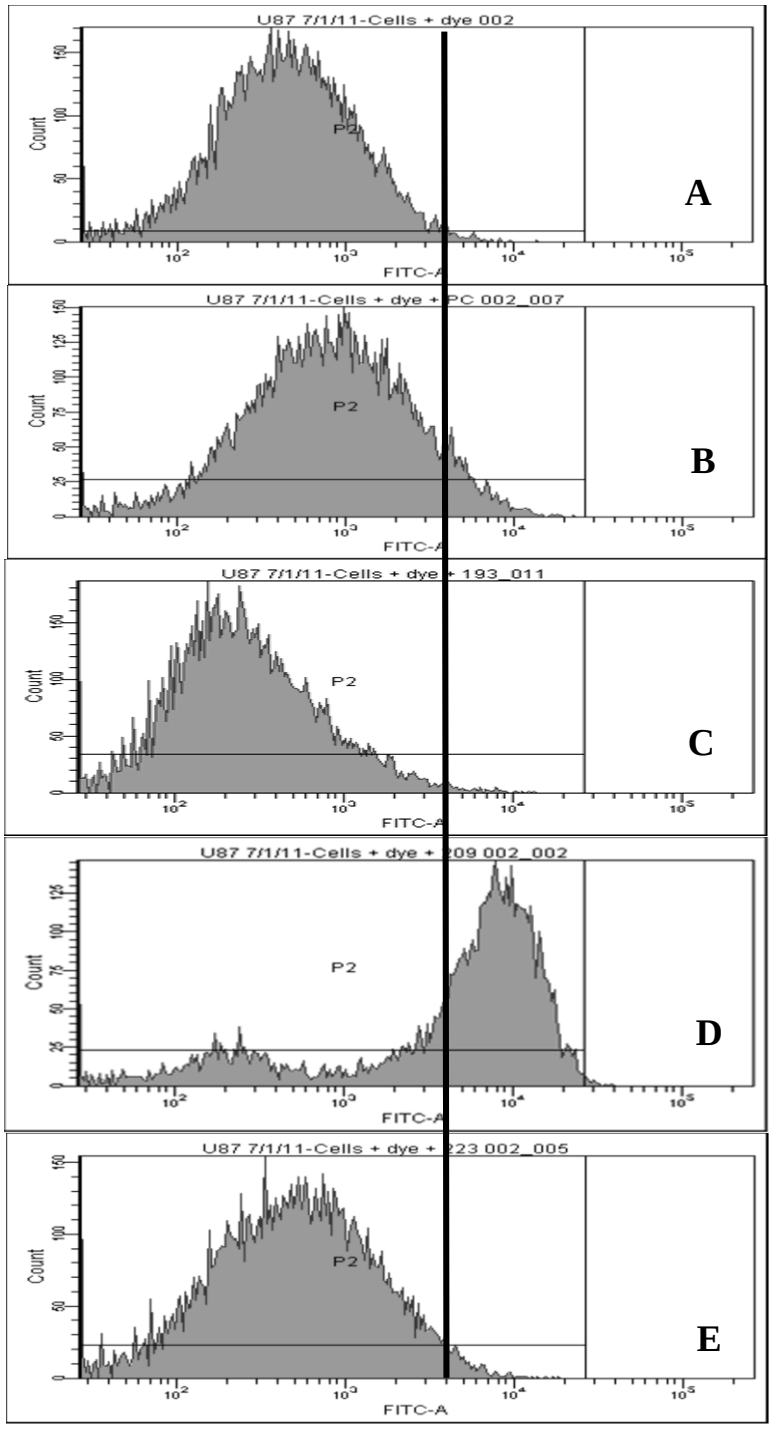

Figure 49: U87MG cells were treated with compound 209 and analogues for 1 h.

(A) Cells + Dye (Control cells). (B) Cells treated with positive control [100 µM *tert*-butyl hydroperoxide (TBHP)] (C) Cells treated with compound 193 (500 µM) (D) Cells treated with compound 209 (500 µM) (E) Cells treated with compound 223 (500 µM). Carboxy-H_2DCFDA staining intensity was quantified by flow cytometry. Representative data from one of three experiments yielding similar results are shown.

3.7.3.2 Dot plots for the selection of cells used in Figure 48 and Figure 49

Dot plots (Figure 50) were used for the assay so that a suitable population could be selected for fluorescence analysis, and cell debris could be discounted by drawing a gate around the population of interest. The manner in which the light bounces off each cell gives information about the cell's physical characteristics. Light scatter or fluorescence data are captured, spectrally filtered and directed to the suitable photodetectors for converting into electrical signals. For example, light scatter is collected at two angles: Forward Scatter (FSC) and side scatter (SSC). FSC measures scattered light in the direction of the laser path and measures the size of the cell while SSC measures scattered light at 90° to the laser path and measures the granularity of the cell. The dot plot charts the coordinates for two parameters, the FSC and the SSC with each cell registered as a single dot.

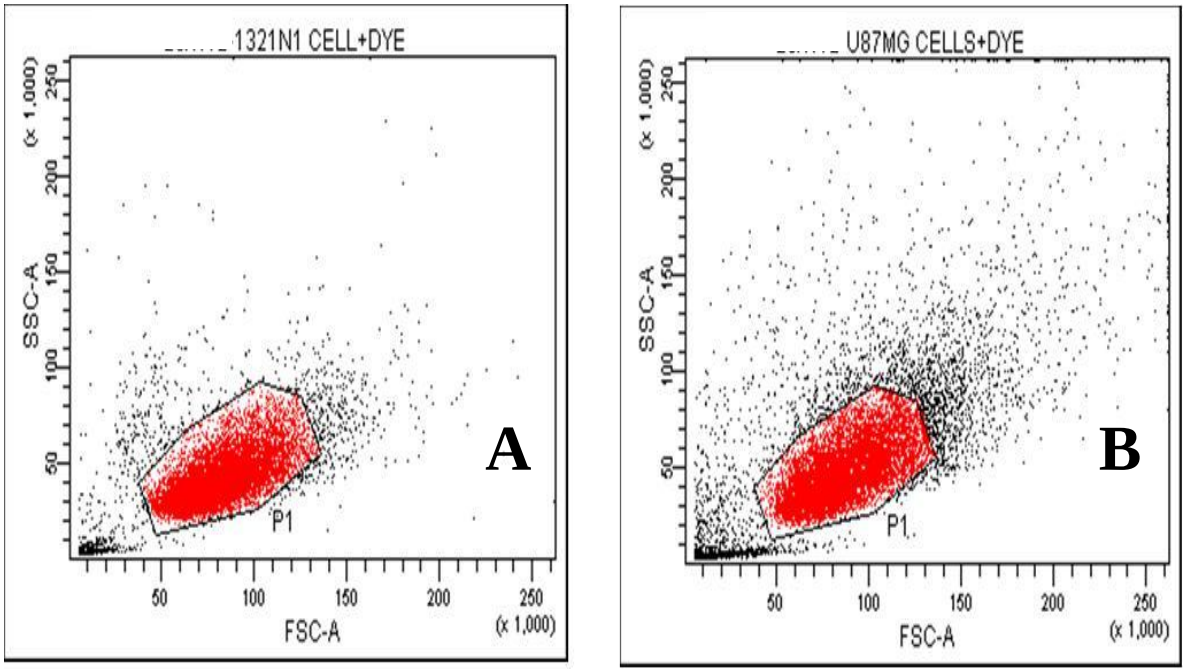

Figure 50: Dot plot with a gate encompassing the A) 1321N1 and B) U87MG cell populations by scatter.

A gate is drawn around the population of interest, which in this case are A) 1321N1 and B) U87MG cells. A gate or a region is a boundary drawn around a sub-population to isolate events for analysis or sorting. Similar gates (Figure 50) indicating the majority of cell populations, have been used in all of the flow cytometry experiments performed herein.

3.7.3.3 Treatment with compound 209 at various concentrations

In order to verify if any dose response relationship exists between treatment of the cell lines with compound 209 and the generation of ROS, both cell lines (1321N1 and U87MG) were treated with various concentrations of compound 209 (100 µM, 250 µM and 500 µM) for 1 h, and the dose response relationship was evaluated. The maximum concentration of compound 209 was maintained at 500 µM which was considered appropriate as anything more than that caused detachment of cells during washing, which hampered the sample collection for flow cytometry analysis (as mentioned above). Compounds 193 and 223 (500 µM) were used as negative controls again since they were not found to be toxic in the MTS assay results (section 3.2.4), as such, their fluorescence should be similar to the control untreated cells. To maintain consistency, the concentration of compounds 193 and 223 used was also 500 µM. Cells were labelled with carboxy-H_2DCFDA dye and analysed by flow cytometry.

The results, on both the cancer cell lines, showed that compound 209 exhibited a dose response with respect to ROS generation, as indicated by the largest deviation away from the control value when treated with 500 µM of compound 209, in comparison to cells treated with 250 µM and 100 µM of the same compound. More specifically, the 1321N1 cell line showed a decrease in the percentage of ROS positive cells from 94 % at 500 µM to 4.6 % at 100 µM whilst, the U87MG cell line showed a decrease from 79 % at 500 µM to

5.1 % at 100 µM, when both cell lines were treated with compound 209 for 1 h. This data suggests that increasing the concentration of compound 209, increases the production of ROS in both the cell lines (table 9). The percentage of ROS positive cells was calculated by comparing them with the control cells, thus eliminating the basal levels of ROS which are present in each of the cells.

Table 9: The percentage of ROS positive cells when treated with compound 209 at various concentrations for 1 h. Carboxy-H_2DCFDA staining intensity was quantified by flow cytometry and the following values are the means of 3 repeats.

Concentration / Cell lines	500 µM	250 µM	100 µM
1321N1	94 ±2 SD	13 ± 1.75 SD	4.6 ±1.5 SD
U87MG	79 ± 6.5 SD	35 ± 5.09 SD	5.1 ±2.15 SD

3.7.3.4 Treatment with compound 209 for 48 h

In order to determine if the production of ROS seen here decreases over time, as already shown by Rogalska *et al*. (2011), the glioma cell lines (1321N1 and U87MG) were treated with compound 209 for 48 h (table 10) and the levels of ROS generation evaluated.

For the extended time period of 48 h, concentrations of 500 µM could not be used since cell detachment was observed, nevertheless, at lower concentations, the 1321N1 cell line showed a decrease in the percentage of ROS positive cells being generated from 19 % at 250 µM to 3.8 % at 100 µM whilst, the U87MG cell line showed a decrease from 17 % at 250 µM to 1.5 % at 100 µM. In these longer time point studies, the results indicated that relatively reduced levels of ROS generation had occurred in both the glioma cell lines (1321N1 and U87MG), compared to the previous study (table 9) in which the cells were

treated with the compound for 1 h, suggesting that ROS production is instantaneous and decreases over time. A previous study on a SKOV3 ovarian carcinoma cell line showed similar results in which ROS production decreased considerably between 24-48 h upon treatment with WP 631, a novel anthracycline antibiotic, when compared to a 2 h treatment (Rogalska *et al.*, 2011), data which supports the results obtained from the current study.

Table 10: The percentage of ROS positive cells when treated with compound 209 at various concentrations for 48 h. Carboxy-H_2DCFDA staining intensity was quantified by flow cytometry and the following values are the means of 3 repeats.

Concentration / Cell lines	500 µM	250 µM	100 µM
1321N1	-*	19 ±2.1 SD	3.8 ±1.2 SD
U87MG	-*	17 ± 3.6 SD	1.5 ±0.43 SD

* At these concentrations over 48 h, the cells detach from the plate.

As the experiments performed in this study contained a single cell population, cell sorting was not required. If the value obtained for the test compound was greater than that of the control data, it would be considered positive for ROS. The greater the difference between the two, the more fluorescent molecules are expressed per cell, and the more positive, or brighter the cell population appears, and therefore more ROS has been produced. Oxidative stress (ROS) was measured by comparing the fluorescence intensities with vehicle controls. The percentage of ROS positive cells (tables 8, 9, 10 and 11) was calculated by comparing it with the vehicle controls and statistical analysis was performed.

3.7.4 Reactive oxygen species (ROS)

Exposure to high-energy or electron-transferring chemical reactions can convert oxygen to various highly reactive chemical forms which are collectively designated as reactive oxygen species (ROS) (Apel and Hirt, 2004). Among all the known reactive oxygen species, the ·OH free radical is possibly the most toxic, as it reacts with a number of biologically important molecules such as DNA, lipids or carbohydrates (Samadi *et al.*, 2011). The generation of ROS is unavoidable for aerobic organisms because they are the by-products of biochemical pathways, such as glycolysis and photosynthesis, which are vital for energy production and storage strategies of aerobic microbes, animals, and plants, and, in healthy cells, it occurs in a controlled manner (Cadenas, 1989; Apel and Hirt, 2004). Therefore, aerobic organisms have advanced enzymatic and non-enzymatic anti-oxidation mechanisms to regulate ROS and avoid oxidative stress (Marian *et al.*, 2004). During conditions of oxidative stress, ROS production is significantly increased, causing subsequent alteration of membrane lipids and oxidation of proteins and nucleic acids (Apel and Hirt, 2004; Harper *et al.*, 2004). Moreover, the oxidative damage of these biomolecules is related to multiple pathological events including atherosclerosis (Singh and Jialal, 2006), carcinogenesis (Klaunig and Kamendulis, 2004), neurodegenerative disorders (Uttara *et al.*, 2009) and with aging (Linford *et al.*, 2006).

Reactive oxygen species (ROS) that are generated from extracellular or intracellular sources can cause DNA damage, which in turn may activate wild-type p53 in normal cells and trigger a stress response, including DNA repair, to eliminate the ROS-mediated damage to genetic material. Nevertheless, in cancer cells which have defective p53, ROS-mediated DNA damage would accumulate due to a defective DNA repair function being present

(Trachootham *et al.*, 2009). In cancer cells with wild-type p53, ROS-mediated DNA mutations or deletions may cause a loss of p53 function, resulting in a defect in DNA repair, which ultimately leads to an accumulation of gene mutations and deletions. This would lead to genomic instability resulting in the activation of oncogenes, aberrant metabolic stress, mitochondrial dysfunction and a decrease in anti-oxidant levels (Trachootham *et al.*, 2009) (Figure 51). All these cellular events may further increase ROS levels, resulting in additional DNA damage and genetic instability. Such a vicious cycle could eventually amplify oxidative stress and cause genomic instability and cancer development.

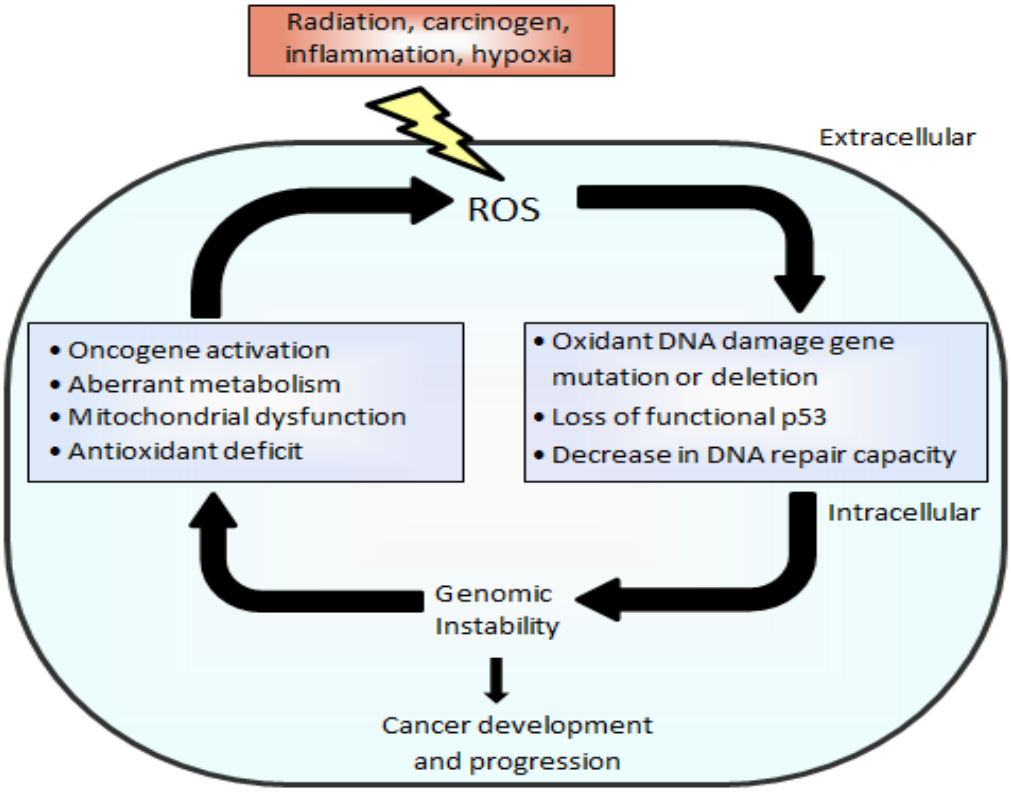

Figure 51: The vicious cycle of ROS stress in cancer (Trachootham *et al.*, 2009).

In the present study the results of section 3.3 suggest that oxidative stress may be mediating cell death in both the glioma cell lines when treated with compound 209.

Carcinogenesis follows a multistep course involving both mutation and greater cell proliferation whilst oxidative stress occurs due to excessive production of reactive oxygen species through either endogenous or exogenous reactions. In the context of carcinogenesis, the unregulated or extended production of cellular oxidants has been linked to mutation which is induced by oxidant-induced DNA damage as well as modification of gene expression (Klaunig and Kamendulis, 2004). In particular, signal transduction pathways, including activator protein 1 (AP-1) and nuclear factor kappa-light-chain-enhancer of activated B cells (NF-κB), are known to be activated by reactive oxygen species, and they lead to the transcription of genes involved in cell growth regulatory pathways (Klaunig and Kamendulis, 2004). Since the excessive production of ROS is capable of inducing many reactions and mutations in cancer cells, in such a short span of time, it was considered as being a potential mechanism via which the potent indole (compound 209), discovered from the current study, mediated cell death.

The relevance of the inclusion of such a study here is corroborated by research which has shown that cancer cells produce higher levels of ROS than normal cells and oxidative damage to cellular DNA can lead to mutations and may, therefore contribute to rapid cancer progression (Pelicano *et al.*, 2004; Schumacker, 2006; Waris and Ahsan, 2006). It has also been shown that rat and human glioma cells overexpress 2-Cys Prx II, a cytosolic peroxide and peroxynitrite-scavenging anti-oxidant enzyme, when compared with their normal cell counterparts, the astrocytes. Additionally, knocking down Prx II led to an increase in radio-sensitivity at clinically relevant doses as low as 1 Gy, and to an increased sensitivity to oxidative stress. These data suggest that overexpression of Prx II protects cancer cells from oxidative stress. As ROS production is increased in cancer cells,

overexpression of Prx II may provide additional protection against ROS while presenting it as a potential therapeutic target (Smith-Pearson *et al.*, 2008).

Recent studies have also found that chemo-resistance to temozolomide (TMZ), the blockbuster drug for the treatment of malignant glioma, is linked to tighter mitochondrial coupling and low ROS production, and this suggests a novel mitochondrial ROS-dependent mechanism underlying TMZ-chemo-resistance in glioma. Thus, alteration of mitochondrial functions and changes in redox status might constitute a novel strategy for sensitising glioma cells to therapeutic approaches (Oliva *et al.*, 2011), suggesting that controlling ROS generation or its levels may hold a promising standard therapeutic strategy for various types of cancers and thus support the continued development of the best compounds found here, compound 209 (and 223a, if its acid-sensitivity can be controlled).

In a related manner, recent studies have also shown that piperlongumine, a natural product constituent of the fruit of the Long pepper, a plant found in southern India and southeast Asia, induces ROS and apoptotic cell death in both cancer cells, and normal cells engineered to have a cancer genotype, irrespective of p53 status, but that it had little effect on primary normal cells (Raj *et al.*, 2011). Substantial anti-tumour effects were observed in piperlongumine-treated mouse xenograft tumour models, with no apparent toxicity to normal mice, which further indicates and supports that ROS mediated cell death pathways hold a promising therapeutic strategy in the future, which in this case is its ability to induce apoptosis selectively in cells that have a cancer genotype (Raj *et al.*, 2011).

3.7.5 Co-treatment of the cells with compound 209 and a ROS scavenger (ascorbic acid)

Under oxidative stress, reactive oxygen species, including free radicals such as superoxide ($O_2^{\cdot-}$), the hydroxyl radical ($HO^{\cdot}$) and hydrogen peroxide (H_2O_2), are generated at high levels, inducing cellular damage and cell death (Pelicano *et al.*, 2004). Ascorbic acid is a naturally occurring organic compound with anti-oxidant properties and is a scavenger of hydroxyl radicals (Biswas *et al.*, 2005; Ozyurek *et al.*, 2008), whereby it reacts with reactive oxygen species, such as the hydroxyl radical formed from hydrogen peroxide, and neutralises it (Jansson *et al.*, 2003). The main objective of these anti-oxidant molecules is to donate an electron to, or to gain an electron from, ROS in order to neutralize them. Therefore, based on this mechanism, ascorbic acid was chosen to validate the ROS production induced by compound 209 in the 1321N1 and U87MG cell lines.

1321N1 and U87MG glioma cells were treated with compound 209 and an anti-oxidant, ascorbic acid (500 µM), a common scavenger for hydroxyl radical reactive oxygen species (Hou *et al.*, 2010), to detect whether oxidative stress decreases after the addition of the anti-oxidant. As before, the MTS assay (section 2.3.1) was used to check the cell viability of the 1321N1 and U87MG cell lines and the amount of viable cells was determined after treating the cells with compound 209 (500 µM) alone for 1 h, and the result of this experiment were consistent with those observed in section 3.2 and Figure 44 and Figure 45, in that only 50-60 % of the cells were viable after treatment. However, upon co-treatment with the anti-oxidant (ascorbic acid, 500 µM) and compound 209 (500 µM) for 1 h, the cell viability increased to *circa* 90 % for both cell lines, Figure 52, suggesting

that the anti-oxidant was able to neutralise the effects of compound 209 almost completely, presumably because the indole is acting through a oxidative stress mechanism.

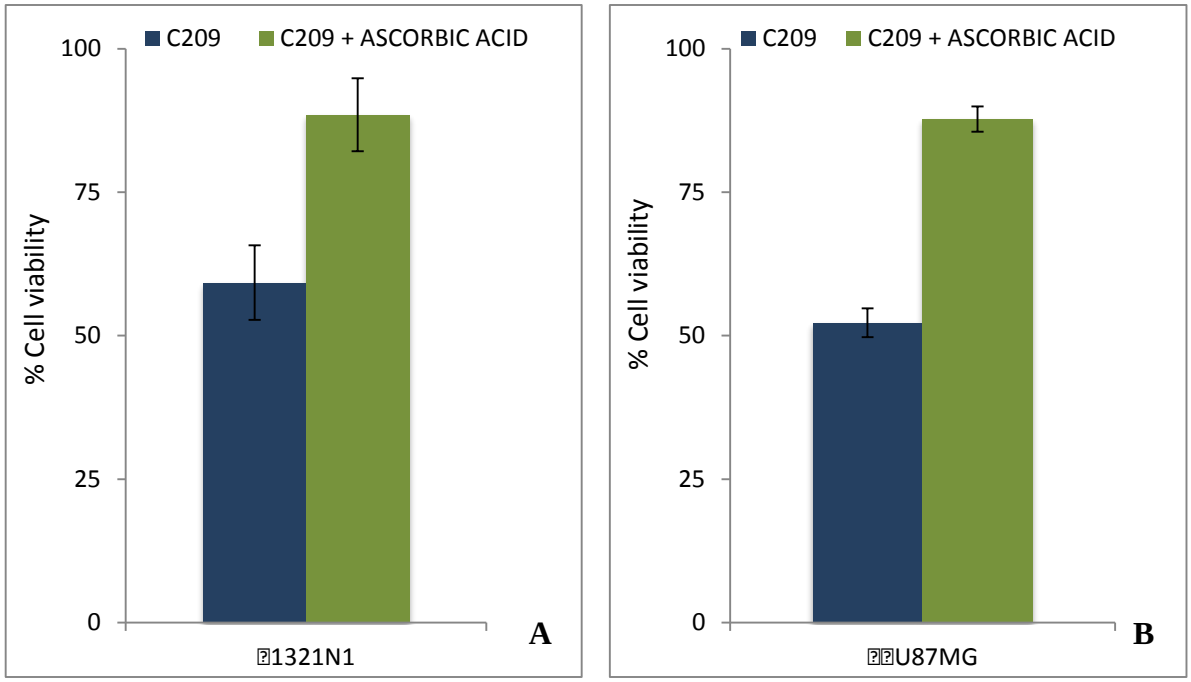

Figure 52: 1321N1 (A) and U87MG (B) cells co-treated with compound 209 (500 µM) and ascorbic acid (500 µM) for 1 h. Ascorbic acid was used as a scavenger for hydroxyl reactive oxygen species and the MTS assay was used to measure the cell viability. The data points are means of 4 repeats and the error bars represent ±SD.

The results were also confirmed by flow cytometry analysis where it was demonstrated that the level of fluorescence produced by the cells treated with compound 209 alone was greater than the fluorescence produced by the cells treated with compound 209 + ascorbic acid. This validated the hypothesis and it was confirmed that the addition of the anti-oxidant, ascorbic acid, reduced the anti-cancer potency of compound 209 by scavenging ROS. The 1321N1 cell line showed a decrease in the percentage of ROS positive cells from 88.53 % when treated with compound 209 alone to 38.6 % with compound 209 + ascorbic acid, whilst the U87MG cell line showed a decrease from 79.33 % when treated with compound 209 alone to 55.96 % with compound 209 + ascorbic acid

for 1 h (table 11). The percentage of ROS positive cells was calculated by comparing them with the control cells, thus eliminating the basal levels of ROS which are present in each of the cells.

Table 11: The percentage of ROS positive cells when treated with compound 209 and compound 209 + ascorbic acid for 1 h. Carboxy-H_2DCFDA staining intensity was quantified by flow cytometry and the following values are the means of 3 repeats. (t-test, $P < 0.05$ for compound 209, SD = Standard deviation).

Compounds / Cell lines	209	209 + ascorbic acid
1321N1	88.53 ± 3.90 SD	38.60 ± 3.3 SD
U87MG	79.33 ± 6.50 SD	55.96 ±3.56 SD

A recent study on human and mouse melanoma cells showed that doxycycline induces intra-cellular ROS production, apoptosis signal-regulated kinase 1 (ASK1), JNK and p38 mitogen-activated protein kinase (MAPK) activation at an early stage of treatment and induces mitochondrial cytochrome c release into the cytosol (Shieh *et al.*, 2010). In that study, the same ROS scavenger to that used here, ascorbic acid, reduced doxycycline-induced JNK activation, caspase cleavage and melanoma cell death. This result is an indication that intra-cellular ROS generation is responsible for doxycycline-induced JNK activation and melanoma cell apoptosis and that ascorbic acid scavenges ROS (Shieh *et al.*, 2010). Therefore, this supports the results here in that the addition of ascorbic acid to the cells treated with compound 209 are showing reduced amounts of ROS production, further confirming that compound 209 is working through a mechanism involving ROS.

3.8 Detection of Autophagy

Further evidence for the ROS-induced mechanism of action of these compounds came about following a recent study which showed that oxidative stress can induce autophagy ahead of apoptosis in U251 glioma cells (Kong *et al.*, 2011). The results of the study indicate that autophagic vacuoles and the expression of the autophagic protein, Beclin 1, increase at 6 h, but that the cell apoptotic ratio and cytosolic cytochrome c protein do not, but only increase after 12 h (Kong *et al.*, 2011). Based on this result, in these glioma cell lines, there appears to be a time dependent relationship of apoptosis with autophagy, indicating that compound 209 used in this study, which induces ROS, is not causing apoptosis mediated cell death (at least at first) but may be causing autophagy mediated cell death initially.

Autophagy is a highly conserved process which is characterised by the sequestration of bulk cytoplasmic proteins and organelles in autophagic vesicles, and subsequent delivery to and degradation by the lysosomal system. It was originally considered as a process for protein recycling and is termed as Type II programmed cell death (Klionsky, 2007). Autophagy is responsible for non-apoptotic cell death, and plays a crucial role in regulating cellular functions (Park *et al.*, 2011). Oxidative stress has been shown to induce autophagy under certain conditions, such as ischemia and reperfusion (Matsui *et al.*, 2007), and cell death by autophagy in tumour cell lines treated with chemotherapeutic agents has been proposed (Levine and Yuan, 2005; Bursch *et al.*, 2000).

As discussed earlier, a recent study by Park *et al.* (2011) on U87MG cells, observed that ROS levels increased within 30 min followed by autophagic cell death following treatment with β-lapachone. Similar to Park's work it was also observed in the current

study that glioma cells treated with compound 209 had elevated amount of ROS production within 1 h (section 3.7.3.1). With this result in mind, and trying to replicate the protocol of Park *et al* (2011), it was decided to determine if the cells were in the stages of an autophagic process, which may have been mediated by the ROS generated and observed in section 3.3.

Autophagy is characterised by acidic vesicular organelle formation (autophagosomes) (Prabhu *et al.*, 2013a) and research has shown that vinblastine, an anti-microtubule drug (section 1.2.2.2.5), triggers autophagosome formation very quickly (30 min) in primary rat hepatocytes (Kochl *et al.*, 2006). Here too, the MTS assay results reported non-viable cells within 2 h upon treatment with compound 209, leading to the hypothesis that such quick cell death might be related to autophagy.

The characteristic AVO formation of autophagy can be detected by staining the cells with acridine orange, and so to try and prove the formations of AVOs in 1321N1 and U87MG cell lines after treatment with compound 209, and that cell death did involve an autophagic process, the cells were treated with compound 209 for 1 h followed by incubation with acridine orange as per the supplied protocol. Acridine orange moves freely across biological membranes and accumulates in acidic compartments, where it can be observed as bright red fluorescence (Paglin *et al.*, 2001). The intensity of the red fluorescence is proportional to the degree of acidity. Therefore, the volume of the cellular acidic compartment can be quantified (Traganos and Darzynkiewicz, 1994). In view of the finding that AVOs accumulate in cells undergoing autophagy (Zou *et al.*, 2011; Kanzawa *et al.*, 2005), acridine orange was used to characterise AVO formation and detect possibly autophagy, in the 1321N1 and U87MG glioma cell lines.

According to the trypan blue exclusion test results (section 3.1.2), membrane lysis occurs after 75 min upon treatment with compound 209, and therefore it was crucial that the cells were not treated with this compound for more than 60 min, since membrane lysis would have hampered acridine orange staining. Membrane lysis would have caused this stain to leak out and possibly generate false negative results.

Upon carrying out such experiments, the cells treated with compound 209 showed a greater amount of red fluorescence compared to the control untreated cells, as indicated by the shift in the control peak. This result suggests that compound 209 induces AVO formation in the 1321N1 (Figure 53) and U87MG (Figure 54) cell lines (table 12), indicating that the cells were in a stage of an autophagic process, and that this may have been mediated by ROS formation (oxidative stress).

Further evidence for this proposal consisted of using an autophagy inhibitor—3-methyladenine (Sigma-Aldrich, UK) (5 mM)—on both the glioma cell lines (1321N1 and U87MG), to determine if autophagy was indeed inhibited after treatment with compound 209 (McFarland *et al.*, 2012). In this event, the results indicated that the peak did indeed shift back towards the control cell level, on both the cell lines (Figure 53C and Figure 54C), indicating that autophagy was being inhibited in the samples which were treated with 3-methyladenine prior to treatment with compound 209. More specifically, compound 209 showed 15.66 % and 16.33 % of acridine orange positive cells on the 1321N1 and U87MG cell lines respectively whilst this reduced to 6.66 % (1321N1) and 2.13 % (U87MG) when pretreated with 3-methyladenine on both the glioma cell lines (table 12).

Table 12: The percentage of acridine orange positive cells when treated with compound 209 and 3-methyladenine for 1 h. Acridine orange staining intensity was quantified by flow cytometry and the following values are the means of 3 repeats. (t-test, $P < 0.05$ for compound 209, SD = Standard deviation).

Compounds / Cell lines	209	209 + 3-methyladenine
1321N1	15.66 ±3.78 SD	6.66 ±0.61 SD
U87MG	16.33 ± 3.51 SD	2.13 ±0.40 SD

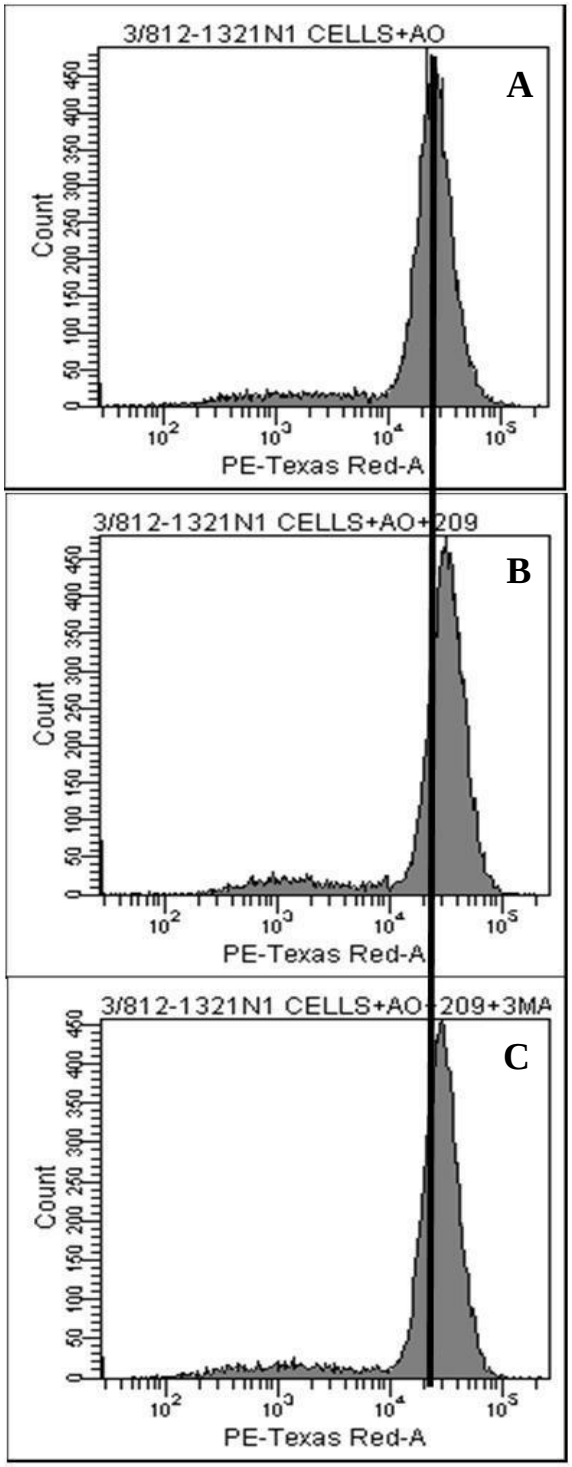

Figure 53: Acidic vesicular organelle (AVO) formation in 1321N1 cells.

(A) 1321N1 control cells + acridine orange (3 µM) (B) 1321N1 cells treated with compound 209 (500 µM) for 1 h + acridine orange (3 µM) (C) 1321N1 cells treated with compound 209 (500 µM) + 3-methyladenine (5 mM) for 1 h. Acridine orange staining intensity was quantified by flow cytometry. Representative data from one of three experiments yielding similar results is shown.

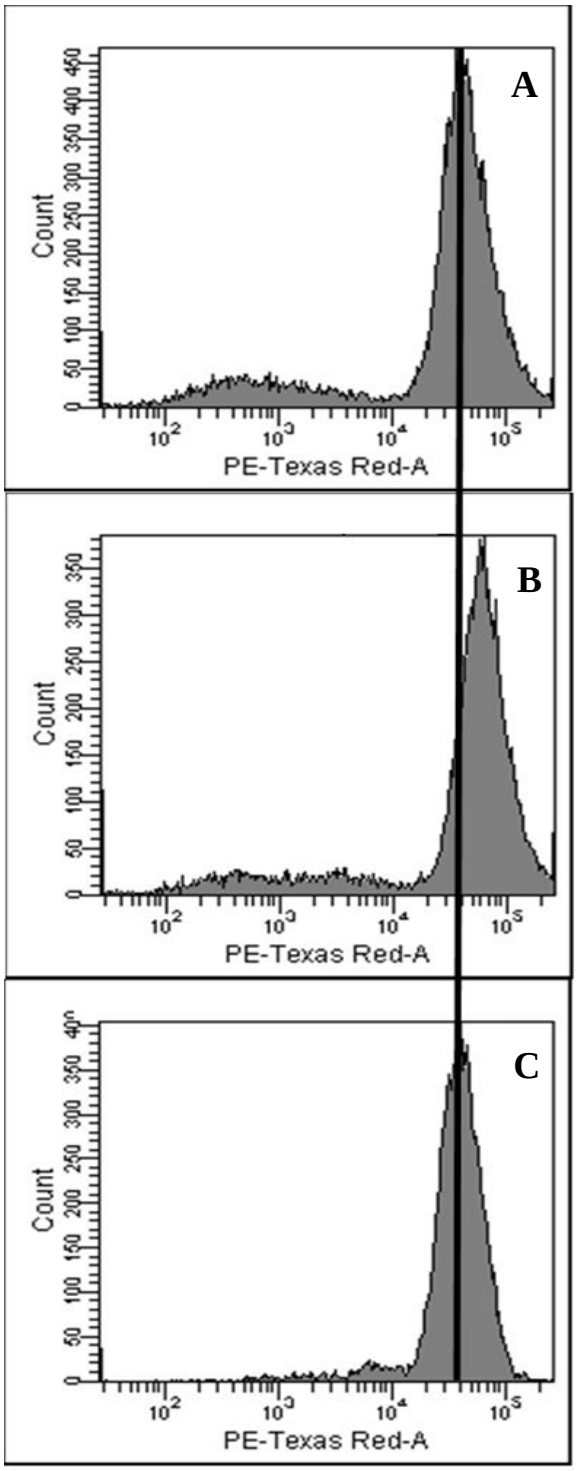

Figure 54: Acidic vesicular organelle (AVO) formation in U87MG cells.

(A) U87MG control cells + acridine orange (3 µM) (B) U87MG cells treated with compound 209 (500 µM) for 1 h + acridine orange (3 µM) (C) U87MG cells treated with compound 209 (500 µM) + 3-methyladenine (5 mM) for 1 h. Acridine orange staining intensity was quantified by flow cytometry. Representative data from one of three experiments yielding similar results is shown.

The results shown here are supported by the research of others which have shown that cell death can occur through an autophagic process in various cancers, including malignant gliomas, ovarian carcinomas and mammary carcinomas (Kanzawa *et al.*, 2005; Opipari *et al.*, 2004; Bursch *et al.*, 1996). It has also been shown that using hydrogen peroxide (H_2O_2) and 2-methoxyestradiol (2-ME) to induce oxidative stress, causes autophagy-induced cell death in the transformed cell line HEK293, and the cancer cell lines U87MG and HeLa (Chen *et al.*, 2008). Resveratrol, which is structurally similar to compound 209 (Figure 30 and Figure 33), has also been shown to induce autophagy in human U251 glioma cells (Li *et al.*, 2009).

Research has also shown that radiation or chemotherapeutic agents such as arsenic trioxide or tamoxifen induce autophagy, but not apoptosis, in several cancers, including: the malignant glioma cell lines U373 and U87MG (Bursch *et al.*, 1996; Yao *et al.*, 2003; Kanzawa *et al.*, 2003; Paglin and Yahalom, 2006). Previous studies have also shown that apoptosis is mediated by caspases, yet caspase inhibitors do not halt arsenic trioxide induced cell death (Kanzawa *et al.*, 2003), as such, the autophagy-induced cell death observed in the above described cell lines, did not exhibit any of the characteristic apoptotic features, such as caspase activation and DNA fragmentation (Voss *et al.*, 2010). Since the onset of cell death was quick (1.5 h) in the current study, it can be speculated that apoptosis may not be the main mechanism of cell death, since the above findings suggest that compound 209 works via a ROS mediated mechanism, which leads to autophagic cell death, in 1321N1 and U87MG cell lines. However, as has been observed by others, it is not being ruled out that apoptosis may be involved at a later stage, after autophagy has taken place (Kong *et al.*, 2011).

A previous study has shown that arsenic trioxide induces autophagic cell death in U373-MG glioma cells when exposed for 24 h, by up regulating the mitochondrial cell death protein BCL2/adenovirus E1B 19 kDa protein-interacting protein 3 (BNIP3) (Kanzawa *et al.*, 2005). Staining of U373-MG glioma cells with acridine orange showed the accumulation of AVO in the cytoplasm of cells exposed to arsenic trioxide (Kanzawa *et al.*, 2005), suggestive of autophagy induced cell death (Zou *et al.*, 2011). Moreover, malignant glioma cells U373-MG when treated with temozolomide for 72 h, are also known to be in an autophagic process (Kanzawa *et al.*, 2004). Collectively, all these findings indicate that autophagic cell death pathways play an important role in inducing cell death in cancer cells.

Another previous study has also shown that the amount of oxidative stress-induced cell death may not be completely blocked by inhibiting either apoptosis or autophagy (Chen *et al.*, 2008). This is an indication that there is a third type of cell death pathway; necrotic cell death. This form of cell death is passive and causes cellular contents to be released into the extracellular space which is indicated by cell lysis (Chen *et al.*, 2008). Reports have shown that when apoptotic or autophagic cell death was blocked, necrotic cell death was observed (Degenhardt *et al.*, 2006). Furthermore, oxidative stress has been shown to trigger a lysosomal-dependent necrotic cell death (Brunk *et al.*, 1997). Therefore, it can be assumed that cells under oxidative stress could undergo cell death through multiple pathways including necrosis. In this current study, membrane lysis was observed within 1.5 h of treatment with compound 209 at high concentrations (> 750 µM) which may suggest that the cells are undergoing necrosis when treated with high concentrations of this indole (compound 209) and hence concentration/time studies are important. From the above results, it may be speculated that the cells may be in a stage of an autophagic process when

treated with compound 209 for 1 h at 500 µM. Following an increase in the concentration of compound 209 to 750 µM, the cells may move to a necrotic stage, since membrane lysis was observed, as indicated by the trypan blue exclusion test (section 3.1.2), at this concentration. This suggests that the concentrations of these indoles may play an important role in deciding the type of cell death pathway to be followed, as has been observed for other phenolic compounds which are either anti-oxidant (at low concentrations) or pro-oxidants (at high concentrations) (Iwasaki *et al.*, 2011; Fujisawa *et al.*, 2005). The pro-oxidant or anti-oxidant activity of phenolic compounds is also dependent on factors such as their metal-reducing potential, pH, chelating behaviour and solubility characteristics (Fujisawa *et al.*, 2005).

It is known that the pro-oxidant activities of phenolic compounds are catalysed by numerous peroxidases, such as plasma myeloperoxidase and cytochrome P-450, which results in the production of pro-oxidant phenoxyl radicals (Fujisawa *et al.*, 2005), and a recent study showed that there are high levels of cytochrome P450 (CYP) expression found in U87MG cells (Stiborova *et al.*, 2011). In the current study, it was shown that the phenolic indole, compound 209, generates ROS in both the U87MG and 1321N1 cell lines, and that the elevated CYP expression known to occur in glioma cell lines might be responsible for compound 209's increased pro-oxidant activity seen here.

Research has shown that the 2-electron reductase, NAD(P)H:quinone oxidoreductase (NQO1) is overexpressed in many solid tumours (Awadallah *et al.*, 2008) and NQO1 is a priority target of glioblastoma chemotherapy (Okamura *et al.*, 2000). As shown herein, the most stable, potent compound used in this study (compound 209) caused the cells to be in a stage of an autophagic process within 2 h. Since the time required for the

cells to induce autophagy was so quick, it may indicate that the mechanism of action of compound 209 may be similar to that of β–lapachone, since β–lapachone induces NQO1-dependent cell death within 2–4 h in NQO1-expressing lung and prostate cancer cells (Park *et al.*, 2011). The U87MG cell line used in this study also expresses the NQO1 gene (Park *et al.*, 2011). The NAD(P)H:quinone acceptor oxidoreductase (NQO) gene family in the human genome consists of two genes (NQO1 and NQO2). These two genes encode cytosolic flavoenzymes that catalyse the beneficial two-electron reduction of quinones to hydroquinones, a reaction which prevents the unwanted one-electron reduction of quinones by other quinone reductases. This reaction is unwanted because it results in the formation of highly reactive oxygen species which leads to cell damage (Vasiliou *et al.*, 2006). Compound 209, used in this study, has a phenolic –OH group which is thought to be an important component for its activity (section 3.3.2) and this –OH group may be participating in a similar redox processes resulting in an unwanted one-electron system and generating reactive oxygen species which could then lead to autophagic cell death. Both the mammalian NQO1 and NQO2 genes are up-regulated as a part of the oxidative stress response and are overexpressed in various types of tumours (Vasiliou *et al.*, 2006). Therefore, considering previous studies and the results obtained from this current study together, it may indicate that compound 209 induces ROS formation within 1 h, which in turn leads the glioma cells to be in an autophagic process, as indicated by AVO formation and the effects of using an autophagy inhibitor, 3-methyladenine. The fact that the cells may undergo cell death via multiple pathways (Chen *et al.*, 2008), which may be triggered any time during the course of cell cycle, means that testing the cell lines for apoptosis induced cell death at a later time point (48 h) would be a topic of future study.

3.9 Effects of compound 209 on a primary cell culture

The activity of compound 209 on the glioma cell lines has been reliably reproduced during these studies, and its mechanism of action appears to include ROS linked to an autophagic process. However, the cell lines used are immortalised and do not completely represent a patient's brain tumour *in vivo*. As such, a primary cell line was obtained from a patient biopsy from Royal Preston Hospital, and screened against compound 209 to see if the activity observed on the established cell lines could be mirrored on cells more reminiscent of an actual tumour.

As such, a dose response curve of compound 209 on the primary cell line, IN859, was plotted using the MTS cell proliferation assay, wherein the cells were exposed to different concentrations of the compound for 2 h. As shown in Figure 55, the IC_{50} value of compound 209 was found to be 400 ±4 µM on this primary cell line, an activity which is almost double that seen in the established cell lines (section 3.2).

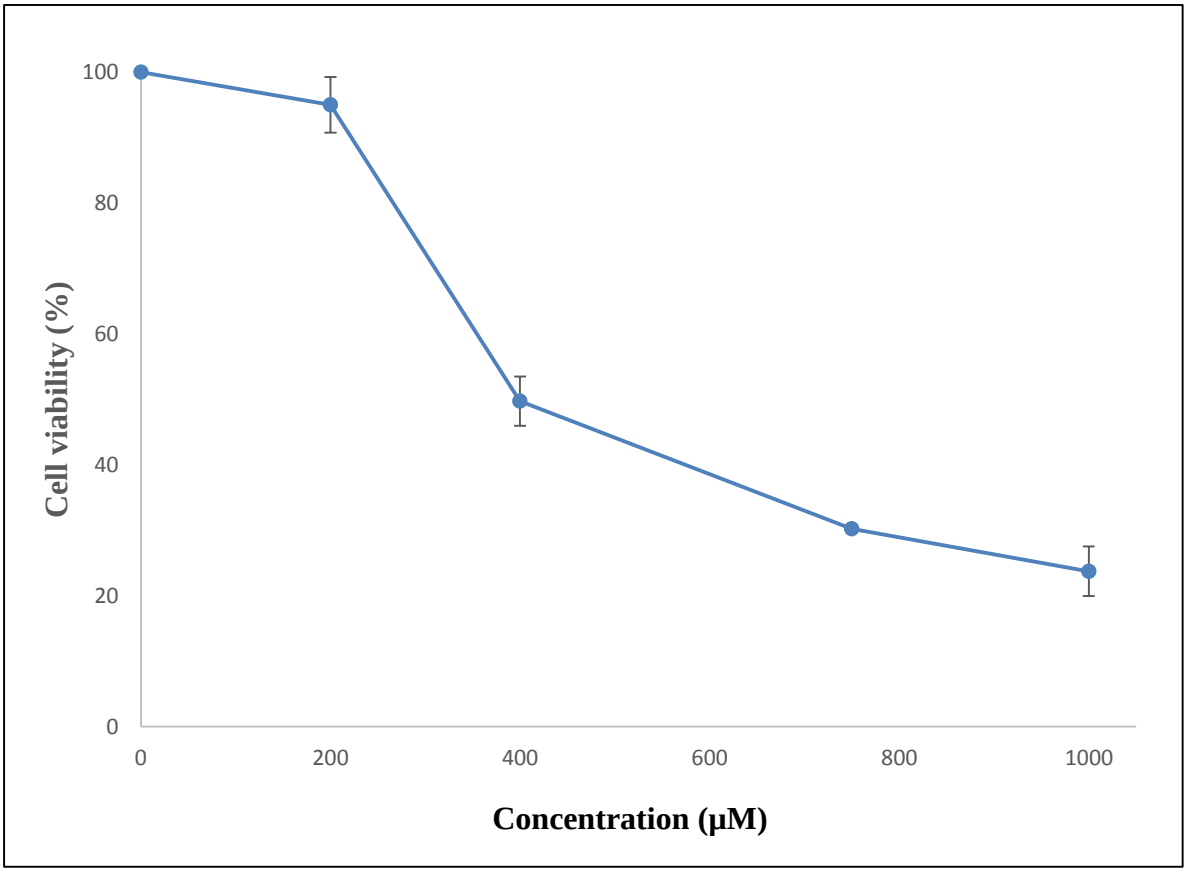

Figure 55: Compound 209 tested on the IN859 primary cell line for 2 h. The data points are means of 4 repeats.

Such a primary cell line was used to substantiate and support the results obtained using the established cell lines, because a primary cell line would mimic *in vivo* conditions more appropriately and closely as compared to established cell lines. There is a greater chance of mutation in the established cell lines because the process of *in vitro* transformation of a primary cell line to a continuous, established cell line leads to genetic variations involving deletion or mutation in the p53 gene. This gene plays a major role in cell cycle arrest if DNA were to become mutated and therefore it is not surprising to find genetic instability perpetuated in continuous established cell lines (Freshney, 2010). Therefore, for the compounds studied herein, and any future analogues prepared, it is

significant that activity is also seen on cells which more closely represent human brain tumours if future therapies for glioma are to be developed successfully.

3.10 Summary of the proposed ROS-induced mechanisms of cell death

As a possible aid for determining the absolute mechanism of cell death induced by ROS, all the above work and literature references have been summarised by building a flowchart model (Figure 56) which demonstrates how ROS-mediated cell death is caused by different types of compound, over differing time points and cell types. The various compounds in this flowchart are categorised under five classes on the basis of the time required to trigger cell death, and also by the type of programmed cell death mechanisms (apoptosis, autophagy and necrosis) taking place. For example, looking at the flowchart, β-lapachone is classified as a class IV compound since it leads to autophagic cell death within 24 h, while compound 209 is classified as a class I compound, since it causes the cells to be in a stage of an autophagic process within 2 h. All other compounds are classified according to the same principle.

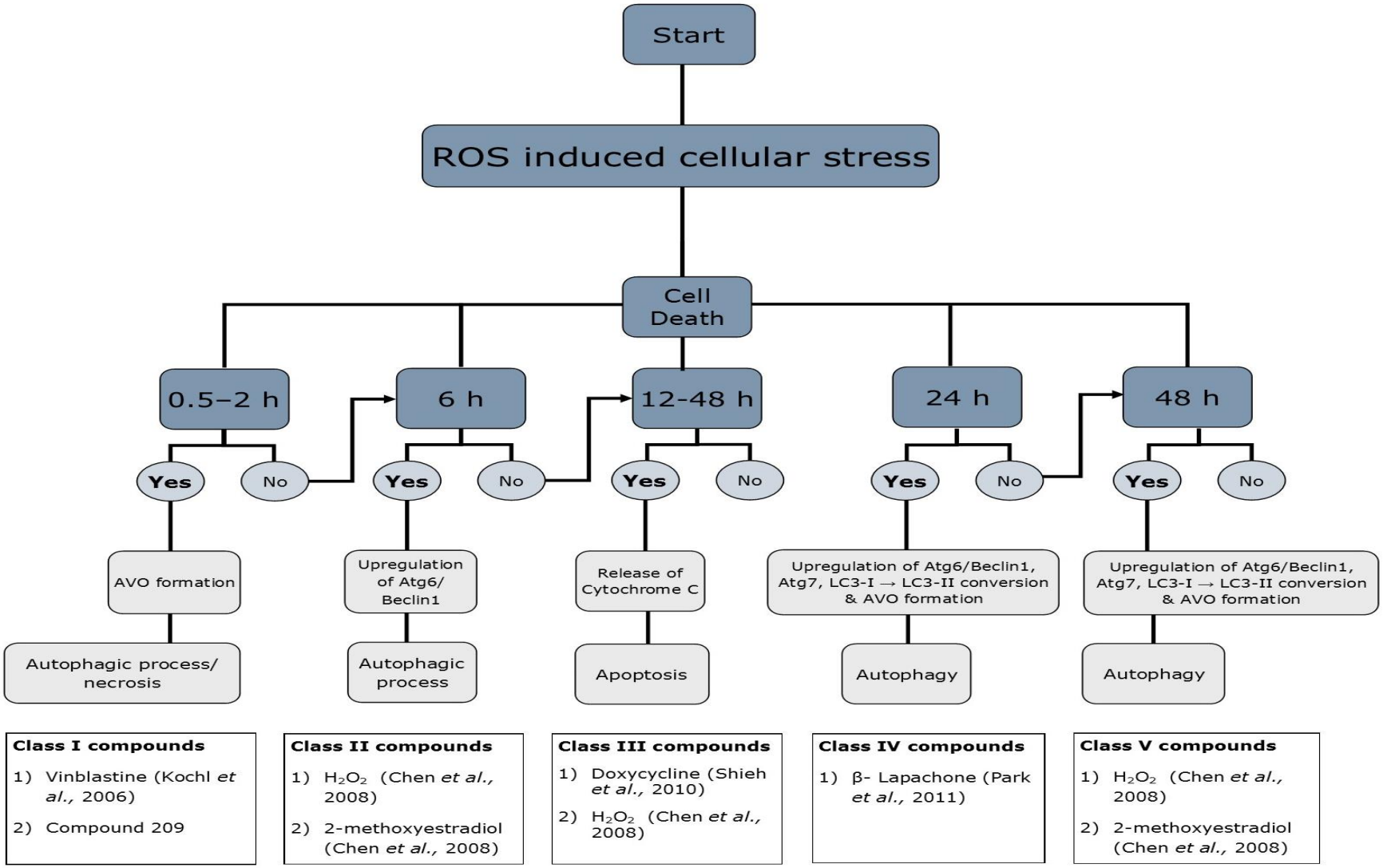

Figure 56: Flowchart model depicting ROS mediated cell death mechanism.

3.11 *Cn*-AMP2, a host defence peptide (HDP) against the glioma cell lines, 1321N1 and U87MG.

Globally, cancer is now one of the leading causes of death, which claimed lives at an annual rate of over 12.7 million in 2008 and is predicted to rise to over 20 million by 2030 (Bray *et al.*, 2012), creating an urgent need for novel approaches to anticancer therapies (Martin Sabroso and Torres-Suarez, 2014; Saraswathy and Gong, 2013; Urruticoechea *et al.*, 2010). In response, there has been a move to develop anticancer strategies that are based on compounds from natural sources (Cragg *et al.*, 2009; Balderas-Renteria *et al.*, 2012; Cragg and Newman, 2013; Newman and Cragg, 2012), including host defence peptides (HDPs) (Harris *et al.*, 2013a; Dennison *et al.*, 2006a; Gaspar *et al.*, 2013). However, presently, the only major candidate in this class of peptides with promise for medical use is the neutraceutical protein, lactoferrin, which has been patented as an anticancer agent and in clinical trials has been shown to reduce the risk of colon carcinogenesis (Tsuda *et al.*, 2010). Given this lack of therapeutically useful HDPs and the fact that most tested in this capacity are cationic, the ability of the anionic plant HDP, *Cn*-AMP2, to serve in this capacity has been investigated. This work constitutes a separate short, parallel study, which extends and complements that described above, in that, it considers the anti-cancer potential of naturally occurring compounds with molecular weights higher than indoles but lower than monoclonal antibodies (mABs). This collaborative project was also undertaken to optimise resource economy, in that, the cell cultures and other systems needed to test the peptide's anti-cancer activity were already in place.

The ability of *Cn*-AMP2, to kill the glioma cell lines, 1321N1 and U87MG was investigated and these data were plotted as dose response curves (Figure 59) and used to estimate the IC_{50} values of the peptide for each cell line. The effect of 72 h incubation with *Cn*-AMP2 on the morphology of these cell lines was examined using an inverted microscope since 48 h incubation did not show any effect. When micrographs of cells from 1321N1 and U87MG cultures, which were treated with the peptide at final concentrations of both 1 mM and 2 mM, were compared to those which acted as controls, cell numbers were seen to be significantly less in the treated cells. These micrographs also showed that cells treated with *Cn*-AMP2 exhibited no significant differences in morphology to that of control cells; no evidence of cell-death was observed, as indicated by a round morphology and detachment from the monolayer; and no sign of cell-lysis, as witnessed by membrane fragmentation. Representative micrographs of these peptide-treated cells are shown in Figure 57.

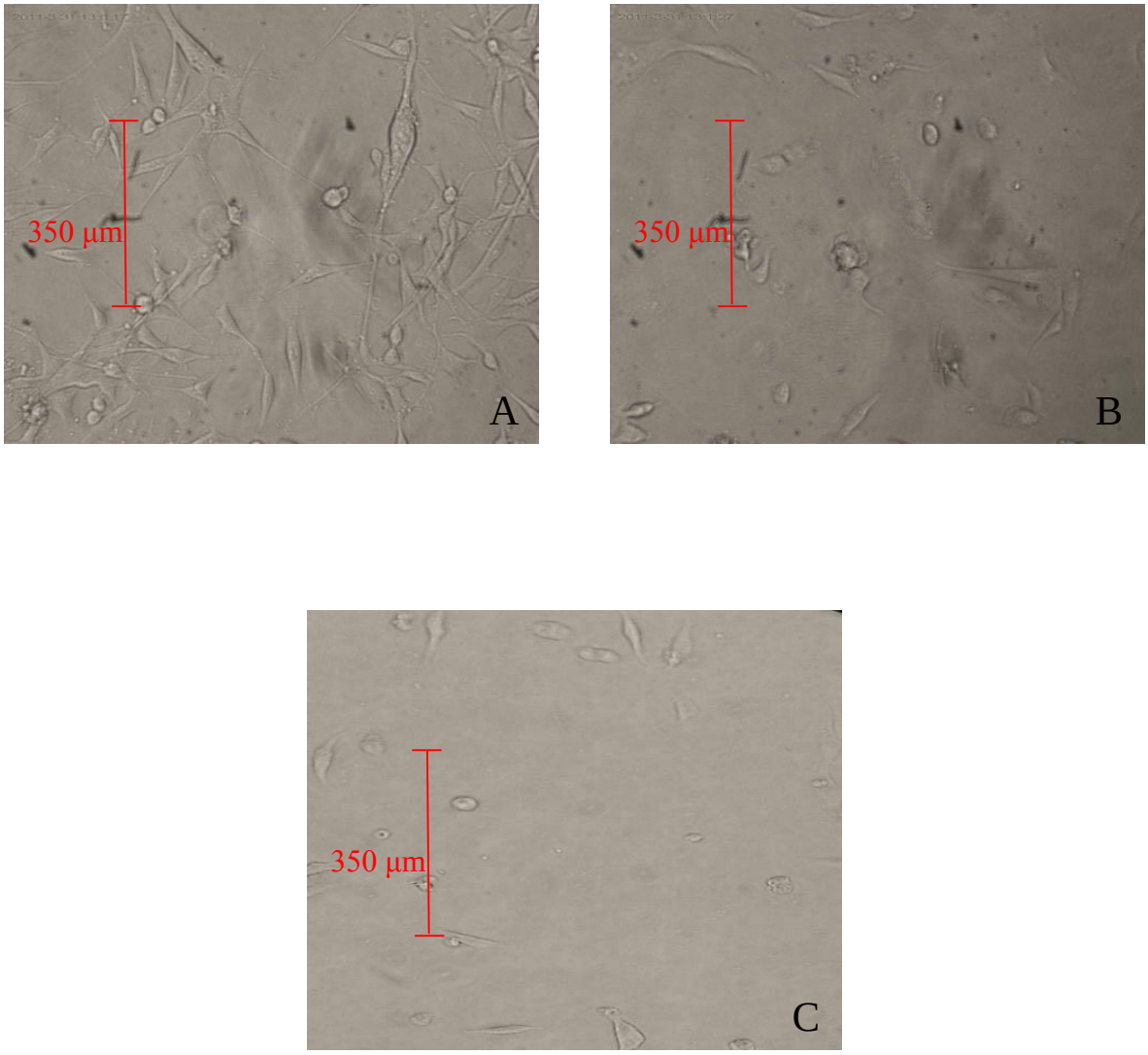

Figure 57: The morphology of 1321N1 cell line after incubation with *Cn*-AMP2.

Inverted microscope acquisitions of the 1321N1 glioma cell line at 10X magnification when cultured in DMEM with an FBS concentration of 2.5 % (v/v) and incubated for 72 h either in the absence (A) or presence of *Cn*-AMP2 at a final concentration of 1 mM (B) or 2 mM (C). It can be seen that there are no significant differences between the morphology in the case of cultures treated with peptide (B), no observable evidence of dead cells, as indicated by a round morphology and detachment from the monolayer, or lysed cells, as witnessed by membrane fragmentation or the release of cellular debris, was seen.

The sequences of the HDPs studied here were represented as two-dimensional axial projections. It was found that *Cn*-AMP2 possessed the potential to form a weakly amphiphilic α-helix with no strongly defined segregation of hydrophobic and hydrophilic amino acid residues (Figure 58). It can be seen that the longest stretch of uninterrupted hydrophobic residues found in this α-helix is the arc formed by the amino acid residues, YMF whilst the peptide's sole negatively charged residue is sandwiched between two hydrophobic V residues (Figure 58A). This contrasts to the α-helix formed by the chosen reference peptide, temporin 1-Ja, which possesses the potential to form a strongly amphiphilic α-helix. It can be seen that this α-helix exhibits a clear segregation of residues to form a short anionic, hydrophilic arc formed by the residues DNPN, which is opposed by a long a hydrophobic arc comprising the residues, LLILVLLL (Figure 58B).

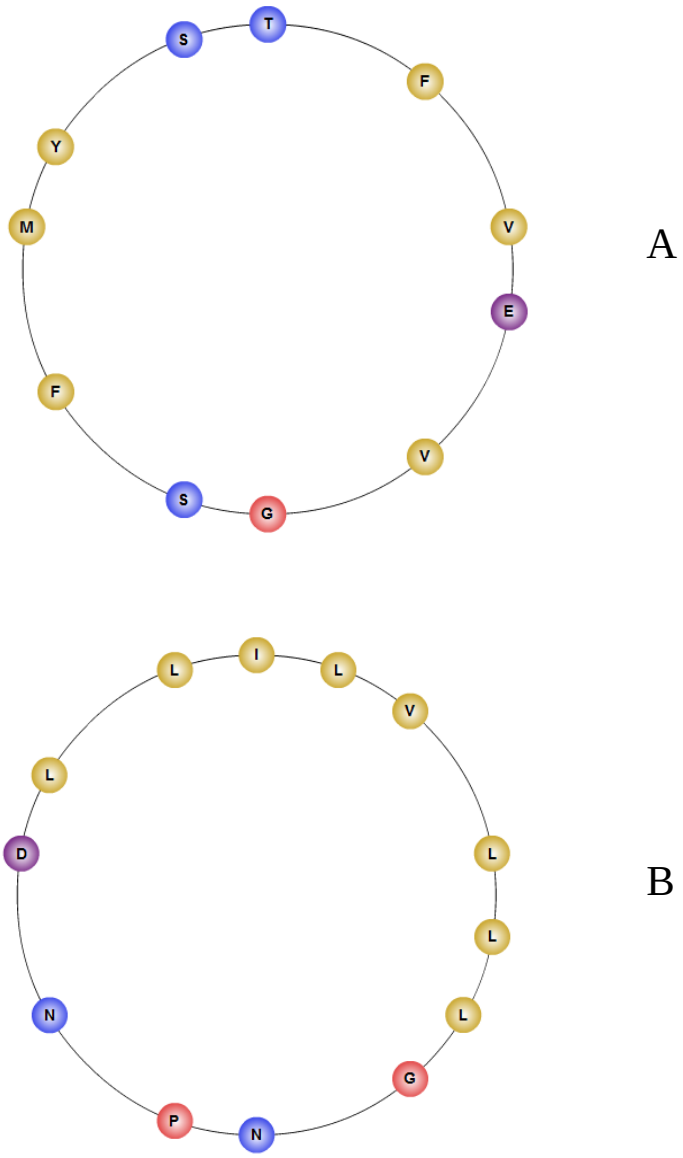

Figure 58: Peptides represented as two-dimensional axial projections.

The sequences of *Cn*-AMP2 (A) and temporin-1-Ja (B) represented as two-dimensional axial projections. It was found that *Cn*-AMP2 possessed the potential to form a weakly amphiphilic α-helix with no strongly defined segregation of hydrophobic and hydrophilic amino acid residues. In contrast, temporin 1-Ja possessed the potential to form a strongly amphiphilic α-helix as indicated by the clear segregation of residues to form hydrophobic and hydrophilic arcs. The single letter code is used to represent amino acid residues, hydrophobic residues are coloured beige, anionic residues are coloured purple, polar residues are coloured blue and neutral residues are coloured red.

It was found by the MTS assay that *Cn*-AMP2 exhibited no apparent effect on the 1321N1 and U87MG cell lines when incubated in DMEM medium containing 10 % (v/v) FBS. However, when FBS levels in DMEM were decreased to 2.5 % (v/v), the presence of the peptide led to large reductions in the viability of cell lines when compared to controls, implying that FBS has an effect on the action of *Cn*-AMP2. Similar findings have been reported by studies on the anti-cancer activity of other host defence peptides (Zhang *et al.*, 2010) and it has previously been suggested that binding of the host defence peptide (HDP) to serum proteins, such as low-density lipoprotein, may contribute to this inhibitory effect on the anti-cancer activity of these peptides (Peck-Miller *et al.*, 1993).

It was found that as the concentration of *Cn*-AMP2 was increased up to 2 mM in the presence of either the 1321N1 (IC_{50} = 1.25 mM) or U87MG (IC_{50} = 1.85 mM) cell lines, the number of viable cells decreased by up to 70 % compared to controls. It can be seen that, as compared to controls, the presence of the peptide at final concentrations of 1 mM and 2 mM led to a reduction in the viability of both the 1321N1 and U87MG cell lines that varied between 25 % and 70 % (Figure 59).

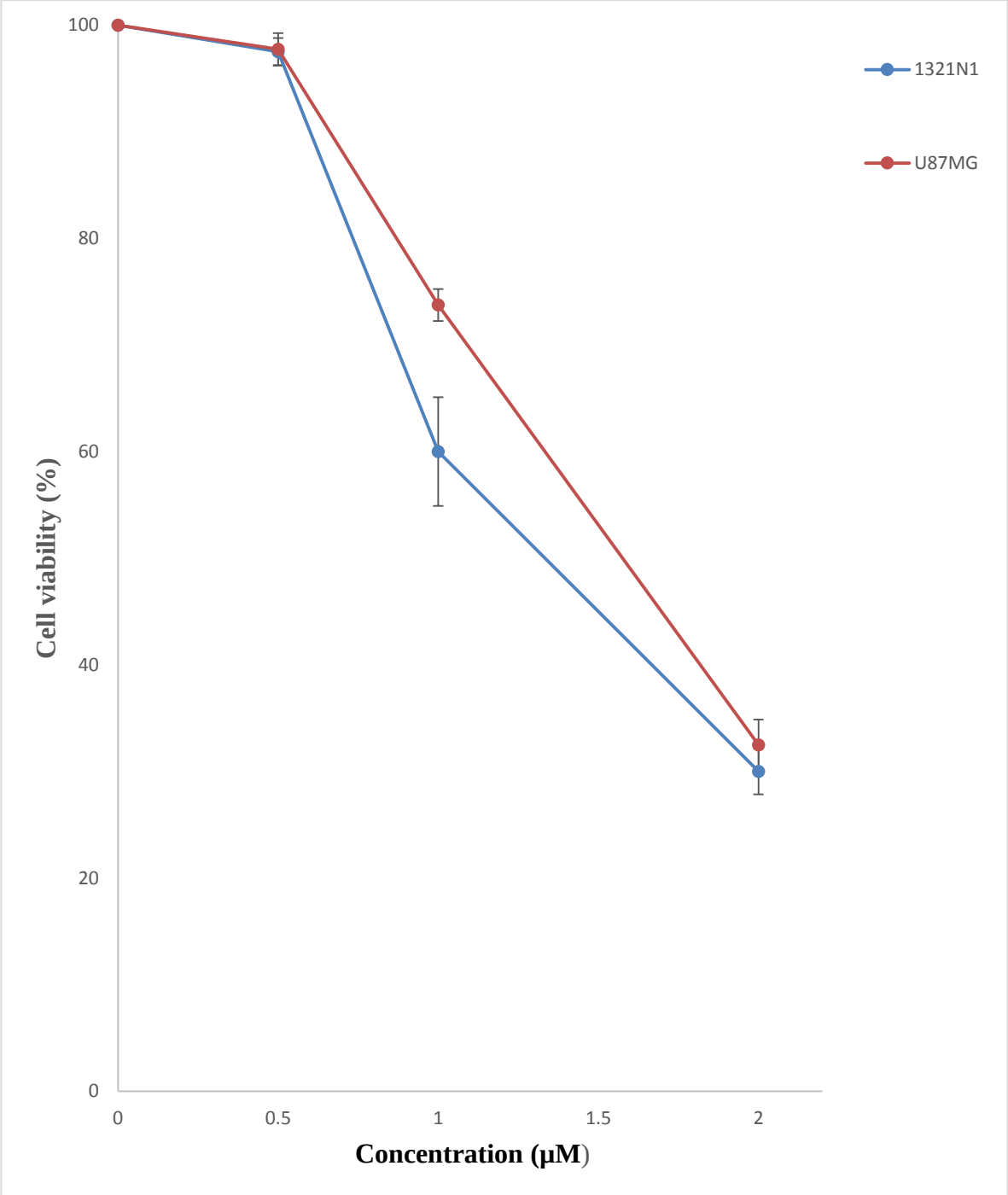

Figure 59: Dose response curves using the MTS assay for the action of *Cn*-AMP2 against the 1321N1 and U87MG glioma cell lines when cultured in DMEM with an FBS concentration of 2.5 % (v/v). The data points are means of 4 repeats and the error bars represent ±SD.

Comparable levels of another plant HDP, *Cr*-ACP1 from *Cycas revoluta*, were recently found to be required for effective activity against the cancer cell lines Hep2A, which is a human epidermoid cancer, and HCT15, which is a colon carcinoma (Mandal *et al.*, 2012). Microscopic examination of these cancer cells peptide-treated showed that these decreases in cell viability did not appear to be accompanied by cell-death or cell-lysis. In combination, these data suggest that *Cn*-AMP2 may be active against the 1321N1 and U87MG cell lines by entering target cancer cells and inhibiting their ability to proliferate using an, as yet, undetermined mechanism. It is well established that a number of HDPs exert their anticancer activity by non-membranolytic mechanisms and enter the cancer cell to attack intracellular targets such as DNA. To exert this inhibitory action it may require *Cn*-AMP2 to translocate across the cancer cell membrane and it has previously been suggested that the peptide may interact with membranes by the adoption of an amphiphilic α-helical structure (Mandal *et al.*, 2009). However, theoretical analysis here showed that *Cn*-AMP2 has the potential to form only a weakly amphiphilic α-helix as it does not possess any strongly defined segregation of hydrophobic and hydrophilic amino acid residues. Moreover, recent biophysical studies showed that the peptide exhibited a linear extended structure in the presence of lipid systems mimetic of cancer cell membranes (Prabhu, 2011) and it seems possible that this could represent the form of the peptide which facilitates its passage across the cancer cell membrane. Visual examination of the primary structure of *Cn*-AMP2 shows that the C-terminal eight residues of the peptide (YFVFSVGM) form a strongly hydrophobic region, which is flanked by a short charged segment (TES). This residue arrangement is an example of primary amphiphilicity that has been reported for other anti-cancer peptides such as indolicidin and is known to mediate the ability of these peptides to traverse membranes. By analogy to indolicidin, the anionic

segment of *Cn*-AMP2 (TES) would interact with positively charged moieties in the cancer cell membrane such as the choline group of phosphatidylcholine. Concomitantly, the hydrophobic region of the peptide (YFVFSVGM) would penetrate the membrane core region, thereby driving translocation of the peptide across the cancer cell membrane to attack intracellular targets. It is also possible that the strongly hydrophobic C-terminal region of the peptide may bind serum components, contributing to the apparent lack of anti-cancer activity shown by *Cn*-AMP2 in media containing high levels of serum.

In summary, this study has shown that *Cn*-AMP2 has activity against several human gliomas, expanding the small repertoire of anionic HDPs known to possess anticancer activity (Harris *et al.*, 2011; Harris *et al.*, 2009a). The action of *Cn*-AMP2 against these cancer cells appears to involve anti-proliferative mechanisms, which result from the ability of the peptide to translocate cancer cell membranes through a hydrophobicity-driven mechanism. Use of this mechanism would seem to reflect the fact that *Cn*-AMP2 is devoid of cationic residues and therefore lacks the capacity to engage in the electrostatically-driven mechanisms of cancer cell targeting utilised by most HDPs (Harris *et al.*, 2013a). However, this lack of cationic residues could also give *Cn*-AMP2 an advantage over cationic HDPs with anticancer action whose possession of lysine and arginine residues makes them highly susceptible to degradation by human proteases (Cho and Kim, 2010; Riedl *et al.*, 2011). Clearly, the levels of *Cn*-AMP2 shown here to be necessary for anticancer activity are prohibitive for the therapeutic application of the peptide. However, this would appear to be one of the first demonstrations that an anionic HDP can exert an anti-cancer effect and given the urgent problems due to the increasing global prevalence of cancer, it is suggested that *Cn*-AMP2 may represent a template for the development of novel HDPs with clinically useful, anti-cancer activity.

Chapter IV

4.Conclusion and future work

4.1 General conclusions

Reactive oxygen species (ROS) induce various types of cell death, depending on the cell type, concentration, and the duration of exposure (Trachootham *et al.*, 2009). In the current study, it was attempted to evaluate whether the novel indoles tested in the current study show any anti-cancer activity and if any, then to find the active compound's mechanism of action. Based on the present findings, it may be concluded that compound 209 induced rapid cell death (< 2 h) in the above mentioned cell lines via the generation of ROS which then may have mediated the cells to be in a stage of autophagic process leading to cell death. The most stable and potent compound (209) was found to be active on the non-cancerous SVGp12 cell line as well as the primary short-term culture designated as IN859. The IC_{50} value of compound 209 was relatively low on the primary cell line as compared to commercial cell lines suggesting that it may act as a potential anti-cancer drug when optimised fully in the future.

The findings from this current study are consistent with previous reports showing an association between ROS generation and autophagic cell death (Chen *et al.*, 2008; Park *et al.*, 2011). Since oxidative stress can induce different types of cell death mechanism including autophagy in various cell types, this may lead to different strategies in developing therapeutic drugs. One of the strategies being, optimising these drugs by analysing their structure-activity-relationships in such a way that they could selectively target cancer cells and undergo autophagy induced cell death independent of apoptosis. Such an approach may reveal a potential mechanism of targeted cytotoxic activity.

In addition to indoles, the anti-cancer potential of the HDP, *Cn*-AMP2, was investigated and the peptide was found to have an anti-proliferative effect against the glioma cell lines tested but only at high concentrations. It would therefore seem that the peptide might not be of therapeutic importance in its current form due to the high concentrations required to show an effect on the cancer cell lines. However, this would appear to be the first demonstration that an anionic HDP can exert an anti-cancer effect and it is possible that *Cn*-AMP2 may serve as a template for the development of future agents with activity against cancer cells.

In conclusion, it has been demonstrated that the ability of certain substituted privileged indoles may have a rapid, deleterious effect on the viability of primary cell line (IN859) and two glioma cell lines (1321N1 and U87MG) and that the mechanism of action of these indoles to cause cell death may be via the generation of ROS, which in turn leads the glioma cells to be in a stage of an autophagic process, as indicated by AVO formation and by using an autophagy inhibitor, 3-MA. Besides, the HDP, *Cn*-AMP2 was found to have an anti-proliferative effect against both the glioma cell lines (1321N1 and U87MG) tested but only at higher concentrations (> 1mM).

4.2 Scope for future studies

There appears to be huge scope for future research on these privileged indoles as they are able to induce rapid (~ 2 h) cell death in high-grade glioma cell lines and in a primary short-term culture, via the generation of ROS leading to autophagy-induced cell death. There are various avenues which could be studied further to tap the full potential of

these 2-aryl indoles. Some of the future studies which can be performed, subject to the availability of adequate funding and resources, are listed below.

Three dimensional (3D) cell culture techniques might be suitable in the immediate future for testing the potent compound (209) so that its mechanism of action could be studied in more detail. Use of 3D culturing techniques may help mimic the mode of action of the potent compound (209) *in vivo* and will also help save money on expensive animal testing. However, 3D cell culture remains open to major improvements at this point in time but can prove very useful once developed properly, and the results using it obtained become reproducible.

Future extensive research will be required to optimise the activity of these indoles. The major criterion to be taken into consideration for future work here is to analyse the structure-activity-relationships further, so that the indoles could be optimised for anti-cancer activity selectively. This study suggested that possessing an –OH group alone is not enough for the anti-cancer activity and that the entire structure (and possible the indole nucleus itself), as a whole, is required. Therefore, future work should be focused on synthesising more derivatives and analogues based on this entire structure after which 3D cell culture studies could be performed on the best compounds obtained.

Another important aspect to look into could be that the indoles can be optimised in such a way that low concentrations (< 100 µM) can prove effective because in the current study the concentrations used are relatively high when compared to the commercial drugs currently used to treat cancer. The potent compound (209) found in this study should also be tested on other types of cancer cell lines and primary cells because it is highly possible that these indoles could be specific in their modes of action such that they might have

differing activities on different cell lines. Furthermore, the indoles, found to be inactive in this study, should not be ignored and must be tested on other types of cancer cell lines and primary cells, as some of these indoles may be specific to certain types of cancers. These above factors may lead to new strategies for the development of therapeutic drugs that will selectively target specific types of cancers and therefore further testing of these compounds is essential in the future. These novel indoles can also be screened in the future with electron paramagnetic resonance (EPR) spectroscopy to check for unpaired electrons as these unpaired electrons may indicate if the compound has the potential to cause ROS mediated cell death in cancer cells. EPR spectroscopy is a technique for studying chemical species that have one or more unpaired electrons, such as organic and inorganic free radicals or inorganic complexes possessing a transition metal ion. Therefore, if compound 209 is able to form a free radical as part of its ROS-forming behaviour, then this would be detected using EPR, thus confirming part of its mechanism of action.

Molecular techniques such as qPCR and western blotting could also open another avenue as they can be used in future studies to find the molecular targets which are being targeted by these novel compounds. Western blotting will help in detecting which proteins are being over expressed in the cancer cells whilst qPCR could be used to study the specific autophagy related genes that may be up-regulated after treatment with these novel indoles. This will give a deeper insight in the workings of cell death mechanisms induced by these indoles.

Currently, two main approaches have been used to develop new autophagy regulators (inhibitors or activators). The first approach is to screen small molecules targeting autophagy (Farkas *et al.*, 2009; Zhang *et al.*, 2007) and the second one is to be

able to design and improve autophagy regulators by studying the structural information of the Atg proteins (Miller *et al.*, 2010). Further characterisation of the known 35 ATG genes (Kanki and Klionsky, 2010; Nazarko *et al.*, 2011) and the discovery of additional genes involved in autophagy regulation will help to understand the autophagy induced cell death in depth. Recently, additional autophagy regulators have been discovered through such a screening approach (Balgi *et al.*, 2009; Choi *et al.*, 2010). For example, drugs already approved for human use, such as perhexiline, niclosamide and amiodarone can reversibly inhibit mTORC1 and stimulate autophagy (Balgi *et al.*, 2009). The mammalian target of rapamycin (mTOR) is a protein which in humans is a serine/threonine protein kinase that regulates cell growth, cell proliferation, cell motility, cell survival, protein synthesis, and transcription (Hay and Sonenberg, 2004). Additional studies using these and various different approaches will be beneficial to understand the regulatory network of autophagy and in making the therapeutic modulation of autophagy a reality in the near future.

In view of the peptide looked in the current study, the sequence of the HDP, *Cn*-AMP2 can be used as a template for future research by performing permutations and combinations within these amino acid sequences as this may prove helpful in designing a new class of peptide. These peptides, including *Cn*-AMP2, should be then tested on different cancerous cell lines to determine if they prove more potent on those compared to the 1321N1 and U87MG cell lines tested in the current study.

Chapter V

Abta (2010). *Brain Tumor Primer A COMPREHENSIVE INTRODUCTION TO BRAIN TUMORS,* Illinois, USA, American Brain Tumor Association.

Aggarwal, B. B. & Ichikawa, H. (2005). Molecular targets and anticancer potential of indole-3-carbinol and its derivatives. *Cell Cycle,* 4**,** 1201-15.

Ahmad, A., Biersack, B., Li, Y., Kong, D., Bao, B., Schobert, R., Padhye, S. B. & Sarkar, F. H. (2013). Targeted regulation of PI3K/Akt/mTOR/NF-kappaB signaling by indole compounds and their derivatives: mechanistic details and biological implications for cancer therapy. *Anticancer Agents Med Chem,* 13**,** 1002-13.

Aminoff, M. J. (2011). *Nervous System In: Current Medical Diagnosis and Treatment,* New York, McGraw-Hill Medical Publishing Division.

Anto, R. J., Mukhopadhyay, A., Denning, K. & Aggarwal, B. B. (2002). Curcumin (diferuloylmethane) induces apoptosis through activation of caspase-8, BID cleavage and cytochrome c release: its suppression by ectopic expression of Bcl-2 and Bcl-xl. *Carcinogenesis,* 23**,** 143-50.

Apel, K. & Hirt, H. (2004). REACTIVE OXYGEN SPECIES: Metabolism, Oxidative Stress, and Signal Transduction. *Annual Review of Plant Biology,* 55**,** 373-399.

Aronchik, I., Chen, T., Durkin, K. A., Horwitz, M. S., Preobrazhenskaya, M. N., Bjeldanes, L. F. & Firestone, G. L. (2012). Target protein interactions of indole-3-carbinol and the highly potent derivative 1-benzyl-I3C with the C-terminal domain of human elastase uncouples cell cycle arrest from apoptotic signaling. *Mol Carcinog,* 51**,** 881-94.

Auborn, K. J., Fan, S., Rosen, E. M., Goodwin, L., Chandraskaren, A., Williams, D. E., Chen, D. & Carter, T. H. (2003). Indole-3-carbinol is a negative regulator of estrogen. *J Nutr*, 133**,** 2470S-2475S.

Avgeropoulos, N. G. & Batchelor, T. T. (1999). New Treatment Strategies for Malignant Gliomas. *The Oncologist*, 4**,** 209-224.

Awadallah, N. S., Dehn, D., Shah, R. J., Russell Nash, S., Chen, Y. K., Ross, D., Bentz, J. S. & Shroyer, K. R. (2008). NQO1 expression in pancreatic cancer and its potential use as a biomarker. *Appl Immunohistochem Mol Morphol*, 16**,** 24-31.

Baeyer, A. & Emmerling, A. (1869). Synthese des Indols. *Berichte der deutschen chemischen Gesellschaft*, 2**,** 679-682.

Balderas-Renteria, I., Gonzalez-Barranco, P., Garcia, A., Banik, B. K. & Rivera, G. (2012). Anticancer Drug Design Using Scaffolds of beta-Lactams, Sulfonamides, Quinoline, Quinoxaline and Natural Products. Drugs Advances in Clinical Trials. *Current Medicinal Chemistry*, 19**,** 4377-4398.

Balgi, A. D., Fonseca, B. D., Donohue, E., Tsang, T. C., Lajoie, P., Proud, C. G., Nabi, I. R. & Roberge, M. (2009). Screen for chemical modulators of autophagy reveals novel therapeutic inhibitors of mTORC1 signaling. *PLoS One*, 4**,** e7124.

Barnet, G. H. (2007). *High Grade Gliomas: Diagnosis and Treatment*.

Batchelor, T. T., Duda, D. G., Di Tomaso, E., Ancukiewicz, M., Plotkin, S. R., Gerstner, E., Eichler, A. F., Drappatz, J., Hochberg, F. H., Benner, T., Louis, D. N., Cohen, K. S., Chea, H., Exarhopoulos, A., Loeffler, J. S., Moses, M. A., Ivy, P., Sorensen, A. G., Wen, P.

Y. & Jain, R. K. (2010). Phase II study of cediranib, an oral pan-vascular endothelial growth factor receptor tyrosine kinase inhibitor, in patients with recurrent glioblastoma. *J Clin Oncol,* 28**,** 2817-23.

Bernstein, M. & Berger, M. S. (2008). *Neuro-oncology- The Essentials,* New York NY, Thieme.

Bhattacharya, S., Gachhui, R. & Sil, P. C. (2011). Hepatoprotective properties of kombucha tea against TBHP-induced oxidative stress via suppression of mitochondria dependent apoptosis. *Pathophysiology,* 18**,** 221-34.

Biernat, W., Aguzzi, A., Sure, U., Grant, J. W., Kleihues, P. & Hegi, M. E. (1995). Identical mutations of the p53 tumor suppressor gene in the gliomatous and the sarcomatous components of gliosarcomas suggest a common origin from glial cells. *J Neuropathol Exp Neurol,* 54**,** 651-6.

Biswas, S., Bhattacharyya, J. & Dutta, A. G. (2005). Oxidant induced injury of erythrocyte-role of green tea leaf and ascorbic acid. *Mol Cell Biochem,* 276**,** 205-10.

Boerman, R. H., Anderl, K., Herath, J., Borell, T., Johnson, N., Klein, S., Kirchhof, A., Raap, A. K., Scheithauer, B. W. & Jenkins, R. B. (1996). The glial and mesenchymal elements of gliosarcomas share similar genetic alterations. *J Neuropathol Exp Neurol,* 55**,** 973-981.

Bradlow, H. L. (2008). Review. Indole-3-carbinol as a chemoprotective agent in breast and prostate cancer. *In Vivo,* 22**,** 441-5.

Brancale, A. & Silvestri, R. (2007). Indole, a core nucleus for potent inhibitors of tubulin polymerization. *Med Res Rev,* 27**,** 209-38.

Brat, D. J., Scheithauer, B. W., Fuller, G. N. & Tihan, T. (2007). Newly codified glial neoplasms of the 2007 WHO Classification of Tumours of the Central Nervous System: angiocentric glioma, pilomyxoid astrocytoma and pituicytoma. *Brain Pathol,* 17**,** 319-24.

Brave, S. R., Ratcliffe, K., Wilson, Z., James, N. H., Ashton, S., Wainwright, A., Kendrew, J., Dudley, P., Broadbent, N., Sproat, G., Taylor, S., Barnes, C., Silva, J. C., Farnsworth, C. L., Hennequin, L., Ogilvie, D. J., Jurgensmeier, J. M., Shibuya, M., Wedge, S. R. & Barry, S. T. (2011). Assessing the activity of cediranib, a VEGFR-2/3 tyrosine kinase inhibitor, against VEGFR-1 and members of the structurally related PDGFR family. *Mol Cancer Ther,* 10**,** 861-73.

Bray, F., Jemal, A., Grey, N., Ferlay, J. & Forman, D. (2012). Global cancer transitions according to the Human Development Index (2008-2030): a population-based study. *Lancet Oncology,* 13**,** 790-801.

Brew, C. T., Aronchik, I., Kosco, K., Mccammon, J., Bjeldanes, L. F. & Firestone, G. L. (2009). Indole-3-carbinol inhibits MDA-MB-231 breast cancer cell motility and induces stress fibers and focal adhesion formation by activation of Rho kinase activity. *Int J Cancer,* 124**,** 2294-302.

Brossi, A. (1992). *The Alkoloids. The Alkaloids: Antitumor Bisindole Alkaloids from Catharanthus Roseus.* , San Deigo, Academic Press.

Brown, D. M. E. (2004). *Drug Delivery Systems in Cancer Therapy,* New Jersey, Humana Press.

Brown, J. E. & Kelly, M. F. (2007). Inhibition of lipid peroxidation by anthocyanins, anthocyanidins and their phenolic degradation products. *European Journal of Lipid Science and Technology,* 109**,** 66-71.

Brunk, U. T., Dalen, H., Roberg, K. & Hellquist, H. B. (1997). Photo-oxidative disruption of lysosomal membranes causes apoptosis of cultured human fibroblasts. *Free Radic Biol Med,* 23**,** 616-26.

Burkhard, C., Di Patre, P. L., Schuler, D., Schuler, G., Yasargil, M. G., Yonekawa, Y., Lutolf, U. M., Kleihues, P. & Ohgaki, H. (2003). A population-based study of the incidence and survival rates in patients with pilocytic astrocytoma. *J Neurosurg,* 98**,** 1170-4.

Bursch, W., Ellinger, A., Kienzl, H., Torok, L., Pandey, S., Sikorska, M., Walker, R. & Hermann, R. S. (1996). Active cell death induced by the anti-estrogens tamoxifen and ICI 164 384 in human mammary carcinoma cells (MCF-7) in culture: the role of autophagy. *Carcinogenesis,* 17**,** 1595-607.

Bursch, W., Hochegger, K., Torok, L., Marian, B., Ellinger, A. & Hermann, R. S. (2000). Autophagic and apoptotic types of programmed cell death exhibit different fates of cytoskeletal filaments. *Journal of Cell Science,* 113**,** 1189-1198.

Burton, E. C. & Prados, M. D. (2000). Malignant gliomas. *Curr Treat Options Oncol,* 1**,** 459-68.

Cadenas, E. (1989). Biochemistry of oxygen toxicity. *Annu Rev Biochem,* 58**,** 79-110.

Chang, S. M., Parney, I. F., Huang, W., Anderson, F. A., Jr., Asher, A. L., Bernstein, M., Lillehei, K. O., Brem, H., Berger, M. S. & Laws, E. R. (2005). Patterns of care for adults with newly diagnosed malignant glioma. *JAMA*, 293**,** 557-64.

Chao, W. R., Yean, D., Amin, K., Green, C. & Jong, L. (2007). Computer-aided rational drug design: a novel agent (SR13668) designed to mimic the unique anticancer mechanisms of dietary indole-3-carbinol to block Akt signaling. *J Med Chem*, 50**,** 3412-5.

Chen, Y., Mcmillan-Ward, E., Kong, J., Israels, S. J. & Gibson, S. B. (2008). Oxidative stress induces autophagic cell death independent of apoptosis in transformed and cancer cells. *Cell Death Differ*, 15**,** 171-182.

Chen, Y. B. & Lacasce, A. S. (2008). Enzastaurin. *Expert Opin Investig Drugs*, 17**,** 939-44.

Cho, J. H. & Kim, S. C. (2010). *Non-membrane Targets of Antimicrobial Peptides: Novel Therapeutic Opportunities?*

Choi, I. K., Cho, Y. S., Jung, H. J. & Kwon, H. J. (2010). Autophagonizer, a novel synthetic small molecule, induces autophagic cell death. *Biochem Biophys Res Commun*, 393**,** 849-54.

Christophersen, C. (1983). *Marine indoles*, New York, Academic Press.

Clinicaltrials.Gov. 2013. *Clinicaltrials.gov* [Online]. Available: http://clinicaltrials.gov/ct2/home [Accessed 16th May 2013].

Cooper, G. M. (2000). *The Cell: A Molecular Approach*, Sunderland, Massachusetts, USA, Sinauer Associates Incorporated.

Cragg, G. M., Grothaus, P. G. & Newman, D. J. (2009). Impact of Natural Products on Developing New Anti-Cancer Agents. *Chemical Reviews,* 109**,** 3012-3043.

Cragg, G. M. & Newman, D. J. (2013). Natural products: A continuing source of novel drug leads. *Biochimica Et Biophysica Acta-General Subjects,* 1830**,** 3670-3695.

Cree, I. A. & Andreotti, P. E. (1997). Measurement of cytotoxicity by ATP-based luminescence assay in primary cell cultures and cell lines. *Toxicology in Vitro,* 11**,** 553-556.

Crocetti, E., Trama, A., Stiller, C., Caldarella, A., Soffietti, R., Jaal, J., Weber, D. C., Ricardi, U., Slowinski, J. & Brandes, A. (2012). Epidemiology of glial and non-glial brain tumours in Europe. *Eur J Cancer*.

Crouch, S. P., Kozlowski, R., Slater, K. J. & Fletcher, J. (1993). The use of ATP bioluminescence as a measure of cell proliferation and cytotoxicity. *J Immunol Methods,* 160**,** 81-8.

Darzynkiewicz, Z. (1991). Flow cytometric methods for RNA content analysis. *Methods,* 2**,** 200-206.

Darzynkiewicz, Z. & Juan, G. (1997). *Differential staining of DNA and RNA,* New York, Wiley- Liss.

Darzynkiewicz, Z. K., J. (1990). *Acridine Orange, a Versatile Probe of Nucleic Acids and Other Cell Constituents.,* New York, Liss, Inc.

De Martino, G., Edler, M. C., La Regina, G., Coluccia, A., Barbera, M. C., Barrow, D., Nicholson, R. I., Chiosis, G., Brancale, A., Hamel, E., Artico, M. & Silvestri, R. (2006).

New arylthioindoles: potent inhibitors of tubulin polymerization. 2. Structure-activity relationships and molecular modeling studies. *J Med Chem,* 49**,** 947-54.

Deangelis, L. M., Seiferheld, W., Schold, S. C., Fisher, B. & Schultz, C. J. (2002). Combination chemotherapy and radiotherapy for primary central nervous system lymphoma: Radiation Therapy Oncology Group Study 93-10. *J Clin Oncol,* 20**,** 4643-8.

Degenhardt, K., Mathew, R., Beaudoin, B., Bray, K., Anderson, D., Chen, G., Mukherjee, C., Shi, Y., Gelinas, C., Fan, Y., Nelson, D. A., Jin, S. & White, E. (2006). Autophagy promotes tumor cell survival and restricts necrosis, inflammation, and tumorigenesis. *Cancer Cell,* 10**,** 51-64.

Deleage, G., Combet, C., Blanchet, C. & Geourjon, C. (2001). ANTHEPROT: an integrated protein sequence analysis software with client/server capabilities. *Comput Biol Med,* 31**,** 259-67.

Dennison, S. R., Wallace, J., Harris, F. & Phoenix, D. A. (2005). Amphiphilic alpha-helical antimicrobial peptides and their structure/function relationships. *Protein Pept Lett,* 12**,** 31-9.

Dennison, S. R., Whittaker, M., Harris, F. & Phoenix, D. A. (2006a). Anticancer alpha-helical peptides and structure/function relationships underpinning their interactions with tumour cell membranes. *Curr Protein Pept Sci,* 7**,** 487-499.

Dennison, S. R., Whittaker, M., Harris, F. & Phoenix, D. A. (2006b). Anticancer alpha-helical peptides and structure/function relationships underpinning their interactions with tumour cell membranes. *Current Protein & Peptide Science,* 7**,** 487-499.

Desimone, R. W., Currie, K. S., Mitchell, S. A., Darrow, J. W. & Pippin, D. A. (2004). Privileged structures: applications in drug discovery. *Comb Chem High Throughput Screen,* 7**,** 473-94.

Doppalapudi, R. S., Riccio, E. S., Rausch, L. L., Shimon, J. A., Lee, P. S., Mortelmans, K. E., Kapetanovic, I. M., Crowell, J. A. & Mirsalis, J. C. (2007). Evaluation of chemopreventive agents for genotoxic activity. *Mutat Res,* 629**,** 148-60.

Dreicer, R., Garcia, J., Rini, B., Vogelzang, N., Srinivas, S., Somer, B., Shi, P., Kania, M. & Raghavan, D. (2013). A randomized, double-blind, placebo-controlled, Phase II study with and without enzastaurin in combination with docetaxel-based chemotherapy in patients with castration-resistant metastatic prostate cancer. *Invest New Drugs,* 31**,** 1044-50.

Efird, J. (2011). *Epidemiology of Glioma* - In Tech.

Engelberg-Kulka, H., Amitai, S., Kolodkin-Gal, I. & Hazan, R. (2006). Bacterial programmed cell death and multicellular behavior in bacteria. *PLoS Genet,* 2**,** e135.

Espinosa, E., Zamora, P., Feliu, J. & Gonzalez Baron, M. (2003). Classification of anticancer drugs--a new system based on therapeutic targets. *Cancer Treat Rev,* 29**,** 515-23.

Evans (2009). *Trease and Evans Pharmacognosy,* New York, Elsevier.

Farkas, T., Hoyer-Hansen, M. & Jaattela, M. (2009). Identification of novel autophagy regulators by a luciferase-based assay for the kinetics of autophagic flux. *Autophagy,* 5**,** 1018-25.

Fda, U. S. F. D. A. 2006. *FDA Approves New Treatment for Gastrointestinal and Kidney Cancer* [Online]. Available: http://www.fda.gov/NewsEvents/Newsroom/PressAnnouncements/2006/ucm108583.htm [Accessed 27th March 2013].

Firestone, G. L. & Bjeldanes, L. F. (2003). Indole-3-carbinol and 3-3'-diindolylmethane antiproliferative signaling pathways control cell-cycle gene transcription in human breast cancer cells by regulating promoter-Sp1 transcription factor interactions. *J Nutr,* 133**,** 2448S-2455S.

Fisher, B. J., Bauman, G. S., Leighton, C. E., Stitt, L., Cairncross, J. G. & Macdonald, D. R. (1998). Low-grade gliomas in children: tumor volume response to radiation. *Neurosurg Focus,* 4**,** e5.

Fisher, J. L., Schwartzbaum, J. A., Wrensch, M. & Wiemels, J. L. (2007). Epidemiology of brain tumors. *Neurol Clin,* 25**,** 867-90, vii.

Frankel, R. H., Bayona, W., Koslow, M. & Newcomb, E. W. (1992). p53 mutations in human malignant gliomas: comparison of loss of heterozygosity with mutation frequency. *Cancer Res,* 52**,** 1427-33.

Freshney, R. I. (2010). *Culture of Animal Cells: A Manual of Basic Technique and Specialized Applications*, John Wiley & Sons.

Fujisawa, S., Atsumi, T., Murakami, Y. & Kadoma, Y. (2005). Dimerization, ROS formation, and biological activity of o-methoxyphenols. *Arch Immunol Ther Exp (Warsz),* 53**,** 28-38.

Gagliano, N., Aldini, G., Colombo, G., Rossi, R., Colombo, R., Gioia, M., Milzani, A. & Dalle-Donne, I. (2010). The potential of resveratrol against human gliomas. *Anticancer Drugs,* 21**,** 140-50.

Galanis, E. & Buckner, J. C. (2000). Chemotherapy of brain tumors. *Curr Opin Neurol,* 13**,** 619-25.

Gaspar, D., Veiga, A. S. & Castanho, M. R. B. (2013). From antimicrobial to anticancer peptides. A review. *Frontiers in Microbiology,* 4.

Gastpar, R., Goldbrunner, M., Marko, D. & Von Angerer, E. (1998). Methoxy-substituted 3-formyl-2-phenylindoles inhibit tubulin polymerization. *J Med Chem,* 41**,** 4965-72.

Gozuacik, D. & Kimchi, A. (2004). Autophagy as a cell death and tumor suppressor mechanism. *Oncogene,* 23**,** 2891-906.

Graff, J. R., Mcnulty, A. M., Hanna, K. R., Konicek, B. W., Lynch, R. L., Bailey, S. N., Banks, C., Capen, A., Goode, R., Lewis, J. E., Sams, L., Huss, K. L., Campbell, R. M., Iversen, P. W., Neubauer, B. L., Brown, T. J., Musib, L., Geeganage, S. & Thornton, D. (2005). The protein kinase Cbeta-selective inhibitor, Enzastaurin (LY317615.HCl), suppresses signaling through the AKT pathway, induces apoptosis, and suppresses growth of human colon cancer and glioblastoma xenografts. *Cancer Res,* 65**,** 7462-9.

Green, C. E., Swezey, R., Bakke, J., Shinn, W., Furimsky, A., Bejugam, N., Shankar, G. N., Jong, L. & Kapetanovic, I. M. (2011). Improved oral bioavailability in rats of SR13668, a novel anti-cancer agent. *Cancer Chemother Pharmacol,* 67**,** 995-1006.

Grose, K. R. & Bjeldanes, L. F. (1992). Oligomerization of indole-3-carbinol in aqueous acid. *Chem Res Toxicol,* 5**,** 188-93.

Gul, W. & Hamann, M. T. (2005). Indole alkaloid marine natural products: an established source of cancer drug leads with considerable promise for the control of parasitic, neurological and other diseases. *Life Sci,* 78**,** 442-53.

Han, J. & Burgess, K. (2010). Fluorescent indicators for intracellular pH. *Chem Rev,* 110**,** 2709-28.

Harper, M. E., Bevilacqua, L., Hagopian, K., Weindruch, R. & Ramsey, J. J. (2004). Ageing, oxidative stress, and mitochondrial uncoupling. *Acta Physiologica Scandinavica,* 182**,** 321-331.

Harris, F., Dennison, S. & Phoenix, D. (2011). Anionic Antimicrobial Peptides from Eukaryotic Organisms and their Mechanisms of Action. *Current Chemical Biology,* 5**,** 142-153.

Harris, F., Dennison, S. R. & Phoenix, D. A. (2009a). Anionic Antimicrobial Peptides from Eukaryotic Organisms. *Current Protein & Peptide Science,* 10**,** 585-606.

Harris, F., Dennison, S. R. & Phoenix, D. A. (2009b). Anionic antimicrobial peptides from eukaryotic organisms. *Curr Protein Pept Sci,* 10**,** 585-606.

Harris, F., Dennison, S. R., Singh, J. & Phoenix, D. A. (2013a). On the selectivity and efficacy of defense peptides with respect to cancer cells. *Medicinal Research Reviews,* 33**,** 190-234.

Harris, F., Dennison, S. R., Singh, J. & Phoenix, D. A. (2013b). On the selectivity and efficacy of defense peptides with respect to cancer cells. *Med Res Rev,* 33**,** 190-234.

Hay, N. & Sonenberg, N. (2004). Upstream and downstream of mTOR. *Genes Dev,* 18**,** 1926-45.

Helm, C. W. & States, J. C. (2009). Enhancing the efficacy of cisplatin in ovarian cancer treatment - could arsenic have a role. *J Ovarian Res,* 2**,** 2.

Hendricks, R. T., Sherman, D., Strulovici, B. & Broka, C. A. (1995). 2-aryl-indolyl maleimides - novel and potent inhibitors of protein kinase C. *Bioorganic & Medicinal Chemistry Letters,* 5**,** 67-72.

Higdon, J. V., Delage, B., Williams, D. E. & Dashwood, R. H. (2007). Cruciferous vegetables and human cancer risk: epidemiologic evidence and mechanistic basis. *Pharmacol Res,* 55**,** 224-36.

Hoang-Xuan, K., Idbaih, A., Mokhtari, K. & Sanson, M. (2005). [Towards a molecular classification of gliomas]. *Bull Cancer,* 92**,** 310-6.

Horakova, K. & Betina, V. (1977). Cytotoxic activity of macrocyclic metabolites from fungi. *Neoplasma,* 24**,** 21-7.

Horton, D. A., Bourne, G. T. & Smythe, M. L. (2003). The combinatorial synthesis of bicyclic privileged structures or privileged substructures. *Chem Rev,* 103**,** 893-930.

Hoskin, D. W. & Ramamoorthy, A. (2008). Studies on anticancer activities of antimicrobial peptides. *Biochimica et Biophysica Acta (BBA) - Biomembranes,* 1778**,** 357-375.

Hou, L., Xie, K., Qin, M., Peng, D., Ma, S., Shang, L., Li, N., Li, S., Ji, G., Lu, Y. & Xiong, L. (2010). Effects of reactive oxygen species scavenger on the protective action of 100% oxygen treatment against sterile inflammation in mice. *Shock,* 33**,** 646-54.

Hu, W., Guo, Z., Chu, F., Bai, A., Yi, X., Cheng, G. & Li, J. (2003). Synthesis and biological evaluation of substituted 2-sulfonyl-phenyl-3-phenyl-indoles: a new series of selective COX-2 inhibitors. *Bioorg Med Chem,* 11**,** 1153-60.

Iwasaki, Y., Hirasawa, T., Maruyama, Y., Ishii, Y., Ito, R., Saito, K., Umemura, T., Nishikawa, A. & Nakazawa, H. (2011). Effect of interaction between phenolic compounds and copper ion on antioxidant and pro-oxidant activities. *Toxicol In Vitro,* 25**,** 1320-7.

Jain, D., Sharma, M. C., Arora, R., Sarkar, C. & Suri, V. (2008). Clear cell ependymoma: a mimicker of oligodendroglioma--report of three cases. *Neuropathology,* 28**,** 366-71.

Jansson, P. J., Asplund, K. U., Makela, J. C., Lindqvist, C. & Nordstrom, T. (2003). Vitamin C (ascorbic acid) induced hydroxyl radical formation in copper contaminated household drinking water: role of bicarbonate concentration. *Free Radic Res,* 37**,** 901-5.

Jemal, A., Siegel, R., Xu, J. & Ward, E. (2010). Cancer statistics, 2010. *CA Cancer J Clin,* 60**,** 277-300.

Jiang, H., Zhang, L., Kuo, J., Kuo, K., Gautam, S. C., Groc, L., Rodriguez, A. I., Koubi, D., Hunter, T. J., Corcoran, G. B., Seidman, M. D. & Levine, R. A. (2005). Resveratrol-induced apoptotic death in human U251 glioma cells. *Mol Cancer Ther,* 4**,** 554-61.

Jin, L., Qi, M., Chen, D. Z., Anderson, A., Yang, G. Y., Arbeit, J. M. & Auborn, K. J. (1999). Indole-3-carbinol prevents cervical cancer in human papilloma virus type 16 (HPV16) transgenic mice. *Cancer Res,* 59**,** 3991-7.

Jo Atten, M., Attar, B. M. & Holian, O. (1998). Resveratrol: A potential chemopreventive agent in human gastric cancer. *Gastroenterology,* 114, Supplement 1**,** A560.

Jordan, M. A., Thrower, D. & Wilson, L. (1992). Effects of vinblastine, podophyllotoxin and nocodazole on mitotic spindles. Implications for the role of microtubule dynamics in mitosis. *J Cell Sci,* 102 (Pt 3)**,** 401-16.

Jordan, M. A. & Wilson, L. (2004). Microtubules as a target for anticancer drugs. *Nat Rev Cancer,* 4**,** 253-65.

Joshi, A. D., Loilome, W., Siu, I. M., Tyler, B., Gallia, G. L. & Riggins, G. J. (2012). Evaluation of tyrosine kinase inhibitor combinations for glioblastoma therapy. *PLoS One,* 7**,** e44372.

Joshi, K. C. & Chand, P. (1982). Biologically active indole derivatives. *Pharmazie,* 37**,** 1-12.

Jovanovic, S. V., Boone, C. W., Steenken, S., Trinoga, M. & Kaskey, R. B. (2001). How curcumin works preferentially with water soluble antioxidants. *J Am Chem Soc,* 123**,** 3064-8.

Kamoun, W. S., Ley, C. D., Farrar, C. T., Duyverman, A. M., Lahdenranta, J., Lacorre, D. A., Batchelor, T. T., Di Tomaso, E., Duda, D. G., Munn, L. L., Fukumura, D., Sorensen, A. G. & Jain, R. K. (2009). Edema control by cediranib, a vascular endothelial growth factor

receptor-targeted kinase inhibitor, prolongs survival despite persistent brain tumor growth in mice. *J Clin Oncol,* 27**,** 2542-52.

Kangas, L., Gronroos, M. & Nieminen, A. L. (1984). Bioluminescence of cellular ATP: a new method for evaluating cytotoxic agents in vitro. *Med Biol,* 62**,** 338-43.

Kanki, T. & Klionsky, D. J. (2010). The molecular mechanism of mitochondria autophagy in yeast. *Mol Microbiol,* 75**,** 795-800.

Kanzawa, T., Germano, I. M., Komata, T., Ito, H., Kondo, Y. & Kondo, S. (2004). Role of autophagy in temozolomide-induced cytotoxicity for malignant glioma cells. *Cell Death Differ,* 11**,** 448-457.

Kanzawa, T., Kondo, Y., Ito, H., Kondo, S. & Germano, I. (2003). Induction of autophagic cell death in malignant glioma cells by arsenic trioxide. *Cancer Res,* 63**,** 2103-8.

Kanzawa, T., Zhang, L., Xiao, L., Germano, I. M., Kondo, Y. & Kondo, S. (2005). Arsenic trioxide induces autophagic cell death in malignant glioma cells by upregulation of mitochondrial cell death protein BNIP3. *Oncogene,* 24**,** 980-991.

Kaufmann, D., Pojarova, M., Vogel, S., Liebl, R., Gastpar, R., Gross, D., Nishino, T., Pfaller, T. & Von Angerer, E. (2007). Antimitotic activities of 2-phenylindole-3-carbaldehydes in human breast cancer cells. *Bioorg Med Chem,* 15**,** 5122-36.

Kazanietz, M. G. (2010). Protein Kinase C in Cancer Signaling and Therapy. *Anticancer Research,* 30**,** 5263.

Ke, L. D., Shi, Y.-X., Im, S.-A., Chen, X. & Yung, W. K. A. (2000). The Relevance of Cell Proliferation, Vascular Endothelial Growth Factor, and Basic Fibroblast Growth Factor Production to Angiogenesis and Tumorigenicity in Human Glioma Cell Lines. *Clinical Cancer Research,* 6**,** 2562-2572.

Keith, A., Alexander, J., Julian, L., Martin, R., Roberts. And Peter, W. (2008). *Apoptosis: Programmed Cell Death Eliminates Unwanted Cells*, New York, Garland Science.

Kim, J. A., Aberg, C., Salvati, A. & Dawson, K. A. (2012). Role of cell cycle on the cellular uptake and dilution of nanoparticles in a cell population. *Nat Nanotechnol,* 7**,** 62-8.

Kim, L. & Glantz, M. (2006). Chemotherapeutic options for primary brain tumors. *Current Treatment Options in Oncology,* 7**,** 467-478.

Kim, Y. S. & Milner, J. A. (2005). Targets for indole-3-carbinol in cancer prevention. *J Nutr Biochem,* 16**,** 65-73.

Klaunig, J. E. & Kamendulis, L. M. (2004). The role of oxidative stress in carcinogenesis. *Annu Rev Pharmacol Toxicol,* 44**,** 239-67.

Kleihues, P. & Cavenee, W. K. (2000). *Pathology and Genetics. Tumours of the Nervous system,* Lyon, IARC Press.

Klionsky, D. J. (2007). Autophagy: from phenomenology to molecular understanding in less than a decade. *Nat Rev Mol Cell Biol,* 8**,** 931-937.

Klionsky, D. J., Cregg, J. M., Dunn, W. A., Jr., Emr, S. D., Sakai, Y., Sandoval, I. V., Sibirny, A., Subramani, S., Thumm, M., Veenhuis, M. & Ohsumi, Y. (2003). A unified nomenclature for yeast autophagy-related genes. *Dev Cell,* 5**,** 539-45.

Kochl, R., Hu, X. W., Chan, E. Y. & Tooze, S. A. (2006). Microtubules facilitate autophagosome formation and fusion of autophagosomes with endosomes. *Traffic,* 7**,** 129-45.

Kojima, T., Tanaka, T. & Mori, H. (1994). Chemoprevention of spontaneous endometrial cancer in female Donryu rats by dietary indole-3-carbinol. *Cancer Res,* 54**,** 1446-9.

Kong, X. X., Zhang, H. Y., Chen, R., Fan, X. F. & Gong, Y. S. (2011). [The time order of autophagy and apoptosis process in the oxidative injury in glioma U251 cells]. *Zhongguo Ying Yong Sheng Li Xue Za Zhi,* 27**,** 471-4.

Koukourakis, G. V., Kouloulias, V., Zacharias, G., Papadimitriou, C., Pantelakos, P., Maravelis, G., Fotineas, A., Beli, I., Chaldeopoulos, D. & Kouvaris, J. (2009). Temozolomide with radiation therapy in high grade brain gliomas: pharmaceuticals considerations and efficacy; a review article. *Molecules,* 14**,** 1561-77.

Kroemer, G., Galluzzi, L., Vandenabeele, P., Abrams, J., Alnemri, E. S., Baehrecke, E. H., Blagosklonny, M. V., El-Deiry, W. S., Golstein, P., Green, D. R., Hengartner, M., Knight, R. A., Kumar, S., Lipton, S. A., Malorni, W., Nunez, G., Peter, M. E., Tschopp, J., Yuan, J., Piacentini, M., Zhivotovsky, B. & Melino, G. (2009). Classification of cell death: recommendations of the Nomenclature Committee on Cell Death 2009. *Cell Death Differ,* 16**,** 3-11.

Lai, A., Tran, A., Nghiemphu, P. L., Pope, W. B., Solis, O. E., Selch, M., Filka, E., Yong, W. H., Mischel, P. S., Liau, L. M., Phuphanich, S., Black, K., Peak, S., Green, R. M., Spier, C. E., Kolevska, T., Polikoff, J., Fehrenbacher, L., Elashoff, R. & Cloughesy, T. (2011). Phase II study of bevacizumab plus temozolomide during and after radiation therapy for patients with newly diagnosed glioblastoma multiforme. *J Clin Oncol,* 29**,** 142-8.

Lake, R., Blunt, J. & Munro, M. (1989). Eudistomins From the New Zealand Ascidian <I>Ritterella sigillinoides</I>. *Australian Journal of Chemistry,* 42**,** 1201-1206.

Lal, S. & Snape, T. J. (2012). 2-Arylindoles: a privileged molecular scaffold with potent, broad-ranging pharmacological activity. *Curr Med Chem,* 19**,** 4828-37.

Laws, E. R., Parney, I. F., Huang, W., Anderson, F., Morris, A. M., Asher, A., Lillehei, K. O., Bernstein, M., Brem, H., Sloan, A., Berger, M. S. & Chang, S. (2003). Survival following surgery and prognostic factors for recently diagnosed malignant glioma: data from the Glioma Outcomes Project. *J Neurosurg,* 99**,** 467-73.

Leete, E. J. (1959). 3-Hydroxymethylindoles. *Journal of the American Chemical Society,* 81**,** 6023.

Leo, A., Hansch, C. & Elkins, D. (1971). Partition coefficients and their uses. *Chemical Reviews,* 71**,** 525-616.

Levine, B. & Yuan, J. (2005). Autophagy in cell death: an innocent convict? *The Journal of Clinical Investigation,* 116**,** 3293-3293.

Li, J., Qin, Z. & Liang, Z. (2009). The prosurvival role of autophagy in Resveratrol-induced cytotoxicity in human U251 glioma cells. *BMC Cancer,* 9**,** 215.

Linford, N. J., Schriner, S. E. & Rabinovitch, P. S. (2006). Oxidative Damage and Aging: Spotlight on Mitochondria. *Cancer Research,* 66**,** 2497-2499.

Lipinski, C. A., Lombardo, F., Dominy, B. W. & Feeney, P. J. (2001). Experimental and computational approaches to estimate solubility and permeability in drug discovery and development settings. *Adv Drug Deliv Rev,* 46**,** 3-26.

Liu, Y. Z., Wu, K., Huang, J., Liu, Y., Wang, X., Meng, Z. J., Yuan, S. X., Wang, D. X., Luo, J. Y., Zuo, G. W., Yin, L. J., Chen, L., Deng, Z. L., Yang, J. Q., Sun, W. J. & He, B. C. (2014). The PTEN/PI3K/Akt and Wnt/beta-catenin signaling pathways are involved in the inhibitory effect of resveratrol on human colon cancer cell proliferation. *Int J Oncol.*

Lonardi, S., Tosoni, A. & Brandes, A. A. (2005). Adjuvant chemotherapy in the treatment of high grade gliomas. *Cancer Treat Rev,* 31**,** 79-89.

Louis, D. N., Holland, E. C. & Cairncross, J. G. (2001). Glioma classification: a molecular reappraisal. *Am J Pathol,* 159**,** 779-86.

Louis, D. N., Ohgaki, H., Wiestler, O. D., Cavenee, W. K., Burger, P. C., Jouvet, A., Scheithauer, B. W. & Kleihues, P. (2007). The 2007 WHO classification of tumours of the central nervous system. *Acta Neuropathol,* 114**,** 97-109.

Mandal, S. M., Dey, S., Mandal, M., Sarkar, S., Maria-Neto, S. & Franco, O. L. (2009). Identification and structural insights of three novel antimicrobial peptides isolated from green coconut water. *Peptides,* 30**,** 633-637.

Mandal, S. M., Migliolo, L., Das, S., Mandal, M., Franco, O. L. & Hazra, T. K. (2012). Identification and characterization of a bactericidal and proapoptotic peptide from Cycas revoluta seeds with DNA binding properties. *J Cell Biochem,* 113**,** 184-93.

Maria Cuervo, A. (2004). Autophagy: in sickness and in health. *Trends in Cell Biology,* 14**,** 70-77.

Marian, V., Mario, I., Milan, M., Christopher, J. R. & Joshua, T. (2004). Role of oxygen radicals in DNA damage and cancer incidence. *Molecular and Cellular Biochemistry,* 266**,** 37-56.

Martin Sabroso, C. & Torres-Suarez, A. I. (2014). Objective: tumor. Strategies of drug targeting at the tumor mass level. *Clinical & Translational Oncology,* 16**,** 1-10.

Martinho, O., Silva-Oliveira, R., Miranda-Goncalves, V., Clara, C., Almeida, J. R., Carvalho, A. L., Barata, J. T. & Reis, R. M. (2013). In Vitro and In Vivo Analysis of RTK Inhibitor Efficacy and Identification of Its Novel Targets in Glioblastomas. *Transl Oncol,* 6**,** 187-96.

Matsui, Y., Takagi, H., Qu, X., Abdellatif, M., Sakoda, H., Asano, T., Levine, B. & Sadoshima, J. (2007). Distinct Roles of Autophagy in the Heart During Ischemia and Reperfusion. *Circulation Research,* 100**,** 914-922.

Matsuoka, S., Huang, M. & Elledge, S. J. (1998). Linkage of ATM to cell cycle regulation by the Chk2 protein kinase. *Science,* 282**,** 1893-7.

Matsuzaki, I., Suzuki, H., Kitamura, M., Minamiya, Y., Kawai, H. & Ogawa, J. (2000). Cisplatin induces fas expression in esophageal cancer cell lines and enhanced cytotoxicity in combination with LAK cells. *Oncology,* 59**,** 336-43.

Mcfarland, A. J., Anoopkumar-Dukie, S., Perkins, A. V., Davey, A. K. & Grant, G. D. (2012). Inhibition of autophagy by 3-methyladenine protects 1321N1 astrocytoma cells against pyocyanin- and 1-hydroxyphenazine-induced toxicity. *Arch Toxicol,* 86**,** 275-84.

Mcgowan, E. M., Alling, N., Jackson, E. A., Yagoub, D., Haass, N. K., Allen, J. D. & Martinello-Wilks, R. (2011). Evaluation of cell cycle arrest in estrogen responsive MCF-7 breast cancer cells: pitfalls of the MTS assay. *PLoS ONE,* 6**,** e20623.

Mckinney, P. A. (2004). Brain tumours: incidence, survival, and aetiology. *J Neurol Neurosurg Psychiatry,* 75 Suppl 2**,** ii12-7.

Meijer, A. J. & Codogno, P. (2004). Regulation and role of autophagy in mammalian cells. *Int J Biochem Cell Biol,* 36**,** 2445-62.

Melino, G. (2001). The Sirens' song. *Nature,* 412**,** 23.

Miller, S., Tavshanjian, B., Oleksy, A., Perisic, O., Houseman, B. T., Shokat, K. M. & Williams, R. L. (2010). Shaping development of autophagy inhibitors with the structure of the lipid kinase Vps34. *Science,* 327**,** 1638-42.

Moore, K. & Kim, L. (2010). *Primary Brain Tomors: Characteristics Practical Daignostic and Treatment Approaches,* New York NY, Springer Science.

Morgan, D. O. (2007). *The Cell Cycle: Principles of Control,* New Science Press.

Mori, H., Niwa, K., Zheng, Q., Yamada, Y., Sakata, K. & Yoshimi, N. (2001). Cell proliferation in cancer prevention; effects of preventive agents on estrogen-related endometrial carcinogenesis model and on an in vitro model in human colorectal cells. *Mutat Res,* 480-481**,** 201-7.

Mosmann, T. (1983). Rapid colorimetric assay for cellular growth and survival: Application to proliferation and cytotoxicity assays. *Journal of Immunological Methods,* 65**,** 55-63.

Mukherjee, A. (2008). *Cell Biology: Fundamentals and Applications.,* India, Oscar Publications.

Nagabhushan M & Sv, B. (1987). Anti-mutagenic and anticarcinogenic action of turmeric (Curcumas longa). *J Nutr Growth Cancer,* 4**,** 82–89.

Nazarko, V. Y., Nazarko, T. Y., Farre, J. C., Stasyk, O. V., Warnecke, D., Ulaszewski, S., Cregg, J. M., Sibirny, A. A. & Subramani, S. (2011). Atg35, a micropexophagy-specific protein that regulates micropexophagic apparatus formation in Pichia pastoris. *Autophagy,* 7**,** 375-85.

Newman, D. J. & Cragg, G. M. (2012). Natural Products As Sources of New Drugs over the 30 Years from 1981 to 2010. *Journal of Natural Products,* 75**,** 311-335.

Newton, H. B. (2006). *Handbook of Brain Tumour Chemotherapy,* London, Elsevier Sceince Inc.

Nguyen, H. H., Lavrenov, S. N., Sundar, S. N., Nguyen, D. H., Tseng, M., Marconett, C. N., Kung, J., Staub, R. E., Preobrazhenskaya, M. N., Bjeldanes, L. F. & Firestone, G. L.

(2010). 1-Benzyl-indole-3-carbinol is a novel indole-3-carbinol derivative with significantly enhanced potency of anti-proliferative and anti-estrogenic properties in human breast cancer cells. *Chem Biol Interact,* 186**,** 255-66.

Nikiforova, M. N. & Hamilton, R. L. (2011). Molecular diagnostics of gliomas. *Arch Pathol Lab Med,* 135**,** 558-68.

Nugumanova, G., Bukharov, S., Tagasheva, R., Kurapova, M., Syakaev, V., Mukmeneva, N., Gurevich, P. & Burilov, A. (2007). Synthesis of sterically hindered phenolic compounds from indole and its derivatives. *Russian Journal of Organic Chemistry,* 43**,** 1797-1803.

Oganesian, A., Hendricks, J. D. & Williams, D. E. (1997). Long term dietary indole-3-carbinol inhibits diethylnitrosamine-initiated hepatocarcinogenesis in the infant mouse model. *Cancer Lett,* 118**,** 87-94.

Ohgaki, H. & Kleihues, P. (2005). Epidemiology and etiology of gliomas. *Acta Neuropathologica,* 109**,** 93-108.

Okamura, T., Kurisu, K., Yamamoto, W., Takano, H. & Nishiyama, M. (2000). NADPH/quinone oxidoreductase is a priority target of glioblastoma chemotherapy. *Int J Oncol,* 16**,** 295-303.

Oliva, C. R., Moellering, D. R., Gillespie, G. Y. & Griguer, C. E. (2011). Acquisition of chemoresistance in gliomas is associated with increased mitochondrial coupling and decreased ROS production. *PLoS ONE,* 6**,** e24665.

Opipari, A. W., Tan, L., Boitano, A. E., Sorenson, D. R., Aurora, A. & Liu, J. R. (2004). Resveratrol-induced Autophagocytosis in Ovarian Cancer Cells. *Cancer Research,* 64**,** 696-703.

Oprea, T. I., Davis, A. M., Teague, S. J. & Leeson, P. D. (2001). {I}s there a difference between leads and drugs? {A} historical perspective. *J Chem Inf Comput Sci,* 41**,** 1308-1315.

Osborne, N. N., Cuello, A. C. & Dockray, G. J. (1982). Substance P and cholecystokinin-like peptides in Helix neurons and cholecystokinin and serotonin in a giant neuron. *Science,* 216**,** 409-11.

Owellen, R. J., Owens, A. H., Jr. & Donigian, D. W. (1972). The binding of vincristine, vinblastine and colchicine to tubulin. *Biochem Biophys Res Commun,* 47**,** 685-91.

Ozyurek, M., Bektasoglu, B., Guclu, K. & Apak, R. (2008). Hydroxyl radical scavenging assay of phenolics and flavonoids with a modified cupric reducing antioxidant capacity (CUPRAC) method using catalase for hydrogen peroxide degradation. *Anal Chim Acta,* 616**,** 196-206.

Paglin, S., Hollister, T., Delohery, T., Hackett, N., Mcmahill, M., Sphicas, E., Domingo, D. & Yahalom, J. (2001). A novel response of cancer cells to radiation involves autophagy and formation of acidic vesicles. *Cancer Res,* 61**,** 439-44.

Paglin, S. & Yahalom, J. (2006). Pathways that regulate autophagy and their role in mediating tumor response to treatment. *Autophagy,* 2**,** 291-3.

Park, D. M. & Rich, J. N. (2009). Biology of glioma cancer stem cells. *Mol Cells,* 28**,** 7-12.

Park, E. J., Choi, K. S. & Kwon, T. K. (2011). β-Lapachone-induced reactive oxygen species (ROS) generation mediates autophagic cell death in glioma U87 MG cells. *Chemico-Biological Interactions,* 189**,** 37-44.

Parker, P. J. (1999). Inhibition of Protein Kinase C—Do We, Can We, and Should We? *Pharmacology & Therapeutics,* 82**,** 263-267.

Peck-Miller, K. A., Darveau, R. P. & Fell, H. P. (1993). Identification of serum components that inhibit the tumoricidal activity of amphiphilic alpha helical peptides. *Cancer Chemother Pharmacol,* 32**,** 109-15.

Pelegrini, P. B., Del Sarto, R. P., Silva, O. N., Franco, O. L. & Grossi-De-Sa, M. F. (2011). Antibacterial peptides from plants: what they are and how they probably work. *Biochemistry research international,* 2011**,** 250349.

Pelicano, H., Carney, D. & Huang, P. (2004). ROS stress in cancer cells and therapeutic implications. *Drug Resist Updat,* 7**,** 97-110.

Petty, R. D., Sutherland, L. A., Hunter, E. M. & Cree, I. A. (1995). Comparison of MTT and ATP-based assays for the measurement of viable cell number. *J Biolumin Chemilumin,* 10**,** 29-34.

Pisanu, M. E., Ricci, A., Paris, L., Surrentino, E., Liliac, L., Bagnoli, M., Canevari, S., Mezzanzanica, D., Podo, F., Iorio, E. & Canese, R. (2014). Monitoring response to cytostatic cisplatin in a HER2(+) ovary cancer model by MRI and in vitro and in vivo MR spectroscopy. *Br J Cancer,* 110**,** 625-35.

Ponten, J. & Macintyre, E. H. (1968). Long term culture of normal and neoplastic human glia. *Acta Pathol Microbiol Scand,* 74**,** 465-86.

Prabhu, S., Akbar, Z., Harris, F., Karakoula, K., Lea, R., Rowther, F., Warr, T. & Snape, T. (2013a). Preliminary biological evaluation and mechanism of action studies of selected 2-arylindoles against glioblastoma. *Bioorganic & Medicinal Chemistry,* 21**,** 1918-1924.

Prabhu, S., Dennison, S. R., Lea, B., Snape, T. J., Nicholl, I. D., Radecka, I. & Harris, F. (2013b). Anionic Antimicrobial and Anticancer Peptides from Plants. *Critical Reviews in Plant Sciences,* 32**,** 303-320.

Prabhu, S., Harris, F., Dennison, S. R., Radek, I., Lea, R., Snape, T. (2011). UK-Netherlands Characterisation of an anionic antimicrobial peptide isolated from green coconut water. *Joint Symposium on Antimicrobial peptides: Isolation, characterization, modification and applications.* University of Durham.

Pratheeshkumar, P., Sreekala, C., Zhang, Z., Budhraja, A., Ding, S., Son, Y. O., Wang, X., Hitron, A., Hyun-Jung, K., Wang, L., Lee, J. C. & Shi, X. (2012). Cancer Prevention with Promising Natural Products: Mechanisms of Action and Molecular Targets. *Anticancer Agents Med Chem*.

Raaphorst, G. P., Mao, J., Yang, H., Goel, R., Niknafs, B., Shirazi, F. H., Yazdi, H. M., Rippstein, P. & Ng, C. E. (1998). Evaluation of apoptosis in four human tumour cell lines with differing sensitivities to cisplatin. *Anticancer Res,* 18**,** 2945-51.

Rachet, B., Maringe, C., Nur, U., Quaresma, M., Shah, A., Woods, L. M., Ellis, L., Walters, S., Forman, D., Steward, J. & Coleman, M. P. (2009). Population-based cancer

survival trends in England and Wales up to 2007: an assessment of the NHS cancer plan for England. *Lancet Oncol,* 10**,** 351-69.

Rahman, K. W. & Sarkar, F. H. (2005). Inhibition of nuclear translocation of nuclear factor-{kappa}B contributes to 3,3'-diindolylmethane-induced apoptosis in breast cancer cells. *Cancer Res,* 65**,** 364-71.

Raj, L., Ide, T., Gurkar, A. U., Foley, M., Schenone, M., Li, X., Tolliday, N. J., Golub, T. R., Carr, S. A., Shamji, A. F., Stern, A. M., Mandinova, A., Schreiber, S. L. & Lee, S. W. (2011). Selective killing of cancer cells by a small molecule targeting the stress response to ROS. *Nature,* 475**,** 231-4.

Rampling, R., James, A. & Papanastassiou, V. (2004). The present and future management of malignant brain tumours: surgery, radiotherapy, chemotherapy. *J Neurol Neurosurg Psychiatry,* 75 Suppl 2**,** ii24-30.

Reef, S., Zalckvar, E., Shifman, O., Bialik, S., Sabanay, H., Oren, M. & Kimchi, A. (2006). A short mitochondrial form of p19ARF induces autophagy and caspase-independent cell death. *Mol Cell,* 22**,** 463-75.

Reggiori, F. & Klionsky, D. J. (2002). Autophagy in the eukaryotic cell. *Eukaryot Cell,* 1**,** 11-21.

Reis, R. M., Konu-Leblebliciogiu, D., Lopes, J. M., Kleihues, P. & Ohgaki, H. (2000). Genetic profile of gliosarcomas. *Am J Pathol,* 156**,** 425-32.

Riedl, S., Zweytick, D. & Lohner, K. (2011). Membrane-active host defense peptides - Challenges and perspectives for the development of novel anticancer drugs. *Chemistry and Physics of Lipids,* 164**,** 766-781.

Riss, T. L. & Moravec, R. A. (2004). Use of multiple assay endpoints to investigate the effects of incubation time, dose of toxin, and plating density in cell-based cytotoxicity assays. *Assay Drug Dev Technol,* 2**,** 51-62.

Rogalska, A., Gajek, A., Szwed, M., Jozwiak, Z. & Marczak, A. (2011). The role of reactive oxygen species in WP 631-induced death of human ovarian cancer cells: a comparison with the effect of doxorubicin. *Toxicol In Vitro,* 25**,** 1712-20.

Rogan, E. G. (2006). The natural chemopreventive compound indole-3-carbinol: state of the science. *In Vivo,* 20**,** 221-8.

Safe, S., Papineni, S. & Chintharlapalli, S. (2008). Cancer chemotherapy with indole-3-carbinol, bis(3'-indolyl)methane and synthetic analogs. *Cancer Lett,* 269**,** 326-38.

Samadi, A., Soriano, E., Revuelta, J., Valderas, C., Chioua, M., Garrido, I., Bartolome, B., Tomassolli, I., Ismaili, L., Gonzalez-Lafuente, L., Villarroya, M., Garcia, A. G., Oset-Gasque, M. J. & Marco-Contelles, J. (2011). Synthesis, structure, theoretical and experimental in vitro antioxidant/pharmacological properties of alpha-aryl, N-alkyl nitrones, as potential agents for the treatment of cerebral ischemia. *Bioorg Med Chem,* 19**,** 951-60.

Samosorn, S., Bremner, J. B., Ball, A. & Lewis, K. (2006). Synthesis of functionalized 2-aryl-5-nitro-1H-indoles and their activity as bacterial NorA efflux pump inhibitors. *Bioorg Med Chem,* 14**,** 857-65.

Sangster, J. (1997). *Octanol-Water Partition Coefficients: Fundamentals and Physical Chemistry,* John Wiley & Sons.

Saraswathy, M. & Gong, S. (2013). Different strategies to overcome multidrug resistance in cancer. *Biotechnology Advances,* 31**,** 1397-1407.

Schiffer, M. & Edmundson, A. B. (1967). Use of helical wheels to represent the structures of proteins and to identify segments with helical potential. *Biophys J,* 7**,** 121-35.

Schilsky, R. L., Milano, G.A. Ratain, M.J (Eds.) (1996). *Principles of Antineoplastic Drug Development and Pharmacology,* New York, Marcel Dekker Inc.

Schultz, S., Pinsky, G. S., Wu, N. C., Chamberlain, M. C., Rodrigo, A. S. & Martin, S. E. (2005). Fine needle aspiration diagnosis of extracranial glioblastoma multiforme: Case report and review of the literature. *Cytojournal,* 2**,** 19.

Schumacker, P. T. (2006). Reactive oxygen species in cancer cells: Live by the sword, die by the sword. *Cancer Cell,* 10**,** 175-176.

Schwartzbaum, J. A., Fisher, J. L., Aldape, K. D. & Wrensch, M. (2006). Epidemiology and molecular pathology of glioma. *Nat Clin Pract Neurol,* 2**,** 494-503; quiz 1 p following 516.

Sersa, G., Miklavcic, D., Cemazar, M., Rudolf, Z., Pucihar, G. & Snoj, M. (2008). Electrochemotherapy in treatment of tumours. *Eur J Surg Oncol,* 34**,** 232-40.

Shah, N., Sattar, A., Benanti, M., Hollander, S. & Cheuck, L. (2006). Magnetic resonance spectroscopy as an imaging tool for cancer: a review of the literature. *J Am Osteopath Assoc,* 106**,** 23-7.

Shankar, S. & Srivastava, R. K. (2012). *Nutrition, Diet and Cancer,* Springer.

Sharma, V., Kumar, P. & Pathak, D. (2010). Biological importance of the indole nucleus in recent years: A comprehensive review. *Journal of Heterocyclic Chemistry,* 47**,** 491-502.

Shaw, E. G., Berkey, B., Coons, S. W., Brachman, D., Buckner, J. C., Stelzer, K. J., Barger, G. R., Brown, P. D., Gilbert, M. R. & Mehta, M. (2006). Initial report of Radiation Therapy Oncology Group (RTOG) 9802: Prospective studies in adult low-grade glioma (LGG). *Journal of Clinical Oncology,* 24**,** 1500.

Shertzer, H. G. & Senft, A. P. (2000). The micronutrient indole-3-carbinol: implications for disease and chemoprevention. *Drug Metabol Drug Interact,* 17**,** 159-88.

Shervington, A., Pawar, V., Menon, S., Thakkar, D. & Patel, R. (2009). The sensitization of glioma cells to cisplatin and tamoxifen by the use of catechin. *Mol Biol Rep,* 36**,** 1181-6.

Shieh, J. M., Huang, T. F., Hung, C. F., Chou, K. H., Tsai, Y. J. & Wu, W. B. (2010). Activation of c-Jun N-terminal kinase is essential for mitochondrial membrane potential change and apoptosis induced by doxycycline in melanoma cells. *Br J Pharmacol,* 160**,** 1171-84.

Singh, U. & Jialal, I. (2006). Oxidative stress and atherosclerosis. *Pathophysiology,* 13**,** 129-42.

Smith-Pearson, P. S., Kooshki, M., Spitz, D. R., Poole, L. B., Zhao, W. & Robbins, M. E. (2008). Decreasing peroxiredoxin II expression decreases glutathione, alters cell cycle distribution, and sensitizes glioma cells to ionizing radiation and H(2)O(2). *Free Radic Biol Med,* 45**,** 1178-89.

Snape, T. J. (2008). A truce on the Smiles rearrangement: revisiting an old reaction--the Truce-Smiles rearrangement. *Chem Soc Rev,* 37**,** 2452-8.

So, C. M., Lau, C. P. & Kwong, F. Y. (2007). Easily accessible and highly tunable indolyl phosphine ligands for Suzuki-Miyaura coupling of aryl chlorides. *Org Lett,* 9**,** 2795-8.

Southon, I. W. & Buckingham, J. (1989). *Dictionary of Alkaloids Index,* London, Chapman and Hall.

Sreejayan & Rao, M. N. (1997). Nitric oxide scavenging by curcuminoids. *J Pharm Pharmacol,* 49**,** 105-7.

Sreejayan, N. & Rao, M. N. (1996). Free radical scavenging activity of curcuminoids. *Arzneimittelforschung,* 46**,** 169-71.

Stiborova, M., Poljakova, J., Martinkova, E., Borek-Dohalska, L., Eckschlager, T., Kizek, R. & Frei, E. (2011). Ellipticine cytotoxicity to cancer cell lines - a comparative study. *Interdiscip Toxicol,* 4**,** 98-105.

Strober, W. 2001. Monitoring Cell Growth. *Current Protocols in Immunology.* John Wiley & Sons, Inc.

Sumpter, W. C. & Miller, F. M. 1954. Indole and Carbazole Systems. *Chemistry of Heterocyclic Compounds.* John Wiley & Sons, Inc.

Sun, Y.-M., Zhang, H.-Y., Chen, D.-Z. & Liu, C.-B. (2002). Theoretical Elucidation on the Antioxidant Mechanism of Curcumin: A DFT Study. *Organic Letters,* 4**,** 2909-2911.

Sundar, S. N., Kerekatte, V., Equinozio, C. N., Doan, V. B., Bjeldanes, L. F. & Firestone, G. L. (2006). Indole-3-carbinol selectively uncouples expression and activity of estrogen receptor subtypes in human breast cancer cells. *Mol Endocrinol,* 20**,** 3070-82.

Sundberg, R. J. (1996). *Indoles,* San Deigo, Elsevier Science Publishing Co Inc.

Surh, Y. (1999). Molecular mechanisms of chemopreventive effects of selected dietary and medicinal phenolic substances. *Mutat Res,* 428**,** 305-27.

Surhone, L. M., Timpledon, M. T. & Marseken, S. F. (2010). *Small Molecule,* Betascript Publishing.

Takahashi, T., Ueno, H. & Shibuya, M. (1999). VEGF activates protein kinase C-dependent, but Ras-independent Raf-MEK-MAP kinase pathway for DNA synthesis in primary endothelial cells. *Oncogene,* 18**,** 2221-30.

Tomasz, M. (1995). Mitomycin C: small, fast and deadly (but very selective). *Chem Biol,* 2**,** 575-9.

Trachootham, D., Alexandre, J. & Huang, P. (2009). Targeting cancer cells by ROS-mediated mechanisms: a radical therapeutic approach? *Nat Rev Drug Discov,* 8**,** 579-91.

Trachootham, D., Zhou, Y., Zhang, H., Demizu, Y., Chen, Z., Pelicano, H., Chiao, P. J., Achanta, G., Arlinghaus, R. B., Liu, J. & Huang, P. (2006). Selective killing of oncogenically transformed cells through a ROS-mediated mechanism by beta-phenylethyl isothiocyanate. *Cancer Cell,* 10**,** 241-52.

Traganos, F. & Darzynkiewicz, Z. (1994). Lysosomal proton pump activity: supravital cell staining with acridine orange differentiates leukocyte subpopulations. *Methods Cell Biol,* 41**,** 185-94.

Tsai, C. W., Lin, C. Y., Lin, H. H. & Chen, J. H. (2011). Carnosic acid, a rosemary phenolic compound, induces apoptosis through reactive oxygen species-mediated p38 activation in human neuroblastoma IMR-32 cells. *Neurochem Res,* 36**,** 2442-51.

Tsuda, H., Kozu, T., Iinuma, G., Ohashi, Y., Saito, Y., Saito, D., Akasu, T., Alexander, D. B., Futakuchi, M., Fukamachi, K., Xu, J., Kakizoe, T. & Iigo, M. (2010). Cancer prevention by bovine lactoferrin: from animal studies to human trial. *Biometals,* 23**,** 399-409.

Tuttle, S., Hertan, L. & Katz, J. S. (2011). Indian gold treating cancer in the age of nano. *Cancer Biol Ther,* 11**,** 474-6.

Urruticoechea, A., Alemany, R., Balart, J., Villanueva, A., Vinals, F. & Capella, G. (2010). Recent Advances in Cancer Therapy: An Overview. *Current Pharmaceutical Design,* 16**,** 3-10.

Uttara, B., Singh, A. V., Zamboni, P. & Mahajan, R. T. (2009). Oxidative stress and neurodegenerative diseases: a review of upstream and downstream antioxidant therapeutic options. *Curr Neuropharmacol,* 7**,** 65-74.

Vanorder, R. B. & Lindwall, H. G. (1942). Indole. *Chem. Rev.,* 30**,** 69-96.

Vasiliou, V., Ross, D. & Nebert, D. W. (2006). Update of the NAD(P)H:quinone oxidoreductase (NQO) gene family. *Hum Genomics,* 2**,** 329-35.

Verhoeven, D. T., Verhagen, H., Goldbohm, R. A., Van Den Brandt, P. A. & Van Poppel, G. (1997). A review of mechanisms underlying anticarcinogenicity by brassica vegetables. *Chem Biol Interact,* 103**,** 79-129.

Von Angerer, E., Prekajac, J. & Strohmeier, J. (1984). 2-Phenylindoles. Relationship between structure, estrogen receptor affinity, and mammary tumor inhibiting activity in the rat. *J Med Chem,* 27**,** 1439-47.

Voss, V., Senft, C., Lang, V., Ronellenfitsch, M. W., Steinbach, J. P., Seifert, V. & Kogel, D. (2010). The pan-Bcl-2 inhibitor (-)-gossypol triggers autophagic cell death in malignant glioma. *Mol Cancer Res,* 8**,** 1002-16.

Wang, T. T., Milner, M. J., Milner, J. A. & Kim, Y. S. (2006). Estrogen receptor alpha as a target for indole-3-carbinol. *J Nutr Biochem,* 17**,** 659-64.

Wang, Z., Yu, B. W., Rahman, K. M., Ahmad, F. & Sarkar, F. H. (2008). Induction of growth arrest and apoptosis in human breast cancer cells by 3,3-diindolylmethane is associated with induction and nuclear localization of p27kip. *Mol Cancer Ther,* 7**,** 341-9.

Waris, G. & Ahsan, H. (2006). Reactive oxygen species: role in the development of cancer and various chronic conditions. *J Carcinog*, 5**,** 14.

Wcislo, G. 2014. Chapter 95 - Resveratrol Inhibitory Effects against a Malignant Tumor: A Molecular Introductory Review. *In:* Watson, R. R., Preedy, V. R. & Zibadi, S. (eds.) *Polyphenols in Human Health and Disease.* San Diego: Academic Press.

Wedge, S. R., Kendrew, J., Hennequin, L. F., Valentine, P. J., Barry, S. T., Brave, S. R., Smith, N. R., James, N. H., Dukes, M., Curwen, J. O., Chester, R., Jackson, J. A., Boffey, S. J., Kilburn, L. L., Barnett, S., Richmond, G. H., Wadsworth, P. F., Walker, M., Bigley, A. L., Taylor, S. T., Cooper, L., Beck, S., Jurgensmeier, J. M. & Ogilvie, D. J. (2005). AZD2171: a highly potent, orally bioavailable, vascular endothelial growth factor receptor-2 tyrosine kinase inhibitor for the treatment of cancer. *Cancer Res*, 65**,** 4389-400.

Weng, J. R., Tsai, C. H., Kulp, S. K. & Chen, C. S. (2008). Indole-3-carbinol as a chemopreventive and anti-cancer agent. *Cancer Lett*, 262**,** 153-63.

Whyte, L., Huang, Y. Y., Torres, K. & Mehta, R. G. (2007). Molecular mechanisms of resveratrol action in lung cancer cells using dual protein and microarray analyses. *Cancer Res*, 67**,** 12007-17.

Wong, G. Y., Bradlow, L., Sepkovic, D., Mehl, S., Mailman, J. & Osborne, M. P. (1997). Dose-ranging study of indole-3-carbinol for breast cancer prevention. *J Cell Biochem Suppl*, 28-29**,** 111-6.

Wu, Y., Feng, X., Jin, Y., Wu, Z., Hankey, W., Paisie, C., Li, L., Liu, F., Barsky, S. H., Zhang, W., Ganju, R. & Zou, X. (2010). A novel mechanism of indole-3-carbinol effects on

breast carcinogenesis involves induction of Cdc25A degradation. *Cancer Prev Res (Phila),* 3**,** 818-28.

Yamanaka, R. & Itoh, K. (2007). Peptide-based immunotherapeutic approaches to glioma: a review. *Expert Opin Biol Ther,* 7**,** 645-9.

Yao, K. C., Komata, T., Kondo, Y., Kanzawa, T., Kondo, S. & Germano, I. M. (2003). Molecular response of human glioblastoma multiforme cells to ionizing radiation: cell cycle arrest, modulation of the expression of cyclin-dependent kinase inhibitors, and autophagy. *J Neurosurg,* 98**,** 378-84.

Youssef, K. M. & El-Sherbeny, M. A. (2005). Synthesis and antitumor activity of some curcumin analogs. *Arch Pharm (Weinheim),* 338**,** 181-9.

Yuan, F., Chen, D. Z., Liu, K., Sepkovic, D. W., Bradlow, H. L. & Auborn, K. (1999). Anti-estrogenic activities of indole-3-carbinol in cervical cells: implication for prevention of cervical cancer. *Anticancer Res,* 19**,** 1673-80.

Zagotto, G., Redaelli, M., Pasquale, R., D'avella, D., Cozza, G., Denaro, L., Pizzato, F. & Mucignat-Caretta, C. (2011). 8-Hydroxynaphthalene-1,4-dione derivative as novel compound for glioma treatment. *Bioorg Med Chem Lett,* 21**,** 2079-82.

Zhang, H., Lei, Y., Yuan, P., Li, L., Luo, C., Gao, R., Tian, J., Feng, Z., Nice, E. C. & Sun, J. (2014). ROS-Mediated Autophagy Induced by Dysregulation of Lipid Metabolism Plays a Protective Role in Colorectal Cancer Cells Treated with Gambogic Acid. *PLoS One,* 9**,** e96418.

Zhang, L., Yu, J., Pan, H., Hu, P., Hao, Y., Cai, W., Zhu, H., Yu, A. D., Xie, X., Ma, D. & Yuan, J. (2007). Small molecule regulators of autophagy identified by an image-based high-throughput screen. *Proc Natl Acad Sci U S A*, 104**,** 19023-8.

Zhang, W., Li, J., Liu, L. W., Wang, K. R., Song, J. J., Yan, J. X., Li, Z. Y., Zhang, B. Z. & Wang, R. (2010). A novel analog of antimicrobial peptide Polybia-MPI, with thioamide bond substitution, exhibits increased therapeutic efficacy against cancer and diminished toxicity in mice. *Peptides*, 31**,** 1832-8.

Zhu, X.-X., Yao, X.-F., Jiang, L.-P., Geng, C.-Y., Zhong, L.-F., Yang, G., Zheng, B.-L. & Sun, X.-C. (2014). Sodium arsenite induces ROS-dependent autophagic cell death in pancreatic β-cells. *Food and Chemical Toxicology*.

Zhu, Y., Guignard, F., Zhao, D., Liu, L., Burns, D. K., Mason, R. P., Messing, A. & Parada, L. F. (2005). Early inactivation of p53 tumor suppressor gene cooperating with NF1 loss induces malignant astrocytoma. *Cancer Cell*, 8**,** 119-30.

Zou, C. F., Jia, L., Jin, H., Yao, M., Zhao, N., Huan, J., Lu, Z., Bast, R. C., Jr., Feng, Y. & Yu, Y. (2011). Re-expression of ARHI (DIRAS3) induces autophagy in breast cancer cells and enhances the inhibitory effect of paclitaxel. *BMC Cancer*, 11**,** 22.

5.Appendices

5.1 Appendix I

Synthesis and characterisation of indoles

Commercially available reagents were used as received without purification. Analytical thin layer chromatography (TLC) was performed with plastic-backed TLC plates coated with silica G/UV_{254}, in a variety of solvents. The plates were visualised by UV light (254 nm). Flash column chromatography was conducted with Davisil silica 60Å (40-63 μm) under bellows pressure. Low resolution mass spectra were recorded on a Thermo Finnigan LCQ Advantage MAX using chemical ionisation (CI). ^{1}H and ^{13}C NMR spectra were recorded on a Bruker Avance DPX 250 (250 MHz) or a Bruker 400 (400 MHz) spectrometer. All chemical shifts (δ) are quoted in parts per million (ppm) relative to a calibration reference of the residual protic solvent; $CHCl_3$ (δ_H 7.26, s) or DMSO (δ_H 2.53, m) was used as the internal standard in ^{1}H NMR spectra, and ^{13}C NMR shifts were referenced using $CDCl_3$ (δ_C 77.0, t) or DMSO (δ_C 40.5, sept) with broad band decoupling.

2-(2'-Methoxyphenyl)-1*H*-indole, 223

2'-Methoxyacetophenone (1.38 mL, 10 mmol) was mixed with phenylhydrazine (0.99 mL, 10 mmol) in ethanol (5 mL) and 4 drops of glacial acetic acid added. The pale yellow solution was heated to 80 °C with stirring for 1 hour which produced a red/brown solution. The solvent was evaporated to yield the phenylhydrazone intermediate as red/brown oil. To this oil was added polyphosphoric acid (20 g) and the reaction heated to 120 °C with stirring for 2 hours. After completion of the reaction (TLC) the reaction mixture was

poured onto crushed ice, followed by the addition of NaOH until a neutral pH was reached. The product was extracted with DCM (3 × 50 mL) and the combined extracts washed with water (50 mL), brine (50 mL), dried ($MgSO_4$), filtered and the solvent evaporated. The product was purified using flash chromatography (SiO_2; 50 % toluene: 50% petroleum ether) to yield the title compound as an off-white solid (532 mg, 24%). Rf 0.64 (100% toluene).

^{1}H NMR (250 MHz, $CDCl_3$) δ_H 4.03 (s, 3H), 6.93 (br. s, 1H) 7.03-7.34 (m, 5H), 7.46 (d, *J* = 8.0 Hz, 1H), 7.67 (dd, *J* = 0.5 and 7.5 Hz, 1H), 7.87 (dd, *J* = 1.5 and 8.0 Hz, 1H), 9.70 (br. s, 1H); ^{13}C NMR (62.5 MHz, $CDCl_3$) δ_C 55.8, 99.5, 110.9, 111.8, 119.8, 120.2, 120.5, 121.5, 121.8, 128.0, 128.3, 128.6, 135.9, 136.1, 155.7; ν_{max} (film, cm^{-1}) 3443, 1577, 1463, 1435, 1308, 1232; *m/z* (CI) 224 ([M+H]$^+$, 100%).

(2-Phenyl-1*H*-indol-3-yl)methanol, 223a

2-Phenylindole-3-carboxaldehyde (300 mg, 1.36 mmol) and $NaBH_4$ (103 mg, 2.72 mmol) were stirred at reflux in ethanol (10 mL) for 1 minute followed by stirring at room temperature for 2 hours. 1% NaOH (10 mL) was added to the reaction mixture and the product was extracted with Et_2O (3 × 10 mL). The combined extracts were dried ($MgSO_4$), filtered and the solvent evaporated to yield a crude product which was re-crystallised in PhMe:EtOAc:petroleum ether, yielding the title compound as a white solid 133 mg, 44%).

^{1}H NMR (250 MHz, DMSO-d6) δ_H 4.81 (d, *J* = 5.0 Hz, 2H), 5.10 (t, J = 5.0 Hz, 1H), 7.14-7.28 (m, 2H), 7.48-7.53 (m, 2H), 7.64 (t, J = 7.5 Hz, 2H), 7.80 (d, J = 7.5 Hz, 1H), 7.92 (d, J = 7.5 Hz, 2H), 11.47 (s, 1H); ^{13}C NMR (62.5 MHz, DMSO-d6), δ_C 54.8, 112.1, 113.3,

119.9, 122.6. 128.5, 128.9, 129.67, 129.71, 133.4, 136.8, 136.9; ν_{max} (film, cm^{-1}) 3488, 3183 (br.), 1638, 1491, 1452, 1392; *m/z* (CI) 206 ($[M-OH]^+$, 100%).

2-(2'-Hydroxyphenyl)-1*H*-indole, 209

1-(2-Hydroxyphenyl)-2-(2-nitrophenyl)ethanone, (105 mg, 0.41 mmol) was dissolved in methanol (4.1 mL). Pd/C (10 mg, 10 wt.%) was added and the flask evacuated and backfilled with hydrogen (3 cycles). The reaction was then stirred under an atmosphere of hydrogen for 18 h. The reaction was filtered through Celite® and eluted with methanol (10 mL) and the solvent removed *in vacuo*. The crude product was purified by column chromatography on silica gel (10% EtOAc in petroleum ether) to give the title compound as a pale yellow solid (62 mg, 72%). Rf 0.39 (30% ethyl acetate in petroleum ether).

m.p. (EtOAc: petroleum ether) 170-172 °C; ν_{max}/cm^{-1} 3500, 3425; δ_H (300 MHz; $CDCl_3$) 9.22 (1H, br. s), 7.70 (1H. dd. *J* = 1.6 and 7.8 Hz, Ar), 7.66 (1H, d, *J* = 7.8 Hz, Ar), 7.42 (1H, d, *J* = 8.1 Hz, Ar), 7.26-7.11 (3H, m, Ar), 7.04 (1H, td, *J* = 1.1 and 7.6 Hz, Ar), 6.91 (1H, dd, *J* = 0.9 and 8.1 Hz, Ar), 6.87 (1H, m, Ar), 6.0-5.0 (1H, br. s); δ_C (75 MHz; $CDCl_3$) 152.0, 136.4, 134.8, 128.9, 128.4, 128.3, 122.2, 121.5, 120.4, 120.1, 119.1, 116.6, 111.0, 100.2; *m/z* (ES+) 210 ($[M+H]^+$, 100%); Found 210.0920, $C_{14}H_{12}NO$ ($M+H^+$) requires 210.0919.

5.2 Appendix II

Shown below is a generic example of how the calculations were performed to obtain the desired cell counts needed to seed the glial cells in well plates from a T75 tissue culture flask.

80-90% confluent T-75 flask comprises of 150×10^4 cells/ml. This cell suspension is serially diluted to get the desired cell count of 20×10^3 cells/ml (4000 cells/200µl) as shown below:

150×10^4 cells/ml or 1500×10^3 cells/ml

1:10 ↓ 1 part of cell suspension + 9 parts of cell culture media

150×10^3 cells/ml

↓ *

20×10^3 cells/ml

$$\text{*Dilution factor} = \frac{\text{Concentration of stock cell suspension}}{\text{Required concentration}}$$

$$= \frac{150 \times 10^3 \text{ cells/ml}}{20 \times 10^3 \text{ cells/ml}}$$

$$= 7.5$$

$$\text{Volume of cell suspension required to make up final concentration} = \frac{\text{Total volume}}{\text{Dilution factor}}$$

$$= \frac{10 \text{ mls}}{7.5}$$

$$= 1.33 \text{ mls}$$

5.3 Appendix III

5.3.1 List of research outcomes

1) **Prabhu, S**., Lea, R., Harris, F. and Snape, T. (2014). A review of experimental small molecules for the treatment of glioma, *Drug Discovery Today*, 19(9):1298-1308.
2) **Prabhu, S**., Dennison, S., Lea, R., Snape and Harris, F. (2014) *Cn*-AMP2 from green coconut water is an anionic anticancer peptide. *Journal of Peptide Science*, (Accepted, *In Press).*
3) Harris, F., **Prabhu S**., Dennison, S., Snape, T., Lea, R., Mura, M. and Phoenix, D. **(2014).** The anticancer activity of anionic host defence peptides from the plant kingdom. *Protein and Peptide Letters*, (Accepted, *In Press).*
4) **Prabhu, S**., Akbar, Z., Harris, F., Karakoula, K., Lea, R., Rowther, F., Warr, T., and Snape, T. (2013). Preliminary biological evaluation and mechanism of action studies of selected 2-arylindoles against glioblastoma. *Bioorganic & Medicinal Chemistry*. 21(7): 1918-1924.
5) **Prabhu, S**., Dennison, S., Lea, R., Snape, T., Radek, I. and Harris, F. (2013). Anionic antimicrobial and anticancer peptides from plants. *Critical Reviews in Plant Sciences*, 32(5):303-320.
6) **Prabhu S**., Harris, F., Lea, R. and Snape, T. (2011). Towards establishing the effects and mechanism of action of a series of indoles in an in vitro chemosensitivity system for glioma treatment, *Neuro. Oncol*., 13 (suppl 2): ii1-ii14.

5.3.2 List of conferences attended

1. Poster presented at the British Neuro-oncology Society (BNOS) conference in Cambridge (July 2013),

Prabhu, S., Snape, T., Lea, R. and Harris, F. (2013). *Cn*-AMP2 from *C.* nucifera is a host defence peptide with anticancer activity. BNOS, Durham University.

2. PhD project nominated at the Royal Pharmaceutical Society awards in London (September 2011).
3. Poster presented at the British Neuro-oncology Society (BNOS) conference in Cambridge (June 2011),

Prabhu, S., Harris, F., Lea, R. and Snape, T. (2011). Towards establishing the effects and mechanism of action of a series of substituted indoles in an *in vitro* chemosensitivity system for glioma treatment. BNOS, University of Cambridge.

4. Poster presented at the UK-Netherlands Joint Symposium on Antimicrobial peptides in Dublin (March 2011),

Prabhu, S., Harris, F., Dennison, S. R., Radek, I., Lea, R. and Snape, T. (2011). Characterisation of an anionic antimicrobial peptide isolated from green coconut water. UK-Netherlands Joint Symposium on Antimicrobial peptides: Isolation, characterization, modification and applications. University of Durham.

5. Attended the conference on "Oxidative Stress in cancer and exploitation of negative regulators as therapeutics" at New York Academy of Sciences, New York, USA (February 2011).

6. Presented work at the 4th Annual Retreat of Brain Tumour Northwest (BTNW) at Preston, England (December 2010).
7. Attended the British Neuro-oncology Society conference at Glasgow, Scotland (June 2010).
8. Presented work at the 3rd Annual Retreat of BTNW at Preston, England (December 2009).
9. Attended various medical seminars and meetings organised by BTNW across the UK.
10. Attended the British Neuro-oncology Society conference at Hull, England (June 2009).